GDAŃSK UNIVERSITY OF TECHNOLOGY

The author of the doctoral dissertation: Aleksander Jakubowski
Scientific discipline: Control, Electronic and Electrical Engineering

DOCTORAL DISSERTATION

Title of doctoral dissertation: Energy efficiency of electric multiple units in suburban operation

Title of doctoral dissertation (in Polish): Efektywność energetyczna elektrycznych zespołów trakcyjnych w ruchu podmiejskim

Supervisor *signature*	Second supervisor *signature*
Andrzej Wilk, Ph.D. D.Sc, Eng., Associate Professor	
Auxiliary supervisor *signature*	Cosupervisor *signature*
Sławomir Judek, Ph.D., Eng.	

Gdańsk, year 2022

GDAŃSK UNIVERSITY OF TECHNOLOGY

STATEMENT

The author of the doctoral dissertation: Aleksander Jakubowski

I, the undersigned, declare that I am aware that in accordance with the provisions of Art. 27 (1) and (2) of the Act of 4th February 1994 on Copyright and Related Rights (Journal of Laws of 2021, item 1062), the university may use my doctoral dissertation entitled:
Energy efficiency of electric multiple units in suburban operationfor scientific or didactic purposes.[11]

Gdańsk,..... .....

signature of the PhD student

Aware of criminal liability for violations of the Act of 4th February 1994 on Copyright and Related Rights and disciplinary actions set out in the Law on Higher Education and Science(Journal of Laws 2021, item 478),[2]as well as civil liability, I declare, that the submitted doctoral dissertation is my own work.

I declare, that the submitted doctoral dissertation is my own work performed under and in cooperation with the supervision of Andrzej Wilk, Ph.D. D.Sc, Eng., Associate Professor, the auxiliary supervision of Sławomir Judek, Ph.D., Eng.*.

This submitted doctoral dissertation has never before been the basis of an official procedure associated with the awarding of a PhD degree.

All the information contained in the above thesis which is derived from written and electronic sources is documented in a list of relevant literature in accordance with Art. 34 of the Copyright and Related Rights Act.

I confirm that this doctoral dissertation is identical to the attached electronic version.

Gdańsk,..... .....

signature of the PhD student

I, the undersigned, agree/do not agree* to include an electronic version of the above doctoral dissertation in the open, institutional, digital repository of Gdańsk University of Technology.

Gdańsk,..... .....

signature of the PhD student

**delete where appropriate*

[1] Art 27. 1. Educational institutions and entities referred to in art. 7 sec. 1 points 1, 2 and 4–8 of the Act of 20 July 2018 – Law on Higher Education and Science, may use the disseminated works in the original and in translation for the purposes of illustrating the content provided for didactic purposes or in order to conduct research activities, and to reproduce for this purpose disseminated minor works or fragments of larger works.

2. If the works are made available to the public in such a way that everyone can have access to them at the place and time selected by them, as referred to in para. 1, is allowed only for a limited group of people learning, teaching or conducting research, identified by the entities listed in paragraph 1.

GDAŃSK UNIVERSITY OF TECHNOLOGY

DESCRIPTION OF DOCTORAL DISSERTATION

The Author of the doctoral dissertation: Aleksander Jakubowski

Title of doctoral dissertation: Energy efficiency of electric multiple units in suburban operation

Title of doctoral dissertation in Polish: Efektywność energetyczna elektrycznych zespołów trakcyjnych w ruchu podmiejskim

Language of doctoral dissertation: English

Supervisor: Andrzej Wilk, Ph.D. D.Sc., Eng., Associate Professor

Auxiliary supervisior*: Sławomir Judek, Ph.D., Eng.

Date of doctoral defense:

Keywords of doctoral dissertation in Polish: trakcja elektryczna, symulacja komputerowa, efektywność energetyczna, transport miejski.

Keywords of doctoral dissertation in English: electric traction, computer simulation, energy efficiency, suburban transport.

**delete where appropriate*

***applies to doctoral dissertations written in other languages, than Polish or English*

Abstract

Rising numbers of agglomeration residents cause increased need for people movement on daily basis. Because of congestion of local roads, limited parking space and rising fuel prices providing mass transit based on electric traction is a logical solution. While the electric rail vehicles are considered highly efficient in themselves, they should be analyzed as a part of a transport network, because energy consumption depends on operating conditions of a whole transport system. Information about energy efficiency of whole system operating under realistic conditions is a basis for research into energy savings. Such data is also useful when modernization of traction power supply, timetable planning or ordering new rolling stock is planned.

This thesis presents approach to analysis of energy efficiency of a suburban rail network, using novel models developed on the Matlab/Simulink basis. Necessary features and requirements for such models were determined thru in-depth review of the source literature in all applicable fields: electrified transportation systems, electric multiple units construction, vehicle drivetrains and finally, existing simulation methods. Existing and applied methods for improvement energy efficiency of electrified transportation were identified.

Original model of electrified transportation system was developed. It can be characterized by unique implementation of the data bus structure that allows for simulating complex transport systems in a straightforward way while retaining high computation performance. Because every part of the program is an independent sub-model, the only limitation to size and complexity of analyzed system is the available computing power.

Verification of the model accuracy was conducted. Precision of vehicle dynamics simulation against recorded run was presented for a reference fragment of analyzed railway line, for an electric multiple unit. Validation of the results for the transport network, generated using the whole model was carried out for exemplary transport network, where detailed measurement data was available (trolleybus system in Pilsen, Czech Republic). Obtained results confirmed accuracy of the developed model, with computed voltage error being consistently below 2% figure, and difference between measured current and final energy balance were below 5%.

Parameters of the analyzed transport system were assumed using technical datasheets, catalogues, tender documentation and a large set of recorded run data. Only vehicles capable of regenerative braking – equipped with induction motor drives were included. Vehicle models take into account detailed parameters, like load and velocity-dependent efficiency, impact that pantograph voltage has on vehicle power and rheostatic braking and relation between the weather and motive force application and heating system operation. Passenger flow was also included – number of passengers carried by the trains varies along the route and during the day, impacting the vehicle mass and consequently, its movement

dynamics and energy consumption. Novel control algorithm was implemented, allowing for semi-random selection of velocity profile for every station-to-station fragment, following the variable selection probability established thru large recorded run data set analysis.

Energy efficiency analysis for suburban railway system of SKM Trójmiasto was carried out, limiting the scope to railway line no. 250 between stations Gdańsk Śródmieście and Gdynia Redłowo. Simulation was executed assuming the whole day of operation, assuming regular workday schedule. Computed daily energy consumption is 56,4 MWh, while recuperation rate lies typically between 25 and 26%.

Practical and easy to implement approach to velocity profile optimization for electric multiple unit was proposed. Presented method allows for energy savings of about 8% while retaining the same travel time, simultaneously reducing drivetrain losses. Possibilities of further energy consumption reduction were suggested.

Conducted research demonstrated that implementing model structure inspired by industrial communication networks improves model scalability and versatility, as it was used for two different electrified urban transport systems, with different power supply layouts. Moreover, proposed approach to energy consumption optimization, based on trackside signs and manageable by human driver was shown to improve energy efficiency of the whole system. This work also includes implementation of passenger flow and variable velocity profiles, which allowed for improvement of calculation accuracy.

Streszczenie

Rozwój obszarów aglomeracyjnych skutkuje zwiększeniem zapotrzebowania na przewóz osób. Ze względu na kongestię sieci drogowej, ograniczoną przestrzeń parkingową oraz rosnące ceny paliw, logicznym rozwiązaniem jest zapewnienie sieci transportu publicznego opartą na trakcji elektrycznej. Chociaż pojazdy elektryczne można uznać za wysokowydajne, powinny być one analizowane jako element składowy zelektryfikowanego systemu transportowego, ponieważ ich zapotrzebowanie na energię jest zależne od warunków pracy tego systemu. Wiedza na temat efektywności energetycznej sieci transportowej pracującej w realistycznych warunkach stanowi podstawę do poszukiwania oszczędności energetycznych. Dane te są także przydatne przy planowaniu modernizacji układu zasilania trakcyjnego, planowania rozkładu jazdy lub zakupu nowych pojazdów.

Niniejsza rozprawa porusza tematykę analizy energetycznej systemu szybkiej kolei miejskiej przy wykorzystaniu nowej generacji modeli bazujących na środowisku Matlab/Simulink. Niezbędne cechy i wymagania dla modelu zostały oparte na przeglądzie literatury dotykającej tematyki zelektryfikowanych systemów transportowych, budowy elektrycznych zespołów trakcyjnych oraz ich układów napędowych oraz istniejących metod symulacyjnych. Zidentyfikowano istniejące oraz stosowane sposoby zwiększenia efektywności energetycznej transportu zelektryfikowanego.

Opracowano autorski model zelektryfikowanego systemu transportowego. Jego cechą jest nowatorska implementacja magistrali danych, umożliwiająca łatwe symulowanie złożonych zelektryfikowanych systemów transportowych przy zachowaniu wysokiej wydajności obliczeń. Ponieważ każdy z elementów składowych jest niezależnym modelem, jedynym ograniczeniem złożoności badanego systemu są dostępne zasoby komputera.

Przeprowadzono weryfikację dokładności modelu. Precyzję symulacji dynamiki ruchu pojazdu zaprezentowano dla elektrycznego zespołu trakcyjnego poruszającego się na referencyjnym odcinku linii kolejowej. Walidację strony energetycznej modelu przeprowadzono bazując na danych oraz wynikach dla sieci trolejbusowej w Pilźnie (Rep. Czeska). Osiągnięte wyniki potwierdziły skuteczność opracowanego modelu, gdzie rozbieżność obliczonego napięcia nie przekroczyła 2% względem pomiaru, a błąd prądu oraz końcowa różnica w bilansie energii zawarły się poniżej 5%.

Parametry badanego systemu zostały ustalone na podstawie kart katalogowych producentów, dokumentacji technicznych i przetargowych oraz dużym zbiorze zarejestrowanych przejazdów. Założono wykorzystanie wyłącznie pojazdów wyposażonych w napędy z silnikami indukcyjnymi, umożliwiające hamowanie odzyskowe. Modele pojazdów uwzględniają szczegółowe parametry, jak zależna od obciążenia napędu sprawność, wpływie napięcia zasilania na dostępną moc pojazdu oraz załączenie hamowania rezystorowego, a także wpływa warunków pogodowych na przeniesienie siły napędowej oraz pracę systemu ogrzewania. Wzięto pod uwagę potoki pasażerów – liczba osób przewożonych przez poszczególne pociągi zmienia się z czasem

oraz wzdłuż trasy, wpływając na masę pojazdu, a tym samym jego dynamikę ruchu i energochłonność. Zaimplementowano nowatorski algorytm sterowania, który dla każdego odcinka międzyprzystankowego wybiera losowo jeden z możliwych profili prędkości, przy czym prawdopodobieństwo wyboru jest zgodne z ustalonym w toku badań systemu transportowego. Profile prędkości pojazdu zostały ustalone na podstawie analizy dużego zbioru danych rejestracji przejazdów.

Dokonano analizy energetycznej systemu transportowego Szybkiej Kolei Miejskiej w Trójmieście na odcinku linii 250 pomiędzy stacjami Gdańsk Śródmieście oraz Gdynia Redłowo. Obliczenia wykonano dla jednej doby pracy systemu, przy założeniu rozkładu jazdy dla dnia roboczego. Obliczone zużycie energii waha się w granicach 56,4 MWh, natomiast sprawność odzysku energii pomiędzy 25 a 26%.

Zaproponowano metodę optymalizacji energetycznej, która jest łatwa w implementacji w rzeczywistym systemie transportowym. Opracowany sposób pozwala na redukcję zużycia energii o około 8% przy zachowaniu dotychczasowego czasu podróży, jednocześnie redukując straty w układzie napędowym. Zwrócono uwagę na możliwe dalsze zabiegi zmierzające do zwiększenia oszczędności.

Na podstawie przeprowadzonych badań wykazano, że modele o strukturze wzorowanej na magistrali danych zwiększają skalowalność oraz wszechstronność programu, który był użyty w analizie dwóch różnych zelektryfikowanych miejskich systemów transportowych, o różnej strukturze układu zasilania. Ponadto, zaproponowana metoda optymalizacji energetycznej, wykonalna przez człowieka przy użyciu znaków przytorowych pozwala na poprawę efektywności energetycznej systemu transportowego. Rozprawa omawia również implementację potoków pasażerskich oraz zmienności profili prędkości, co zwiększa dokładność obliczeń.

Ackowledgements

I would like to express my gratitude towards the people that supported my research work, enabling this dissertation to come to fruition.

I am grateful to my supervisor, prof. Andrzej Wilk for supporting my scientific endeavors and providing inspiration and guidance in both academic work and research.

This work would not have been possible without prof. Krzysztof Karwowski, who provided me with invaluable suggestions and advice.

I would like to express my thanks towards everyone from Department of Electrified Transportation, especially dr Sławomir Judek, who was my supervisor for Master's thesis, prof. Leszek Jarzębowicz, who helped me with various problems and publishing papers, prof. Mikołaj Bartłomiejczyk, who suggested me taking part in EfficienCE, prof. Jacek Skibicki, who provided me with advice and prof. Dariusz Karkosiński, who helped with suggestions. I also thank eng. Paweł Bawolski for professional support in laboratory work.

Also, I thank dr Zygmunt Giętkowski, who was my lecturer in Electric Traction and provided me with not only knowledge, but multitude of scientific resources as well.

Thanks should also go to all people who helped me with all the formal issues and document preparations: Ms. Halina Kwiatkowska – Kasperowicz, Ms. Katarzyna Urbanowicz, Ms. Dorota Kodź, Ms. Bogusława Horiszna and Mr. Andrzej Wojewódka, and everyone who supported my work in any way and whom I forgot to mention.

Contents

Symbols and Abbreviations

a	-	acceleration
B	-	magnetic flux density
D	-	duty cycle
d	-	deceleration
E	-	energy
F	-	motive force
f	-	frequency
G	-	conductance
g	-	gravitational acceleration
I, i	-	current
i_r	-	curve resistance
J	-	moment of inertia
k	-	rotating mass coefficient
L_f	-	inductance of field windings
M	-	mechanical torque
m	-	mass
O	-	occupancy rate
P	-	power
R’	-	kilometric resistance
R_w	-	motor windings resistance
S	-	electromechanical switch
s	-	slip (in induction motor)
T	-	period
t	-	time
U, u	-	voltage
U_{d0}	-	idle traction substation voltage
v	-	velocity
W	-	motion resistance force
x	-	absolute location
η	-	efficiency factor
η_{reg}	-	regenerative braking efficiency
μ	-	surface adhesion coefficient
σ	-	material conductivity
τ	-	absolute time
Φ	-	flux
φ	-	in cosfi
ω_r	-	angular velocity

AC	–	Alternating Current
AGV	–	Automotrice à Grande Vitesse (High Speed Electric Multiple Unit)
ATO	–	Autonomous Train Operation
BART	–	Bay Area Rapid Transit
BEMU	–	battery electric multiple unit
CFD	–	computational fluid dynamics

DC	–	Direct Current
DoD	–	depth of discharge
EEA	–	European Environment Agency
EMU	–	Electric Multiple Unit
ERTMS	–	European Rail Traffic Management System
ETCS	–	European Train Control System
EV	–	electric vehicle
FEM	–	Finite Elements Method
GNSS	–	Global Navigation Satellite Systems
GTO	–	Gate Turn-Off thyristor
HVAC	–	Heating, Ventilation and Air Conditioning
ID	–	identifier
IGBT	–	Insulated Gate Bipolar Transistor
IPEMU	–	independently powered electric multiple unit
JR	–	Japan Railways
LZB	–	Linienförmige Zugbeeinflüssung (Continuous Train Influence)
MARTA	–	Metropolitan Area Rapid Transit Atlanta
MGU-K	–	motor-generator unit – kinetic
OS	–	operating system
PI	–	Proportional-Integral controller
PKP	–	Polskie Koleje Państwowe (Polish State Railways)
PM	–	Permanent Magnet
PMDP	–	Plzeňské Městské Dopravní Podniky (Pilsen City Transport Company)
PSR	–	Przekaźnik Samoczynnego Rozruchu (automatic acceleration controller)
PT	–	podstacja trakcyjna (traction substation)
RER	–	Réseau Express Régional
RMSE	–	root mean square error
RNG	–	random number generator
SDB	–	Supply Data Bus
SG	–	Savitzky – Golay filter
SKM	–	Szybka Kolej Miejska (Rapid Urban Railway)
SN	–	Section Number, supply section identifier
SoC	–	State of Charge
SQP	–	Sequential Quadratic Programming
TS	–	traction substation
UIC	–	Union Internationale des Chemins de fer (International Union of Railways)
VDB	–	Vehicle Data Bus
VVVF	–	Variable Voltage, Variable Frequency
WKD	–	Warszawska Kolej Dojazdowa (Warsaw Commuter Railway)
WUT	–	Warsaw University of Technology
ZNTK MM	–	Zakład Naprawy Taboru Mińsk Mazowiecki (Rolling stock repair company in Mińsk Mazowiecki)

1. INTRODUCTION

1.1. Background

Growing importance of decarbonization of economy implies modernization of energy sources and rationalization of energy usage. Because virtually all of the environmentally friendly power is generated as an electrical energy, intensified electrification of basically all industries is the result [37]. This is especially highlighted in case of transportation, where electromobility is being dynamically developed, in form of the electric cars, but also smaller vehicles like electric bicycles, drones and small sized aircraft [2,13,72,121,153]. It is worth noting that while transition to electrified individual transportation allows for reduction in emissions, it does not address the general low efficiency of the individual transport means itself, especially in highly urbanized areas characterized with large population density [16,19,92,135]. Therefore, electric public transit is a logical solution to a growing movement demand within agglomerations [10,13,78,86,116,143,144,147,161].

Applicable means of transport depend on potential passenger numbers, route length, existing infrastructure and terrain within intended operation zone. Moving smaller number of people can be realized with electric buses or trolleybuses, while large cities require efficient railway-based systems, like subway or suburban railway [16,19,135]. However, enlargement of transport network or introduction of new connections into existing system results in increased energy demand. To accommodate more rolling stock and ensure reliable operation of the whole system, appropriate power supply is needed, for both new and modernized routes [3,10,42,44,56,125,151,159]. Because of this, analyses are required to find the optimal parameters of the rolling stock and infrastructure [30,49,50,85,142].

New vehicles have often higher power and are more demanding when it comes to energy quality (e.g. require high enough line voltage). It is important to verify, if vehicle will be adequate for desired task and if it will not cause disturbances in power supply [12,15,27,38,84,97,139]. Moreover, the growth of electrical energy prices motivates research for energy efficiency improvement, through vehicle design but also driving technique and timetabling. Energy management strategy is an important factor too, especially for hybrid and storage-powered vehicles [117]. Depending on route geometry and vehicles used, optimization of velocity profile allow to save about 10 – 20% of energy [18,42,56,125,147]. Use of integrated optimization algorithms can improve that to about 30%, which translates to substantial reduction of operating costs. Integrated means that both velocity profiles of multiple vehicles and the timetable are optimized simultaneously, with some of the applications designed for on-line operation. In papers [28,86,159,161] authors proposed multiple optimization methods, with different levels of complexity. However, their validation was carried out only for specific cases, and many of those have high requirements infrastructure-wise in order to use in real system.

Currently, the need for precise evaluation of energy consumption of a rail vehicle before making an order is widely acknowledged. There are many approaches to the problem, with varying complexity.

The simplest method operates on assumption of constant parameters of line voltage, efficiency factors and even simplify velocity profile to trapezoidal shape or assume ideal braking energy recuperation [13,81,129]. Such approach might be sufficient for timetabling or generalized energy calculations, however for the power supply and losses analysis use of more advanced models is advisable.

One of such methods assume single vehicle movement, computing electrical parameters of the whole transport system through superposition [17,40,98]. While the method is viable, determination of energy regeneration and potential impact of pantograph voltage on traction drive performance is challenging.

The most complex programs are designed to simulate whole system simultaneously, allowing for in-depth analysis of energy flow and efficiency as well as accurate values of currents and voltages [30,141-143,162]. However, program stability and computation performance are a major challenge, often limiting such applications to simulate single section of power supply, or at best, single route. Those programs are also developed for one certain task and often cannot be used for different analysis.

There is also commercial software available – allowing for calculations of energy consumption and timetables. However, those programs are developed aiming for maximum versatility and used primarily for timetabling [32,33,114,145]. Considering number of input parameters needed to run the simulation and output data, usability of such software is limited. Algorithms used are also unknown, being internal secret of companies developing the programs, and implementing custom modifications or extensions is not possible. Some of the developers also employ “calculations as service” business model. This is especially true for more advanced simulators that allow for multi-vehicle analysis [104,140]. Because of this, commercial software cannot be considered well-suited for research purposes.

Despite large number of analyses of energy efficiency in transportation systems aimed at reduction of energy consumption, most researchers focus heavily on development of advanced optimization algorithms (using for timetabling or velocity profile setting) or the power supply [21,56,71,86,93,125,151,159]. The vehicle itself in such analyses is often being oversimplified, despite consuming the most energy in analyzed system.

On the other hand, papers on traction drives analyze the vehicle in idealized conditions or even only the drive itself are presented. They assume simplified operation conditions, such as theoretical routes or trapezoidal velocity profiles, often skipping the power supply part entirely [3,10,12,36,43,76,90,94,152,156]. While every element of the transportation system need to be depicted accurately in simulation in order to provide meaningful results, there are very few analyses that attempt to do so [66,118,165].

Every program based on mathematical model that computes parameters in continuous time domain can be characterized as dynamical system [70]. Such model contains dynamic sets of data, and both relations between the sets as well as operations within the system are specified within the program. For the electric traction system, vehicles and power supply

elements can be considered as dynamic sets, relations between them are determined by the system structure and the operations are defined by all the equations coded within the model. However, for certain applications, discrete systems are a better fit – discontinuous changes in signal values are useful for modeling logical systems with finite number of states, such as communication networks.

There is a possibility of implementing discrete system under dynamical system [73]. Such solution can be used for describing dynamical systems where subsystems working in continuous time exchange information or are controlled by discontinuous signals. Example of this can be found within industrial communication networks, where devices performing continuous–time tasks communicate thru common transmission medium called data bus (wired or wireless), using discrete–time protocol [105,158]. For models involving multiple subsystems that exchange information, adoption of such solution seems advantageous.

1.2. Research theses

Analysis of the source literature shown the scarcity of comprehensive models that could allow for in-depth analysis of electric vehicle as a part of transportation system. Seeing potential benefits that better accuracy of such calculations would bring, author decided to focus on development of an original software, which will provide results of practical significance, implementable in real transport systems.

Consequently, the author stated research theses:

1. **Implementation of data bus structure within electrified transport system model improves its versatility and scalability. Therefore, model is useful for complex power supply layouts, found in electrified urban transport networks.**
2. **Implementation of optimized velocity profile using trackside signs executable by human driver improves energy efficiency of the whole transport system in relation to current operating conditions. The signs define movement phases: acceleration/cruising, coasting and braking, along with set velocity.**
3. **Consideration of passenger flow and variability of velocity profiles improves accuracy of transport system energy efficiency calculations. Obtained results constitute for a large set of data that can be further used in statistical analyses.**

1.3. Dissertation objectives

In order to prove stated research theses, author defined dissertation objectives that include:

- Development of novel simulation models for comprehensive, in–depth analysis of energy efficiency of vehicles operating in suburban electrified transportation systems;

- Implementation of vehicle model accounting for its drivetrain electrical and mechanical characteristics along with power supply model, that allow for computation of all parameters necessary for energy efficiency evaluation;
- In-depth analysis of electrified transport system operation, based on large set of measurements, data published by the system operator and technical documentations;
- Simulation of energy efficiency of selected vehicle classes under realistic operating conditions;
- Verification of obtained results for analyzed system and for alternative electrified transport network;
- Proposal of method allowing for energy-saving measures such as optimized velocity profiles that is simple and quick to implement in real systems.

1.4. Scope of the research

The scope of this dissertation is as follows:

- Analysis of source literature, focusing on subject matter of energy consumption and efficiency in electrified suburban railway systems. That included both power supply and vehicle drivetrain construction, its auxiliary needs, possibility of energy storage implementation and impact of operating conditions, like passenger service, timetable and velocity profile (chapter 2).
- Review of existing simulation methods, looking into their advantages, shortcomings and possible room for improvements (chapter 2).
- Development of novel models of the vehicle, power supply and traffic control allowing for detailed analysis of the energy flow, losses assessment and energy efficiency under realistic operating conditions (chapter 3).
- Analysis of operation of a suburban rail vehicles in typical conditions, assuming actual transportation network, technical parameters of analyzed infrastructure and rolling stock and large set of recorded data (chapter 5, 6).
- Verification of the results of the simulation against measured data from real objects, including electrical and mechanical parameters (chapter 4).
- Proposal for implementation of an algorithm allowing for optimization of energy consumption, defining the most significant parameters that need to be taken into account (chapter 7).
- Analysis of energy efficiency using optimized velocity profiles, showing potential for energy savings (chapter 7).
- Summarization of obtained results, proving the stated theses and indicated possibilities of further development of the work (chapter 8).

Novel aspects of the dissertation include:

- Introduction of industrial data network structure into electrified transport system model, which improves versatility and computation performance;

- Adaptive structure of the model: elements of the vehicle or power supply are easily replaceable for different analyses; simulating every part independently is possible also outside the main program;
- Simulation of interconnected systems: each vehicle can be of different type, follow different route and schedule; power supply can have different parameters for each section; interconnected systems (e.g. tram and trolleybus) or smart grids can be analyzed;
- Statistic-based determination of input parameters for the analysis;
- Original algorithm for automatic analysis of large set of recorded vehicle run data, that returns the summary of all velocity profiles;
- Implementation of original semi–randomized velocity profile selection, with variable probabilities based on runs recorded in real system;
- Unique control algorithm: vehicle movement is controlled by the set of logical functions, with the Permission function being the highest in hierarchy;
- Implementation of passenger flow data, which impacts mass of the vehicle, and consequently, its movement dynamics and energy consumption;
- Variability of station dwelling time: this includes not only prolonged stops at main stations, but also random variability occurring in real systems;
- Consideration of weather conditions: air temperature has an impact on heating and air conditioning, and dry, wet or icy conditions have a consequences in wheel adhesion. This can vary with time and/or distance;
- Differentiation between route and power supply section: parameters of the route (inclination, curvature) are independent from power supply – the vehicle can change track during the run or travel outside the electrified route if equipped with energy storage;
- Original approach to energy consumption optimization, which is practically implementable with minimal cost and infrastructure requirements;
- Scalability: it is possible to simulate a whole day of the network operation or focus only on short timeframe, with reduced timestep – as the initial parameters are loaded from external file;
- Evaluation frame: it is possible to simulate only a part of larger system, where vehicles enter and leave analyzed fragment – but all the calculations are carried out only for the selected part.

Procedure of model development and energy efficiency analyses were shown for electrified transport systems of SKM Trójmiasto (suburban railway) and PMDP Pilsen (Czech Republic, trolleybus system).

2. ENERGY CONSUMPTION IN SUBURBAN RAILWAY SYSTEMS

2.1. Suburban railway system

In this subsection typical characteristics of suburban railway system were described. Literature review included publications about infrastructure, rolling stock and operating conditions worldwide. As the vehicles utilize wide range of drivetrains, author decided to look into most common solutions found in suburban rail rolling stock. Analysis focused on modern electric multiple units and DC power supply system.

2.1.1. Electrification system

Majority of suburban railway transportation systems worldwide utilize electrical energy for vehicle movement. Better acceleration, elimination of local exhaust gas emissions, braking energy recuperation and relatively silent drivetrain operation are the main advantages of electric traction in comparison to diesel traction [78]. Lower maintenance costs and better reliability are the factors as well. However, feeding electrical energy to vehicles require additional infrastructure, known as traction power supply system, which is costly to construct and maintain and can have negative impact on aesthetics of environment. Therefore, route electrification need to be prefaced with study of feasibility of investment to verify if savings from lower operation costs of electric vehicles outweigh costs of electrical infrastructure [72,138]. In case of lines with smaller passenger flow it might be cheaper to operate diesel trains, or taking ecological aspect into account – hydrogen powered (fuell–cell) or full–battery vehicles [41,96]. Both of those solutions have been introduced into service and are expected to fully replace diesel traction and compete against catenary-fed electric trains on local routes. In case of urban transport, trolleybuses equipped with battery storages are successfully introduced into a bus lines, replacing diesel-powered vehicles.

Because agglomeration railway networks often are, contrary to subways or trams, a part of a larger transportation system, interoperability is a concern. Therefore, power supply system used for suburban railways is often determined by national railway electrification system, to make the line accessible for intercity and freight trains as well (e.g. in case of maintenance works on mainline, suburban railway line can be used as a bypass). Many of those were electrified using most modern solutions available at the time, which also impacted which electrification system was chosen. There are also independent systems, which have different power supply, e.g. *S–Bahn* in Berlin, fed from third rail with nominal voltage of 800 V DC, while the whole railway in Germany is electrified in 15 kV AC system [39,133], using overhead contact line. Similar solutions can be found in countries that electrified their railways with 25 kV AC system – 750 V DC fed Thameslink in London or 1500 V DC powered Réseau Express Régional (RER) in Paris.

Such solutions are mostly the result of implementation electric railway in agglomeration before the intercity routes were electrified – because of that, many suburban railway systems are powered by relatively old in design DC systems, often with lower nominal

voltages (600 V – 1500 V). In Poland, there were originally two purpose-built urban railways: *SKM* (Szybka Kolej Miejska) in Tricity, and *WKD* (Warszawska Kolej Dojazdowa) in Warsaw, both of which used different power supply than national railways PKP – SKM utilized 800 V DC till 1976 (rolling stock consisted of refurbished pre-war Berlin *S-Bahn* trains), WKD – 600 V DC till 2016 (rolling stock based on tram parts). Currently, all suburban railway networks in Poland utilize 3 kV DC power supply, the same as the whole national railway network. Typically, DC power supply systems are considered adequate for suburban operation, with many systems utilizing 1500 V nominal voltage [85].

Urban transport networks like trams or trolleybuses utilize lower voltages not only because of lower power needed, but for safety reasons as well – it is easier to provide adequate electrical insulation within lower voltage range. Moreover, letting catenary with higher voltage into densely populated areas is also not advisable.

DC railway electrification system consists of traction substations, feeder cables, overhead catenary with single or double contact line or third rail, and railway track. Substations are fed from public power system either by medium voltage line (double step transformation), or by high voltage line (single step transformation) where such infrastructure is available. To ensure reliability, each substation must be connected to power system with at least two lines from two separate power stations. In most cases, there is no possibility to send energy back to public power grid, as substations are equipped with diode rectifiers, though reversible substations see limited, experimental use [71,72,138,165]. Alternatively, substations can be equipped by energy storage that absorbs excessive energy from regenerative braking and is discharged when the substation load increases, for improving both energy efficiency and voltage stability. Such devices are growing in popularity in urban electrified transport systems like trams, trolleybuses and also in subway [86]. Implementation of energy storage in railway systems is also considered, however very high costs of purchase and maintenance of device with adequately high capacity is the major drawback. Nevertheless, trackside energy storages can be assembled from multiple used batteries from electric cars and buses, decreasing the costs greatly [37].

It is worth noting that in Poland such device has been built and is currently in operation near Wrocław, being one of the largest in Europe, with construction of more being planned [111]. In this application, the storage allows for lowering demand for energy from public power system in peak hours, decreasing cost of operation.

Electrified route is divided into power supply sections that can be fed by one or two substations. Section length typically varies from about 5 to 25 kilometers, depending on substations' power, catenary parameters, route inclination, speed limits and expected traffic. For double track sections that are longer or located in mountainous terrain, transverse connections (section cabins) are used to reduce losses and voltage drops [72,120,138]. There may be one or more of such connections, depending on the route. In case of breakdown or maintenance works, substations can also work as such connection (with transformer-rectifier units switched off and decoupled from power supply). Conversely, portable substation installed in easy to transport container, can be coupled into such connection to provide power during substation refurbishment. In some cases, one

substation can be connected to more than two sections (star topology, found in urban transport systems, like trams or especially trolleybuses). Typical layouts found in railway DC power supply systems are shown in Fig. 2.1.

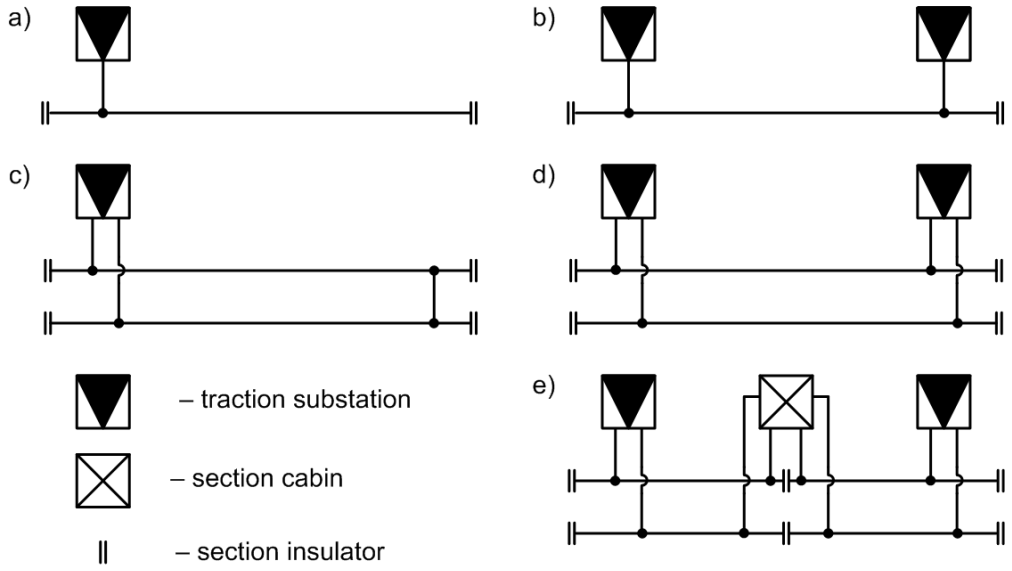

Fig. 2.1. Simplified diagrams of typical layouts of DC power supply system: a) powered from one side, single track; b) powered from two sides, single track; c) powered from one side, double track with interconnection at the end; d) powered from two sides, double track; e) powered from two sides, double track with transverse connection (section cabin)

Substations' main task is to convert parameters of electrical energy from public power system to match requirements specified for railway electrification system. Allowed voltage values and maximum time they can occur is specified in European standard EN50663, to ensure both reliability and interoperability of rolling stock [35,119].

Because of that, units of transformers coupled with rectifiers are used. Typically, 6 and 12 pulse rectifiers are utilized, with the latter being preferable due to better output voltage stability and less harmonics emitted [126]. They require, however, use of transformers with three windings, so the output of the transformer is six-phase. Such units are characterized by parameters like idle voltage U_{d0}, nominal voltage U_{dN} (typically 3300 V), nominal current I_{dN}, nominal power and internal (equivalent) resistance (Fig. 2.2). It is worth noting, that in real substations, output characteristic bend upwards when load current decreases to zero as a result of energy stored in filter capacitors. Because of this, actual value of idle voltage is slightly higher than value approximated by linear characteristics. There is also overload class, which informs of maximal possible current value and time in which such current can be fed to the catenary. The transformers are also equipped with tap-switch, which allows for some degree of output voltage regulation [120].

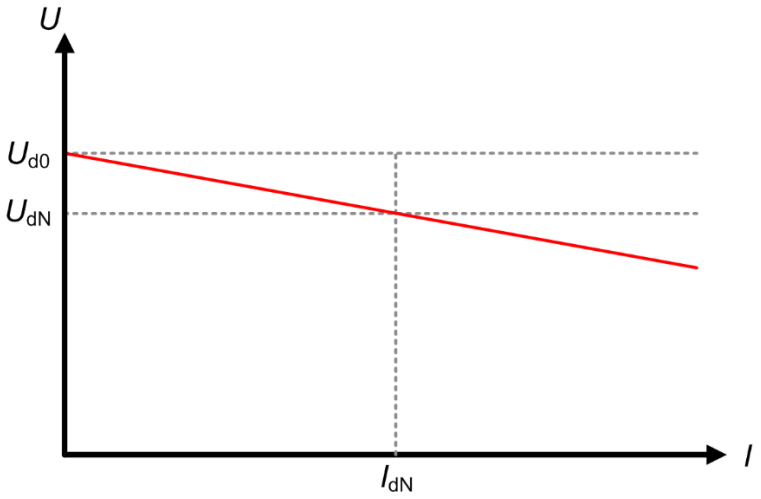

Fig. 2.2. Output characteristic of traction substation (used in calculations), where U_{dN}, I_{dN} – nominal voltage and current, U_{d0} – no-load voltage

Other equipment installed in traction substation is used to ensure energy quality and short-circuit protection. Therefore, LC filter designed to decrease typical voltage harmonics is equipped (higher current harmonics in catenary cause additional losses and electromagnetic disturbances which can interfere with signaling systems). There is also protection against under-voltage. However, in models developed for the purpose of analyzing energy efficiency of transportation systems, substation are simplified into voltage source, connected in series with resistor and diode. This is done to depict the output characteristics of the substation without considering internal structure of the rectifier, which would require significantly shorter timestep to properly analyze [8,38,143].

Losses in railway DC power supply system are caused by resistance of each element [49,51,52,132]. Most losses on catenary are in overhead contact line – rail track have such a large cross-section that their resistance is an order of magnitude smaller than contact line resistance and is sometimes omitted. Losses in feeder cables are generally extremely small in comparison to catenary and substations, because of large cross-section and relatively short length of such cables. In substations there are losses in power transformer windings, rectifier and LC filter. Because of complexity of substation equipment, in energy efficiency analyses substations are either omitted or modelled with efficiency curve, obtained either experimentally or thru simulation. It is worth noting that substation can be analyzed separately from a transportation systems, as losses are power-dependent; therefore, efficiency can be measured as a quotient of input and output power.

2.1.2. Electric multiple units

Every transportation system can be divided on infrastructure and rolling stock. In case of suburban railways, the most numerous type of vehicle is an electric multiple unit (EMU). EMUs are characterized by distributed drivetrain – there is no separate locomotive and carriages, but every section of vehicle is accessible for passengers and can have motorized bogies (Fig. 2.3) [26,79]. Motors typically drive single axle each, through single-step gear

train that reduces angular velocity and increases torque to ensure adequate motive force for the vehicle. Rarely, multiple units are equipped with direct drive, as this solution is mostly found in trams, because it allows for the vehicle to be fully low–floor. The advantage of having multiple motors is enhanced reliability – in case of failure, vehicle can continue its run with reduced dynamics [48].

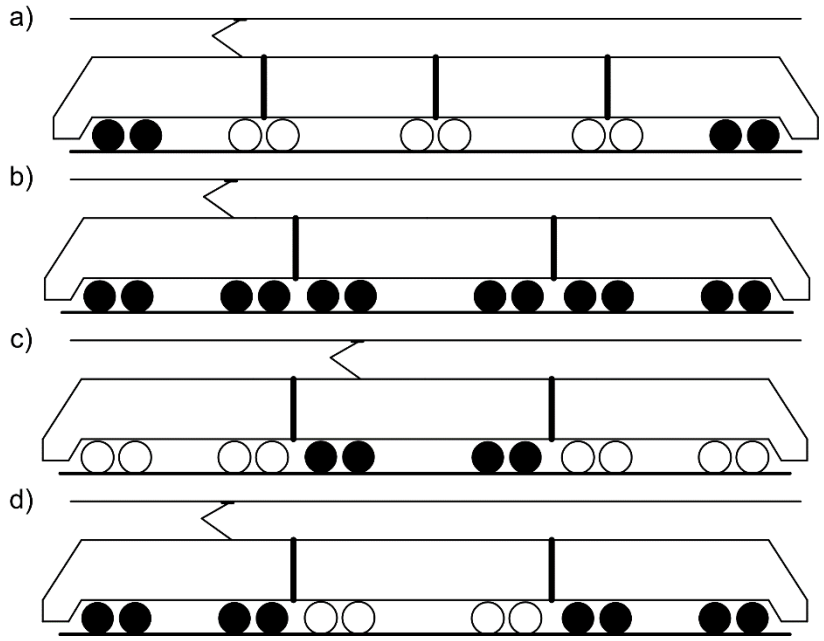

Fig. 2.3. Examples of electric multiple unit drivetrain layouts: a) with motorized front and back bogies; b) all axles powered; c) motorized middle section; d) motorized driving cars

EMUs construction is advantageous for suburban operation – more equal weight distribution than classic train, higher number of powered axles and generally lower weight means more efficient motive force application, and consequently better movement dynamics, because the same motive force is transferred through higher number of wheels [1]. This also reduces value of adhesion coefficient required to retain movement dynamics in bad weather conditions [130]. Lower axle load in relation to locomotives reduces track wear and stress on bridges and switches. Another advantage of having high number of powered axles is the possibility of switching off part of drivetrain while cruising, reducing losses occurring in inverters and motors. Electric multiple units also tend to have lower movement resistance, thanks to lower amount of vehicles in train with comparable number of passenger places and better aerodynamics [113]. Furthermore, some of the rolling stock manufacturers equip their vehicles with Jacobs bogies thus lowering number of axles, which translates to lower rolling and friction resistance. This also reduces mutual movement of carriages, improving passenger comfort.

The drawback of such design is fixed number of carriages in train consist, but that can be mitigated to an extent by coupling multiple vehicles into a single train [147]. This is done easily even at intermediate stations as the vehicles are equipped with automatic couplers. Most of the railway vehicle manufacturers offer their EMUs in variants of length from 1 to 16 carriages, which can be coupled interchangeably for maximum versatility. On the other

hand, because it is possible to forecast passenger numbers, fixed length of trains is a minor issue. Possibility of quick direction change is an advantage too, especially when terminal station has no infrastructure for maneuvers with locomotive. It is worth noting that in most of European EMUs driver cabin placement makes it impossible for passengers or personnel to walk thru the whole length of the train – though, some manufacturers tried to mitigate that by using adaptable cabin with tilt-dashboard and door within the front of the vehicle, with notable example being the Danish/Swedish IC4/X31 operating regional routes, including the Malmö – Copenhagen thru the Øresund Bridge [149]. In other countries, like Japan, most of the suburban EMUs have door built in the front of the vehicle for maximum versatility [74]. Some operators also use EMUs with bi–level carriages for larger passenger capacity, with most prominent being RER in Paris or JR East within Tokyo agglomeration.

For the suburban vehicles top speed is not the most important parameter, and many vehicles are designed for 100 – 120 km/h. However, power is still important as it allows for good movement dynamics (acceleration of around 1 m/s^2 is common) – because of this, vehicles with 6 – 8 carriages (also called sections) have typically 3 – 4 MW of continuous power. Comparison between suburban rail vehicles used worldwide is shown in Table 1.

Table 1. Comparison of selected suburban electric multiple units

Vehicle	35WE Impuls	MI 09	DB-Class 484	3100 series
Manufacturer	Newag	Alstom	Stadler/Siemens	Nippon Sharyo
Operator	SKM Warszawa	RER Paris	S-Bahn Berlin	Keisei Electric Railway (Tokyo)
Vehicle length	6 sections	5 sections*	4 sections	8 sections
Nominal voltage	3000 V DC	1500 V DC 25 kV AC**	800 V DC	1500 V DC
Rated power	3600 kW	3900 kW	1680 kW	3360 kW
Traction drive	Inverter, induction motors	Inverter, induction motors	Inverter, induction motors	Inverter, induction motors
Acceleration	1,1 m/s^2	0,9 m/s^2	1 m/s^2	0,97 m/s^2
Top speed	160 km/h	120 km/h	100 km/h	120 km/h
Pass. capacity	903	2600	398	1042
*Bi-level carriages **Dual voltage vehicle: AC power is used for regional routes, outside the agglomeration				

Because the most energy in electrified transportation system is consumed by vehicles, for both movement and losses, it is justified to use vehicle type that allow for energy savings. Electric multiple units are considered optimal for suburban rail service [44,78,147,163].

2.1.3. Passenger service

Suburban railway transportation systems are characterized by large number of passengers moved at relatively short distances. In Poland, most railway passengers travel within agglomerations, with largest numbers within Warsaw and Tricity [75]. Because such rail service is used to commute to work, school or shopping centers, passenger numbers vary with time of the day and day of the week and are both predictable and measurable [16,135,163,167]. Knowledge about those allow for calculation of timetable that provides both adequate passenger service and is energy–efficient. Possibility of sending shorter train consists outside of rush hours is also a factor in energy saving [4,8,12,28].

Trains often run in regular time intervals called tact [78,161]. Such traffic organization is comfortable for passengers, because not only is the service regular, but allows synchronization between various means of transport as well. It is worth noting, that regular schedule enables improvement of regenerative braking efficiency, because it is easier to synchronize acceleration and braking for vehicles on route for increase of recuperation efficiency [24,108].

There are also similarities between urban rail and high-speed rail, because both systems operate under regular schedule and often on dedicated lines, using electric multiple units as dominant type of rolling stock. The differences are running velocity, distance between stops, and mostly electrification systems [40,151]. The high–speed systems also use signaling systems allowing for full control over vehicle, like ETCS or LZB, which are often absent in local suburban railway systems.

2.2. Determinants of energy consumption

This subsection is focused on determining factors that impact energy consumption. Research papers review provided an insight, which elements of transportation system need the most energy and where do losses come from. Such information is helpful for setting the focus points of energy efficiency analysis.

2.2.1. Electrical drivetrain

Most of energy consumed by the vehicle is consumed by its drivetrain [40,78,90,159]. A part from energy is used for vehicle movement, while the rest is dissipated, mainly in form of heat. Scale of that losses depends on type of electric motors, their power, control strategy and mechanical construction of the vehicle. Therefore, losses approximation is a crucial part of energy efficiency analysis and cannot be neglected. Simplest form of calculating losses in vehicles powertrain is by use of efficiency factors, given by the manufacturers in datasheets [13]. This, however can be inaccurate, as catalogue parameters are specified for steady-state operation, typically under nominal conditions. Traction drives, however, are often working under transient states, with torque load and angular velocity of the motors continuously changing. Because efficiency of traction drive changes

depending on those operating conditions, it has also impact on overall energy consumption of the vehicle and, consequently – on the whole transport network. Therefore, drivetrain of the vehicle should be more accurately analyzed as described in [12,36,38,43].

There are three major drivetrain types used in suburban rail EMUs: DC motors with starting rheostat (installed in older vehicles, continually retired from service), DC motors with pulse voltage controller (DC-DC chopper) and AC motors (mostly squirrel cage induction motors) with variable voltage, variable frequency (VVVF) inverters. There are also vehicles with single–phase AC motor with tap–switching transformer (in AC voltage systems) and unconventional drivetrains like linear motor built along the track or maglevs, mostly built as short airport lines [39,133].

Because rail vehicles are designed to be used for long periods of time, some of the rail operators still use vehicles with DC motors and starting rheostat. For a long time it was the only drivetrain used in DC voltage systems, when there were no power electronics available. Moreover, series–wound DC motors were generally well suited for the early electric traction drives: they have high starting torque, high tolerance for input voltage changes and simple regulation of angular velocity, achievable with electromechanical switchgear [39,72]. The principle of such solution is regulation of motor angular velocity through input voltage regulation, as the angular velocity is directly dependent on voltage as given by:

$$\omega_r = \frac{U - i \cdot R_w}{c \cdot \Phi(i)} \tag{2.1}$$

where: ω_r – angular velocity, U – input voltage, i – motor current, R_w – windings resistance, c – motor constant, $\Phi(i)$ – magnetic flux (current-dependent, because field windings are connected in series with armature).

Angular velocity can also be controlled by changing circuit resistance value and flux of the magnetic field. The former is also resulting in change of input voltage, while the latter is used in the vehicles as it provides additional velocity regulation in steady state. It is worth noting that by increasing of angular velocity, the motor is de-magnetizing itself, leading to further acceleration (current is decreasing as a result of rotational electromotive force increasing along with angular velocity). If series–wound DC motor is working without torque load, it can accelerate till centrifugal force damages it permanently. However, traction motor is loaded by the mass of the vehicle itself, so this risk is reduced in practice.

Voltage regulation is achieved by connecting the motor in series with resistors, which are sequentially switched off, increasing voltage on motor terminals in steps (Fig. 2.4). Switching sequence is determined by position of cams on shaft connected to regulator. The process itself is controlled by the vehicle driver.

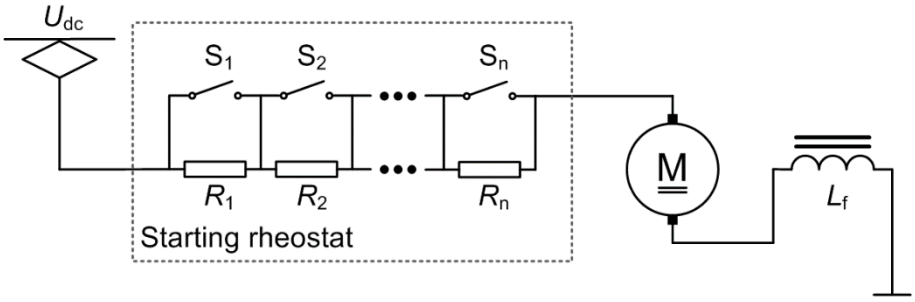

Fig. 2.4. Layout of rheostatic DC drive, where: U_{dc} – dc catenary voltage, $R_1..R_n$ – starting resistors, $S_1..S_n$ – switches bridging resistors, M – dc commutator motor, L_f – field windings

The main criterion for switching off the starting resistor is the current value that should not exceed nominal current value for the vehicle. Therefore, in simplest application rheostatic DC drive is consuming full power, while dissipating energy in resistors [72,133]. In order to reduce losses in vehicles equipped with multiple motors, motor groups switching was introduced – possibility of lowering voltage through connecting motors in series (Fig. 2.5).

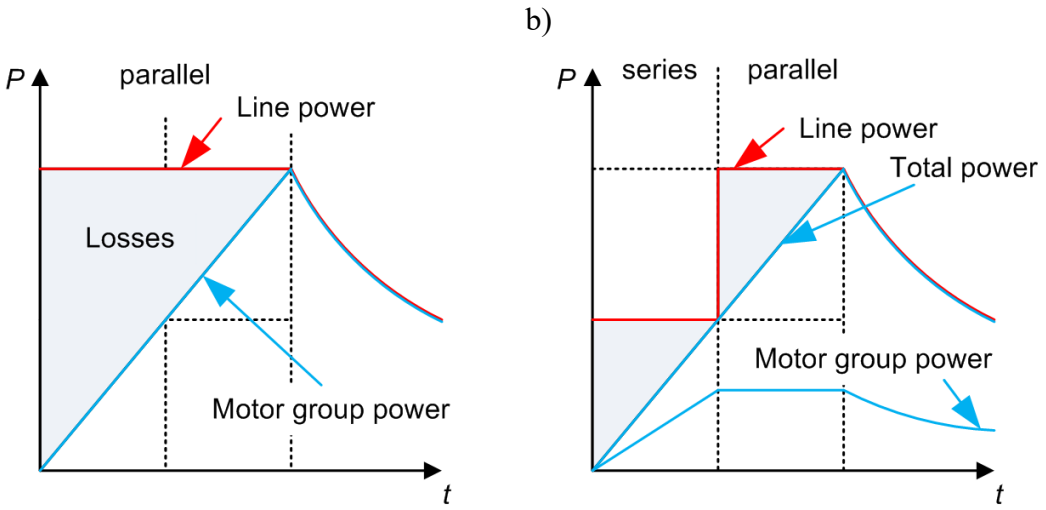

Fig. 2.5. Power and losses in DC rheostatic drive: a) without, b) with motor group switching

Sometimes, vehicles were equipped with automatic regulator, based on electrical relays. Such solution allowed to mitigate jolts (to an extent) while switching resistors, resulting with smoother acceleration. Example of such starter is the PSR (Polish: Przekaźnik Samoczynnego Rozruchu) installed in older EMUs, most numerous in Poland being EN57 class trains [97]. It is worth noting, that running with constant speed is possible only for natural characteristics (with all resistors switched off), with possibility of slight regulation thru/by field control. While electrodynamic braking is achievable, energy recuperation is practically impossible due to lack of precise voltage control. Along with excessive losses during acceleration phase, this make rheostat-based electric drives unfit for suburban railway service.

Significantly better efficiency was achieved through change of rheostatic starter to voltage chopper. This solution is also based on controlling voltage on motor terminals, albeit this

is achieved by regulating duty cycle of semiconductor switch [72]. Nominal voltage is switched on and off, resulting in proportional average value. Because this process is precise, regenerative braking was made possible and losses during acceleration vastly reduced (Fig. 2.6). While such drive is the most efficient energy-wise, there is still energy dissipation in power-electronic switch (GTO thyristor or transistor). Some implementations have also electromechanical switch installed in parallel to the transistor in order to reduce losses when duty cycle approaches 100% [25].

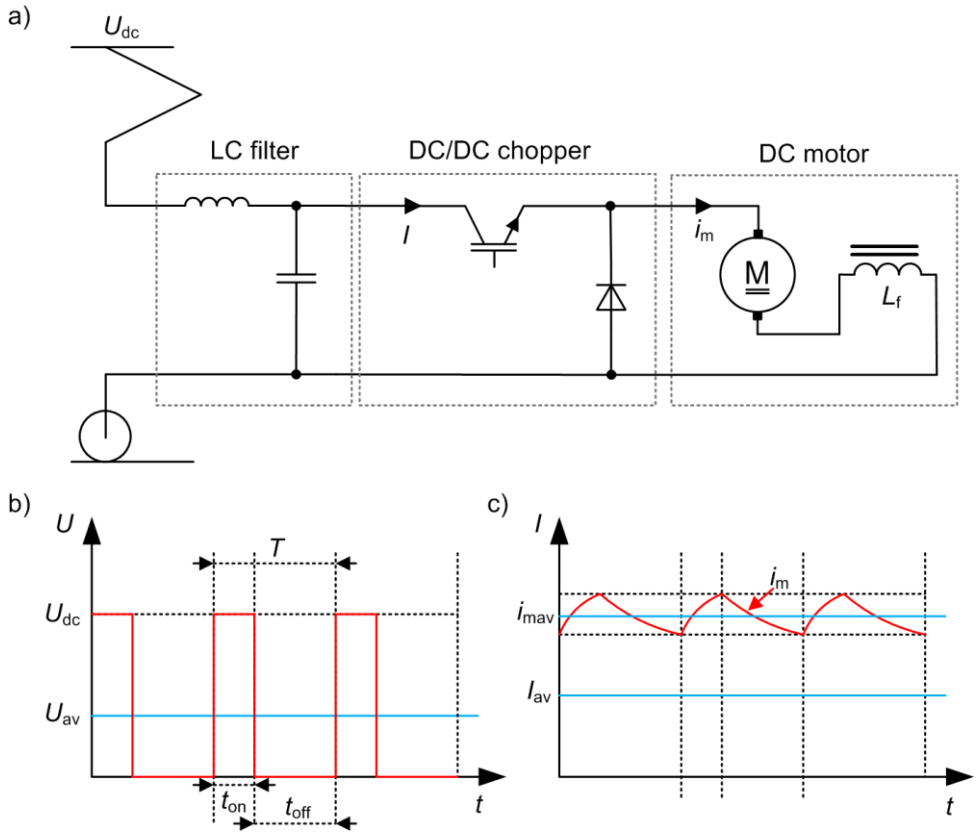

Fig. 2.6. Diagram (a), voltage (b) and current (c) of chopper DC drive

Despite the good efficiency and simple implementation, choppers were never widely used because of higher mass of DC motors and need for regular maintenance (commutator and brushes). Because this solution relies on the power electronics, it was also outpaced by quick implementation of AC induction motor drives in rail vehicles [133]. Currently, only railway vehicles in Poland that utilize this drivetrain are those of 14WE class (rebuilt from EN57 between 2005 and 2007). However, it can still be found in older trams, e.g. Düwag N8C in Gdańsk.

Rapid progress of power electronics allowed for mass production of variable speed drives based on AC induction motors controlled by inverters. In railway vehicles, one inverter is used to control two motors installed in one bogie (Fig. 2.7). Those were better suited for vehicle use, because of lower mass and size, absence of friction elements and lower purchase price [39,90,133]. Inverter drive allow for wide regulation of motor angular velocity and torque, enabling good movement dynamics and regenerative braking.

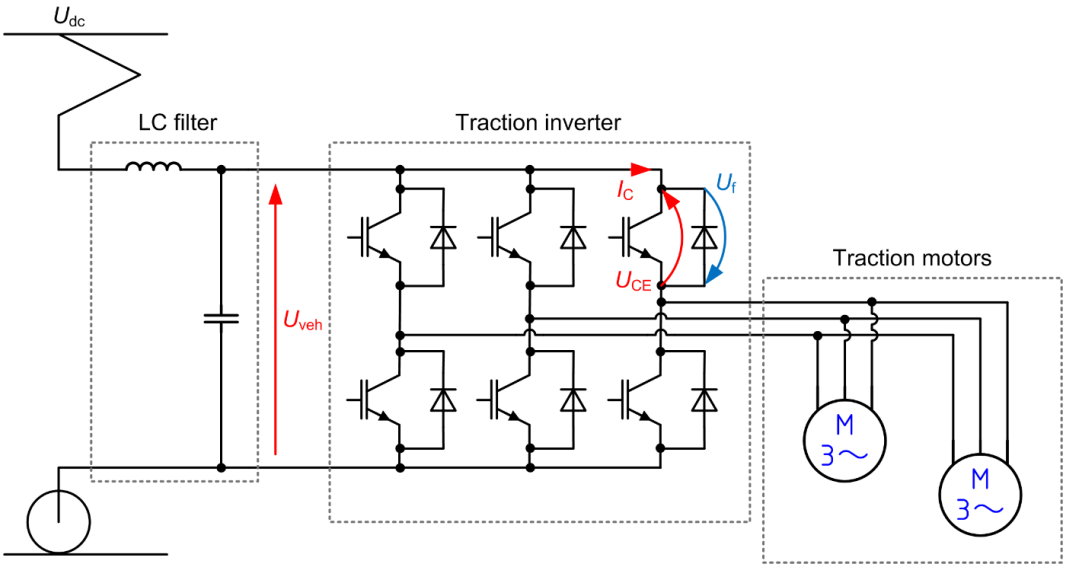

Fig. 2.7. Simplified diagram of induction motor drive

Typically, induction motors were used in industrial drives rotating with constant velocity, fed from public power network. However, vehicles require variable velocity drive, which in this case can be achieved thru changing number of pole pairs, slip value or controlling voltage frequency (2.2).

$$\omega_r = \frac{2 \cdot \pi \cdot f}{p}(1 - s) \tag{2.2}$$

where: ω_r – angular velocity, f – voltage frequency, p – number of pole pairs, s – slip (relative difference between angular velocity of stator rotating magnetic field and angular velocity of rotor).

Pole pair change is implemented in so–called multispeed (or Dahlander) motors, typically found in elevators and historically used by vehicles in polyphase AC systems, found in mountain railroads in Switzerland [39]. Changing slip value can be achieved thru connecting additional resistances into the rotor (done in slip-ring induction motors, used in cranes). Change of input voltage frequency and also voltage value requires use of inverter.

Regulation of voltage frequency requires also regulation of its value, as the magnetic flux must remain constant. Thus, older inverters realized so–called scalar control strategy, where constant relation of U/f was retained. However, at low angular velocity values voltage cannot satisfy the constant voltage to frequency value because of the impact of the winding resistance. Similarly, dynamic braking down to stop cannot be realized as fully regenerative because of too low voltage induced. Because of this, most vehicles require engaging friction brakes below certain threshold, typically around 10 km/h [116]. Accelerating the motor further over the nominal velocity is done thru increasing frequency without increasing voltage – the velocity rises, torque decreases and the generated power is remaining constant, at rated value. This way, the motor can be accelerated until the maximum slip value is achieved. In order to accelerate further, the slip value must be controlled to remain constant thru voltage decrease, resulting in further decrease of generated torque because motor power is also reduced.

Considering requirements of traction drive, ability to precisely control behavior of the motor, under both steady and transient states is required. Currently, inverter drives have vector control strategy implemented, allowing for much better control over the drive, especially in transient states. In order to analyze such drive, adequate models for the motor and inverter are required [2,10,76,152]. The control of the motor is often analyzed within 3-phase or 2-phase reference frame, which can be static or dynamic depending on strategy employed. One of the most commonly used, 2–axes d–q model is particularly useful for analysis of traction drives, as it makes the induction motor model similar to a dc-motor [14,20,48,127]. Consequently, d–axis current is proportional to excitation current and q–axis armature current, which results in simple torque control. This synergizes well with traction drive requirements as the regulator in real vehicle is also designed to control the motive force [3].

Precise modeling of induction motor should include the possibility of analysis of transient states of the machine. For such task, general equations describing induction motor [2,36,91] are used as given by:

$$\mathbf{M}(\varphi)\frac{d}{dt}\mathbf{i} + \frac{\partial}{\partial\varphi}\mathbf{M}(\varphi)\cdot\mathbf{i}\cdot\omega_r + \mathbf{R}(s)\cdot\mathbf{i} = \mathbf{u}(t) \tag{2.3}$$

$$J\cdot\frac{d}{dt}\omega_r - \frac{1}{2}\mathbf{i}^T\frac{\partial\mathbf{M}(\varphi)}{\partial\varphi}\cdot\mathbf{i} + D\cdot\omega_r = T_{ext}(t) \tag{2.4}$$

where: **M** – matrix of inductances, **i** – vector of currents, φ – rotor angle, **R**(s) – matrix of resistances (slip dependent), **u** – vector of voltages, J – moment of inertia, D – moment of resistance, T_{ext} – external torque.

The equation (2.3) describes equivalent electrical circuit of induction motor, and second (2.4) is torque equation.

The model utilizes differential equations enabling calculations of dynamic and static motor behavior. Because linearization of electromagnetic coupling is the only simplification considered, the precision of this method is very high. However, parameters necessary for completing the models are also precise and obtainable only during laboratory test or finite elements method (FEM) calculations, and information about internal geometry of the machine is necessary. The model itself also requires significant computing power, as the size of the matrices depend on the motor structure. Such models are useful in motor design process or in research into possible construction improvements as well as design of energy-efficient control strategies.

There are also simplified models which neglect transient states of the motor [10,38,131]. While they require less parameters and are simpler to implement, such solutions are accurate only for motors operating in steady state, and their use for the transient states would result in errors. Nevertheless, they are sometimes used as the parameters of such model are not time–dependent, so they are still usable even with long timestep.

Popular simplification of the induction motor drive relies on implementing the torque curves with the value dependent on angular velocity $M = f(\omega)$ [40,143,162]. Energy

consumption in this model is approximated using efficiency curves or efficiency maps, which is sufficient for calculation of energy use in the whole transport system.

2.2.2. Losses in drivetrain components

The induction traction motor is the most powerful element of the whole drivetrain, so approximation of its losses is necessary for energy efficiency analysis. Power losses dissipated in the induction machine are:

- losses in windings – the so–called "copper losses",
- losses in the iron core due to eddy-currents and hysteresis effect,
- loss due to friction and ventilation – mechanical losses.

The "cooper losses" can be determined if windings currents and their resistances are known. The winding loss is defined as product of square of the effective current in this winding and winding resistance. Total losses in windings are taken as the sum each winding loss:

$$P_{cu} = P_{cu1} + P_{cu2} = 3I_1^2 R_1 + 3I_2'^2 R_2' \tag{2.5}$$

The total loss in iron core is sum of two components. These components are: eddy–current loss and hysteresis loss [94].

Eddy–current losses are generated in conducting material when it is subjected to a magnetic field varying in time. In the volume of an iron core there are loops of induced currents as stated by Faraday's law. These currents are referred to as eddy–currents. The power dissipated due to eddy-current effect is normally expressed by:

$$K_e V_c f^2 \sigma h^2 B_{max}^2 \tag{2.6}$$

where: K_e is a constant coefficient obtained from suitable experimental data, V_c is the core volume, f is the frequency, σ is the material conductivity, h is the thickness of plate, B_{max} is the maximum value of flux density.

In order to reduce eddy–current losses, the steel cores induction motors are laminated – they consist of assembly of thin steel plates with thickness $h = 0{,}27 \div 0{,}5$ mm.

The hysteresis loss is caused by the magnetic properties of ferromagnetic material. When a ferromagnetic material is under the influence of a periodic, time–dependent magnetic field, an amount of energy proportional to the area of hysteresis loop is dissipated in the material for each cycle of flux variation. The power dissipated due to hysteresis effect is typically expressed by:

$$P_h = K_h V_c f B_{\max}^x \tag{2.7}$$

where: V_c is the core volume, f is the frequency, B_{max} is the maximum value of flux density, K_h is a material dependent constant obtained usually from experimental data. The exponent x is called the Steinmetz exponent and has a range of values from 1,5 to 2,5 for the magnetic steels used in transformers or electrical machines.

Implementing full traction drive model within simulation of transport system operating electrical vehicles might be undesirable, as such simulations focus on vastly different timeframes – for motor or inverter, it is within single seconds to minutes; for the whole system it is hours to days. Because of this, depiction of motor efficiency changing in relation to torque load and angular velocity can be implemented in a form of lookup table, named efficiency map [109]. Such maps are typically calculated using simulation methods: there are finite number of points under torque curve defined, and for each of them simulation of steady–state operation of traction drive is carried out. Results are then saved into the table, allowing for estimation of motor efficiency with sufficient accuracy even within models using longer time step [141,162].

Inverter also dissipates energy – not only during transistor commutation, but due the high power of the traction drives, conduction losses need to be taken into consideration as well [23,122]. It is worth noting, that inverter energy losses are unavoidable, so in some situations, e.g. long run with constant speed, it might be less efficient than DC drive with starting rheostat. There is also need for additional cooling for the inverter. However, inverters have generally high efficiency within their practical power range and there is constant research into possible improvements. For such analyses, digital twin model of the inverter is used, closely depicting the equivalent electrical circuit, with simulation timestep allowing for switching process analysis [23,122].

For the analysis of energy efficiency of the whole transport system, efficiency of the inverter can be also depicted as efficiency map, or considering lower losses variability in relation to the motor, in form of efficiency curve. There is also method allowing for approximation of losses using analytical equations, using parameters from transistor datasheet and taking into account variability of switching frequency with vehicle speed [107,153]. In such case, inverter losses are computed as a sum of switching losses of transistors, reverse–recovery diode losses and conduction losses for both diodes and transistor. The latter need to be included, because typical voltage drop of 1,2 – 2,5 V on semiconductor switch translates to kilowatts of losses.

For the single transistor, as represented in Fig. 2.7, switching losses P_{t_sw} are calculated using:

$$P_{\mathrm{t\_sw}} = \left(\frac{U_{\mathrm{veh}}}{U_{\mathrm{veh\_n}}}\right) \cdot \left(E_{\mathrm{sw\_on}} + E_{\mathrm{sw\_off}}\right) \cdot \left(\frac{f}{\pi}\right) \tag{2.8}$$

where: U_{veh} – voltage of dc bus, U_{veh_n} – nominal voltage of dc bus, E_{sw_on}, E_{sw_off} – energy loss for switching the transistor, f – switching frequency.

Conduction losses for transistor and freewheeling diode are computed as (2.9) and (2.10):

$$P_{\mathrm{t\_cond}} = I_{\mathrm{c}} \cdot U_{\mathrm{CE}} \cdot \left(\frac{1}{8} + \frac{D \cdot \cos\varphi}{3\pi}\right) \tag{2.9}$$

$$P_{\mathrm{d\_cond}} = I_{\mathrm{c}} \cdot U_{\mathrm{f}} \cdot \left(\frac{1}{8} + \frac{D \cdot \cos\varphi}{3\pi}\right) \tag{2.10}$$

where: D is the duty cycle of the corresponding semiconductor switch.

Reverse recovery losses of the freewheeling diode are calculated using (2.11):

$$P_{\mathrm{d\_rec}} = \left(\frac{U_{\mathrm{veh}}}{U_{\mathrm{veh\_n}}}\right) \cdot E_{\mathrm{rec}} \cdot \left(\frac{f}{\pi}\right) \tag{2.11}$$

Because expressions allow to calculate losses for the single transistor and single diode, total power of losses in the inverter are approximated as sum of losses for 6 elements (2.12):

$$P_{\mathrm{inv\_loss}} = 6 \cdot \left(P_{\mathrm{t_{sw}}} + P_{\mathrm{d_{rec}}} + P_{\mathrm{d_{cond}}} + P_{\mathrm{t_{cond}}}\right) \tag{2.12}$$

While accuracy of this method may not be the highest, possible errors introduced are minuscule as general efficiency of inverters lies within 95 – 98%, and is nearly constant within the useful power range [122].

Improvement of efficiency can be achieved by using permanent magnet (PM) motors instead of induction motors [90]. Use of permanent magnets reduce size and weight of the machine, while also reducing because the filed winding is replaced by permanent magnets. To accelerate the motor beyond its base velocity, armature reaction effect is used. The armature current is controlled in such a way that the total magnetic flux inside the air gap is reduced [2,127]. As the excitation field from PMs cannot be switched off, so in case of voltage deficiency or inverter failure, voltage surge will be generated. If fault happens, PM motor will still generate energy powering the short-circuit current, which can cause several damage, with a risk of fire. Using PM motors is also relatively expensive – because of PMs pricing and higher safety requirements for maintenance works. Currently, only rail vehicle equipped with permanent magnet synchronous motors is the high speed multiple unit Alstom AGV. However, PM motors are used on regular basis by automotive industry, as compact size of the motors allow for in–wheel direct drive, without need for mechanical geartrain [121].

Between the motors and wheels there are often mechanical gearboxes installed. While they also dissipate energy because due to friction, their efficiency is also variable and depends on type of gearbox used. Most rail vehicles utilize single step velocity reducer, which is characterized by higher losses at low speed [150]. Values of efficiency curve of the mechanical gears can be measured thru laboratory test or using simulation methods. However, in vehicle simulations the mechanical efficiency factor is typically assumed at constant value (between 85% and 95%, depending on transmission type), because variability is relatively small and takes place only during few percent of the time, while vehicle is moving at low speed. However, this dependency is relatively simple to implement in model, as dependence of gearbox efficiency on vehicle velocity.

Use of alternative traction drives such as linear motors does not provide improvement of energy efficiency [133]. Most of such solutions have lower rated efficiency than rotating machines because of significantly larger air gap (up to 1 cm), and they rely on feeding inverter controlled current through long windings installed along the track. Similarly, maglevs are less efficient within velocities typical for suburban railway because of additional energy required for levitating the vehicle.

2.2.3. Auxiliary systems

Vehicle energy efficiency analyses often disregard auxiliary needs of vehicle, focusing only on energy consumption of the drive itself. It is, however a part of energy that is used by the vehicle while not being directly responsible for its movement. Some of those systems are mandatory for vehicle to move, while others serve improving passenger comfort.

Motive force that allow for train movement is generated by the traction motors. While it can be reversed decelerating the vehicle, it is not possible to stop without injecting additional energy at low speeds or using friction brakes. Similarly, electrodynamic braking force at higher speeds would not be able to effectively slow down the vehicle. Friction brakes, however are powered by the pneumatic system that need compressed air – so the adequately powerful compressor is needed. The air compressor, however does not work constantly – it is switched on only when pressure within braking reservoir falls below set threshold. The frequency of compressor work is determined by the route profile and driver behavior. Use of dynamic braking reduces the compressor working time [98].

There are also systems responsible for traction drive control and cooperation with trackside signaling that need power to work. Those are operating all the time, however their power is within few kilowatts, so their impact on overall consumption is minuscule. Similarly, energy is supplied constantly to passenger information system screens and, depending on time of the day and weather – to lighting. This also can be assumed constant, and the power is typically within few kilowatts [27].

Passenger vehicles also require power for systems ensuring comfort, like heating, ventilation and air conditioning (HVAC), which can consume amount of energy comparable to traction drive (depending on conditions). It should be noted that energy consumption by the auxiliary systems, especially heating and climate control is a subject of ongoing research in itself, aiming at improvement of its efficiency and its impact on regenerative braking [54,106]. To be able to approximate when those systems are active, researchers build thermal models of the vehicles, implementing their geometry, passenger numbers and air circulation, which allows them for computing temperature changes within the vehicle and CO2 concentration, as those are parameters used by HVAC controllers. Many of these models use computational fluid dynamics (CFD) as their basis, so they are unfit for implementation in comprehensive model of transportation system, used for energy efficiency calculations [83].

Energy consumption caused by auxiliary needs is not negligible, it should be taken into consideration. Not only could it affect total energy consumption, but values of line voltage and even regenerative braking efficiency as well. Value of auxiliary power is also hard to specify – because auxiliary converters normally do not work under full load. While about 20% of vehicle's energy consumption tend to be accepted value in calculations [161], accuracy of such statement is questionable as it would impact not only the consumed energy figure but values of voltages, currents and regeneration as well. It would be the best to actually measure power of auxiliaries during vehicle run and make assumptions. If such measurements are not available, the power of auxiliaries can be averaged.

2.2.4. Energy storages

Electrified suburban railway networks often operate large number of trains at the same time. Because all of the modern EMUs use regenerative braking, there is a risk that multiple vehicles start braking simultaneously. Alternatively, they can accelerate at the same time causing overload. Both situations are undesirable, as they lead to excessive losses and voltage fluctuations. This can be a significant problem if transport network uses timetable created without considering regenerative braking or if tact is irregular.

In such situation, installation of energy storage might be worthwhile. Trackside storage can be installed in substation or in place on route, where simultaneous braking/accelerating occur [66]. Alternatively, there is possibility of equipping the vehicle with onboard storage, which on top of absorbing recuperated energy might also enable movement outside of power supply system (widely used in trolleybuses). Well–designed energy storage significantly improves efficiency of regenerative braking while reducing losses in catenary and voltage fluctuations [121].

Because regenerative braking yield large amount of energy sent into the power supply in short period of time, trackside storage should be built using technology that allow high enough currents to absorb this energy. There is, however, no need to store the energy for long period of time, so using supercapacitors or kinetic storages can be adequate [115]. On the other hand, trackside storage may be a part of a smart grid system, allowing not only for improvement of regeneration efficiency, but supply energy for other use (e.g. EV charger) as well [37].

Supercapacitors' key advantage is the possibility of very fast charge and discharge. They are also more reliable and have longer lifespan than electrochemical batteries, while their capacity is much less dependent on temperature. On the other hand, their voltage decreases linearly during discharge, so some of the stored energy cannot be used. They also require DC/DC converter and are relatively expensive [11].

Kinetic energy storages, much like supercapacitors can quickly store energy. However, their capacity is relatively low and losses are quite high (due to mechanical resistance) [99]. They also require energy converter and electric motor coupled with the flywheel. Therefore, efficiency of kinetic storages in trackside application seems questionable,

especially considering relatively high cost of investment. On the other hand, there is possibility of coupling such storage directly with mechanical gear, allowing for operation with any type of drivetrain (including combustion engines) and improving braking efficiency, however it is possible only with onboard application. Such devices currently see automotive applications, in both regular automobiles (start–stop systems) and racecars (MGU–K in Formula 1 vehicles).

Battery storages are limited by maximal values of charge and discharge current which are of importance when absorbing regenerative braking energy is considered. However, their capacity is high and voltage during discharge is stable. They can also store energy for a longer time than capacitors or flywheels. On the other hand, deep discharge may permanently damage the battery, and capacity is dependent on value of charging or discharging current as well as weather conditions.

Hybrid storages are designed to combine advantages of battery and supercapacitors while minimizing their drawbacks – limitation of maximum charge/discharge current in battery and relatively small energy capacity of supercapacitors. It can also improve battery longevity reducing frequency of charging cycles.

In this approach, the battery is buffered by the supercapacitors that absorb regenerative braking energy and then provide additional power during acceleration. Battery is powering the vehicle during acceleration and cruising while being energy source for auxiliary needs [41,121]. Such design allows for decrease size and weight of onboard storage while providing the vehicle with adequate power and retaining designed capacity.

Use of every type of energy storage might be viable depending on its application requirements, therefore knowledge of their characteristics is crucial for optimal design of such device. Major characteristics of currently used solutions were compared in Tab. 2.

Table 2. Comparison of energy storage types

Parameter	**Electrochemical (battery, Li-ion)**	**Supercapacitor**	**Kinetic storage (flywheel)**
Source type	Voltage source	Current source (converter required)	Electrical / kinematic energy source
Specific energy	Up to 200 Wh/kg	Up to 15 Wh/kg	Up to 5 Wh/kg
Specific power	1-3 kW/kg	10 kW/kg	Up to 5 kW/kg
Charge/discharge time	hours	seconds	Seconds to minutes
Discharge efficiency	Up to 98%	Up to 98%	Up to 80%
Lifetime	Up to 1000 cycles	Up to 1 M cycles	Over 1 M cycles

Currently, independently powered vehicles (BEMU, IPEMU) are seeing rise in popularity, replacing diesel multiple units on partially unelectrified routes. Those vehicles are designed to run under catenary normally while recharging their energy storages at the same time [64]. Some vehicle are also equipped with battery allowing for reduced dynamics run in

order to move out of tunnel or damaged section in case of catenary failure. Such solution was implemented in new N700S series Shinkansen high speed train [139].

2.2.5. Driving technique

Energy consumption in suburban railway system depend not only on physical objects, like infrastructure and rolling stock, but on driving technique as well. The timetable specifies travel time between stations, while maximal velocity is limited by the infrastructure [75]. The method of executing that schedule, however depends on the driver's knowledge about energy-efficient driving and route geometry.

Train movement on route can be described using four basic phases:

- acceleration – motive force F is greater than resistance force W,
- cruising – motive force F is counteracting the resistance force W,
- coasting – motive force F equals zero,
- braking – motive force is negative, and vehicle is decelerating.

Combinations of those constitute for velocity profiles [42,72,151]. Example of simplified velocity profile consisting of all the described movement phases is shown in Fig. 2.9. Velocity profiles can contain multiple movement phase changes, depending on the speed limits on the route and traffic situation. Those changes might be defined in relation to route location, being denoted as $x_1 \ldots x_n$, depending on how many there are.

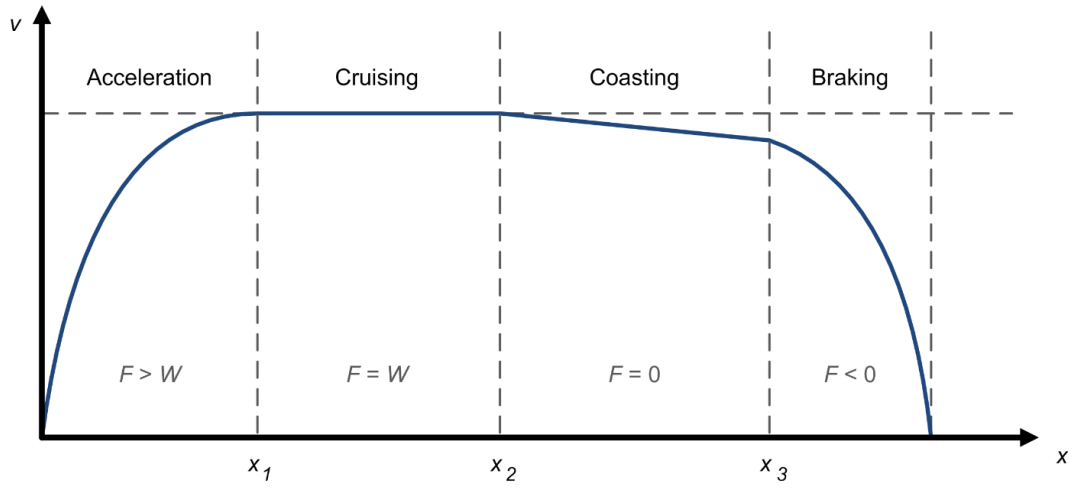

Fig. 2.9. Movement phases of rail vehicle

During acceleration, motive force is higher than motion resistance. Generally, it is desirable to accelerate with maximum available force, because of shorter time of maximum power usage and better overall efficiency, as the drive is working under full load. However, risk of wheel slip and passenger comfort must be taken into account. Typical maximal value of acceleration varies between 0,8 and 1,2 m/s^2 in case of suburban trains and up to 1,5 in subway, tram and trolleybus systems [13,116,138]. Acceleration value might also be reduced by vehicle current limitation or power limit engaged with low catenary voltage.

Cruising phase is also called constant velocity phase. To achieve that, motive force must be equal to motion resistance – and it can be positive or negative (when running downhill). While modern traction drives allow cruising with set velocity, it is not efficient to do so, because unless running at high speed or uphill, traction drive works under low load. On the other hand, cruising through downhill parts of the route might result in slight energy recuperation, which is clearly better than use of friction brakes. Also, covering some distance with set speed instead of coasting and accelerating again might be more efficient, depending on velocity and route profile [28,138,143].

Coasting means running with zero motive force – vehicle is slightly decelerating or accelerating depending on motion resistance and route inclination. It is often considered as fundamental part of energy efficient driving style and used widely instead of cruising, because traction drive needs no power to generate motive force [44,72]. Currently, coasting is sometimes replaced by slight regenerative braking, where deceleration is only marginally higher, but regenerative braking energy allows to mitigate auxiliary demands of the vehicle and cover traction drive losses.

Braking is a process of slowing vehicle down, to speed limit or to stop. While modern electric vehicles allow for regenerative braking, combined brake systems with pneumatic friction brakes are mostly used [110,160]. Fully electric braking is also considered [68], but meeting the requirements of deceleration distance is a major problem (because of maximum power of motors, there is relatively low motive force available at higher speeds). Deceleration should also take into account passenger comfort and wheel adhesion, which further promotes combined braking as most of the vehicles do not have all axles motorized.

There are also alternative methods of slowing the vehicle down – namely the eddy current brake and aerodynamic brakes. Eddy current brake is typically installed in vehicles designed for high speed service, as an additional emergency brake. It consists of electromagnets installed typically below the bogies, close to rails; they are powered by the energy provided by regenerative braking, inducing eddy currents in rails, which causes counteracting magnetic field that slows down the vehicle. However, electromagnetic disturbances from this kind of braking were deemed as undesirable for signaling system and telecommunication networks. Additional dynamic forces and thermal exposure are proved to negatively impact rail infrastructure, reducing its durability – so usage of eddy current brake under normal operating conditions is avoided. There is also an ongoing research focused on improvement of electromagnetic brakes, where authors claimed reduction of environmental impact of bogie-installed electromagnets. In principle, this solution is analogous to typical eddy–current brake, however it is powered by regenerative braking current and acts as additional braking system, improving recuperation efficiency and reducing friction brakes wear [123].

Calculation of train braking distance is required for any transportation system model. In real systems, braking distances are approximated in relation to vehicle speed, its mass, route grade and allowed deceleration value. Some methods introduce reaction time of the driver or delay between moving the brake handle and brakes application [53]. Because of necessity of ensuring safe operation, such measures are needed, however, in energy

efficiency analyses such details are often either absent or implemented differently. Moreover, precise modeling of pneumatic system of the train is skipped as it has little impact on consumed energy, being rather a vehicle design problem.

Analysis of velocity profile and its impact on energy efficiency is continuously studied from 1960s, with Ishikawa's work considered to be the first publication on the subject [56]. First works defined criterions allowing for evaluation of velocity profile, concluding that optimally, vehicle should accelerate with full motive force, then coast and brake to stop. However, only DC drives with starting rheostat were in use back then in DC systems, so possibilities of speed regulation were limited. Currently, optimization algorithms are developed in order to compute the most efficient velocity profile within route and timetable constraints [9,0,42,44,78,86,161]. Many of the works focus on the algorithm itself, without considering its practical applicability, therefore not all of them are possible to implement as they require very precise velocity regulation, achievable only thru automated train operation [125,128,159]. This should not be however considered as the only option, because energy savings between 10–15% can be achieved thru relatively simple calculation of movement phase change location. It is worth mentioning that optimized timetables and velocity profiles are used in suburban railway systems worldwide: in Hamburg, S–Bahn network operates within optimized schedule, using optimal velocity profiles, with ETCS-based ATO implementation being planned for the near future [46]. It is safe to assume that some degree of optimization will be introduced to most electrified transport networks because of rapidly rising prices of electrical energy and pressure for greenhouse gases emission reduction in transportation.

There are also alternative methods of lowering energy consumption in electrified transport systems – using either vehicle construction or power supply system. The first option is considered mostly from the manufacturers standpoint, with solutions like vehicle mass or movement resistance reduction [90,102,113]. Even simpler energy saving method was proposed by Tseng et al. [147], where decoupling part of the units from train outside peak hours was discussed. Interesting and nearly zero-cost is the second option – regulation of idle substation voltage thru tap switching transformer. As the braking energy regeneration is voltage-dependent, lowering line voltage might increase regeneration efficiency. On the other hand, it can lead to higher losses and potential voltage dips, so it should be implemented with caution. Similar operation can be done with changing voltage levels in regenerative braking controller [85].

2.3. Existing simulation models

Simplest analyses of energy efficiency of electrified transport networks are conducted using empirical equations, parameters of which are determined based on vehicles power, timetable and speed limit. However, no information about vehicle movement is analyzed and thus, actual values of current and possible regenerative braking efficiency are unobtainable. Because of this, conducting simulations is preferable [72].

Basic models used for vehicle simulation often disregard many parameters, assuming constant values of line voltage or efficiency factors. Such models are very easy to implement and, because of simplifications, their versatility is very high. However, they provide very limited information about vehicle, which is simplified to current source with value dependent on mechanical power. Programs like that are therefore best suited for educational needs (explicit movement equation), basic timetabling or general efficiency evaluation, where accurate calculation of vehicle dynamics and energy efficiency is not the focus point [134].

Where the vehicles are considered, multiple types of models exist: for simulating mechanical structure of the vehicle (including its impact on tracks and infrastructure) and precise electric drive models. First group use either chain of mechanical actuators [2,57] or multibody models [145,154] for either parts of vehicle or the carriage as a whole. This allows for calculating construction strength, specifying geometry and materials of analyzed parts or interaction of vehicle and railway infrastructure. Depending on number of considered parameters, those models can provide very good results, being of value for vehicle and infrastructure design. However, implementation of complex mechanical model of every vehicle within general energy efficiency model is rarely done, as possible accuracy improvement would be minuscule or even offset by stacked numerical errors. Analogically, precise traction drive models are used for testing control strategy or determining required parameters of the inverter, but in analysis considering hours of operation of multiple vehicles implementation of full drive model is not advisable and is usually not implemented, because of required time step discrepancy [36,43,65]. Consequently, considering traction drive losses in models is currently done thru efficiency curves or efficiency maps. Only when calculating behavior of traction drive under realistic conditions is needed, run of single vehicle thru short route fragment is conducted [3,10,65,80,81,156].

Because of rising interest in electrified transport, need for energy savings arose. Seeking for efficiency improvement forced progress in simulation methods – there was need to take into account power supply system architecture and evaluate losses in transport network in order to develop improvements. Therefore, models allowing for line voltage and mean useful voltage were developed. Introduction of simulating multiple vehicles running within analyzed route was required. Some of them assume single vehicle movement and then calculate global values of substation currents and line voltages thru superposition. However, such method is computing parameters in fixed distance steps, so its accuracy is limited. Computation performance is an issue too [8,28,164].

The most advanced models calculate the whole analyzed system at once [47,66,140,143,144,159,162]. While it can provide most accurate results, getting closest to realistic operating conditions, overall complexity of model can cause problems. The major issues that may arise are solver stability and computation performance due to multiple algebraic loops. Because of that, such detailed analyses are often limited to single line or power section, with limited (constant) number of vehicles. Some of those also use fixed distance step and store parameters in single, global matrix [5,129]. There are also solutions that employ two separate models working together – one conducts simulation of vehicles

movement, while the second synthetizes and calculates electrical circuit. This structure allows to solve layout limitation, as the electrical circuit is derived for every time step of the simulation, however it requires two coupled programs running at the same time [69]. The most notable example of such system is the commercial software *OpenPowerNet*, that combines motion dynamics simulator and timetabling tool *OpenTrack* with electric power supply simulator [104]. Mechanism of this interconnection have not been described clearly, so it is hard to determine if, and to what extent line voltage impacts the vehicle performance.

Some of the simulation software come equipped with tools for analysis of electromagnetic compatibility and stray currents [30]. Such solutions take into account catenary construction (spatial location of wires), rail-to-ground resistance and cross connections between rail tracks. It should be mentioned, however that obtained results are of quantitative value and can be used for improvement of reliability, not energy efficiency in itself.

Other common commercial software, used by both railway operators and vehicle manufacturers is the *Dynamis*. It has been developed mostly in order to enhance timetable planning process, being equipped with tools to do so. While mechanical calculations are generally accepted as credible – verified thru measurements, there are not enough information to determine energy computations accuracy [32,114]. It can be assumed that results of energy consumption are of statistical value, because structure of power supply is simplified into constant voltage value and vehicle model need only basic parameters to run. Moreover, commercial software does not provide insight in internal program structure as their source code is a property of the developers, and any improvement or possible custom functionality extensions might be limited.

Despite the existence of commercial vehicle simulators, many analyses are carried out using models developed by the researchers precisely for the considered problem [5,40,147,151,164]. This is because many researchers came up with solutions on their own, which can be more advanced than their commercial counterparts as there is no need to care about versatility and user–friendliness. Moreover, knowledge of source code allows for flexibility in modifications, without license restraints. Literature review revealed that many research institutions worldwide conduct energy efficiency analyses of transport systems using their own software. In Poland, there are also models developed for electrified transportation networks simulations. Significant achievements in this matter belong to the Warsaw University of Technology, where models for both railway and urban transport systems (including subway) were developed [29,67,115,136,137]. Gdańsk University of Technology also conducted research in this matter, focused on detailed vehicles modeling as well as multi–vehicle transport network simulation [12,65,69] Therefore, availability of ready-made software should not be considered as final word of vehicle run simulations (Tab. 3).

Table 3. Comparison of selected simulation software

	Dynamis	**OpenPower Net**	**Tian et al.**	**Frilli et al.**	**Szeląg et al. (WUT)**
Base program	Stand-alone application (Windows)	OpenTrack addon (Windows)	Stand-alone application (Windows)	Matlab/Simulink/ Simscape	Stand-alone application (Windows)
Type	Commercial software		Research		
Multi-vehicle	No	Yes	Yes	Yes	Yes
Complex layout	N/A	Yes	Not specified*	No	Not specified*
Power supply	U = const.	DC, AC	DC	DC	DC,AC
Method	N/A	Nodal voltages		Superposition	Nodal voltages/mesh currents**
Timestep	0,5 - 1 s fixed	0,5 – 1 s fixed	1 s fixed	5 s fixed	0,5 – 2 s fixed
Velocity profile	Pre-set	Pre-set, signals considered	Pre-set	Pre-set	Pre-set
Multisystem	N/A	No	No	No	Yes
Impact of traffic	N/A	Signals only	No	No	No
Vehicle mass	Constant	Constant	Constant	Constant	Constant
Efficiency	Constant	Constant, variable /curve	Variable/map	Variable/map	Variable/curve
Movement control	Switch	Switch	Switch	PI controller	Switch
Schedule	Timetabling tool	Timetabling tool included	Rigid	Rigid	Rigid
Drive model	No, $F = f(v)$	No, $F = f(v)$	No, $F = f(v)$	No, $F = f(v)$	No, $F = f(v)$
Non-electrified routes	Yes	Yes	No	No	No
Energy storages	No	Yes	Yes	No	Yes
Losses calculation	No	Yes (power supply)	Yes (power supply)	No	Yes (power supply)

*Research papers described particular implementation of the model, not its full features
**There are multiple versions of the model, with varying features

2.4. Summary of literature review

Overview of the subject matter of suburban railway systems efficiency shows that determination of losses and reducing energy consumption is of importance, both economically and ecologically. Seeking improvement is mostly done thru computer simulations, which allow for evaluation of energy efficiency of analyzed vehicle or its influence on power supply before entering the service. Credibility of obtained data, however is highly dependent on quality of used model and factors considered by its developer. Many of the existing software use over–simplified models or do not disclose all the information needed for detailed analysis. Some of the simplifications occur consistently within most of the research papers, and are justified (e.g. traction drive represented by motive force curve $F = f(v)$ and efficiency factors). However, including some degree of variability (changing mass depending on passenger flow, multiple possible velocity profiles) could improve accuracy of obtained results, as such data is obtainable thru measurement. Despite the availability of the commercial software, research is typically conducted basing on self–developed models because of license limitations or better suitability for task.

Seeing room for possible improvements in computer simulation methods used in suburban railway energy efficiency evaluation, author decided to develop novel models, which can offer improvements over existing solutions, especially when versatility is considered. While the software should provide consensus between complexity and robustness of the model, author argues that implementation of advanced digital twin of every part of the vehicle should still be possible; therefore implementation of modular structure is desirable. Moreover, the well-designed model needs to be easily modified and updated, so utilization of adequate programming environment is required. Similarly, the model should not be limited by its solver as the future extensions may require modification of time step without loss of accuracy.

In order to show possibilities created by multi-criterial analysis, implementation of optimizing algorithms was considered. Because suburban railway networks operate mostly on separated infrastructure, with regular time intervals energy efficiency improvement thru velocity profile forming and timetable planning is possible. With installation of advanced traffic control systems (ERTMS/ETCS), obtained data might be useful for fully automatic train operation system (ATO), however it should still be implementable even without such measures, as those are rarely found in suburban railway systems.

3. GENERAL DESIGN OF TRANSPORT SYSTEM MODEL

3.1. Programming environment

Implementation of transport system model using certain programming environment requires knowledge about its features. There is a wide selection of tools that can be used, however this also translates into usage of specified programming languages. While all the environments allow to achieve very similar results, some of them offer additional tools or addons that makes implementation of transportations system model easier and simulation more efficient. It is worth noting that most of the commercial simulation programs were developed in C++ or C# (Microsoft Visual Studio), which allow them to run on any machine with Microsoft Windows operating system (OS) installed. Some of the programs, however, use dedicated mathematical simulation software, like Matlab, Saber, PSpice etc. as those have better tools for simulations and data analysis while also being popular worldwide.

Author decided to use the Matlab/Simulink software as a basis for model development. This programming environment is widely used by both researchers and industry, offering numerous tools for mathematical analysis, data handling, optimization and simulation of physical systems [89]. Because of that, compatibility of developed models is improved as they can be used on computer with any operating system. It is, however, worth noting that Matlab relies mostly on its own programming language, which is used for implementing functions and programs (scripts). Those can be executed without relying on external compiler, but there are differences in syntax in relation to e.g. C++.

In order to run the simulation, the adequate numerical solver must be used. Standard programming environments require user to implement solver manually, which is a challenge in itself, considering required compromise between accuracy and computation performance. In case of Matlab, there are multiple solvers already implemented, allowing to choose the best suited one. The solver can be set up with multiple parameters – length of the timestep, tolerances or number of iterations. For this application, author chosen the fixed-step solver, as in transportation systems values are continuously variable. Because such a complex model require compromise between robustness and precision, the ode3 solver was selected. The solver, proposed by P. Bogacki and L. Shampine, is a variant of the Runge–Kutta method [82]. It is worth noting that the model can be built so it retains its stability regardless the timestep value (within practical bounds).

Using programming environment also requires to keep in mind its limitations. Because this analysis widely employs matrices for both calculations and data handling, the most notable shortcoming is the lack of dynamic matrix (array) sizing – the size needs to be specified before executing the model and must remain constant during the simulation. On the other hand, determination of matrix size as a constant improves calculation performance. Consequently, width of block input and output ports must also be constant and specified inside the block. Moreover, the arrays containing different data types, e.g. integer and character type variables are not supported by the Simulink. While there is a solution to problems stated above in form of the cell arrays, they are not supported by the Simulink,

so their use would require to employ extrinsic coder – command that send the simulation data to Matlab workspace in order to carry out outside of Simulink. This, however, negatively impacts computation performance; therefore it is not advisable to use within complex models. Similarly, there are functions that allow the script to interact with the running simulation, but those also slow down the process.

3.2. Proposed structure and data handling

Analysis of electrified transportation system requires model that allow for simulating operation of multiple vehicles at the same time. Those vehicles, however, can be of different types, following different routes; time intervals can also differ depending on time of the day. In case of transportation systems equipped with DC power supply, analysis of separated route fragment might be inaccurate, because of possibility of powering section from two sides or lines branching off, which requires inclusion of their load in calculations.

Because of this, the model needs to be designed in such a way to enable flexibility of its subsystems while binding them together to calculate electrical circuit of the power supply system accurately. Typical solution to this problem, where motion dynamics calculation and electrical circuit calculation are conducted separately is complicated and require cooperation of two programs, one for vehicle movement dynamics and another for electrical calculations. Other possibility is the model where there is fixed electrical circuit for the power supply – but this on the other hand can be problematic for simulating variable service tact during the day and implementation of branches considerably increase the size of the parameter matrix. Also, such matrix needs to be prepared in advance, and is not reusable for other analyses.

Therefore, author decided to propose original approach to simulating electrified transportation systems that can offer improvement of model versatility and computation performance over existing solutions without losing reliability. The general model structure is inspired by industrial communication networks, where the devices are connected to the data bus [105,158]. The information between the devices is exchanged using so–called data frames that contain sender identifier, address of recipient and encoded information. Thanks to this, every device can communicate with all the others; adding more vehicles or power supply sections requires only to connect them to the bus and configure their address.

Implementation of this structure in the model means that both vehicles and power supply sections are separate subsystems with no direct connections between them. All of the data, parameters and results are handled using unique identifiers, allowing for highly flexible structure of the simulated transportation network. This also means that the only effective limitation for the route configuration and number of vehicles is the available computing power. Constant connections exist only between models of substations and power supply sections as those are not expected to change within the simulation timeframe. Simplified diagram of the proposed model is shown in Fig. 3.1.

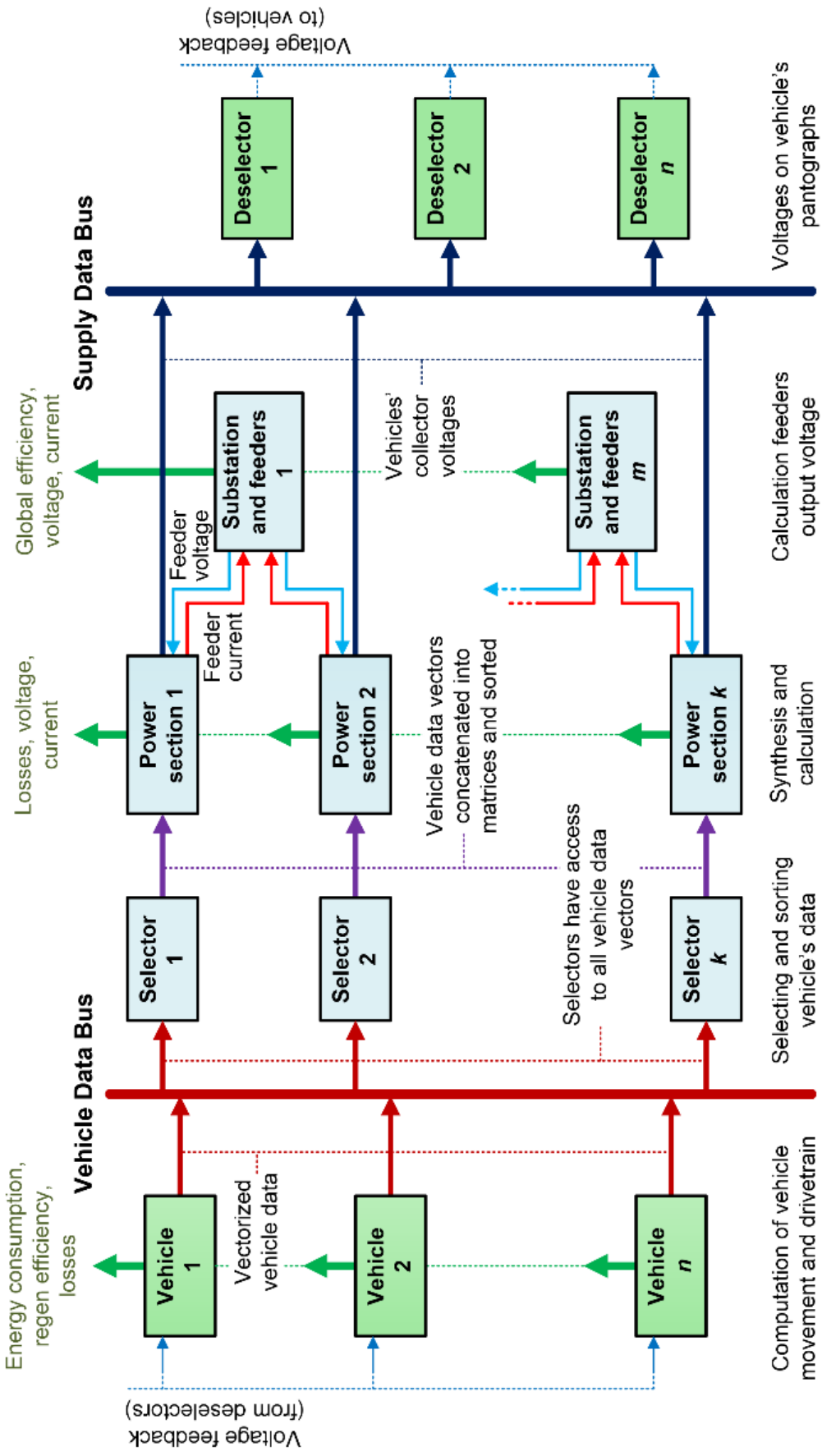

Fig. 3.1. General structure of developed model [62]

Data from vehicle models is grouped into vectors which are broadcasted into the *Vehicle Data Bus* (VDB). Those vectors are analogous to data frames found in industrial networks, but as numerical data, they are all delivered simultaneously, within one timestep of the simulation. Information sent to the VDB is intended for power supply section models, which receive data vectors using *Selectors*. *Selectors* are introduced in order to extract the data of the vehicles within corresponding section at given time from VDB and prepare them for further calculations. Vehicle data is fed to power supply section model, which calculates electrical parameters, interacting with models of substations through physical connection. Results of computation carried out within power section models are then broadcasted into the Supply Data Bus, where they are accessible for vehicle subsystems. Similarly to power supply section models, vehicles obtain their data through *Deselectors* – algorithms that isolate data corresponding to a particular vehicle, completing the feedback loop. It is worth noting that both vehicles and sections have their unique identifiers, so in case of line branching off in the middle of power supply section, the branch section can programmatically act as both power supply and a vehicle, with fixed location within one section.

Author decided to implement two data buses instead of using one because of computation performance – the model runs considerably faster this way. This is also reasoning between Selectors and Deselectors, as executing multiple simple algorithms is faster than using one complex one instead. Moreover, editing the source code is significantly easier for possible future updates.

Flexibility of proposed model stemming from modular structure and information exchange using data buses allows for comprehensive analysis of transportation systems. Implementation of traction power supply sections as subsystems opens a possibility for simulation of virtually any power supply layout, including branches and loops as all the data is processed locally – transport system model can be synthesized thru connecting adequate blocks. This also means that with sufficient parametrization, the model can be used as a basis for universal software, similar to commercial programs currently available. More detailed insight in the model operation is shown in Fig. 3.2, depicting interaction between single vehicle and power supply section.

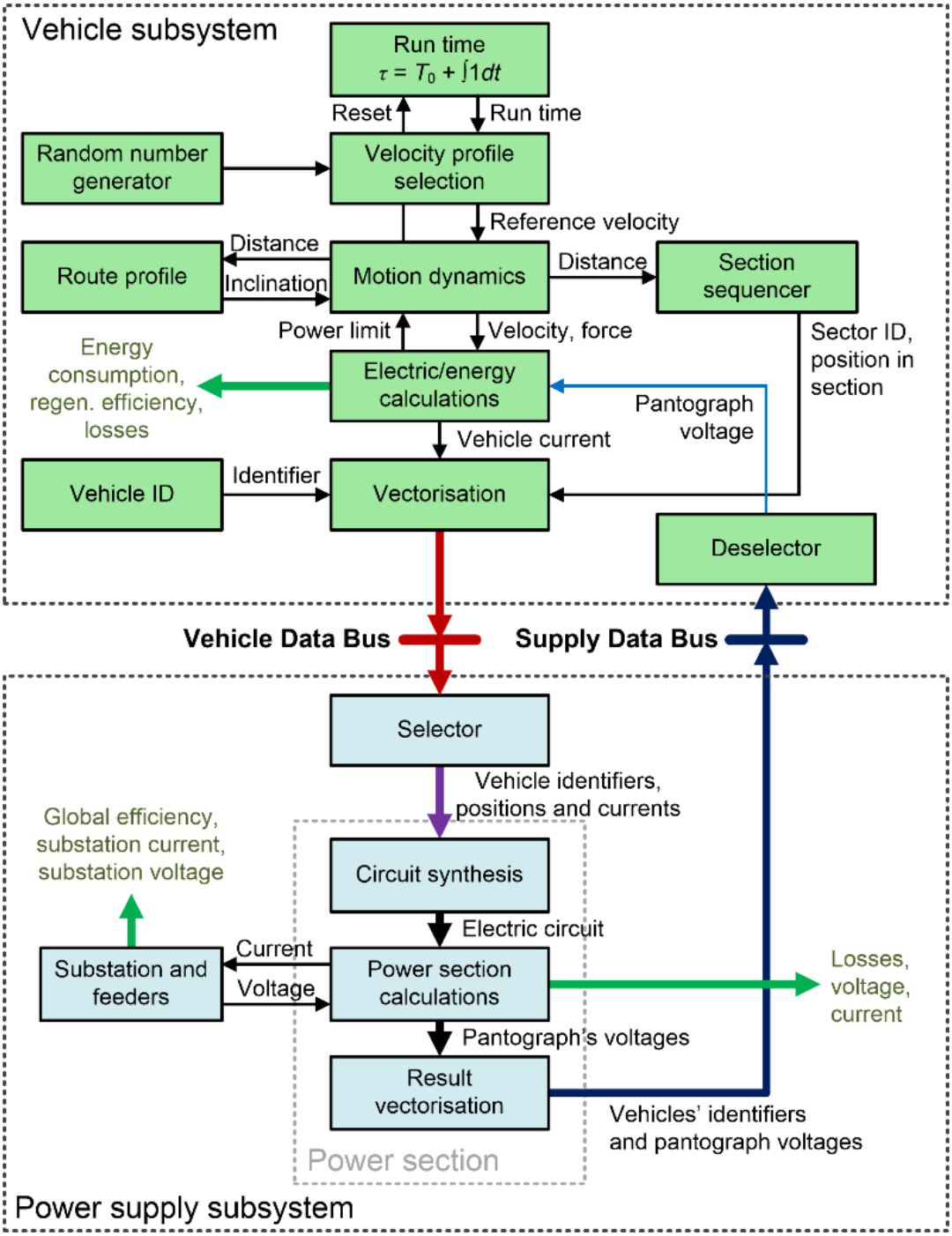

Fig. 3.2. Interaction between vehicle and power supply model [62]

Vehicle movement calculation is based on set velocity profile – it provides the value of set velocity for motion dynamics subsystem. Random number generator provides a value used for determination of station dwell time and velocity profile selection (according to its probability). Then, values of mechanical variables, such as motive force, velocity and distance are computed in Motion dynamics block. Route profile subsystem provides values of route inclination and curvature which are used to reflect additional motion resistances. By design, route parameters are localized within vehicle subsystem, because vehicle models are independent allowing them to follow different routes. Section sequencer uses covered distance value to determine power supply section the vehicle currently runs

through, and then computes distance within that section. Electric/Energy subsystem calculates electrical parameters: pantograph current, energy consumption and regeneration based on mechanical power, motive force, efficiency factors and pantograph voltage value. Energy is split into consumed, regenerated and dissipated. Drivetrain losses are computed as well, allowing for comprehensive vehicle efficiency analysis. Vectorization subsystem awaits four values to synthetize the data frame: vehicle identifier (ID), current power supply section identifier (SN), vehicle current value (i_{veh}) and location within the sector (x_{veh}). Those frames are broadcasted to the *Vehicle Data Bus*, where they are available for all *Selectors* within the model.

Selectors retrieve from VDB vectors containing their section identifier in order to prepare matrix of vehicle parameters for the power supply section model. Because size of electric circuit parameter matrix in power supply section model is constant, logic for accommodating varying number of vehicles within the section was implemented. For this reason, "dummy vehicles" were introduced – with constant location and current equal to zero, they can occupy unused nodes without influencing the results.

It is worth noting, that vehicles may not always enter power supply section in the same order, especially when they follow different paths or when some of them are stopped outside of peak hours. Therefore, sorting operation is carried out in relation to distance within section, to ensure that value of distance difference between the vehicles is always positive. Such prepared vehicle data matrix is then sent to the power supply section model. Thanks to this, one vehicle overtaking another (e.g. at the terminal) is not an issue.

Power supply section model synthesizes electrical circuit, using data provided by the *Selector*, traction substation model and section layout coded inside the model. Therefore, "Circuit synthesis" can be interpreted as calculation of equivalent circuit parameters (in this case – resistances) and linking vehicle and substation parameters to corresponding sources and loads. Depending on the layout, section is connected to one or two substations, and this connection is fixed as it does not change during the simulation. Traction substation model accepts value of the load current and provides value of the voltage at the end of the corresponding feeders, caused by the current and voltage drops on the internal resistance and feeder resistance. Because typical substations in DC systems are equipped with diode rectifiers, reverse current is not allowed. To ensure non–negative output current, internal resistance is set to value a few orders of magnitude higher than normal when current approaches zero. Alternatively, model can be fitted with iterative current limiter, if the relation between braking chopper installed in vehicle and its pantograph voltage is unknown. The results of power supply section model calculations are the voltages on the vehicles' pantographs, as well as transmission losses. Voltage values are vectorized, combining them with vehicles' identifiers – because all the operations were conducted on the sorted matrix, the order of the identifiers and voltages is the same, so concatenation is straightforward. Output matrix is then broadcasted into the *Supply Data Bus*, where it is accessible for all the *Deselectors*. The *Deselectors* are searching the SDB for the vehicle identifier and load corresponding vector in order to extract voltage value (Fig. 3.3).

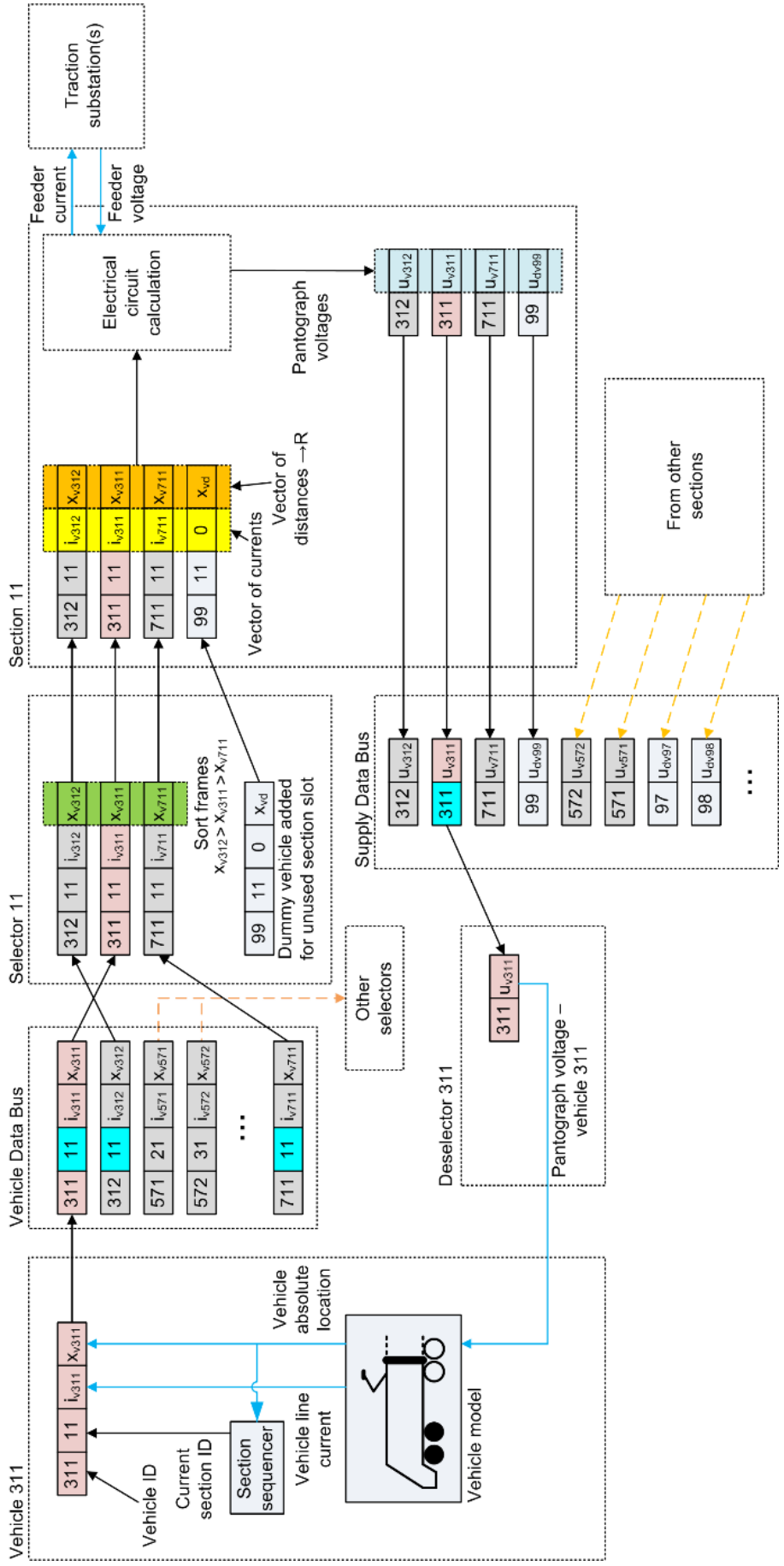

Fig. 3.3. Diagram of data circulation from the single vehicle standpoint

The model relies on external script for loading input parameters and initial conditions. This way, changing simulation conditions is straightforward, and the key parameters are accessible from Matlab workspace, where they can be interacted with. Thanks to that there is a possibility to conduct analysis simulating model in the loop or use one of Matlab Toolboxes, e.g. for optimization purposes. Saving simulation results to file or displaying waveforms is also done using additional scripts. This also means that the model can be connected to visual interface and operated like standard Windows application. It is worth noting that completed application can also be compiled to use on computer without Matlab, either under Windows, MacOS or Linux operating systems. Examples of model realization can be found in Appendix 1.

3.3. Vehicle motion dynamics

Simulation of vehicle movement dynamics is a basis for energy efficiency analysis, because it binds mechanical and electrical systems. Level of detail, however, may vary depending on the type of vehicle, assumed velocities or traction drive architecture. There is also a concern about computation performance, solver stability or cumulative error, when developed model is too complicated.

In case of electric multiple unit, the vehicle is considered as a lumped inertia element, where all of the vehicle mass is concentrated in single point. Such simplification reduces greatly size of the model, introducing only negligible error – because of equal mass distribution throughout the vehicle and relatively short length of the train [72]. Because of this, the basic movement equation can be applied:

$$a = \frac{F(v) - W(x,v)}{k \cdot m(x,t)} \tag{3.1}$$

where: a – acceleration, F – motive force, v – vehicle velocity, W – motion resistance, x – absolute distance, k – coefficient of rotating mass, m – total vehicle mass, t – absolute time.

Under such circumstances, vehicle velocity is calculated thru integration of (3.1) and distance, consequently, thru double integration of (3.1). Motive force F is generated by the traction motors and controlled by the driver, cruise control or ATO through the inverters in order to execute the velocity profile and satisfy requirements of the timetable. Therefore, an algorithm capable of simulating such system was implemented.

Motion resistance W is sum of resistances that can be attributed to the vehicle (aerodynamic, rolling and friction, so called basic resistance) and the route (inclination and curvature, additional resistance). There are also resistance forces from running through tunnels and wind.

Coefficient of rotating mass k defines the impact on movement dynamics that inertia of the rotating parts of a drivetrain has. The rotating mass includes motor rotors, disc brakes and wheels. It is worth noting, that this coefficient is applied only to dynamics equation – because it does not modify the weight of the vehicle; it is used only to depict how certain parts behaving as a flywheels can impact movement dynamics.

3.3.1. Motive force calculation

For every type of vehicle, movement calculation is based on motive force, generated by the motors. To drive the vehicle means "to execute velocity profile", to achieve desired velocity and to stop in determined place. Looking at the basic movement equation, only the motive force is a parameter that can be actively controlled, as acceleration and deceleration are the results of the force application, while movement resistance forces counteract the traction effort. In case of electric vehicles, diagram of motive force in relation to velocity can be depicted with 2 or 3 areas: constant motive force, constant power and in case of induction motors, reduced power area or constant induction motor slip (Fig. 3.4). It should be pointed out, that the curve is only showing maximum nominal value – the traction drive can achieve any points lying below the curve as well.

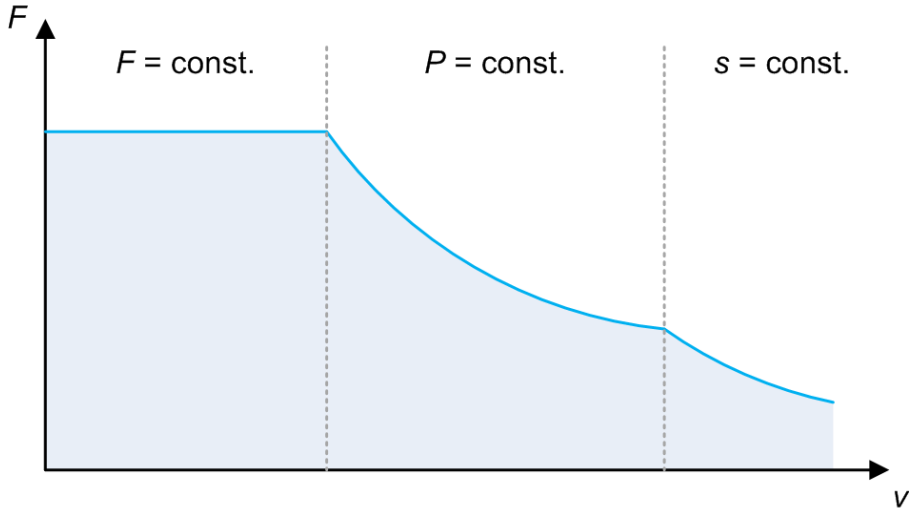

Fig. 3.4. Motive force curve for induction motor powered vehicle

The motive force curve can be implemented in model either in form of a lookup table or mathematical function. In case of this work, author decided to use the latter approach, as it allows for easier implementation of power limitation caused by the undervoltage. Relation between line voltage and available power percentage is specified in a lookup table, and the vehicle rated power is a single parameter. This way, maximum power in any given moment can be obtained as multiplication of limitation value and the rated power. The motive force value is specified as constant (for the constant torque region) and as division of available power and vehicle velocity for the constant power region. Selection between the two is dependent of which one is smaller, as the constant power curve is hyperbolical. Third operating region of induction motor drive was not implemented because in this case vehicles do not achieve high enough velocity. During braking, motive force is limited at around 10 km/h and falls to zero with velocity decrease – this depicts low efficiency of electrodynamic brakes at low speeds.

In simplest implementation, regulation of velocity can be achieved thru switching between values of motive force adequate for movement phase:

- maximum available force for acceleration,

- force equal to motion resistance for cruising,
- zero for coasting and adequate constant value,
- maximum motive force for braking or deceleration (friction/electrodynamic brakes).

Such approach is sufficient for educational purposes, because it allows to explicitly show relation between movement phases and movement equation.

This simplicity, however, limits model accuracy – there is instantaneous and significant change of applied motive force that causes numerical spikes and, because of high inertia of the vehicle and inductance of electrical system, does not occur in real vehicles. Additionally, setting the motive force as equal to sum of motion resistance force might result in incorrect values when analyzing vehicle run on steep gradients – in that case, resulting set value of motive force might be higher than maximum possible tractive effort of the traction drive. Therefore, such model would allow the vehicle to cruise regardless of the motion resistance, while in reality vehicle would slow down until maximum available motive force and the resistance force will balance out. Similarly, setting motive force value of exactly zero for coasting may result in uncontrolled acceleration while moving downhill, while in reality the driver would apply brakes to keep the velocity within required limit. It is also worth noting that in case of modern electric vehicles precise control of motive force is possible, so it is desirable for model to have the same capacity.

In order to ensure realistic motive force application, author implemented proportional–integral (PI) controller that carries out regulation in relation to velocity error [61]. The gain values for proportional and integrating terms are tuned to ensure force application dynamics similar to recorded during the real train run. Derivative term of the controller was skipped, because it brings very little to no improvement of accuracy, while impacting negatively computation performance. There is also a risk of program returning error if velocity error is not derivable because of discontinuities in set velocity value, because the set velocity value is determined by the algorithm that uses multiple signal switches. Therefore, this model is suitable for forward simulation, where the vehicle reacts to velocity profile as it would in reality. In order to ensure reliable stopping at the stations, the set velocity is assumed negative in value – thanks to this there is still non–negligible velocity error fed into the controller, resulting in brakes being applied when vehicle does not move. The risk of backward movement (because of a negative force) is averted thru limitation of minimal output value of the velocity integrator to zero.

Because of this, the tractive effort chart serves only as limitation, while the force is applied fluently aiming at the set velocity (Fig. 3.5). Also, other limitations, like wheel adhesion or limitation due the undervoltage can be applied easily – the lowest value is selected as maximum force. Selection between cruising and coasting phase is done by the control function, as it is closely related to algorithm executing velocity profile. This selection can be done using pre–set distance values, speed–dependent hysteresis switch or even using random number generator (RNG). For the coasting, upper limit of the motive force is set to zero, while lower limit still allows for braking – such solution is much more reliable than arbitrary switching between driving and braking at set distance. Cruising was selected as default movement phase – because coasting requires additional input for switching on and

off the traction drive. Because maximum available force is variable, limitations were implemented using *dynamic saturation* block from basic Simulink library.

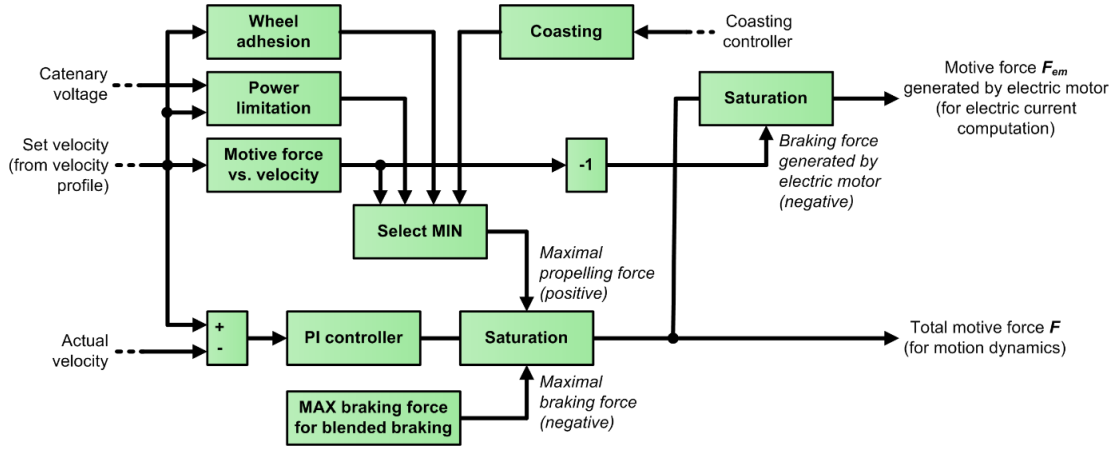

Fig. 3.5. Diagram of motive force control algorithm

Brakes were implemented as combined system of electropneumatic (friction) and electrodynamic brakes (regenerative). Relation between the two can be customized, along with maximum ratio of energy regeneration; by default use of electrodynamic brake is prioritized. Because of timestep and utilization of PI controller for motive force application, pneumatic brake system is simplified – it acts only as additional force component, without considering delay of brakes activation. Braking is realized with constant deceleration rate that can be set separately for every vehicle. To achieve this, braking curve calculation was implemented into set velocity generator. Because the braking curve is parabolic (Fig. 3.6), at the beginning of the run its value is very high; however, the closer the vehicle is to the desired stopping point, the value of velocity from the braking curve will fall below speed limit thus initiating braking phase (algorithm selects the lowest value of set velocity as its output). Purely electric braking is not considered, as it would be impractical due to prolonged braking distance and necessity of either injecting additional energy or engaging friction brakes at low speeds [68].

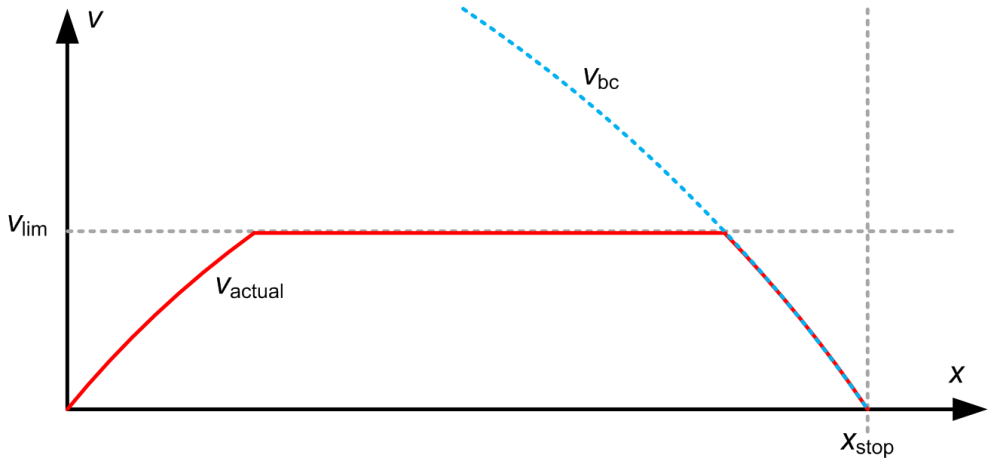

Fig. 3.6. Implementation of braking curve

Adhesion limit calculation was implemented in simplified version, taking into account surface coefficient and axle load (3.2), which is sufficient for modeling transportation system in order to evaluate energy efficiency of vehicles as given:

$$F_{max} = \mu_s \cdot m_a \cdot g \tag{3.2}$$

where: $F_{\max}$ – maximum applicable motive force, μ_s – surface adhesion coefficient, m_a – mass loaded on motorized or braked axles, g – gravity acceleration.

Constant adhesion value might however be insufficient for comprehensive energy efficiency analysis, when optimization of velocity profile is planned. Because of this, correction of surface coefficient in relation to train velocity was implemented:

$$\mu_s = \frac{\mu_0}{1+0{,}01 \cdot v} \tag{3.3}$$

where: μ_s – corrected adhesion coefficient, μ_0 – base adhesion coefficient (typically 0,3 for steel wheels on steel track under dry conditions), v – vehicle velocity.

For braking, adhesion limit was lowered to 80% of starting value for dynamic braking and set as 50% for friction brakes [138]. There are also more complex methods for calculating the adhesion, however their implementation requires significant amount of additional parameters, while possible improvement of accuracy in this case would be minuscule [1,57,103]. Because not all of the axles are motorized, maximum applicable force is different for acceleration and braking.

It is worth mentioning that under dry conditions that are often assumed for such analyses, impact of wheel adhesion on vehicle dynamics and consequently energy consumption is negligible. However, the model was developed with maximum versatility in mind, so there is a possibility to look into influence that weather conditions have on vehicle movement. Those conditions can be set as variable, both in time and distance allowing to represent realistic weather – loading the values into a lookup table instead of setting single constant. Similarly, because of modular structure of the model, presented motive force controller can be replaced by the complete traction drive model thus allowing for computing efficiency maps or testing inverter control algorithms.

3.3.2. Motion resistance

Motion resistance of the vehicle is calculated as sum of aerodynamic drag, friction and rolling resistance. In most cases, the empirical equations are used in order to approximate the value of the resistance force, typically in form of second order polynomial (Davis equation):

$$W = \mathrm{A} + \mathrm{B}v + \mathrm{C}v^2 \tag{3.4}$$

Where A is coefficient of rolling resistance, B – coefficient of friction and C – coefficient of aerodynamic drag.

The coefficient values are obtained from running tests, where measurements are taken during coasting phase [102]. In case of multiple units, where the whole train is considered

as a single vehicle, formulae might be more complex, taking into account parameters as number of axles, length or weight of the vehicle, though they can still be reduced to the quadratic equation. This can be especially useful when multiple variants of the same vehicle exist. For trains consisting of locomotive and carriages, total resistance should be calculated as sum of resistance for each vehicle in the consist. In current implementation, the model accepts only polynomial parameters A,B,C as it is intended for multiple units.

Resistance of the route is calculated as a sum of equivalent coefficients for both inclination and curvature, expressed in promiles. By multiplying these by the vehicle mass and gravitational acceleration, value of the force is obtained. Route inclination is stated directly in the route profile map, as well as curves' and transitional radiuses. To compute equivalent movement resistance on curves, empirical formula needs to be employed. Typically, for normal gauge railroad, the following expression (Röckl equation) is used:

$$i_c = 690/R \tag{3.5}$$

where: i_c – equivalent resistance (in promiles), R – curve radius.

Because the route includes transition curves, they need to be included in the resistance value as well. In this case, the equivalent resistance is calculated in relation to adjacent curve [72], however such approach requires time consuming data preparation and introduces error to the calculation. Because of that, author decided to import the route data directly into the model, using lookup table with linear interpolation.

Additional resistance forces attributed to running through tunnels or wind speed and direction were not implemented, because of their presumed minimal impact on energy consumption in analyzed situation. Relatively low velocity values and frequent stops translate to low value of these forces, and wind speed would need to be unlikely high and consistent in order to have impact on the results.

3.3.3. Electrical system of the vehicle

Electrical parameters of the vehicle are computed on the basis of mechanical power and motive force. In order to calculate the electrical power, losses in vehicle's drivetrain need to be considered, preferably in form of an efficiency factor. Datasheets and catalogues usually contain basic information about efficiency of a device, however the parameter holds true only under certain, mostly nominal conditions – so for the electric motor its efficiency factor is given for nominal angular velocity, with nominal torque load in steady state. Therefore, efficiency factors in train run simulations are often assumed constant, however such approach can result in considerable errors [59], as the traction drive rarely works with constant velocity or torque load. There is a possibility of using lower, averaged values of efficiency factor, however their calculation is not straightforward and introduces errors, sometimes significant in value [58]. While using it allows for relatively good coincidence with measurement for the energy balance, current values resulting from lower constant efficiency factor can be severely distorted. Because of that, author decided to implement variable efficiency factors for electric motors and traction inverters.

Induction traction motor is converting electrical energy to mechanical energy using electromagnetic field. Because it is the most powerful element of the drivetrain, possible losses are also the largest in value. Moreover, efficiency of induction motor is highly dependent on both angular velocity and torque load, reaching very low value especially when rotating at lower speed or under low load. Because of that, simple graph with dependency of efficiency factor on generated mechanical power might not be sufficient. In order to depict the motor losses accurately, efficiency map $\eta = f(M,\omega)$ was computed by the author [59]. The map contains values of motor efficiency in steady–state for certain values of angular velocity and load torque (Fig. 3.7). Because the data is loaded into the 2–dimensional lookup table, values for arguments between assumed points are computed using linear interpolation.

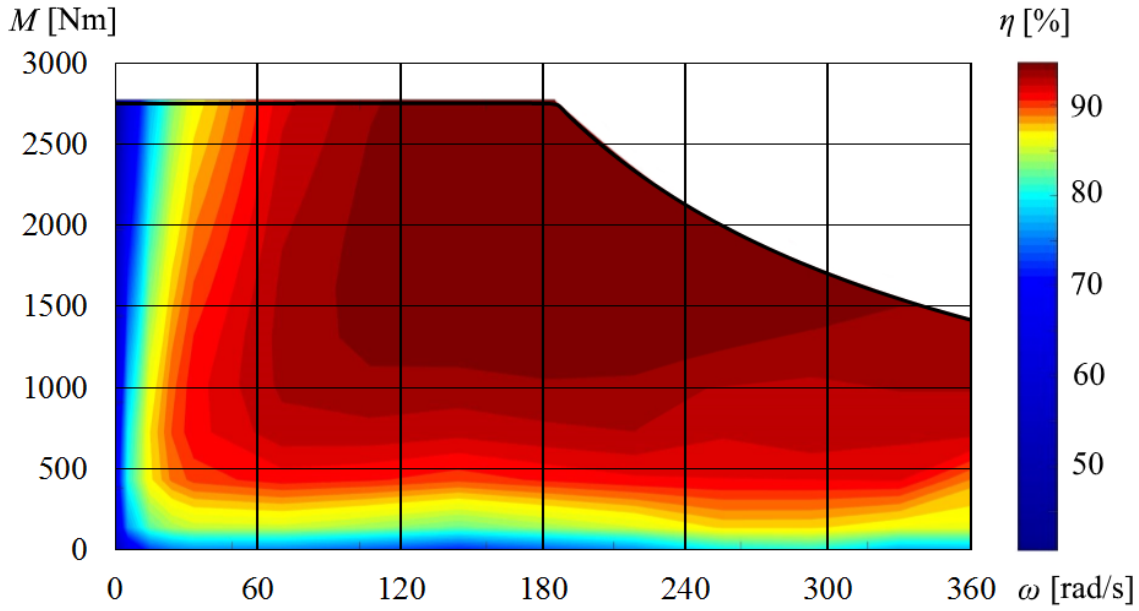

Fig. 3.7. Computed motor efficiency map for 500 kW traction induction motor [59]

Efficiency map of traction motor was calculated using model of vehicle dynamics, with basic motive force controller and its constraints replaced by detailed model of the electric drive. For each point, the target velocity was set and the drive accelerated without any torque load. After achieving steady speed, the torque load with value adequate to data point was applied; after the drive achieved equilibrium, the efficiency value was saved into the map.

Such approach allows for improvement of assessment of motor losses during train run over existing simplified models while retaining good computation performance. Further improvement would require using detailed drivetrain model that enables transient states analysis, however negative impact on simulation time would be severe. Moreover, for analysis of energy efficiency of vehicles running for a longer period of time, using extremely detailed model is not justified because of required short timestep.

Detailed analysis of the traction inverter would require time step allowing for calculation of transient states in transistors and diodes, which are a few orders of magnitude lower than time step used for the train run simulation. Running analysis of the whole transportation system with such a small time step is therefore undesirable. However, it is possible to estimate inverter losses using parameters of power electronic components (transistors and freewheeling diodes) specified in their datasheets. For this analysis, inverter losses are approximated using efficiency curve dependent on output power $\eta = f(P)$, shown in Fig. 3.8.

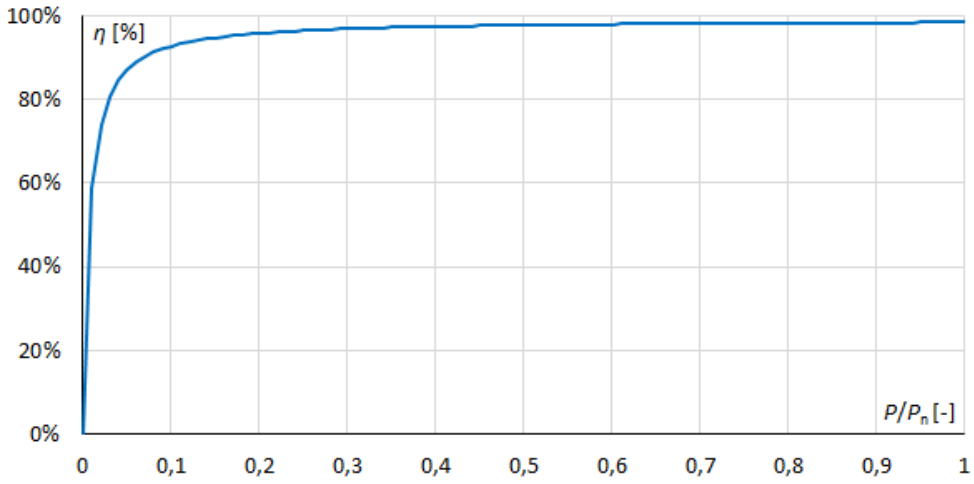

Fig. 3.8. Computed efficiency curve of the traction inverter

The efficiency curve has been calculated using additional program that included analytical equations as described in 2.2.2. [58,60,107,153] and datasheets of semiconductor switches used in traction inverters (IGBT transistors and freewheeling diodes). Use of full inverter model was considered unnecessary, because of relatively little value variability and very short timestep required for its proper analysis, rendering it unfit for transport system energy efficiency analysis.

All of the vehicles considered in this work utilize regenerative braking. However, to recuperate energy there is need for other vehicles to consume the surplus. When there is none, excess energy must be dissipated in braking rheostat. Typically, this is related to the voltage on vehicle pantograph – when the vehicle decelerates with energy regeneration enabled, the voltage is rising; if the certain set threshold is exceeded, braking chopper is activated, allowing for energy dissipation. Depending on the vehicle, there may be one threshold (resulting in switching on rheostatic braking) or two, allowing for voltage–dependent reduction (Fig. 3.9). As the model aims at depicting realistic operation of the transport system, such measure was implemented. This also functions as countermeasure against negative substation current while being more robust than iterative reductor (which is also present in the model, but is triggered rarely – which improves computation performance).

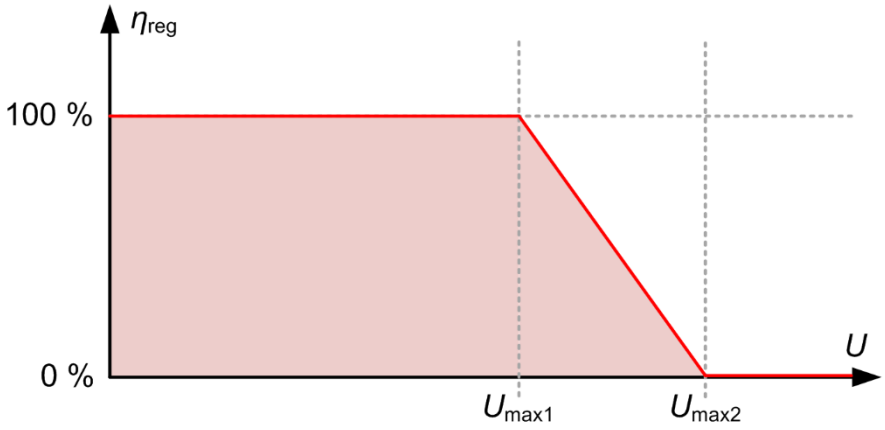

Fig. 3.9. Voltage–dependent reduction of regenerative braking power; U_{max1} – rheostatic brake activation voltage, U_{max2} – fully rheostatic braking threshold

Auxiliary power can be set to 20% of the vehicle consumed energy, which provides insight in maximum potential energy consumption; it is however not very precise, as in practice full auxiliary power is used rarely [106]. Because of this, author decided to split auxiliary power to three main elements, each of which may work with different duty rate (Fig 3.10). These systems contain base auxiliary power (traction drive controllers and cooling, onboard computers) and passenger information systems with monitoring that work continuously, HVAC that is switched on depending on temperature and air compressor that works depending on pneumatic brakes usage (in this case – it is triggered by vehicle stopping). While it is possible to simply calculate average values of the energy consumption considering parameters stated above, such simplification may lead to incorrect vehicle current values as the heating system requires significant power when turned on.

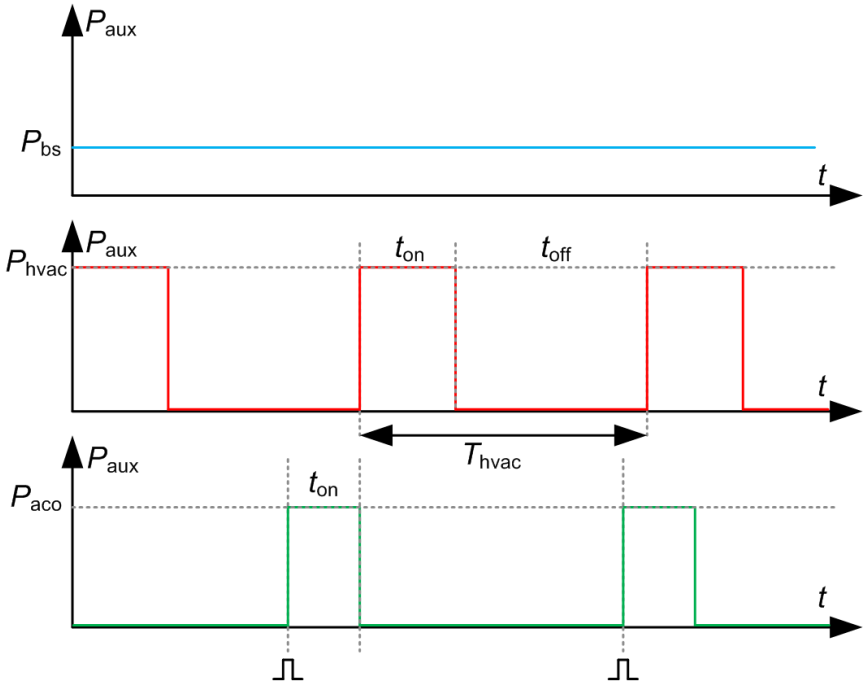

Fig. 3.10. Components of auxiliary power, where: P_{bs} – power of basic systems, P_{hvac} – power of heating and air conditioning, P_{aco} – power of air compressor

Therefore, author decided to model the auxiliaries as sum of constant value (for base systems), square–wave signal with pulse width dependent on temperature (for heating/HVAC) and step signal every stop (for air compressor). Time period for the HVAC system was set to 10 minutes, based on author's observations. This way, auxiliaries operation simulation is more realistic than use of maximum values or ignoring it at all.

It should be noted that energy consumed by the auxiliaries is not considered a part of the losses. This is because those systems are either required to move the vehicle (drive controller, lighting, signaling), or required for passenger comfort (HVAC, lighting, information screens, etc.).

3.3.4. Schedule setting

Simulation of rail vehicle operating under realistic conditions require setting adequate schedule for all the vehicles in the analyzed transport network. In order to achieve that, knowledge about all the travel times between stops, dwelling time on stations and terminals and time reserve is necessary. While recording of real train run might be helpful for determination of velocity profile, it should be placed in corresponding time of the day and traffic situation – dwelling time and velocity profile is different, when the driver is trying to reduce the delay. Because of this, velocity profile in the simulated schedule need to fit within timeframe, including time reserve and providing no less than adequate station dwelling time [77].

Author decided to implement schedule as a part of control function, which arguments consist of time, section ID and logical values. For every vehicle, there is section sequence specified, allowing vehicles to follow different paths. Depending on analyzed network layout, section identifier is used to determine current power supply section and track section as well. For every station to station run, time is measured; moreover, there is measurement of time for each route run (including terminal dwelling time). Such feature allows for easy control over the timetable and vehicles circulation (Fig. 3.11). It is worth noting, that author decided not to implement clock using corresponding Simulink block, but rather used time integrator fed with constant value of 1. Because of this, possibility of local time counting was achieved, with easy access to initial value, reset and introducing delay for timetabling purposes.

Random number generator (RNG) provides value that allows for introduction of variable station dwelling time and selection between multiple velocity profiles, according to their probability. RNG algorithm is triggered by vehicle finishing its station stop, allowing for update of the value, along with target station location – stations are numbered, and the number is linked to the location; because of this, counting trigger events allow for reliable identification of the stations. The algorithm is presented in detail in Appendix 1.

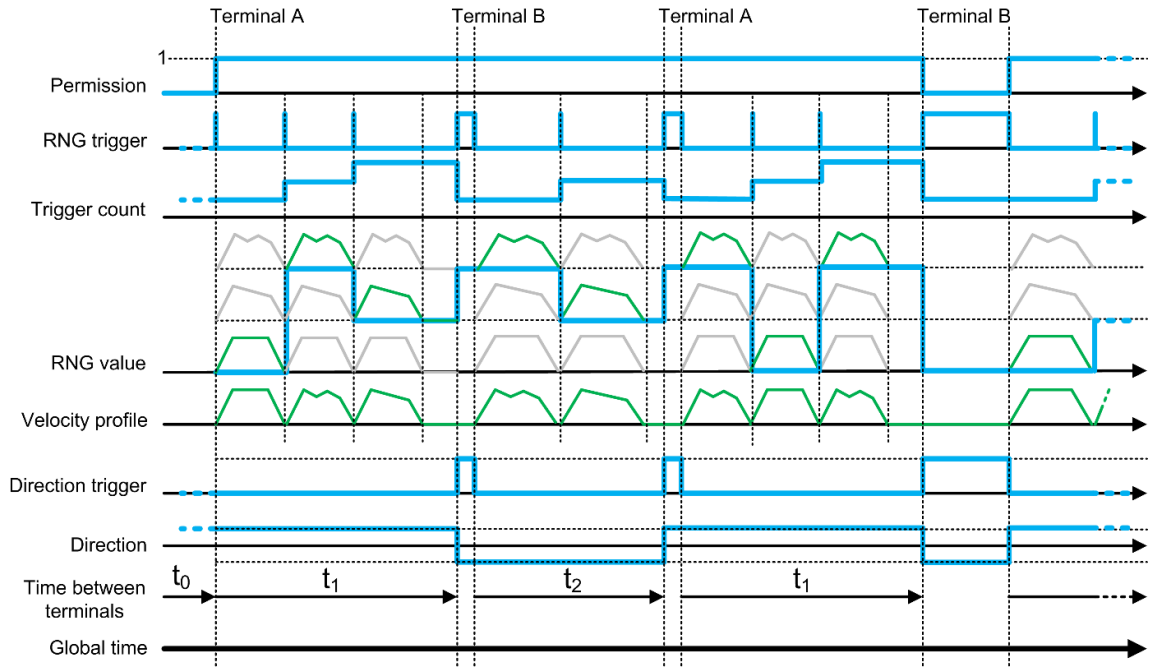

Fig. 3.11. Diagram of control function algorithm

Each vehicle run can be interpreted as a set of station to station runs, contained within terminal to terminal frames. Stations within the analyzed route are numbered, with parameters like station location and occupancy rate linked to that number. Because of this, for every route fragment, there is a target station location. In order to ensure reliable stopping regardless the set vehicle and route parameters, the target needs to be updated after vehicle called at the station and dwelled for the required amount of time. The most efficient way of implementing this algorithm is based on multiple triggers.

First, the velocity value of zero resets stop time integrator. While the vehicle is stopped, time is counted and compared to required dwell time. The dwell time consists of constant value and randomized variable, allowing to reflect the realistic differences in station stop time. For certain stations, the dwell time can be set independently, overriding variability algorithm. When the integrated time value is equal or greater than the target dwell time, the value “true” of this logical test acts as a trigger for the parameters update: target station location, vehicle load mass and RNG value for next stop dwell time. It is worth noting, that change of the target station location while permission function value is 1 results in vehicle immediately starting the run. Those triggering events are counted, as the value can be linked with station number on the route.

If the direction switch at the terminal is necessary, it is triggered by rising slope of logic function that requires run time to be equal or higher than set value for terminal to terminal route and permission function value to be true. Those impulses are being counted, and their number divided modulo 2; depending on set direction, reverser value is set as 1 or -1, which is directly multiplied by the velocity, allowing for travel in both directions. In case of loop line, reverser value is always set as 1 or -1 resulting in consistent direction. Similarly, station number is counted using the reverser value to be added to previous value, reducing number of required parameters.

Some situations require taking into account some variability of vehicle velocity. This is especially important in case of urban transport vehicles that utilize public roads, but can be of value for railway transport as well, when there are multiple different trains in service, or trains do not follow consistent velocity profiles. In such case, random number generator triggered by the station stop used for stop time determination has another purpose. Its value can be used to compare against thresholds specifying probability of selecting one of velocity profiles. Those thresholds can be variable with respect to simulation time or stop number, so the vehicles can follow different velocity profiles depending on time of the day or localization (Fig. 3.12). This way, developed model can still provide meaningful results even if there is a degree of randomness in real transportation system. This also allows for bypassing the impossibility of compilation Matlab functions responsible for variable–probability RNG (extrinsic coder is inefficient).

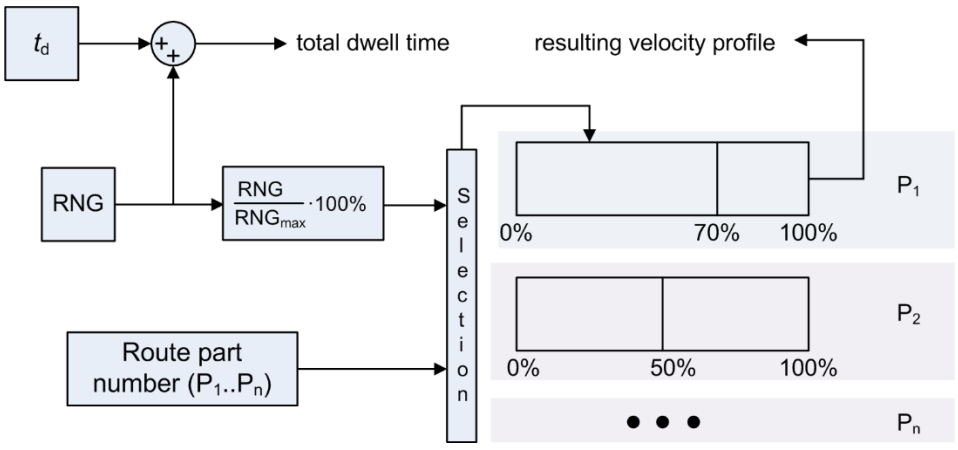

Fig. 3.12. Algorithm for semi–random selecting velocity profiles with variable probability for every part of the route (station–to–station); t_d – base dwell time

Permission function is the key to setting realistic timetable – it controls, which and when vehicles are allowed to move. It is a logical function – value of 1 permits the vehicle to execute its timetable, value of 0 unconditionally stops the vehicle and pauses its timers and counters. Because of that, it is simple to stop additional vehicles during off–peak hours or control moment of departure from station to synchronize acceleration of vehicle with other decelerating in order to improve regenerative braking efficiency. There is also a possibility of further expansion that could take into account signaling and analysis under nontypical conditions, like power supply failure or construction works, as those conditions are possible to be depicted as logical functions dependent on location or distance between vehicles. For this analysis, permission function was set manually for each vehicle, to execute realistic timetable.

Scheduling algorithm contains also implementation of changing mass during the station dwelling, which stem from varying number of passengers during the day. When vehicle stops, the percentage occupancy value which is a function of time and station number is loaded and multiplied by maximum vehicle load. Then, it is added to empty vehicle mass. Varying vehicle load has noticeable impact on energy consumption [63].

3.4. Traction power supply

This work is focused on analysis of the DC power supply system, that is used by the suburban railways, metros and urban transport like trams and trolleybuses. In comparison to AC systems, more complicated layouts are often found that may require simultaneous computation of electrical parameters in multiple sectors.

3.4.1. Power supply model architecture

Analysis of the whole electrified transport network as a single electrical circuit is very challenging and may even be impossible to carry out efficiently for complex systems. There is also a concern about vehicles that cover part of the route independently from power supply, using onboard energy storage. Because number of vehicles on every supply section may vary depending on timetable, modeling single circuit with moving nodes for the whole system can be problematic. Because of this, author proposed model using separate subsystems for each section, where circuit layout remains constant. These subsystems are building blocks for the power supply system model that act as a load. They are bound together by the models of substations, which are the sources. Therefore, equivalent circuit for the power supply system is compiled from such sources and loads, improving computation performance.

Power supply sections accept vehicle parameters from main data bus through *Selectors*. Based on number of vehicles and their localization, the parameters of electrical circuit are determined. Power supply sections differ based on their real structure, thus equations for the electrical circuit are coded into them and cannot change during the simulation. Next, the node voltages of vehicles and feeder currents are computed. Every section is connected to corresponding substations that provide voltage depending on load current. Pantograph voltage values are put into the data vector and forwarded to *Supply Data Bus*, where *Deselectors* await input. Then, *Deselectors* send data back to adequate vehicles, completing feedback loop from power supply system.

Because all vehicles communicate with power supply using data bus, there is virtually no limitation to the system layout. In case of one sector branching off another, it can be implemented as both the sector and vehicle (stationary in the place where it is connected to the main line). Implementation of trackside energy storages might be done similarly, if they are not installed in the substation or section cabin.

3.4.2. Traction Substations and feeders

Typically, substations in DC power supply systems are modelled as an ideal voltage source connected in series with a resistance to depict load–dependent voltage drop, known as output characteristics. Because there can be multiple power transformers–rectifiers units installed in the substation, possibility of simulating various scenarios was implemented. Firstly, number of transformer–rectifier units connected to the catenary can be either pre–

set or specified as time function. This means that simulation of rectifier unit failure at any given time is possible. Additionally, simulation of output voltage regulation thru tap switching is implemented – it results in moving output characteristics up or down.

Substations are normally equipped with diode rectifiers, so they do not accept reverse current. Acknowledging this fact, internal resistance value starts rising when load current is nearing zero and is set to 1 GΩ, if the current value equals zero. This synergizes well with voltage–dependent reduction of regenerative braking efficiency, implemented in vehicle model. There is also a possibility of using iterative loop (do–while) triggered by substation current approaching zero, that reduce braking current of vehicles within affected sector, when no data about braking chopper is available.

Feeder resistance is coded into the substation model, because its value is constant during the analyzed timeframe. Moreover, implementing the feeders within substation model allows for simplification of section models, improving computation performance. Despite the large cross–section of the feeder cables, losses calculation was implemented (3.6):

$$E_{feeder} = \sum_{k=1}^{n} \int I^2 R_{feeder} dt \tag{3.6}$$

where: E_{feeder} – total feeder energy loss, n – number of feeders, I – current of n–th feeder, R – resistance of n–th feeder.

3.4.3. Catenary

Catenary in DC electrification systems is modeled as pure resistance – for both overhead contact line and rail track. Analysis of such electric circuit is however not trivial, because its layout changes in every time step of simulation. While simulation of system containing constant number of vehicles within single section is straightforward, movement of multiple trains through multiple sections and beyond analyzed area can be challenging.

To address this, author developed catenary models that compute all the parameters for single section. Number of vehicles – or nodes is predetermined, and their data is provided by the *Selector*. *Selector* also performs sorting the vehicles by their localization, so they can be linked to the corresponding nodes. Therefore, physical structure of the catenary model does not change – only the loaded values are variable, and the same vehicle can occupy different nodes during the simulation. Conversely, unused nodes (e.g. in off–peak hours) are linked with dummy vehicles with current equal zero and constant location. Because of this, implementation of local matrix of parameters is possible. Additionally, branch line implementation is straightforward – it can act as both "vehicle" and "power supply section", having both IDs, as well as own Selector and Deselector – the former loads parameters of vehicles within the branch, the latter provides information about voltage. The principle of implementation of such layout is shown in Fig. 3.13.

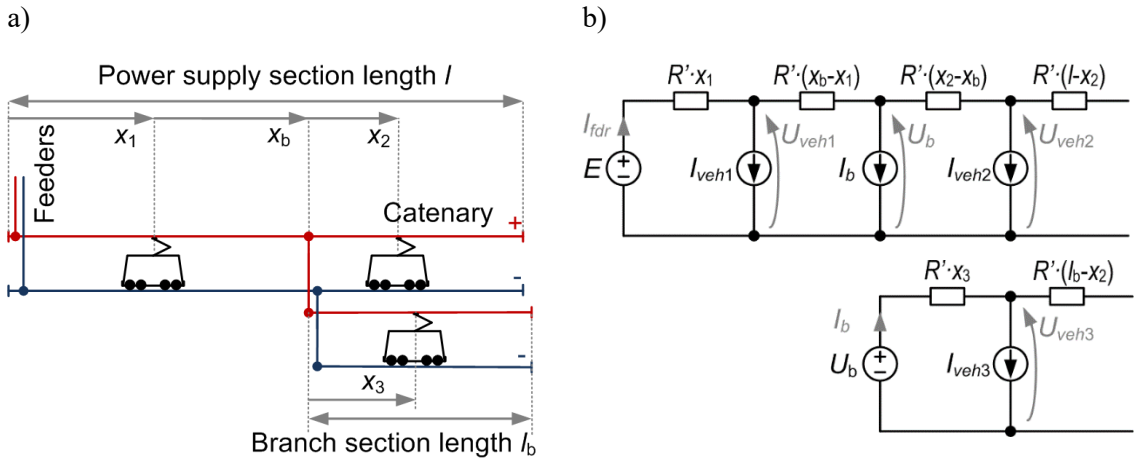

Fig. 3.13. Implementation of branch line within power supply section: a) general structure, b) electrical diagram

Values of the resistance are loaded from external file, being expressed in Ω/km. Precise calculation of kilometric resistance of the catenary using material conductivity, cross section and temperature can be done in setup script, executed before starting the simulation. This also includes possible contact line wear. Because power sections within analyzed network might be constructed using different wire types and rail tracks, resistance is set separately for every section. Author decided to simplify the diagram by assuming rail tracks resistance being lumped together with overhead contact line. In this case, such assumption would not influence the results, as the tracks have significantly larger cross–section than the overhead catenary, and interval between the trains is quite long.

There are multiple connection layouts of the catenary – powered from one or two sides. Double track sections can mostly be analyzed for every track independently. Two basic layouts of catenary and their circuit equivalents are shown in Fig. 3.14.

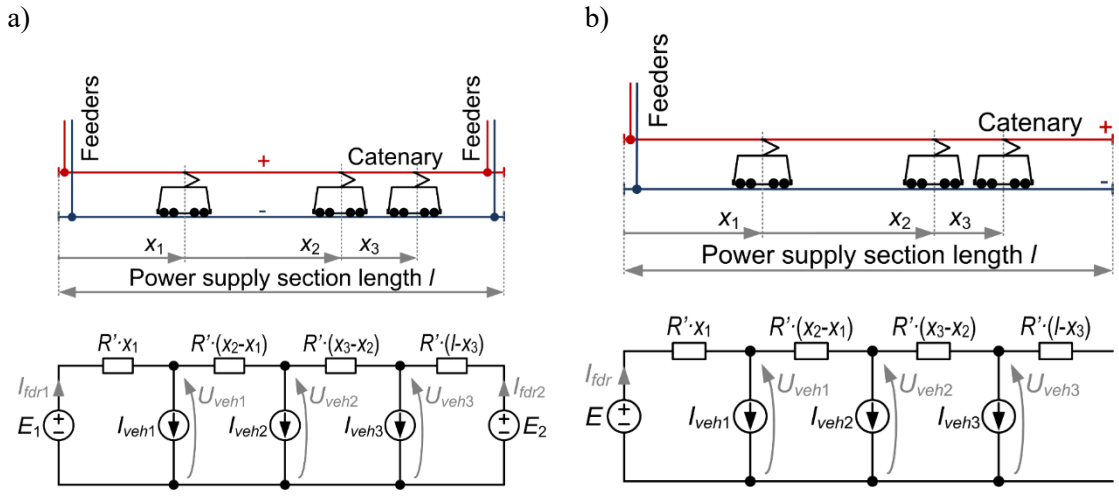

Fig. 3.14. Examples of equivalent circuit for sections powered: a) from two sides, b) from one side, where $x_1 \ldots x_3$ – vehicle location within section, $I_{veh1} \ldots I_{veh3}$ – vehicle current, R' – kilometric resistance of catenary

In case of double track electrified routes, there are also methods of connecting catenary to reduce resistance between vehicle node and feeder node. Typically, it is done through transverse connection (so–called section cabin) or in case of sections fed from one side, the catenary over both tracks is connected at the end of the section. While the former require building dedicated power supply section model, the latter can be depicted using layout shown in fig. 3.13 a), because the section model operates on relative distances between nodes. Explanation of the simplification process is shown in Fig. 3.15.

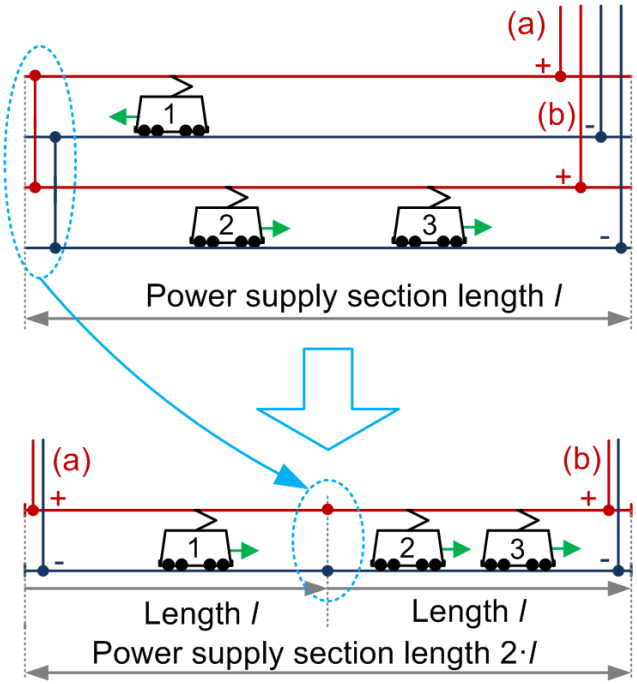

Fig. 3.15. Implementation of double track section powered from one substation, connected at the end

In order to carry out electrical calculation, parameters from *Selector* are loaded. Values of resistance between nodes are computed, taking into account their localization and pre–set catenary parameters. Values of voltage sources are loaded from substations/feeders model, based on feeders' currents; initial condition is assumed as no–load voltage, because analysis starts before the first vehicle begins its run. Matrices of parameters are obtained basing on circuit equations for nodal voltage method (example shown for layout from Fig. 3.13 a):

$$\begin{cases} U_{veh1}\left(\frac{1}{R_1}+\frac{1}{R_2}\right) - U_{veh2}\left(\frac{1}{R_2}\right) + U_{veh3}\cdot 0 = \frac{E_1}{R_1} - I_{veh1} \\ -U_{veh1}\left(\frac{1}{R_2}\right) + U_{veh2}\left(\frac{1}{R_2}+\frac{1}{R_3}\right) + U_{veh3}\left(\frac{1}{R_3}\right) = -I_{veh2} \\ U_{veh1}\cdot 0 - U_{veh2}\left(\frac{1}{R_3}\right) + U_{veh3}\left(\frac{1}{R_3}+\frac{1}{R_4}\right) = \frac{E_2}{R_4} - I_{veh3} \end{cases} \tag{3.7}$$

where: $V_1 \ldots V_n$ – vehicle node voltages, $1/R_1 \ldots 1/R_n$ – conductances, $I_1 \ldots I_n$ – vehicle currents, E_1, E_2 – voltages at the feeder connection point.

Numerical values of conductances found by the nodal voltages are loaded into the matrix **G**. Values on the right sides of the equations are also numerical, and are loaded into the current coulmn vector **I**. Line voltage for the vehicles is computed using node voltage method, where results are obtained in a column vector **V** (3.8), thru multiplication of inverse matrix of conductance and current vector:

$$\mathbf{V} = \mathbf{G}^{-1}\mathbf{I} \tag{3.8}$$

where: **V** – resulting voltage matrix, **G** – matrix of conductance, **I** – matrix of currents.

Calculated values are loaded into the output data vectors, along with corresponding vehicle identifiers – order of the results is consistent with order of the vehicles, so this can be done without utilizing any search functions or multidimensional matrices, improving simulation performance. Data vectors are then broadcasted into *Supply Data Bus*, where they are awaited by the *Deselectors*, which send the line voltage value to corresponding vehicle.

Author recognized the need for possible losses assessment – because it is beneficial to be able to optimize cross section of the contact line, ensuring compromise between resistive losses reduction and modernization costs. Therefore, catenary losses calculation was implemented. Those losses, resistive in nature are computed as sum of losses caused by current between the nodes within power supply section (3.9):

$$E_l = \sum \int I^2 R \, dt \tag{3.9}$$

Losses are calculated independently for each section, therefore it is possible to localize weak points of power supply system, where losses are the highest and test the impact of catenary cross–section on system efficiency.

Some analyses (including this work) focus only on a fragment of a larger transport network. In such situation, parameters from outside of an analysis area should not be taken into consideration and should be specified clearly in order to exclude them from results. To achieve this, author decided to implement additional power supply section specified in sequencer. This "out–of–scope" section is detected by the energy computation algorithm, resulting in all parameters calculation being halted. However, the voltage value is still set at a constant level, equal to nominal power supply voltage in order to improve solver stability (vehicle model is still being fed with parameters which may result in divisions by zero inside).

4. MODEL VERIFICATION

Every model used in analysis should be verified against measurement conducted on the physical object to ensure that obtained results are credible. Because the models are used in order to seek improvement in energy efficiency in transportation systems, bad precision may lead to false conclusions. Therefore, developed program was verified against measurements in two steps – dynamic model test for single vehicle and energetic model test for part of a transportation network.

4.1. Movement dynamics – single vehicle

Testing of movement dynamics model was carried out against recorded train run. After loading prepared train parameters and tuning the controller (PI motive force controller), simulation was executed for selected route fragment, between stations Sopot and Gdynia Redłowo. The fragment has been selected to include longer distances between stops in order to compare behavior of the model while running at constant velocity over varying inclination and curvature to real vehicle.

Approach for performance of this test was as follows:

- GNSS recorder was used to measure the vehicle velocity; from the large set of data, run with the best position accuracy (<3 m) was selected,
- Additionally, selected run was required to be recorded in dry conditions and without traffic disturbances,
- Measured velocity profile was filtered and analyzed in order to develop the target speed signal for the controller,
- Program allowing for movement of the single vehicle was prepared, using the same vehicle model as in transportation system simulation,
- Considered vehicle was the same as the one which run was recorded – EN57AKM, two units coupled in a single train,
- Vehicle load mass was computed basing on passenger number during the recorded run (uniform distribution of occupation along the train was assumed),
- Pantograph voltage was assumed constant at 3400 V to ensure nominal vehicle movement dynamics.

Comparison between recorded and simulated run between stations Sopot and Gdynia Orłowo is shown in Fig. 4.1 (in relation to time) and Fig. 4.2 (in relation to distance, with route inclination included). Figure 4.3 shows location in relation to time, for recorded and computed runs.

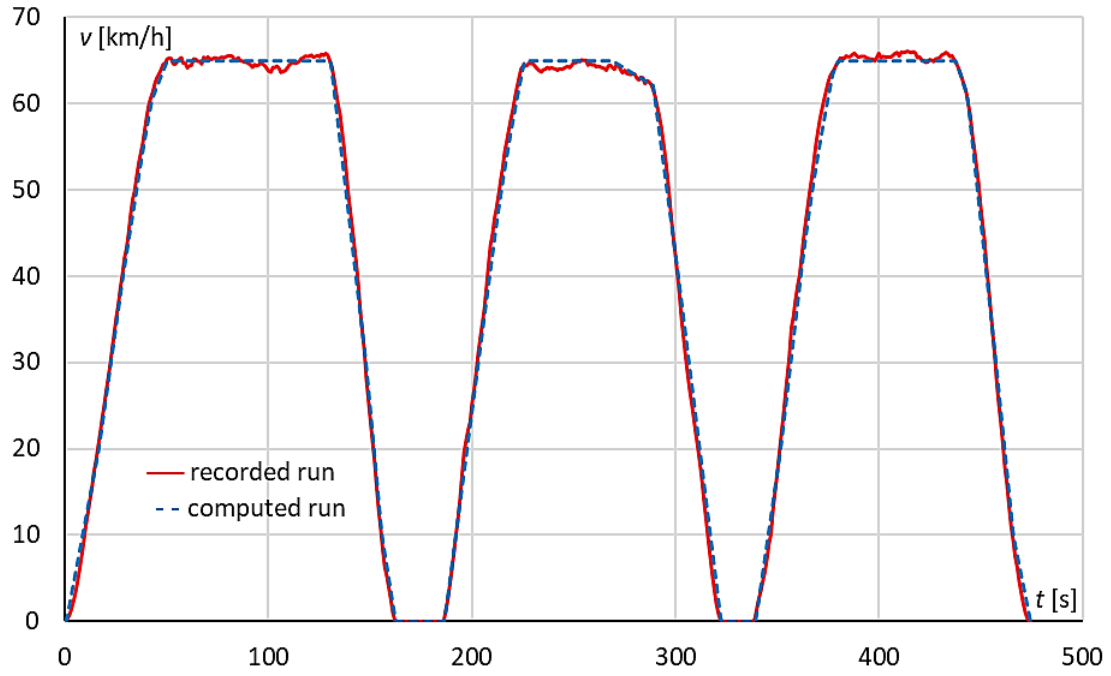

Fig. 4.1. Comparison of velocity in relation to time for recorded and simulated run – route Sopot – Gdynia Redłowo (Track 501)

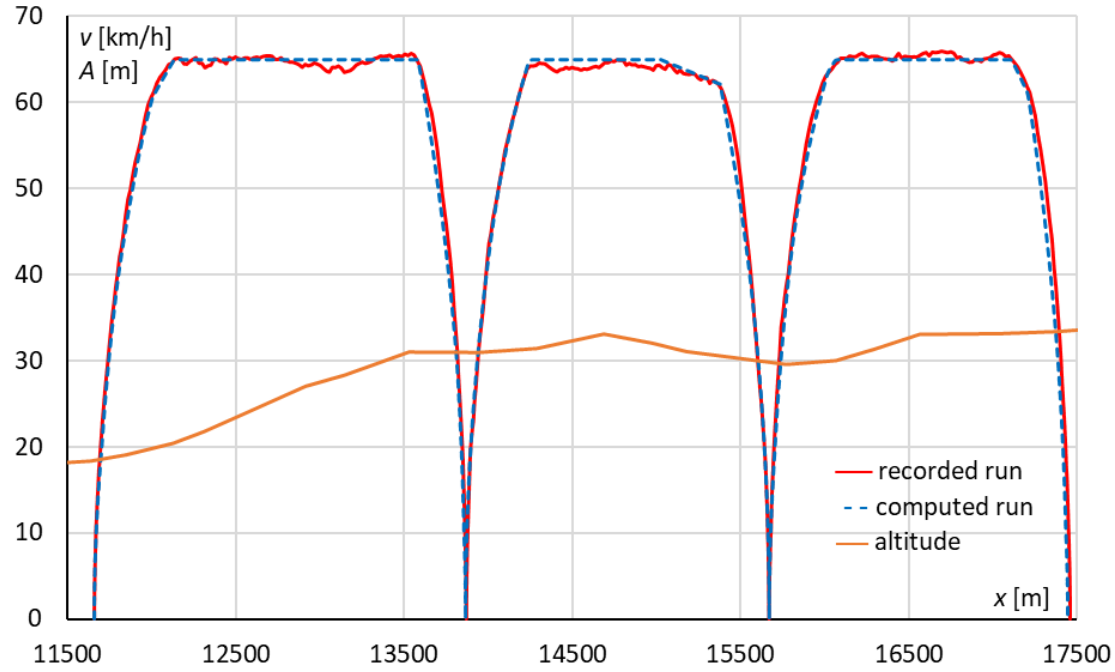

Fig. 4.2. Comparison of velocity in relation to distance for recorded and simulated run – route Sopot – Gdynia Redłowo (Track 501)

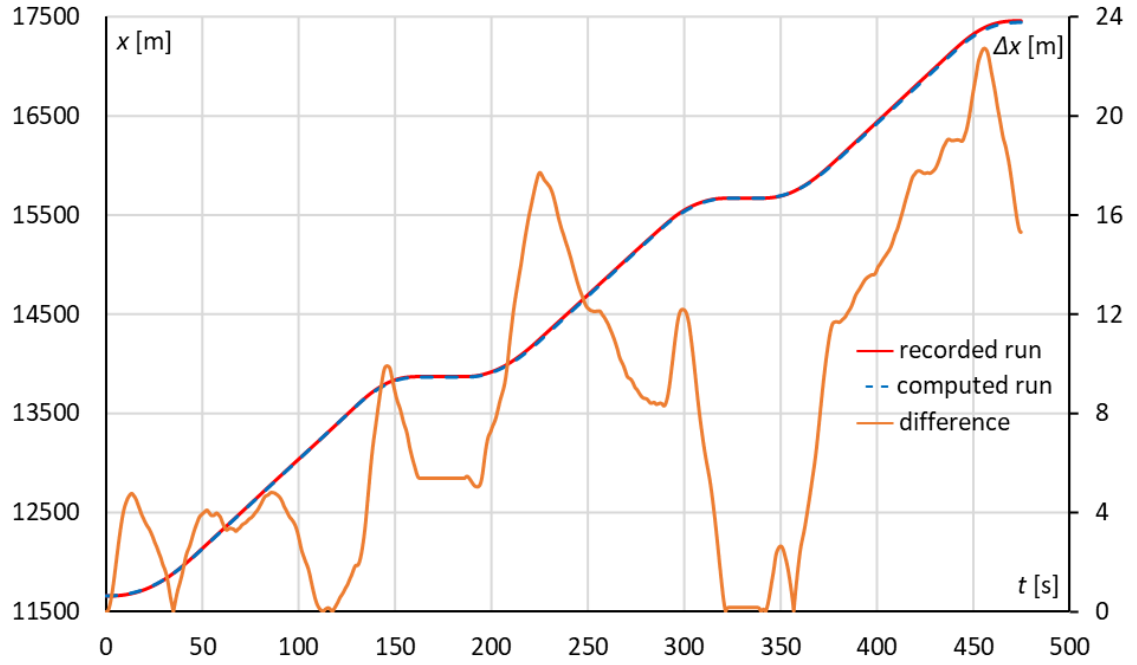

Fig. 4.3. Comparison of location in relation to time for recorded and simulated run – route Gdynia Orłowo – Gdynia Redłowo (Track 501)

Velocity waveforms obtained as a result of simulation closely resemble recorded velocity profiles. The discrepancies may be a result of limited GNSS recorder accuracy, however they are smaller than 0,4 m/s or 2,5% of the cruising velocity which can be considered satisfactory (2 km/h is the cruise control system accuracy). There might be slight discrepancies between simulated and recorded run during acceleration and braking phase, as in real vehicle the driver controls the motive force manually, not necessarily holding it at the same level for the whole duration of the movement phase. However, those differences are minuscule as the simulated run is extremely close to the recorded one, with differences in stopping point being within a single centimeter.

It is worth noting that the better results were obtained using set velocity value based on record analysis, setting coasting override than using recorded run directly as set velocity value (after filtering) – in case of recorded velocity, there was high discrepancy at low speed because of too low velocity error value (difference between set and actual speed) and velocity oscillations in cruising phase, because filters could not produce steady waveforms. Adequate movement dynamics of the vehicle was achieved through tuning the gain values of controller terms. All the adjustments were done using single vehicle model, however it was exact same model used for complete analysis of transportation system.

4.2. Transportation system – current and energy

Verification of the whole model was impossible for the analyzed urban railway system, because of high number of old vehicles with rheostatic DC drive still in service, insufficient information about train circulation and ongoing mutiple maintenance works – resulting in

additional speed limits or changes in traffic organization. Conducting simulation for such abnormal conditions may not hold true to regular system operation, and therefore, would be inconclusive as a basis for optimization of velocity profile.

However, author is involved in Interreg "EfficienCE" project [34], where the improvement of energy efficiency in urban electrified transport is the main objective. The scope of author's work for this programme is simulation and optimization of trolleybus network in city of Pilsen, Czech Republic. Large amount of measurement data for every part of this transportation system and its power supply created an opportunity for validation of the obtained simulation results and model credibility. As the model was designed with high versatility in mind, author argues that with sufficiently precise parameters provided, the simulation results will hold true for different means of transport – therefore validation for different transportation system is of value.

For this task, modified version of model developed for this thesis was used. The differences are found mostly in vehicle models – using adequate parameters for road vehicles on rubber tires, as the trolleybuses were the focus of this analysis. Velocity setting requires wide usage of randomization methods in order to account for road traffic conditions and random events, such as on–demand stops or red light on intersections. For this reason, velocity profiles based on data measured by onboard recorders have been specified for various times of the day, with typical profiles for morning, midday and evening determined. Those profiles were selected randomly during simulation for every between–stops route fragment, with selection probability varying with time (Fig. 4.4).

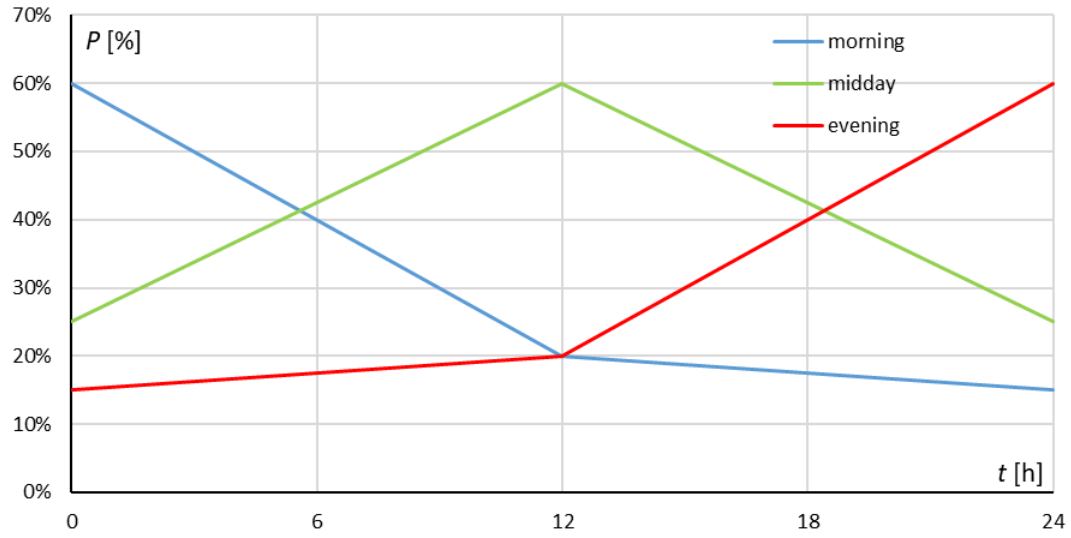

Fig. 4.4. Values of probabilities of selection of velocity profile from set corresponding to time of the day

Probability values for selection of each profile and division between morning, midday and evening were assumed after analysis of the measured velocity profiles. This analysis shown similarities between vehicle runs during the time intervals; however, possibility of profile similar to those recorded in different hours still existed. Therefore, during morning hours, probability of selection of morning profile is not at 100%. The probabilities were set to

above 15% because below this threshold possibility of selection of such profile was very small in practice. Probabilities as shown were determined thru series of simulations, conducted to find good conformity between measurements and computation results.

Testbed for the developed program was the area powered by substation MR5 (Zatiši). The substation is feeding 5 two–track trolleybus sections, with large roundabout and a short branch (Fig. 4.5). The branch is powered directly from catenary thru connecting wire (there is no feeder from substation). Traction substation is located close to the location of feeder no. 52 connection.

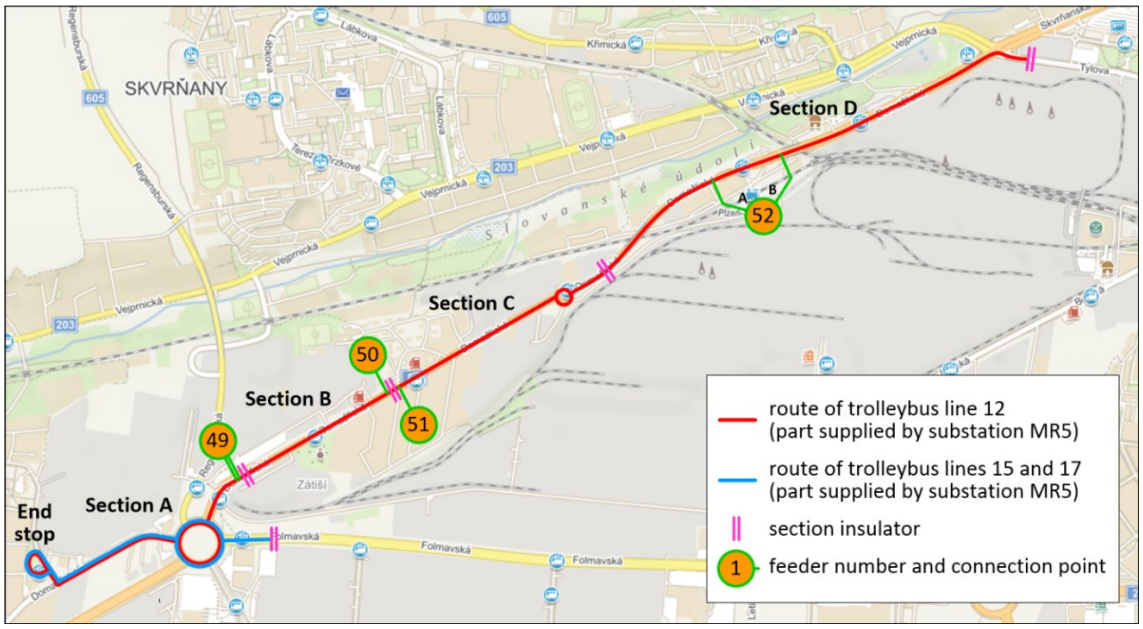

Fig. 4.6. Map of the analyzed trolleybus network fragment

The area lies within bounds of trolleybus lines 12, 15 and 17. It was selected for the results verification, because vehicle types used on these lines are consistent, and equipped with induction motor drives with energy recuperation enabled – lines 12 and 15 are served by single trolleybuses (Škoda 26Tr), line 17 by articulated ones (Škoda 27Tr). Parameters of the vehicles were provided by the manufacturer, Škoda Electric, and parameters of power supply as well as measurements were provided by the network operator, Plzeňské Městské Dopravní Podniky (PMDP). Key parameters of modelled vehicles are presented in Tab. 4.

Table 4. Parameters of modelled trolleybuses

Parameter/vehicle	26tr (single)	27tr (articulated)
Vehicle length	12 m	18 m
Number of axles (powered)	2 (1)	3 (1)
Nominal motor power	200 kW	250 kW
Drive type	Induction motor, VVVF	Induction motor, VVVF
Maximum motive force	36 kN	36 kN
Maximum speed	70 km/h	70 km/h
Mass (empty)	11400 kg	18290 kg
Passenger capacity	91	131
Nominal voltage	660 V DC	

Analysis was carried out for the whole day of regular operation. Schedule was set according to regular workday timetable. For line 12, service begins at around 4:00 with a 15–minute intervals. During the morning peak hours, tact is decreased to 5 minutes. From 8:00 to 13:00 vehicles operate with interval of 10 minutes; at 13:00 another peak with 5–minute tact begins and lasts until 17:00, when service frequency is decreased to 10 minutes. From 19:00 in the evening, interval is further increased to 15 minutes, and it is retained till the last service. Line 12 requires about 12 minutes to run thru analyzed route fragment one–way. Line 15 enters analyzed area at 5:15, and operates regularly throughout the day. Line 17 operates in the area from 5:20 to 6:00 in the morning with 5–minute tact; after that there are a few single services on this route. Lines 15 and 17 operate on the shorter fragment, thru the branch line, which requires about 4 minutes to travel in single direction. Dwelling time at the terminal (end stop) is typically about 10 minutes.

Electrical parameters, including currents and voltages, were calculated for the vehicles and the substation. The substation current was computed as well, including 10 s, 2 min, 5 min, 15 min and 1 h average current. Analogically, average values were calculated from measurements taken traction on substation. Comparison between measurement and outcome of the simulation is shown on waveforms (Fig. 4.7, 4.8, 4.9, 4.10, 4.11).

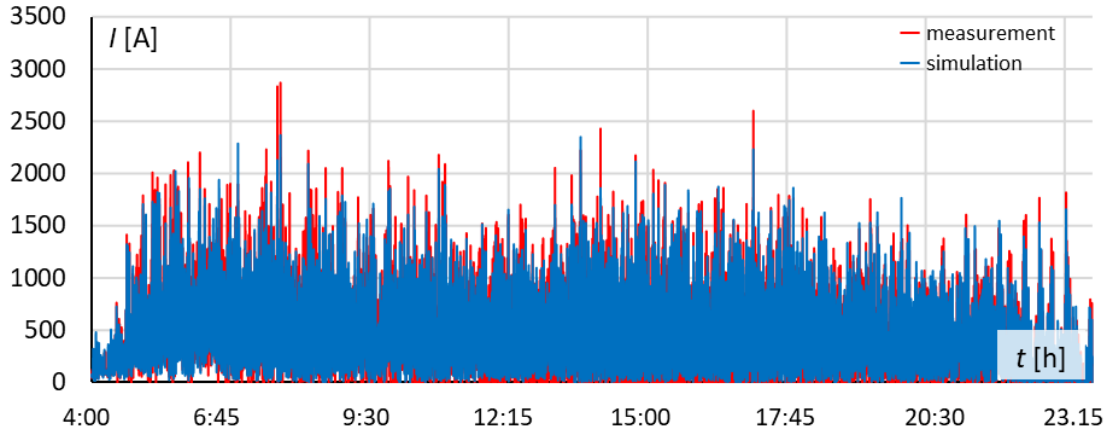

Fig. 4.7. Substation current: 10 second average

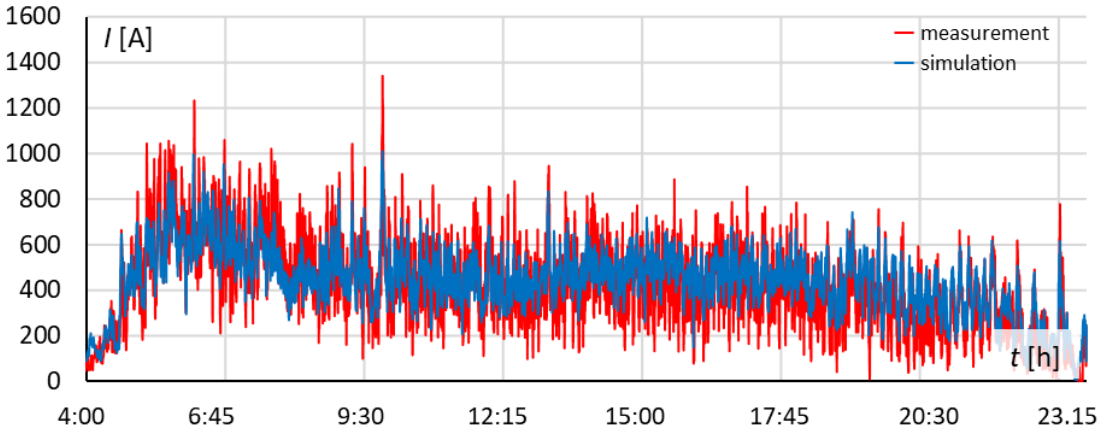

Fig. 4.8. Substation current: 2 min average

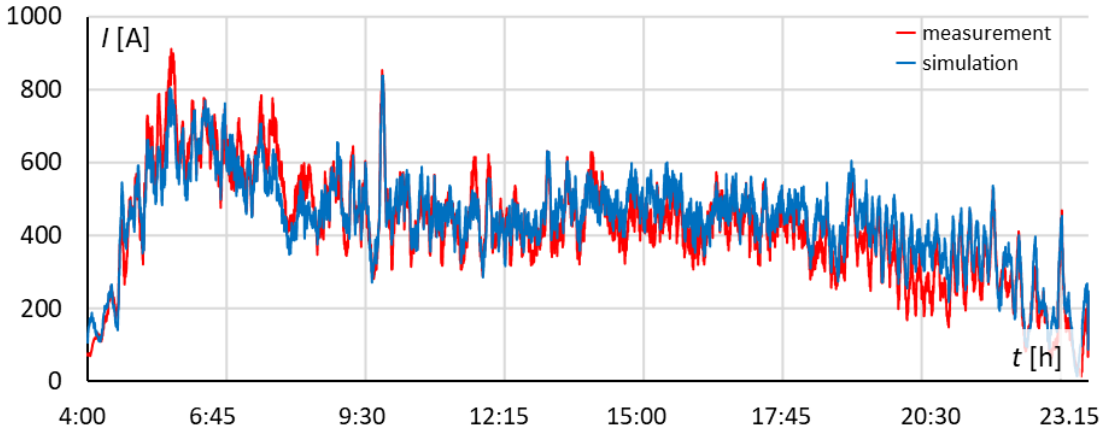

Fig. 4.9. Substation current: 5 min average

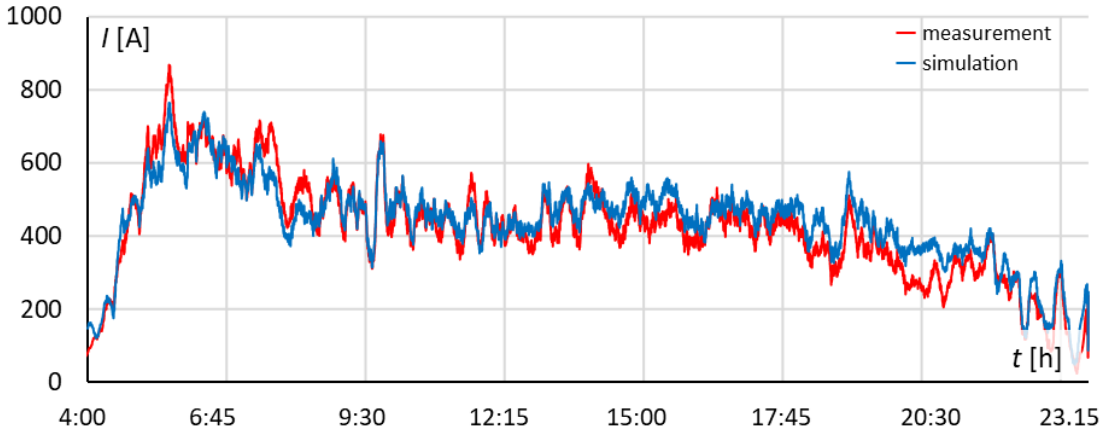

Fig. 4.10. Substation current: 10 min average

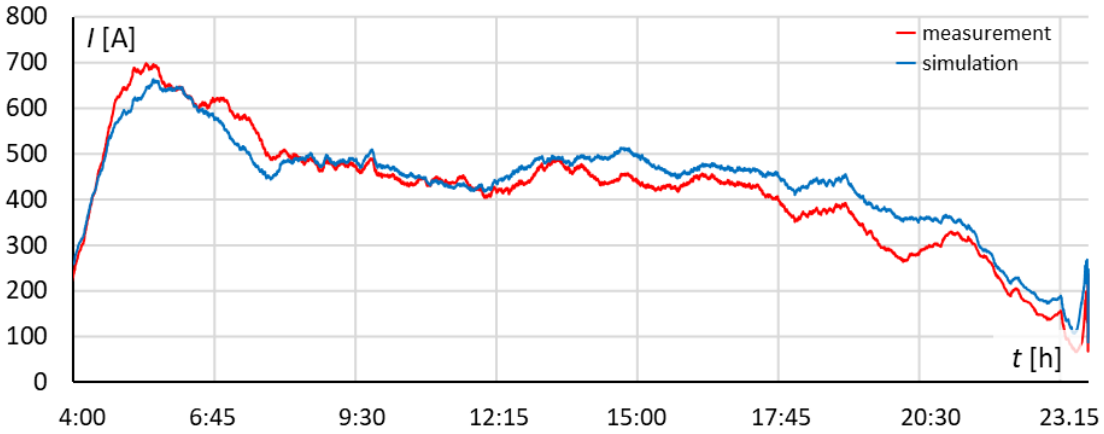

Fig. 4.11. Substation current: 1 h average

Results show that good conformance between measurement and simulation was achieved. The general shape of waveforms is the same for both simulated and measured operation, with characteristic points and peaks occurring precisely at the same time. Slight deviations can be attributed to differences between real and simulated traffic conditions and estimated HVAC power (measurement was taken early March of 2021). Differences between the waveforms for 2 minute average currents stem from different sampling rate of measurement device and simulation timestep; those are less noticeable for longer averaging periods.

Voltage chart confirms high accuracy of executed analysis – maximum error between measured and simulate value does not exceed 14V or 2,8%, and can be expected as the variability of voltage is a result of differences between actual and simulated vehicle movement (Fig. 4.12). Calculated root–mean–square–error (RMSE) for voltage is 8,8 V or about 1,5% of idle voltage. For current, RMSE value is 49,2 A, or 7% of the highest measured current. It should be noted that for 15 minute averages of current that are equal for both recording and the simulation, 15 minute average voltage values are also equal (Fig. 4.12, Fig. 4.13), confirming both model accuracy and correctness of electrical circuit calculation.

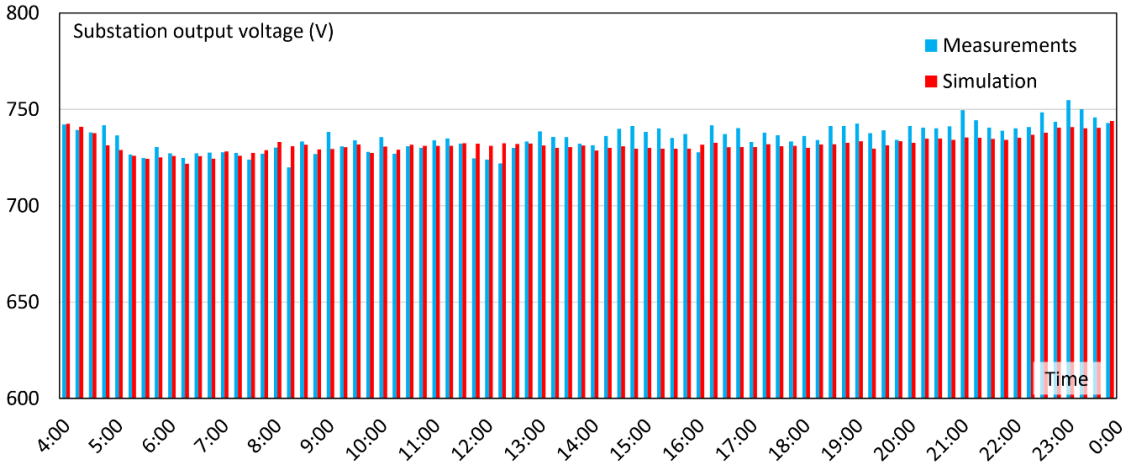

Fig. 4.12. Average 15 min voltages (substation)

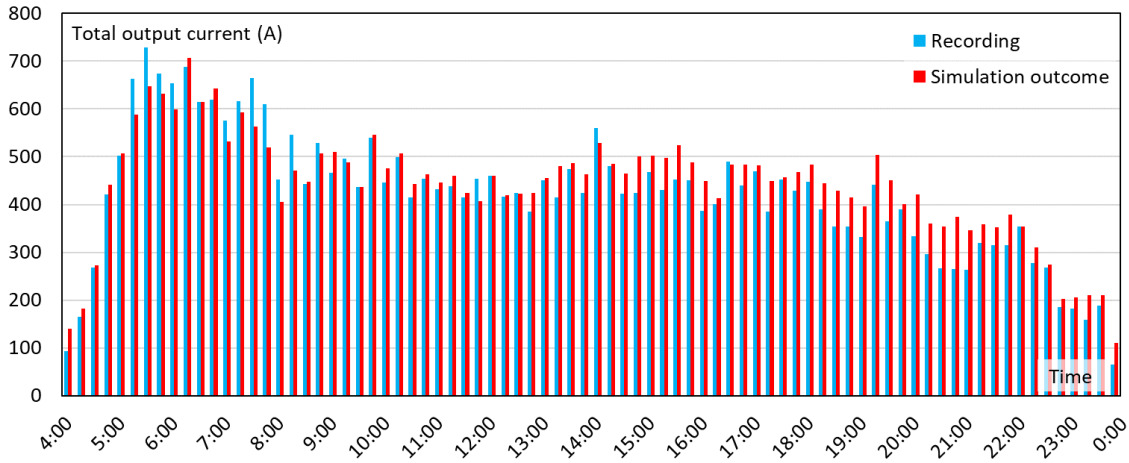

Fig. 4.13. Average 1 min current (substation)

Energy waveform (Fig. 4.14) shows that for the most of the time (up to about 19.00 in the evening) error is negligible; after this, simulated value of energy exceeds measured value slightly. This discrepancy can be attributed to difference between real and simulated traffic conditions – in reality vehicles were running slightly slower than it was assumed, probably due to the increased traffic (there is no separated bus lane on this route). Overall error is however still below 5%, which for such a complex system can be considered a good match, considering that road traffic and random events (on–request stops, traffic lights, pedestrian

crossings, roundabouts) might potentially result in large difference between simulation and measurement.

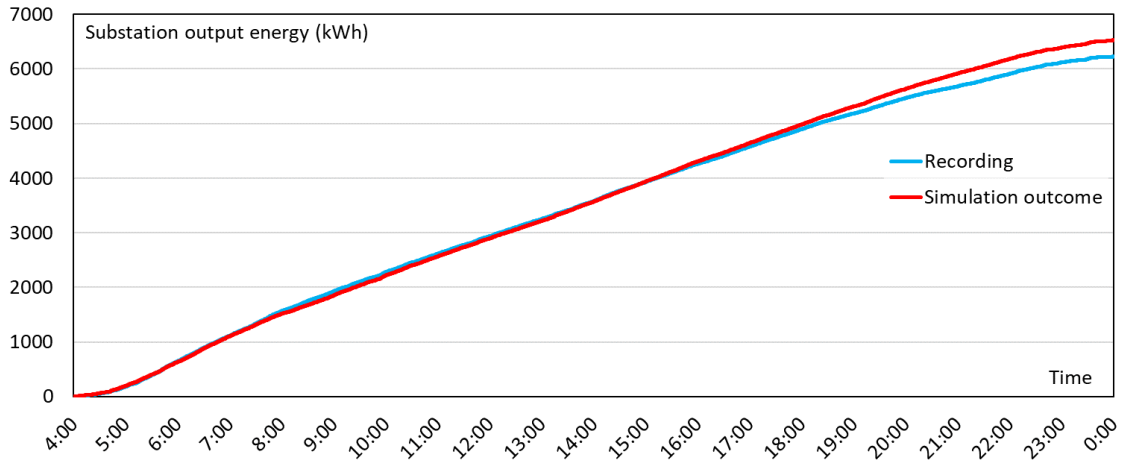

Fig. 4.14. Energy waveforms

Efficiency of regenerative braking for the whole route was computed at 8,5%, with vehicles achieving from 2% to 32% of regeneration during the single run. Measurements confirmed these figures, with average regeneration of 8,7% and vehicle recuperation between 1,5% and 33%. This can be considered a good match, as the simulation was using finite set of the velocity profiles, while in reality each run was slightly different, as the vehicles are operated by human drivers.

Validity of the developed model was confirmed, as the results were published in JCR–listed paper [62], and are further used for development of energy saving methods for trolleybus network in Pilsen. Future work will include analysis of in–motion charging of onboard battery storages and its impact on the system efficiency.

5. IDENTIFICATION OF TRANSPORT SYSTEM OPERATING CONDITIONS

Proposal of the improvement of the energy efficiency of electrified transport should be sufficiently motivated. Evaluation of theoretical algorithms viability for reduced energy consumption can be challenging, when there is no Figure to compare it with. This is because the value of how much energy can be saved or how the CO2 emissions can be reduced is something that can be translated into possible monetary savings. Because of very high costs of railway equipment and their lifespan expressed in decades, careful planning is recommended.

5.1. Assumed bounds of transportation system

The analysis was carried out for a selected part of SKM Trójmiasto urban railway network, localized in northern Poland. This transport system fits the scope of this work well, being an example of suburban railway, with all of its basic characteristics. With 32,7 milion annual ridership [75], it is also one of the biggest people movers in Poland, so looking into possible energy efficiency improvements is desirable.

5.1.1. Rolling stock

For the sake of the analysis, vehicles being currently in service of SKM Trójmiasto were modelled. However, the scope of this work was limited only to include electric multiple units equipped with induction motor drives, as they are capable of regenerative braking and allow for wide motive force regulation. Moreover, because of the ongoing plans for purchasing new vehicles for this service, it is expected that the older vehicles with rheostatic DC motor drives will be gradually modernized or retired from service. Therefore, excluding them from this analysis is justified. Similarly, multiple units equipped with chopper DC drives were modernized and are currently equipped with induction drives. Parameters of vehicles considered in analysis are shown in Tab. 5.

Tab. 5. Basic parameters of analyzed trains

Vehicle	**EN57AKM [15]**	**EN71SKM [15]**	**31WE [27]**
Manufacturer /modernization	Pafawag/Pesa+ ZNTK MM	Pafawag/Newag	Newag/-
Assumed number	double	single	double
Axle layout	2'2'+Bo'Bo'+2'2'	2'2'+Bo'Bo'+Bo'Bo' +2'2'	Bo'2'2'2'Bo'
Nominal power (continuouns)	1000 kW	2000 kW	2000 kW
Acceleration	0,8 m/s^2	1,4 m/s^2	1,1 m/s^2
Mass (empty)	125 Mg	180 Mg	135 Mg
Mass (full load)	160 Mg	225 Mg	175 Mg
Res. coefficients	A = 2560,790 N B = 66,195 N/m/s C = 7,245 N/m/s^2	A = 3512,127 N B = 96,379 N/m/s C = 8,516 N/m/s^2	A = 2617,378 N B = 95,321 N/m/s C = 7,516 N/m/s^2
Passenger cap.	158/468	242/624	202/460
Aux. power	67,7 kW (HVAC) 26 kW (other)	89,6 kW (HVAC) 26 kW (other)	120 kW (incl. HVAC, 75 kW)

Electric multiple units of classes EN57AKM and 31WE typically operate as trains consisting of two coupled units; EN71 class operates as single unit, due to incompatibility of control systems between vehicle classes. Despite very high nominal starting acceleration values, in reality vehicles accelerate slower. Because during the acceleration and braking phases the motive force is controlled manually, setting catalogue parameters for the simulation would be incorrect. There is a need for analysis of measured velocity profiles.

The duty cycle of the HVAC systems is dependent on the temperature. Because the analysis does not include air circulation within vehicles, the percentage of time with heating turned on has been measured during the large number of train runs. Measurement results are shown on Fig. 5.1.

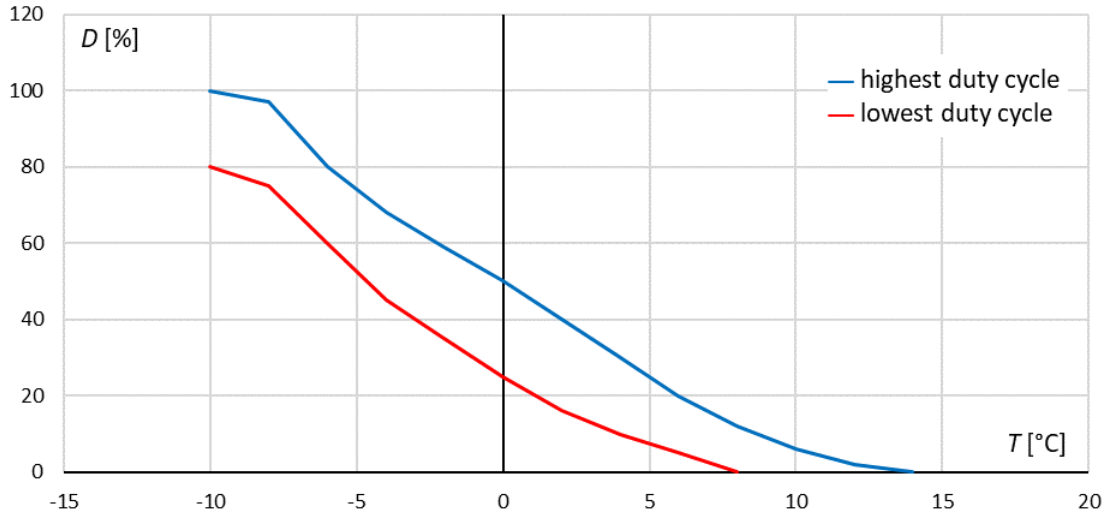

Fig. 5.1. Percentage of running time with heating turned on (HVAC duty cycle) vs. outside air temperature – maximum and minimum value

During recorded runs, heating could be working for a longer or shorter time even when the outside temperature was the same, therefore maximal and minimal percentages for each temperature was noted. Consequently, duty cycle of simulated HVAC system is selected randomly with measurements serving as limitations for selected value.

5.1.2. Considered route

Trains of the SKM Trójmiasto operate on multiple routes within Pomeranian Voivodeship. The main and most popular service, however, is found within Tricity agglomeration, with separate infrastructure between stations Gdańsk Śródmieście and Rumia (railway line no. 250). Railway line is built as double track and has length of 32 km, with 24 stations [157]. Electrification system is 3000 V DC, with dedicated traction substations located in Gdańsk Wrzeszcz, Sopot Wyścigi and Gdynia Redłowo.

This thesis focused on fragment of the railway line 250 between stations Gdańsk Śródmieście and Gdynia Redłowo, totaling 18,5 km in length (Fig. 5.2). The motive is the

possibility of analysis the suburban railway system independently from parallel intercity line 202, industrial sidings and port connection, which have their power supply interconnected beginning from Gdynia Redłowo substation (further northwest, there is section cabin in Gdynia Grabówek that connects all the tracks, and traction substation in Gdynia Cisowa powers intercity line, SKM line and industrial lines).

Fig. 5.2. Map of the analyzed line fragment, with stations (blue) and traction substations (orange) locations shown

Route profile does have multiple altitude changes, with maximum inclination of 10‰ (Fig. 5.3). Curvature and inclination differs slightly between the two tracks, having a few curves with a radius below 400 m, mostly in proximity of stations (platforms are in most cases located between the tracks). The profile was implemented using data from route plan, where inclination, curve radiuses and length were stated directly. There is also a 250 m long tunnel between Gdańsk Śródmieście and Gdańsk Główny stations, however its large cross–section and relatively low speed allows to neglect additional aerodynamic drag. The whole route has speed limit of 70 km/h with few exceptions seen on track 501 (tight curves near Sopot station platform, pedestrian crossing in Gdańsk Zaspa, switches in tunnel between Gdańsk Śródmieście and Gdańsk Główny).

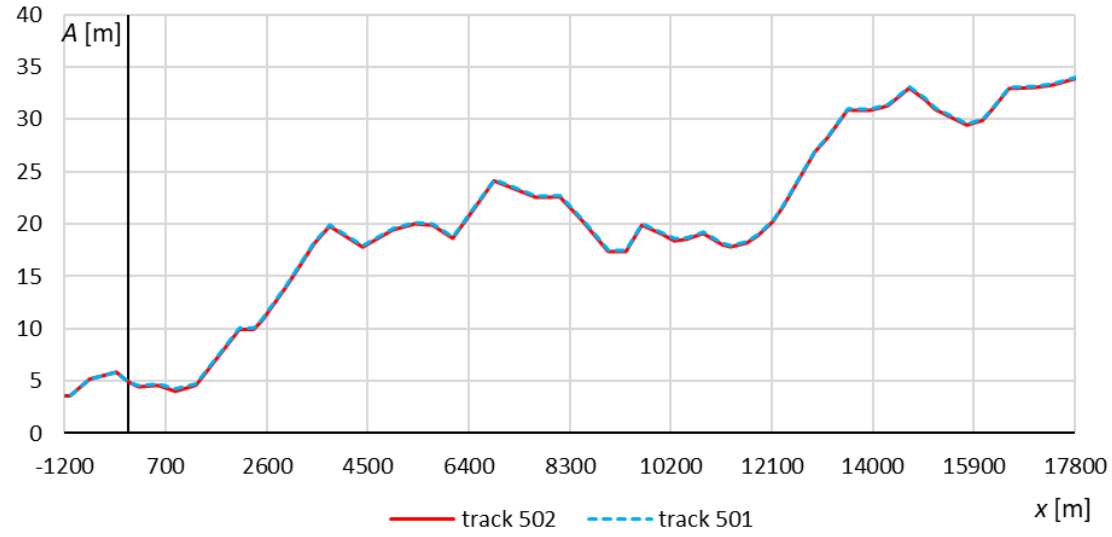

Fig. 5.3. Inclination profile of analyzed route (absolute route distance in m)

Analyzed fragment consists of 3 power supply sections, powered by traction substations localized in Gdańsk Wrzeszcz, Sopot Wyścigi and Gdynia Redłowo (Fig. 5.4). The substations are equipped with four PD16/3,3 12–pulse rectifier units each. The feeders were laid using 630 mm^2 aluminum cables. First of the sections (between Gdańsk Śródmieście and Gdańsk Wrzeszcz) is powered only by one substation, with transverse connection at the end, while remaining two are fed from two sides, without transverse connection. Catenary is made from copper wire and consists of two contact lines, 100 mm^2 each, catenary line, 95 mm^2 and additional "booster cable" with cross section of 120 mm^2. Booster cable is installed in order to reduce voltage drops in catenary and suspended on the same pylons as the catenary. The tracks were built using welded S49 rails along the whole analyzed route.

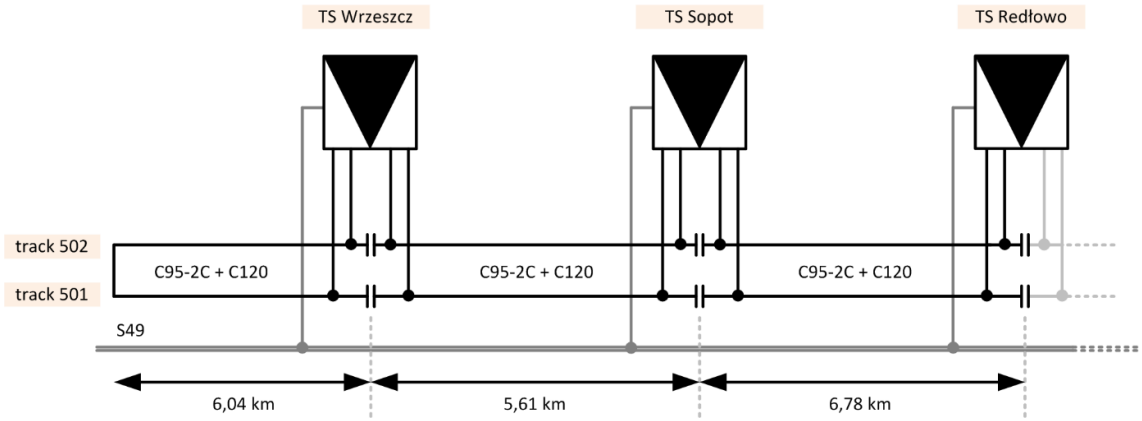

Fig. 5.4. Diagram of power supply for analyzed route

To ensure adequate passenger service, timetable was formulated with 7–8 minute tact during peak hours, prolonged to 15 min off peak and 30 min early in the morning or at night. According to timetable calculation rules [55], for every 100 km of route length, 5 minute time reserve must be added for local train. This results in travel times are specified in Table 6.

Tab. 6. Travel times between stations and their location along the route [157]

No.	km	Abbrev.	Station	Direction Gdańsk/ Track 502	Direction Gdynia/ Track 501
1	-1,01	GDS	Gdańsk Śródmieście	-	2
2	0,00	GDG	Gdańsk Główny	3	3
3	1,04	GDT	Gdańsk Stocznia	2	2
4	2,52	GDP	Gdańsk Politechnika	2	2
5	4,18	GDW	Gdańsk Wrzeszcz	3	3
6	5,39	GDZ	Gdańsk Zaspa	2	3
7	6,98	GDU	Gdańsk Przymorze – Uniwersytet	2	2
8	8,08	GDO	Gdańsk Oliwa	3	2
9	9,27	GDA	Gdańsk Żabianka – AWFiS	2	3
10	10,41	SPW	Sopot Wyścigi	2	2
11	11,66	SPT	Sopot	3	4
12	13,56	SPK	Sopot Kamienny Potok	2	3
13	15,90	GAO	Gdynia Orłowo	3	2
14	17,54	GAR	Gdynia Redłowo	2	-
			Total time	31 min	33 min

Typical station dwelling time is between 20 and 40 seconds, with exception of Gdańsk Główny (2 min) and Sopot (1 min). There is also around 10 minutes of time at the Gdańsk Śródmieście terminal, giving necessary time for changing direction. Because the dwelling time can differ between runs, degree of variability was implemented: in simulation, dwell time consists of constant base time, equal to 15 seconds and variable additional time, which is RNG based and can achieve values between 5 and 25 seconds. Seed for random number generator is selected independently for every analyzed vehicle; therefore there are no identical runs. For stations that require setting longer dwell time, it is done independently, overriding randomization algorithm. First and last trains of the day begin and end their runs on Gdańsk Główny station, with first train arriving at Gdańsk Śródmieście is the fourth service of the day bound for Gdańsk. Terminal dwell time is set at about 10 minutes, coded into travel time. This however is sometimes prolonged using permission function in order to synchronize vehicles with required tact.

Passenger numbers are also variable, depending on time of the day and station. Basing on published passenger flow statistics [92,124] and author's own observations, two occupancy charts were assumed – vehicle occupancy depending on station and depending on time of the day (Fig. 5.5). Those values are multiplied, along with mass of the maximum allowed vehicle load, resulting in additional weight of vehicle load (passengers). Author argues, that it is more reliable approach than setting absolute passenger numbers, and 70 kg per passenger because of risk of vehicles exceeding maximum allowed axle load with all places (sitting and standing) occupied. This introduces variability of vehicle mass, which has an impact on energy consumption (shown in chapter 6).

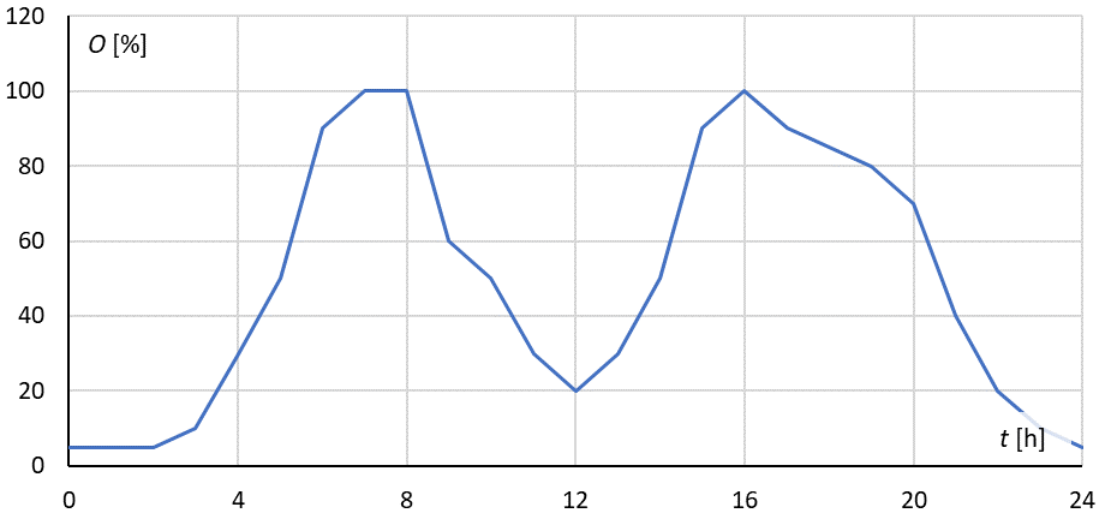

Fig. 5.5. Occupancy rate *O* depending on time of the day

It is worth noting that the route between Gdańsk and Gdynia is covered on average over 100 times in every direction every day, therefore even minor improvement of energy efficiency for single run will add up to much greater total savings given service frequency.

Analysis has been carried out for single day of regular operation, from 2:00 at night, right before first train to around 1:30, after the last train. There is about two hours break between two night trains and beginning of the regular service, dedicated for safety and maintenance inspection.

5.2. In–depth analysis of velocity profiles

Velocity profiles set in simulation are based on large number of measurements, taken on real trains running on analyzed route, during various hours and days of year, from 2017 up until 2021. The recordings have been carried out by author using standard GNSS recorder. Only recordings with 14 satellites or more were taken into account, because of resulting position precision of 5 m or below. This, combined with observation of movement dynamics and sound from traction drive, allowed to determine realistic velocity profiles. On fragments where signal from the satellites was unreliable due to obstruction caused by buildings covering the route, measurement was taken using accelerometer.

Recorded velocity data was filtered using Savitzky–Golay (SG) filter [87,155] with variable window length, in order to obtain smooth waveforms suitable for further analysis. For this task, Analyzer application was developed – its algorithm is explained in subsection 5.2.2. The application is suitable for calculating vehicle acceleration values from GNSS data, comparing them against accelerometer data and manually collected run information. Because of this, database comprising all the recorded runs along with their parameters is synthesized, enabling not only single run analysis, but the statistical data as well. The application calculates also cruising velocities and detects movement phases.

5.2.1. Movement dynamics analysis

Acceleration values are important for setting the velocity profile, because in the real vehicle, the motive force is controlled manually by the driver. Therefore, it is not guaranteed that it will be always set at 100%, especially when there are multiple vehicle types in use and timetable is typically computed for the slowest vehicles in operation [55]. To address this, author analyzed large set of train run records, computing starting acceleration values (up to 40 km/h), as the parameter is specified in vehicle datasheets. Runs with interrupted acceleration (because of maintenance, track change or pedestrian crossing) were ignored. Obtained data, as a percentage of all recorded runs is presented on Fig. 5.6 and 5.7:

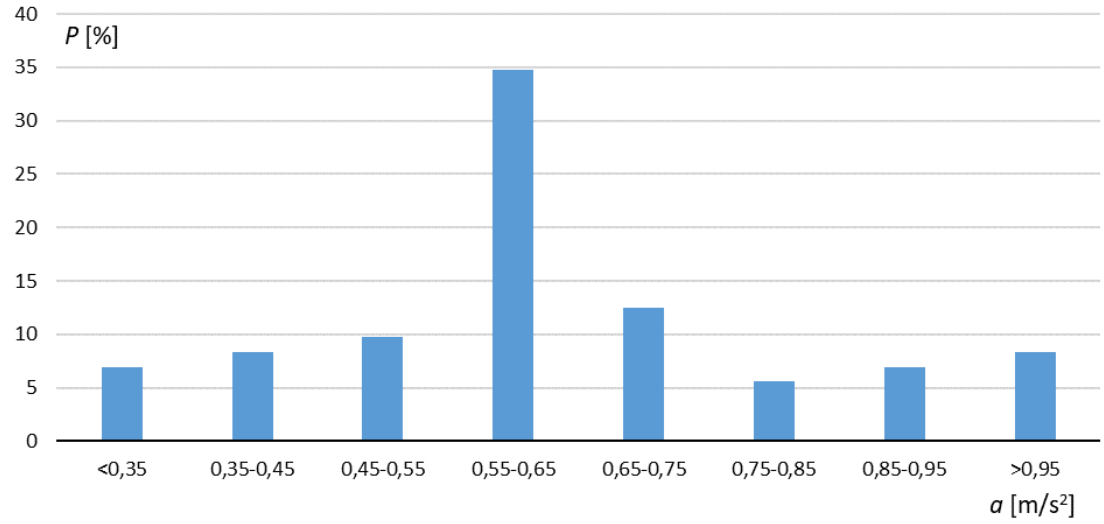

Fig. 5.6. Percentage of acceleration values – track 501 (direction Gdynia)

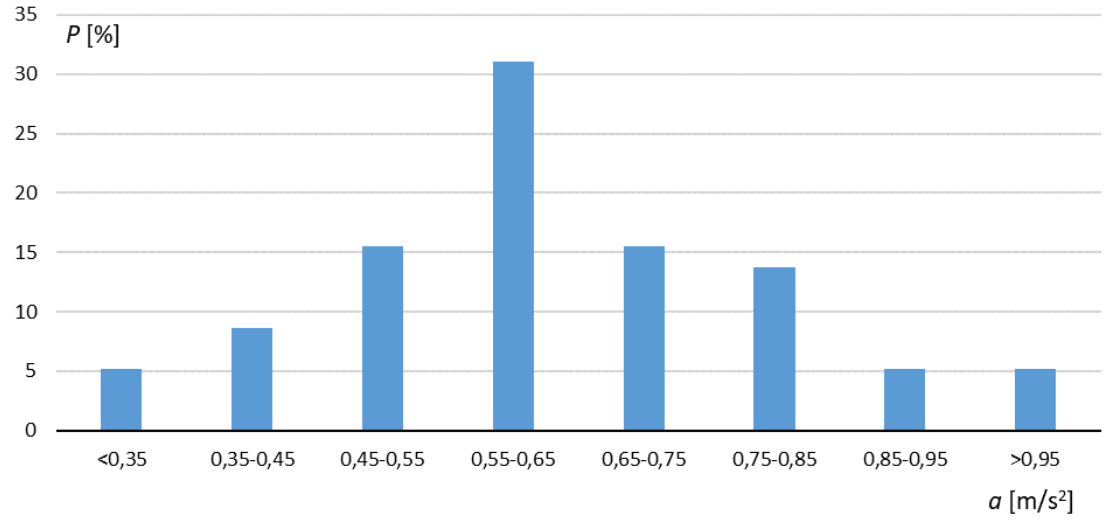

Fig. 5.7. Percentage of acceleration values – track 502 (direction Gdańsk)

It can be concluded, that in most runs trains accelerated with about 0,6 m/s^2, constituting for over 30% of recorded runs. Runs with slower acceleration amount to 25% combined, while the most probable higher value of acceleration is about 0,7 m/s^2. It is worth noting

that maximum acceleration of modernized EN57AKM is only about 0,8 – 0,9 m/s^2; higher values of acceleration were only recorded onboard 31WE and especially EN71SKM. Therefore, for the sake of the analysis, acceleration of all the vehicles was set at 0,6 m/s^2 as a middle ground and most common acceleration value. Trains bound for Gdańsk accelerate slightly faster, probably because of larger part of the route being downhill.

Similar analysis was carried out for braking (Fig. 5.8, 5.9). Because deceleration of vehicle is also controlled manually, the value used in the analysis should not be based on maximum nominal values, but on typical measured ones. This should be highlighted as the maximum braking mass will guarantee much higher deceleration value than is ever achieved during everyday service.

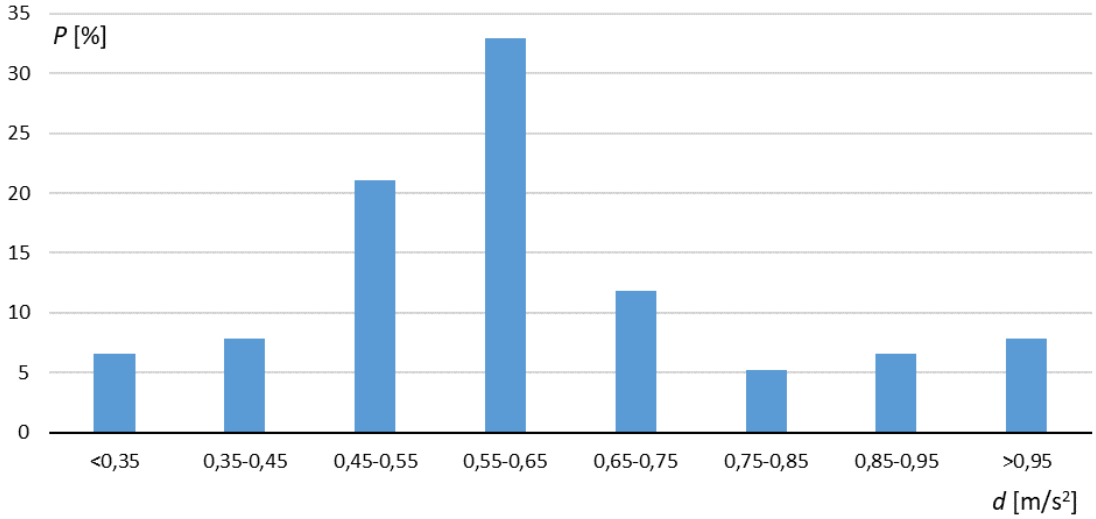

Fig. 5.8. Percentage of deceleration values – track 501 (direction Gdynia)

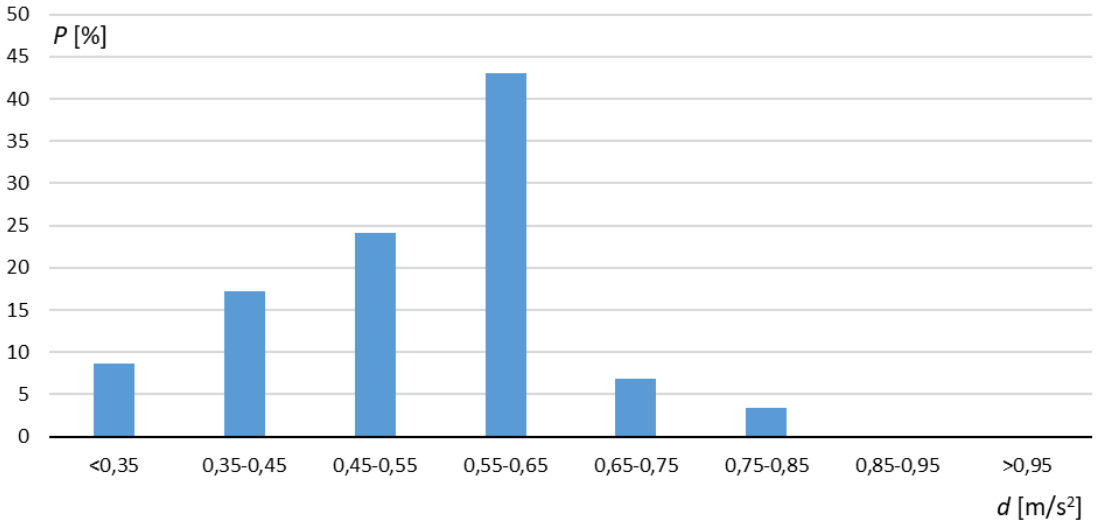

Fig. 5.9. Percentage of deceleration values – track 502 (direction Gdańsk)

Analysis shows that braking is characterized by similar values of deceleration, mostly about 0,6 m/s^2, and more often below 0,55 m/s^2 than acceleration. More dynamical deceleration

is observed rarely, and this was also mostly onboard the EN71SKM vehicle. Trains running towards Gdynia were more likely to decelerate more intensively as the route is going uphill.

It should be noted that drivers rarely engage brakes with fixed force value; more often the braking force is applied fluently, with slight increases and decreases. As implementation of such behavior would result in inconsistent braking distances, the Analyzer software was set to compute average values of deceleration from movement phase change point down until vehicle stop. Therefore, in simulation braking was assumed with constant deceleration of 0,6 m/s^2.

5.2.2. Movement phases vs. distance

Knowledge about acceleration and braking is necessary for setting benchmark velocity profile, however it is also important to look into movement that happens between. In case of analyzed route, speed limit is consistent at 70 km/h, which does not mean that all vehicles run at that exact speed with cruise control active. Because change of movement phase is often described as distance–dependent [9,21,93,118,125,151], insight in relation between the velocity and distance is preferable, as this will allow to find the movement phase change locations. There is also a potential of finding multiple possible velocity profiles for each station–to–station run, which is a basis for improvement of simulation accuracy, as the model has the random–with–variable–probability velocity profile selection implemented. Because vehicles are driven by human operators, variability of velocity profiles is expected. However, dealing with large dataset directly, manually deciding which movement phase occurs where is inefficient and prone to human errors. Because of this, the author proposed alternative approach, using Analyzer software developed for this task.

In this case, the route was divided into equal blocks, 50 m in length. The length of the blocks is adjustable, but selected value should be a middle ground between the accuracy and readability of the results. For each block and each run, average values of acceleration were computed and stored. Then, values of acceleration were compared to the threshold values of movement phases, deciding where they belong to. Such solution allowed for analysis of many velocity profiles at the same time, with probability of movement phase occurrence at determined location included. Author would like to point out that such approach is more reliable than analyzing few recorded velocity profiles directly, as it shows how often possible profiles are realized. Improvement of the algorithm precision was achieved, when the GNSS recording data is enhanced by information about traction drive work (collected manually). Detailed algorithm of this Analyzer program is shown in Fig. 5.10.

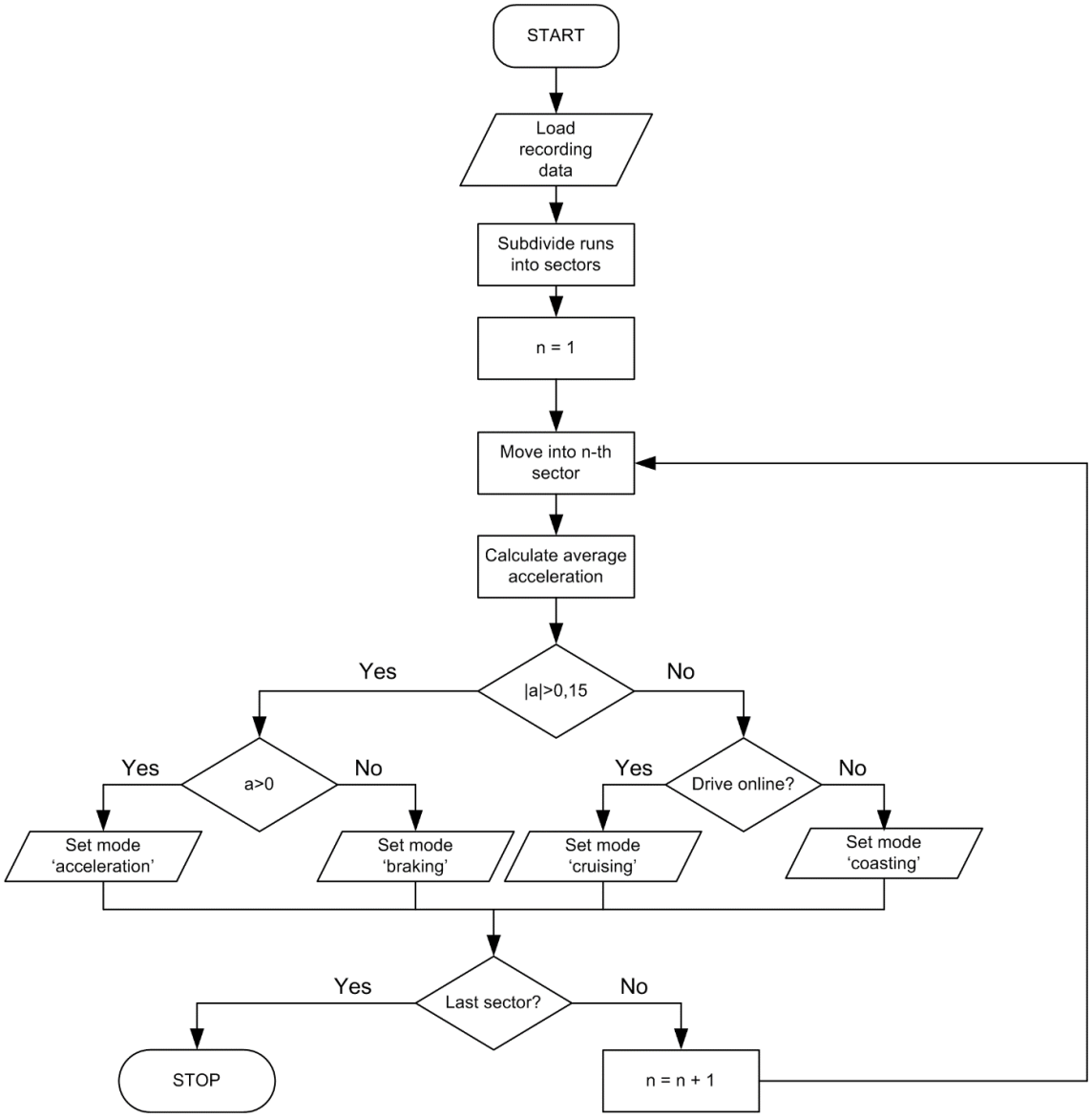

Fig. 5.10. Movement phase determination algorithm – Analyzer application

Such data is helpful in determining velocity profiles executed in normal transport system operation. Proposed method is also advantageous over analyzing a few runs displayed as a velocity waveforms because it is based on a large set of recorded runs. Therefore, general information about velocity profiles and driving technique is obtained, and the data can be compiled into reference velocity profiles with variable probability of executing any of those in simulation. Author argues that such preparation of input parameters will increase quality of the analysis, similarly to what was done in case of Pilsen trolleybuses [62].

For the first three stations of the route, author managed to record less runs than for the remaining ten – because of the tunnel and multiple viaducts, precision of the GNSS recorder was unsatisfactory, and accelerometer was of limited use because of the vehicle swaying while travelling through the switches. Movement phases data for runs between Gdańsk Śródmieście and Gdańsk Główny are shown in Fig. 5.11 for track 501 and Fig. 5.12 for track 502.

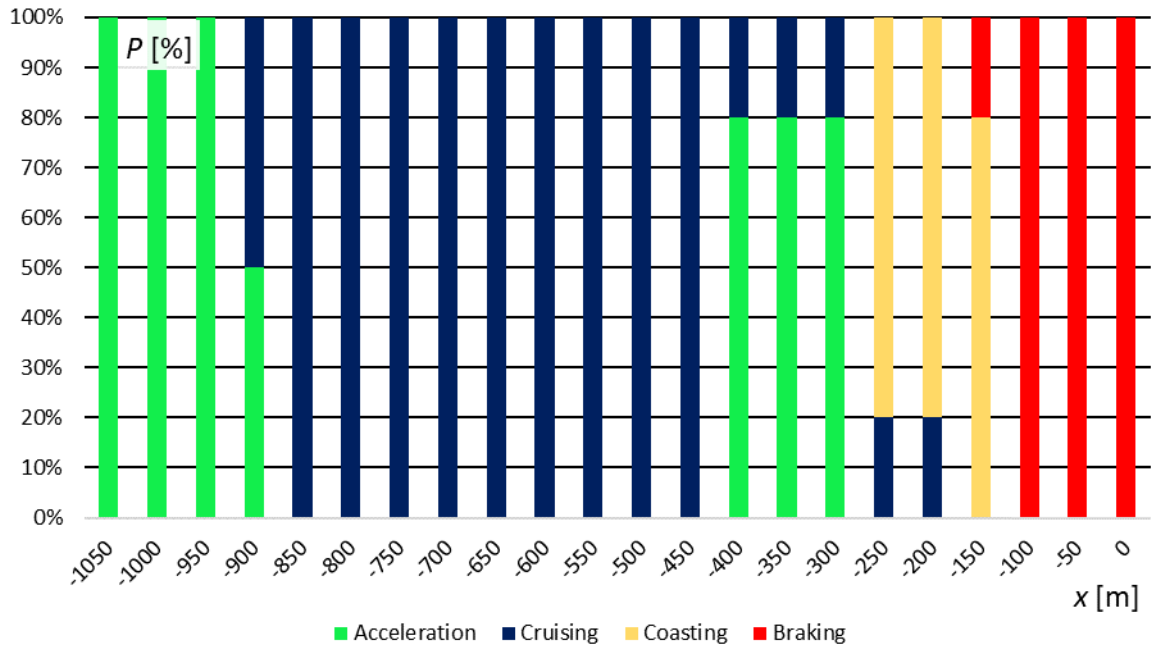

Fig. 5.11. Movement phases – route Gdańsk Śródmieście – Gdańsk Główny, track 501 (direction Gdynia)

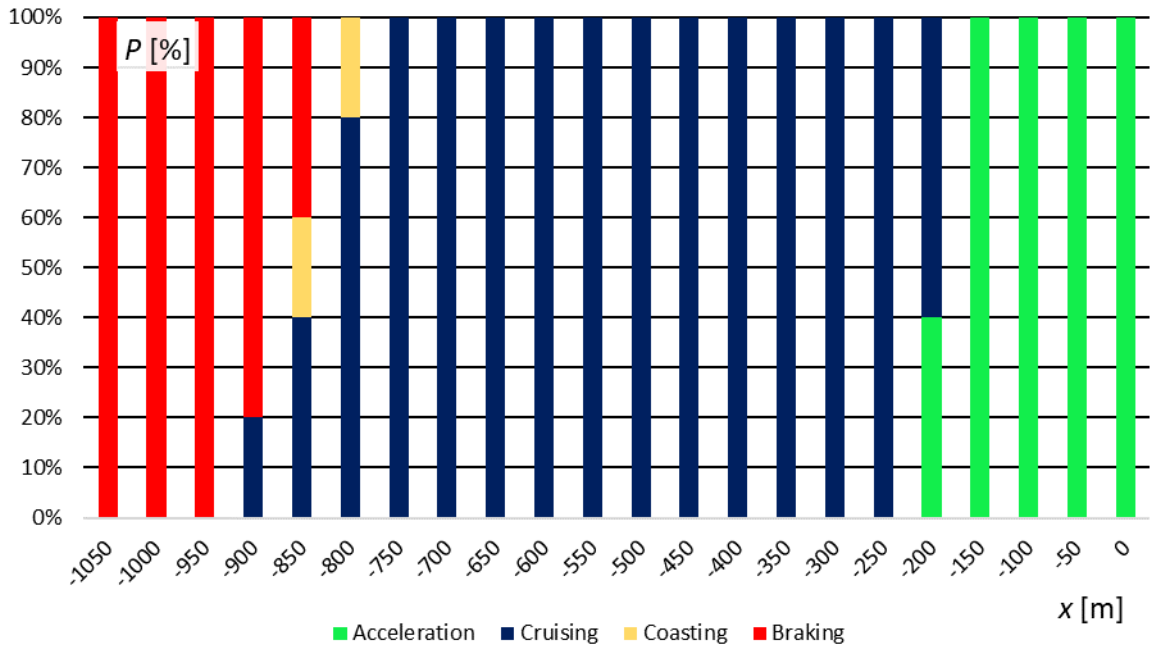

Fig. 5.12. Movement phases – route Gdańsk Śródmieście – Gdańsk Główny, track 502 (direction Gdańsk)

It can be concluded that most of the distance is covered with constant velocity. Running towards Gdynia, trains accelerate slightly when out of the tunnel, then coast up to the platform. Further, the trains go between Gdańsk Główny and Gdańsk Stocznia (Fig. 5.13, Fig. 5.14).

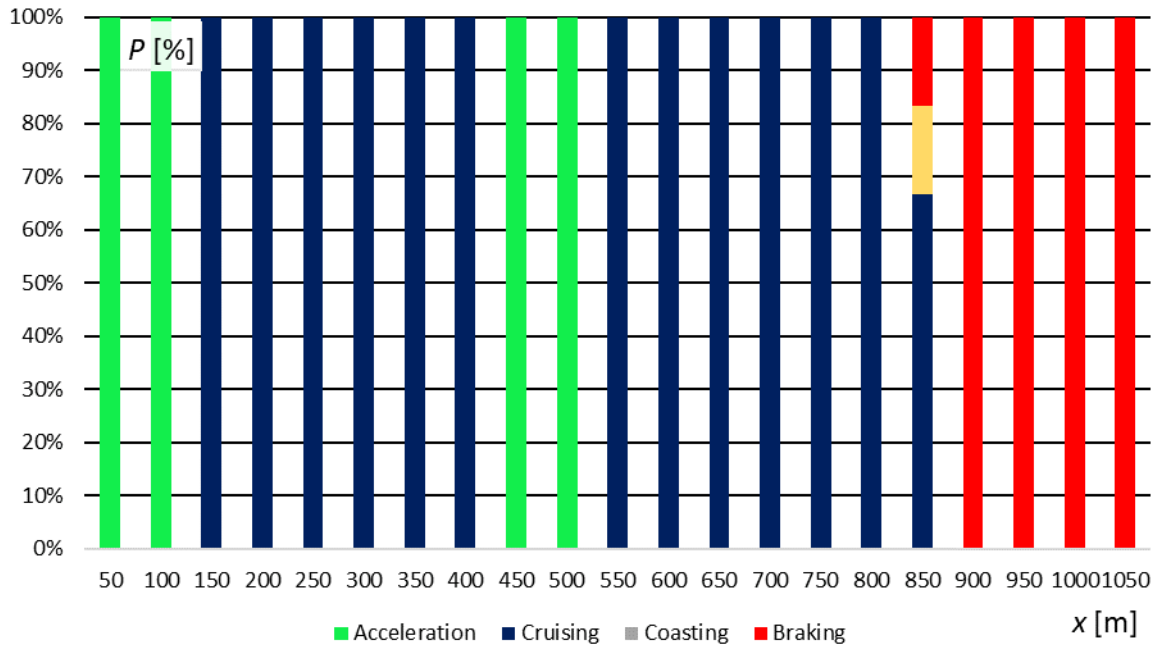

Fig. 5.13. Movement phases – route Gdańsk Główny – Gdańsk Stocznia, track 501 (direction Gdynia)

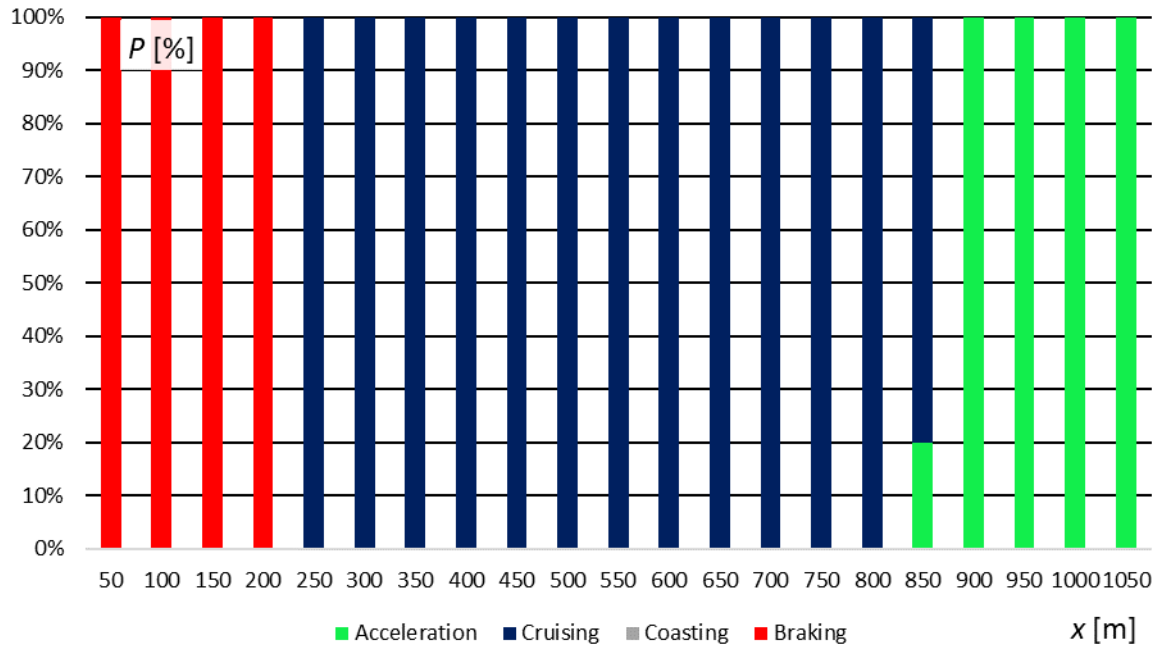

Fig. 5.14. Movement phases – route Gdańsk Główny – Gdańsk Stocznia, track 502 (direction Gdańsk)

Going towards Gdynia, trains go slower thru switches, then accelerate to constant velocity. Towards Gdańsk, route goes straight thru switches and track curvature has significantly larger radius, so deceleration is not needed. The next part of the route is between Gdańsk Stocznia and Gdańsk Politechnika (Fig. 5.15, Fig. 5.16).

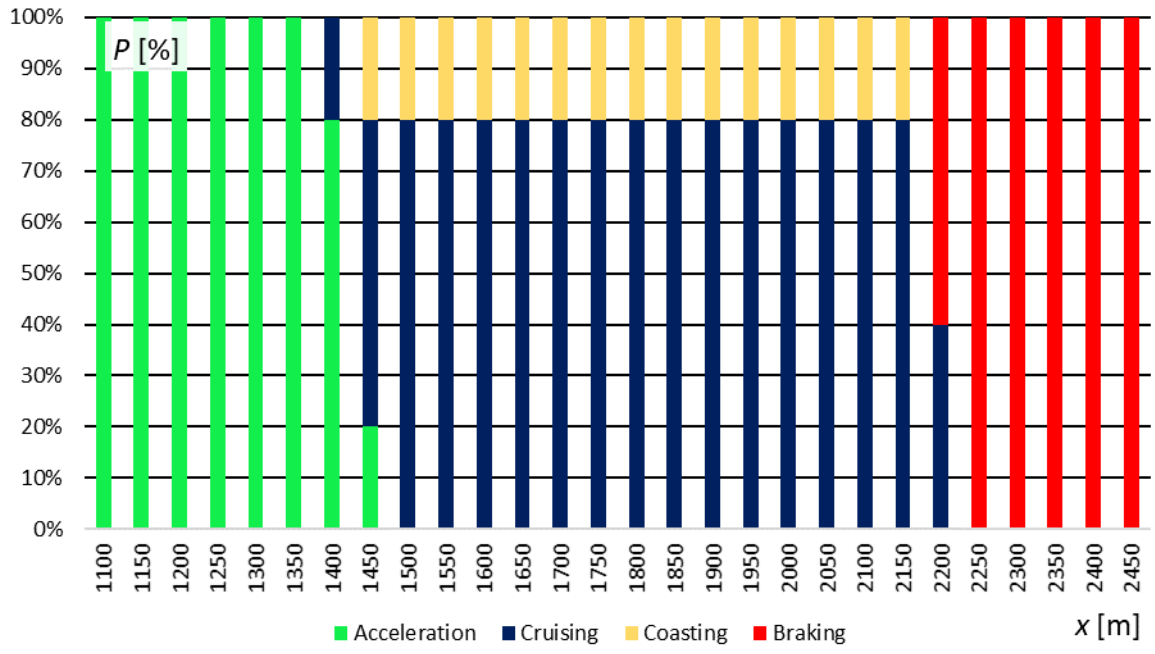

Fig. 5.15. Movement phases – route Gdańsk Stocznia – Gdańsk Politechnika, track 501 (direction Gdynia)

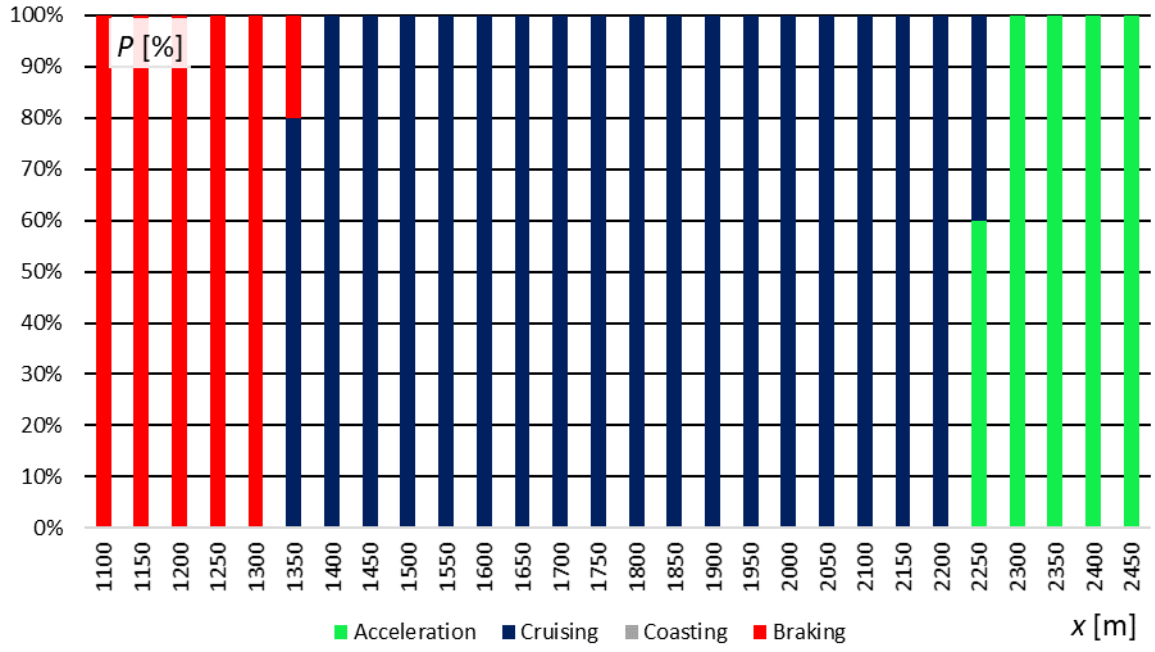

Fig. 5.16. Movement phases – route Gdańsk Stocznia – Gdańsk Politechnika, track 502 (direction Gdańsk)

This fragment is covered mostly at a constant velocity. This might be because of additional resistance from a long curve that trains run thru. The next fragment is between Gdańsk Politechnika and Gdańsk Wrzeszcz (Fig. 5.17, Fig. 5.18).

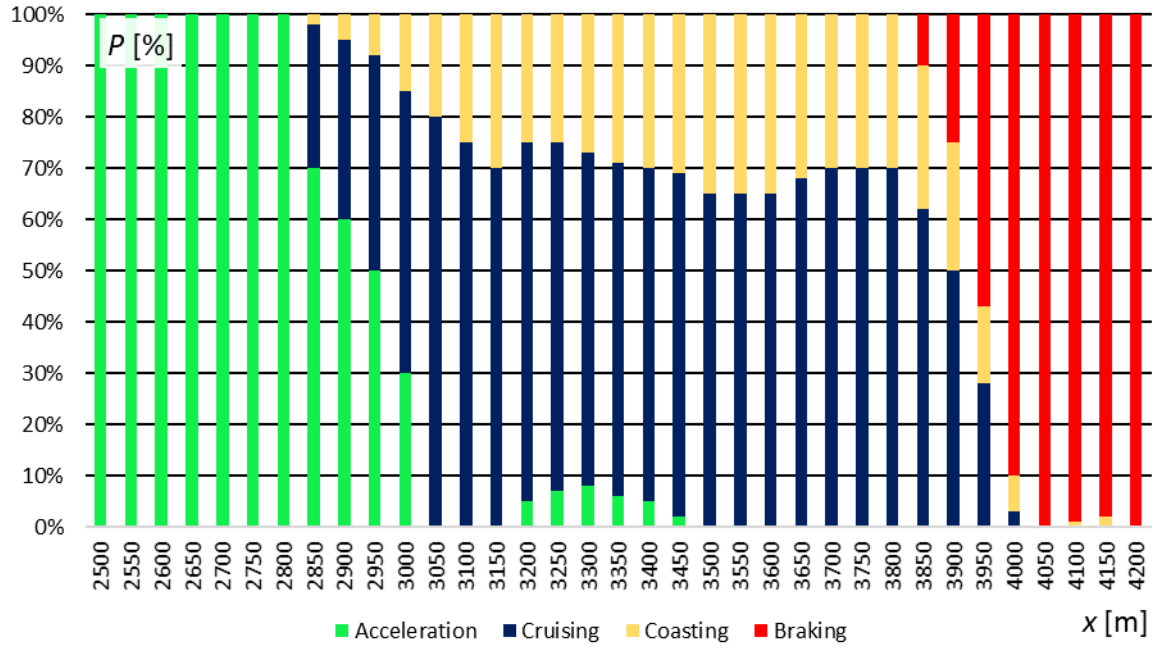

Fig. 5.17. Movement phases – route Gdańsk Politechnika – Gdańsk Wrzeszcz, track 501 (direction Gdynia)

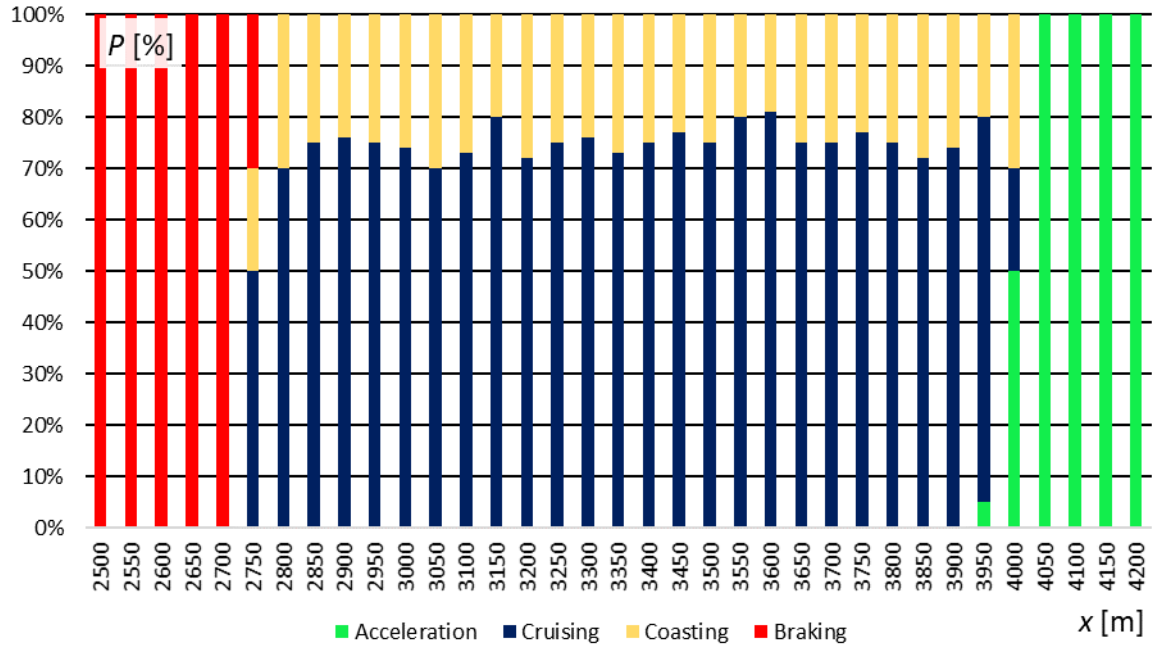

Fig. 5.18. Movement phases – route Gdańsk Politechnika – Gdańsk Wrzeszcz, track 502 (direction Gdańsk)

Towards Gdynia, vehicles accelerate slowly, and run more often with constant velocity (up to 80% of runs) than with coasting. In opposite direction situation is similar. Then, the route goes towards Gdańsk Zaspa (Fig. 5.19, Fig. 5.20).

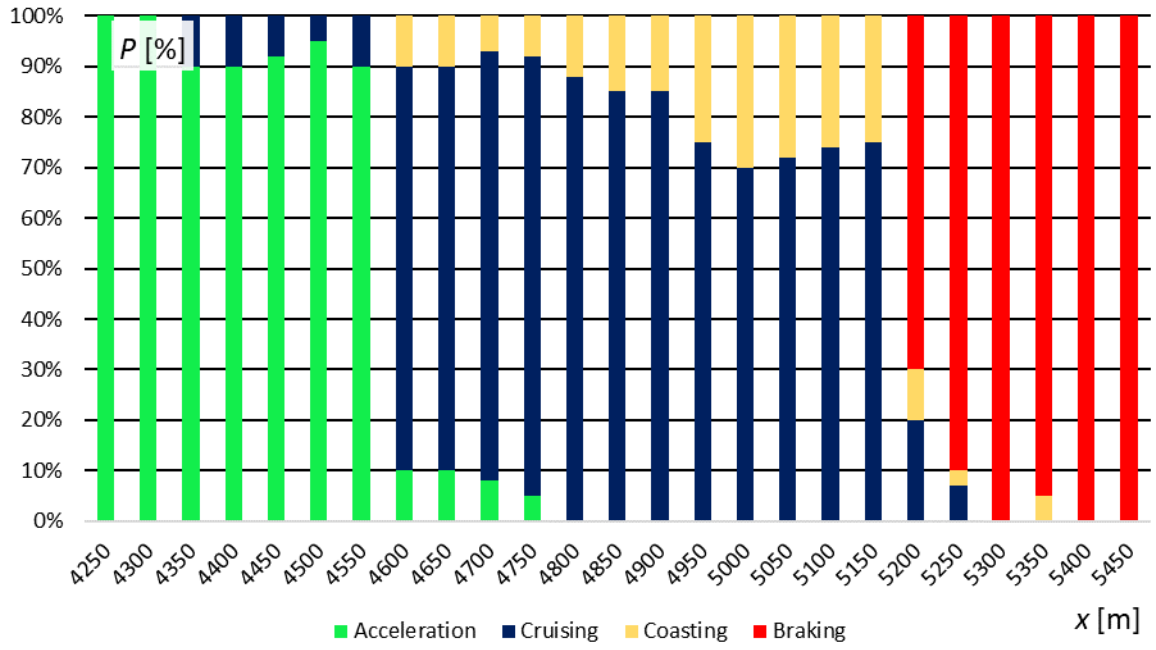

Fig. 5.19. Movement phases – route Gdańsk Wrzeszcz – Gdańsk Zaspa, track 501 (direction Gdynia)

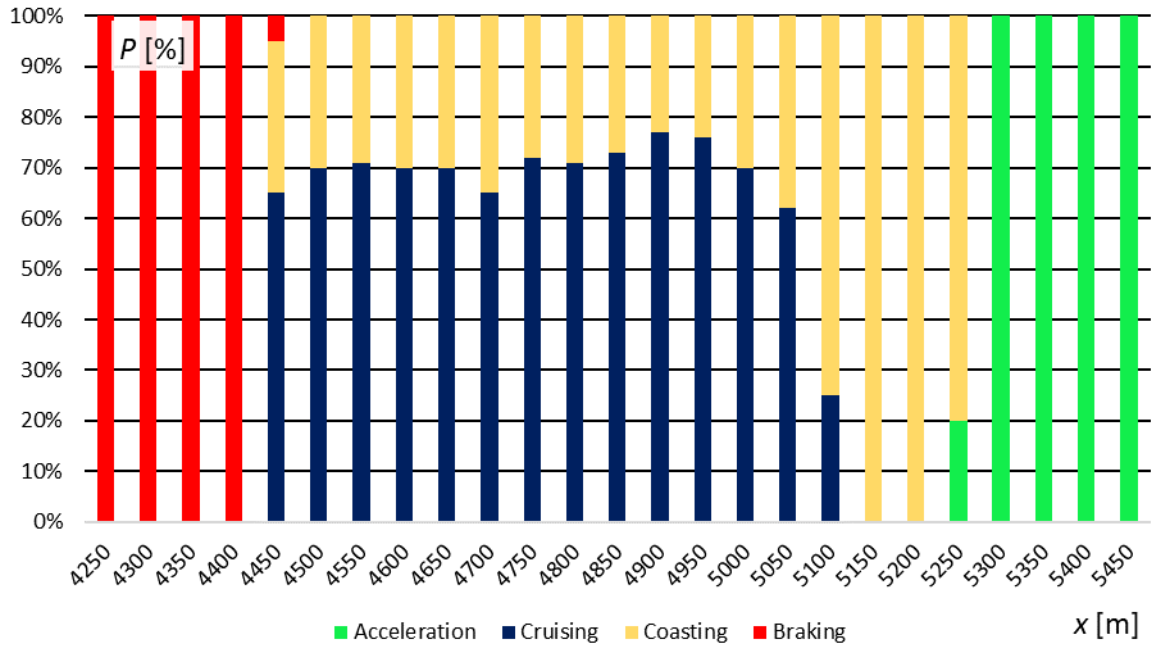

Fig. 5.20. Movement phases – route Gdańsk Wrzeszcz – Gdańsk Zaspa, track 502 (direction Gdańsk)

Majority of the recorded runs were driven with constant velocity. There is route fragment when all the trains were coasting, probably because of section insulator located there. Then, route continues to Gdańsk Przymorze (Fig. 5.21, Fig. 5.22).

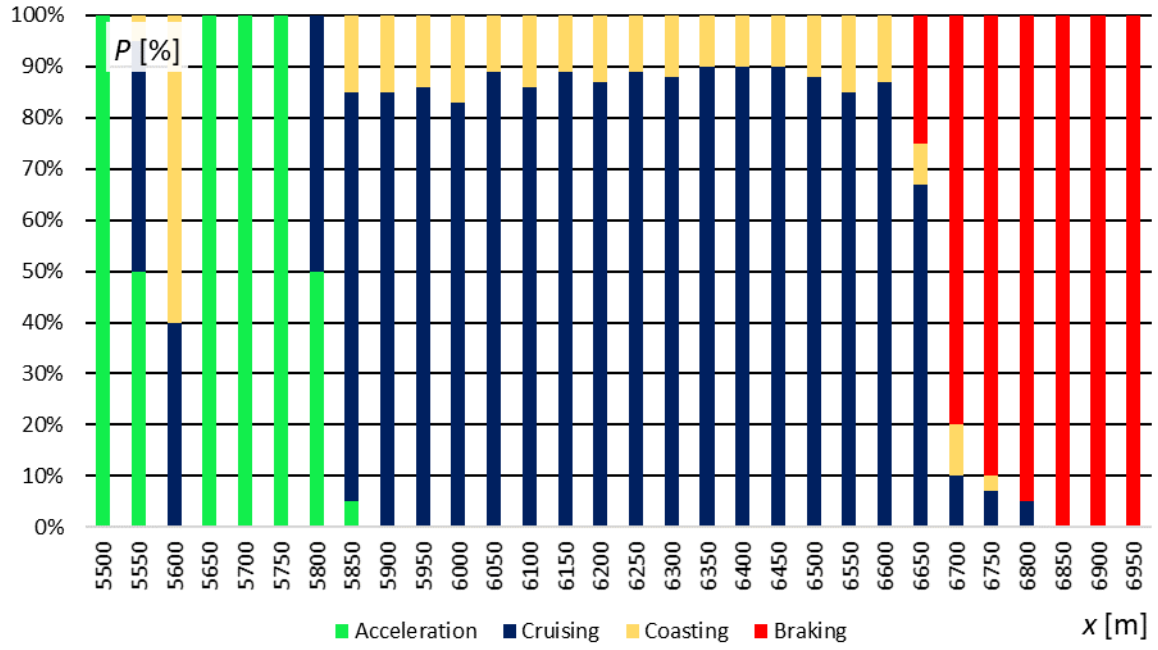

Fig. 5.21. Movement phases – route Gdańsk Zaspa – Gdańsk Przymorze–Uniwersytet, track 501 (direction Gdynia)

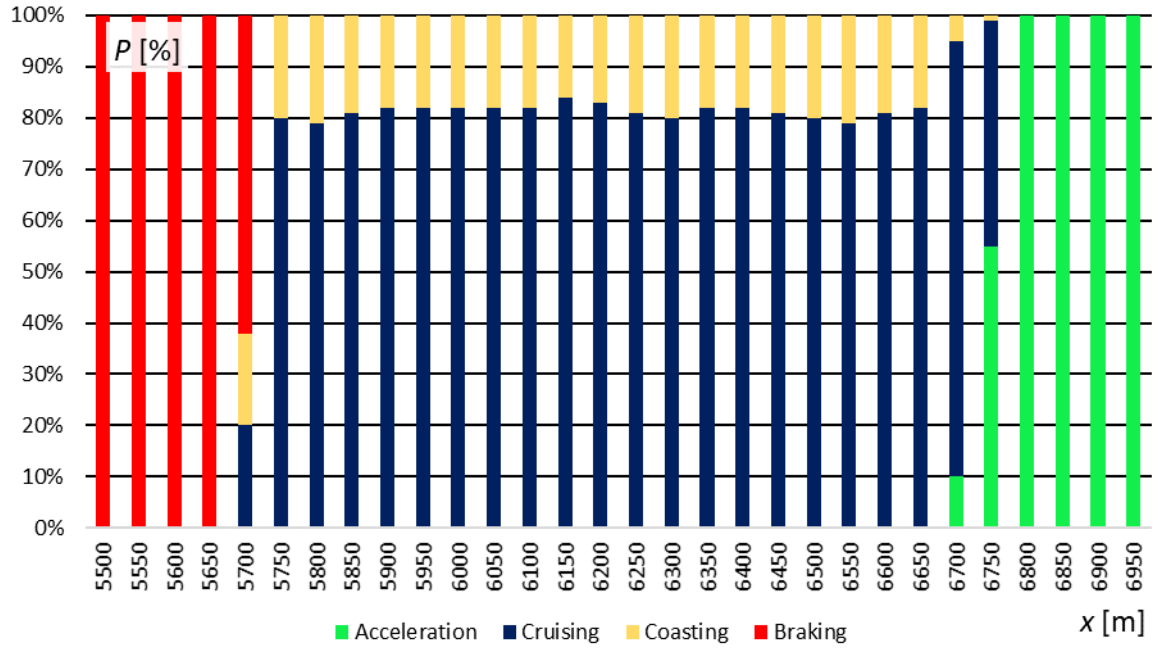

Fig. 5.22. Movement phases – route Gdańsk Zaspa – Gdańsk Przymorze–Uniwersytet, track 502 (direction Gdańsk)

Most vehicles consistently run with constant speed. The acceleration of trains going towards Gdynia is interrupted because of speed limit at northern end of the platform. The next part ends at Gdańsk Oliwa (Fig. 5.23, Fig. 5.24).

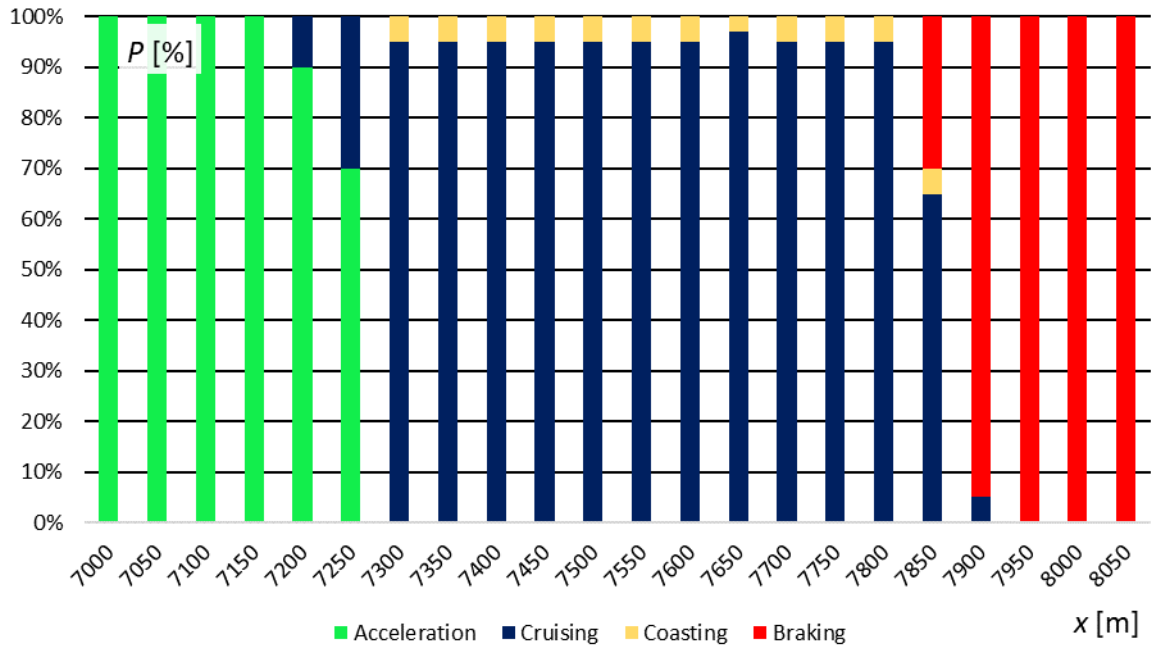

Fig. 5.23. Movement phases – route Gdańsk Przymorze–Uniwersytet – Gdańsk Oliwa, track 501 (direction Gdynia)

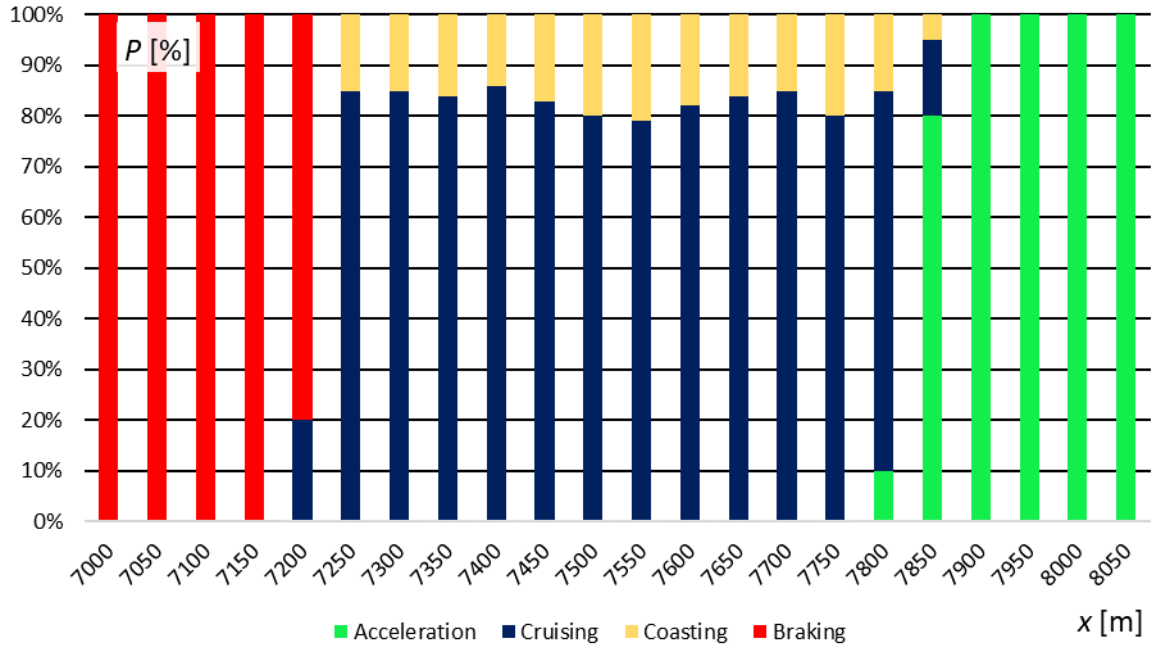

Fig. 5.24. Movement phases – route Gdańsk Przymorze–Uniwersytet – Gdańsk Oliwa, track 502 (direction Gdańsk)

Between Gdańsk Przymorze and Gdańsk Oliwa most services cruise with constant speed. Coasting was observed in about 20% of runs, despite the route being nearly straight. The next fragment runs towards Gdańsk Żabianka (Fig. 5.25, Fig. 5.26).

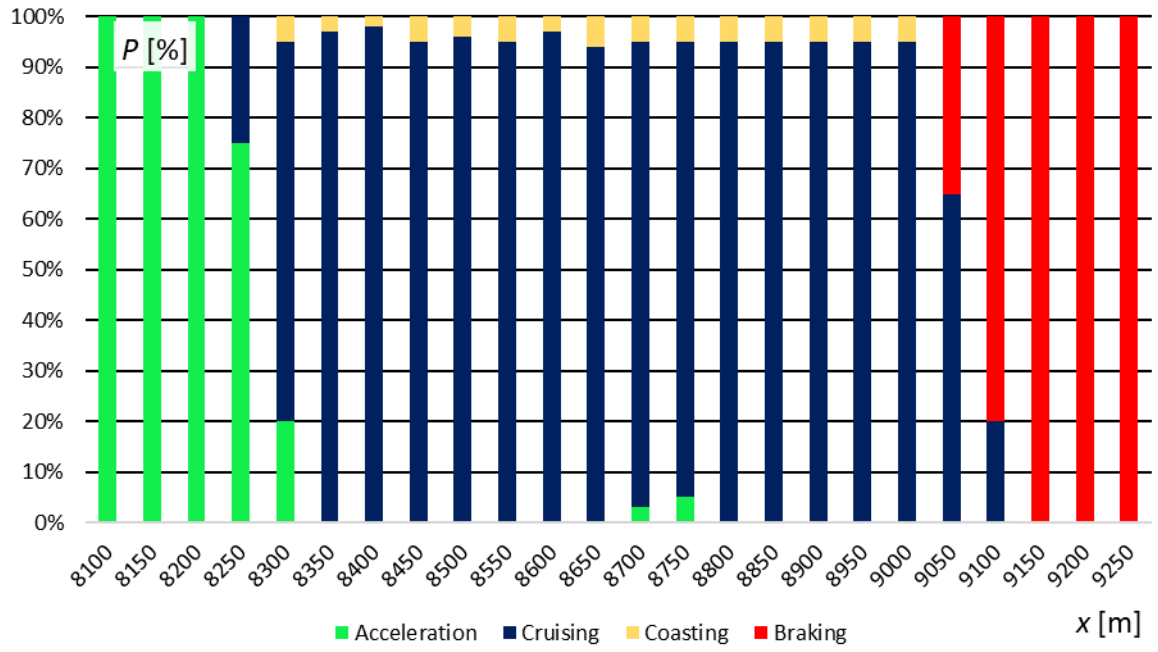

Fig. 5.25. Movement phases – route Gdańsk Oliwa – Gdańsk Żabianka–AWFiS, track 501 (direction Gdynia)

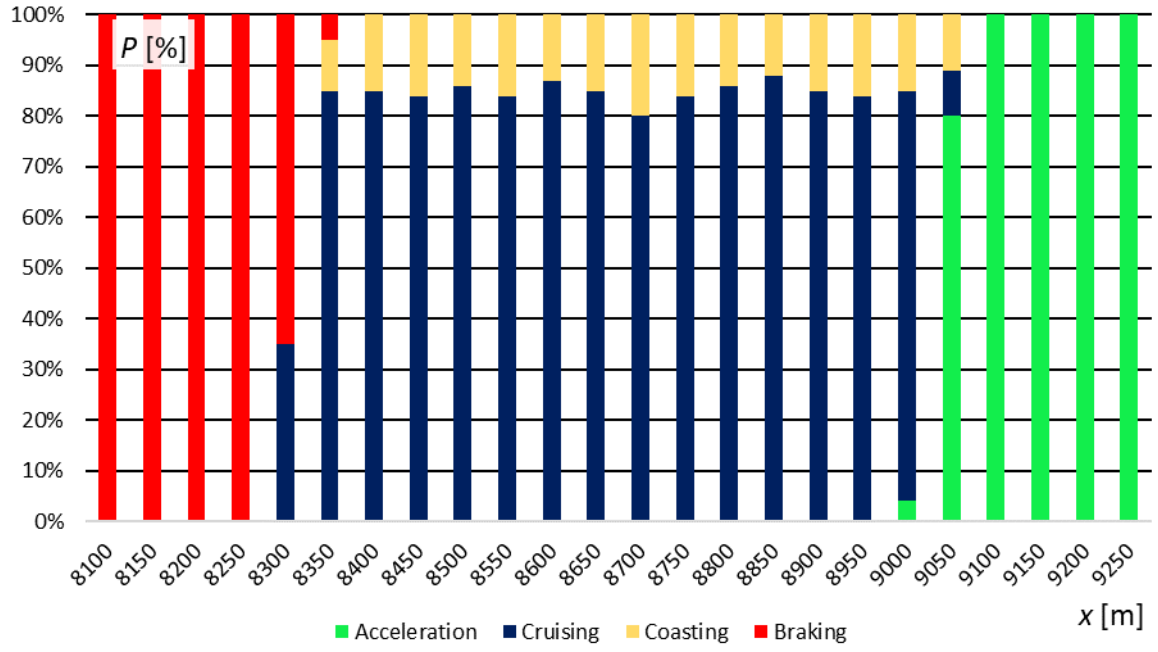

Fig. 5.26. Movement phases – route Gdańsk Oliwa – Gdańsk Żabianka–AWFiS, track 502 (direction Gdańsk)

Similarly, only minority of the runs include coasting phase, with negligible amount of re–acceleration in the middle when going towards Gdynia. The next station on the line is Sopot Wyścigi (Fig. 5.27, Fig. 5.28).

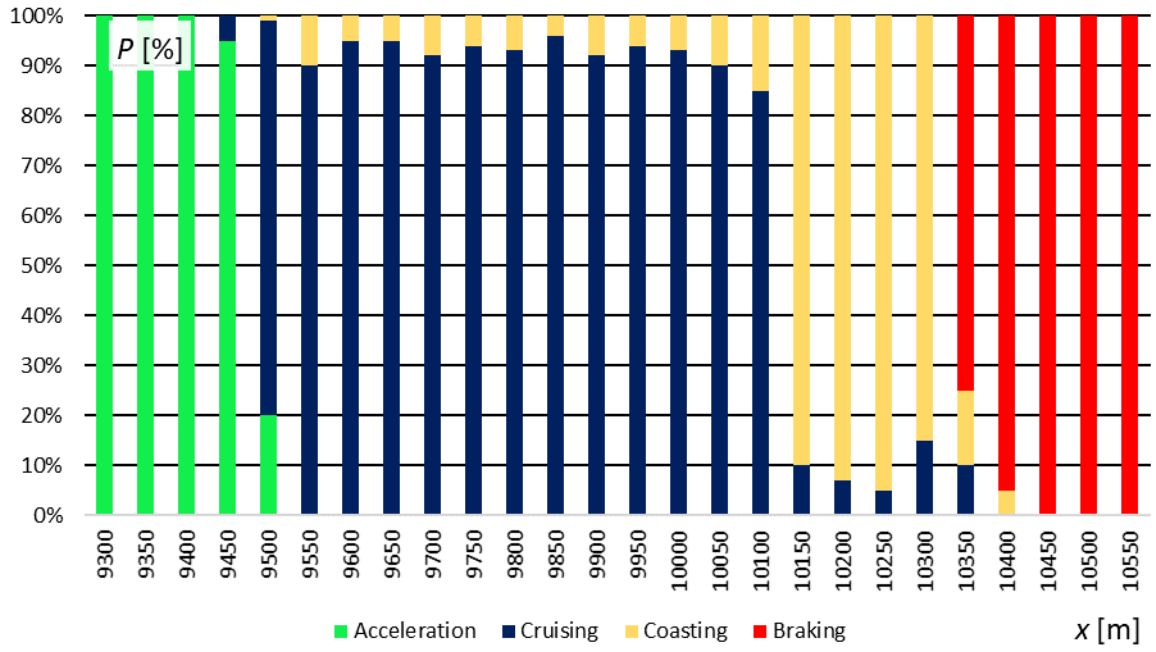

Fig. 5.27. Movement phases – route Gdańsk Żabianka–AWFiS – Sopot Wyścigi, track 501 (direction Gdynia)

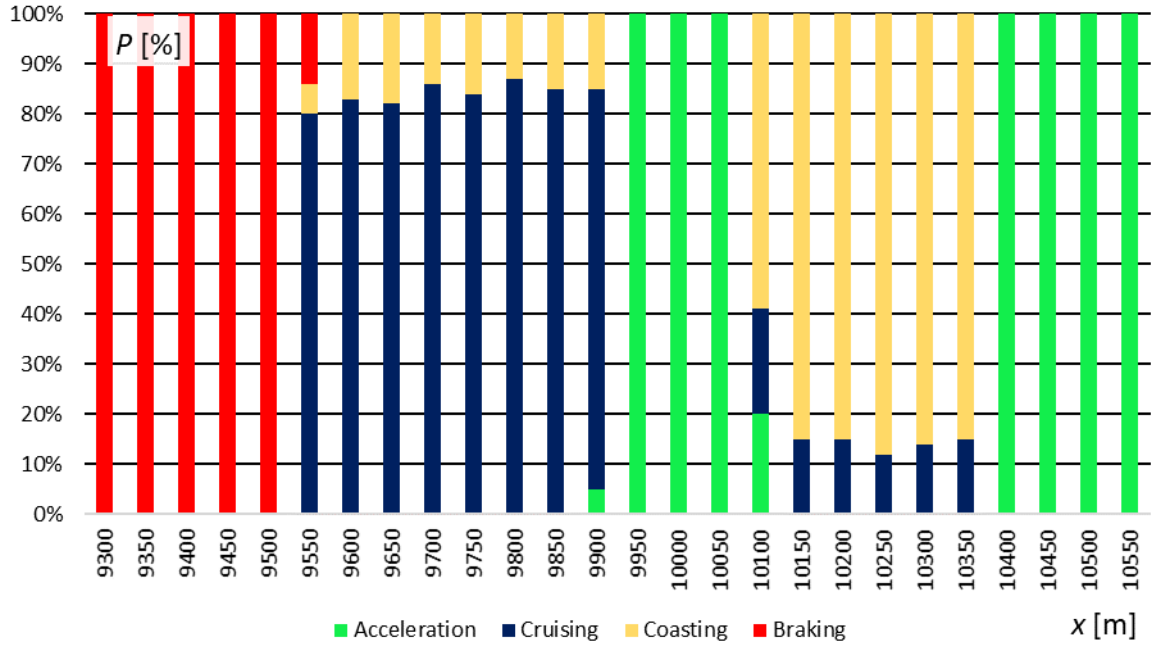

Fig. 5.28. Movement phases – route Gdańsk Żabianka–AWFiS – Sopot Wyścigi, track 502 (direction Gdańsk)

Significant part of the route is covered with constant velocity. There is visible part where vehicles are coasting in both directions – there is section insulator located there. After that, the route continues towards Sopot (Fig. 5.29, Fig. 5.30).

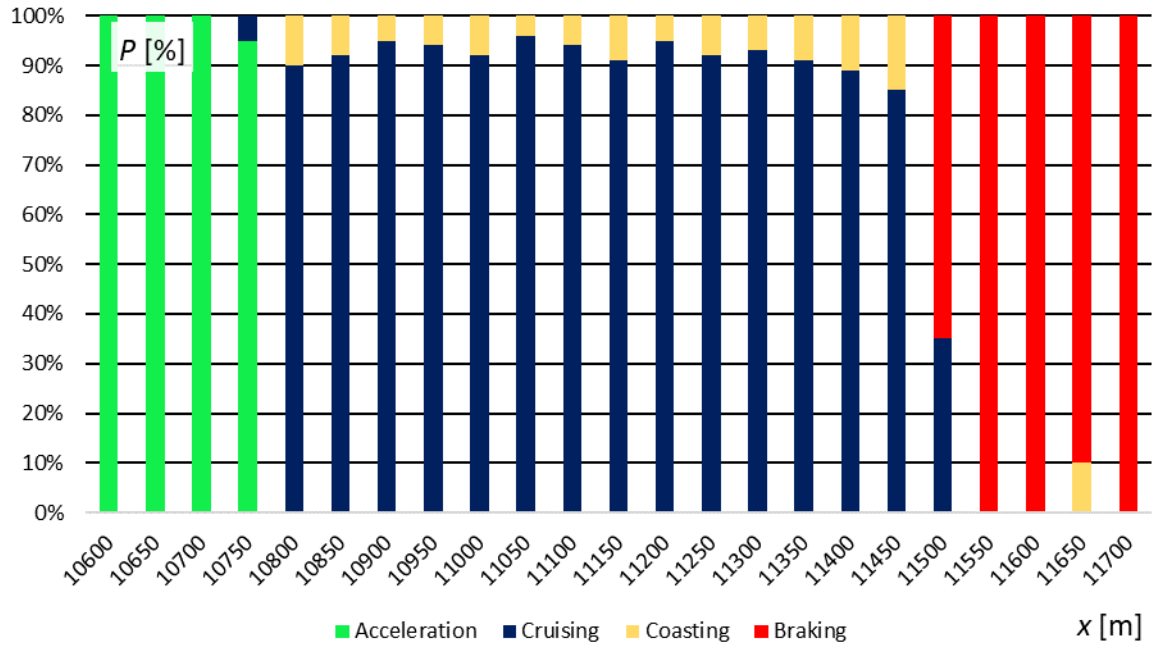

Fig. 5.29. Movement phases – route Sopot Wyścigi – Sopot, track 501 (direction Gdynia)

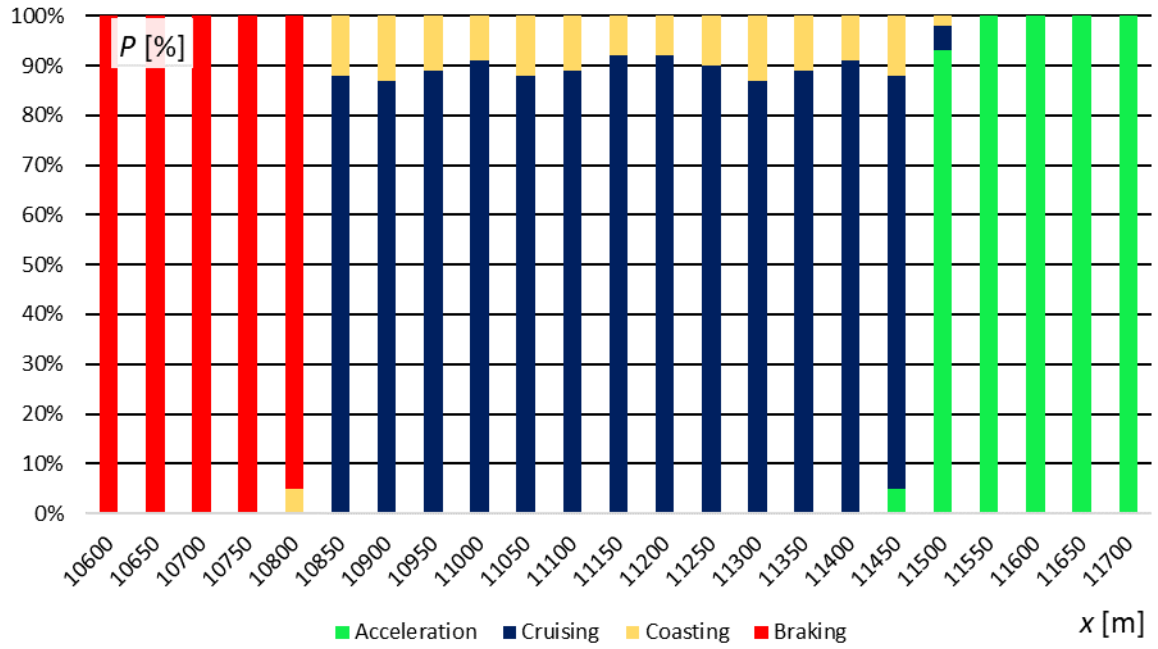

Fig. 5.30. Movement phases – route Sopot Wyścigi – Sopot, track 502 (direction Gdańsk)

This route fragment is relatively short and straightforward. In both directions, trains accelerate, cruise and brake to stop. Coasting was observed rarely, despite short distance. Then, route goes to Sopot Kamienny Potok (Fig. 5.31, Fig. 5.32).

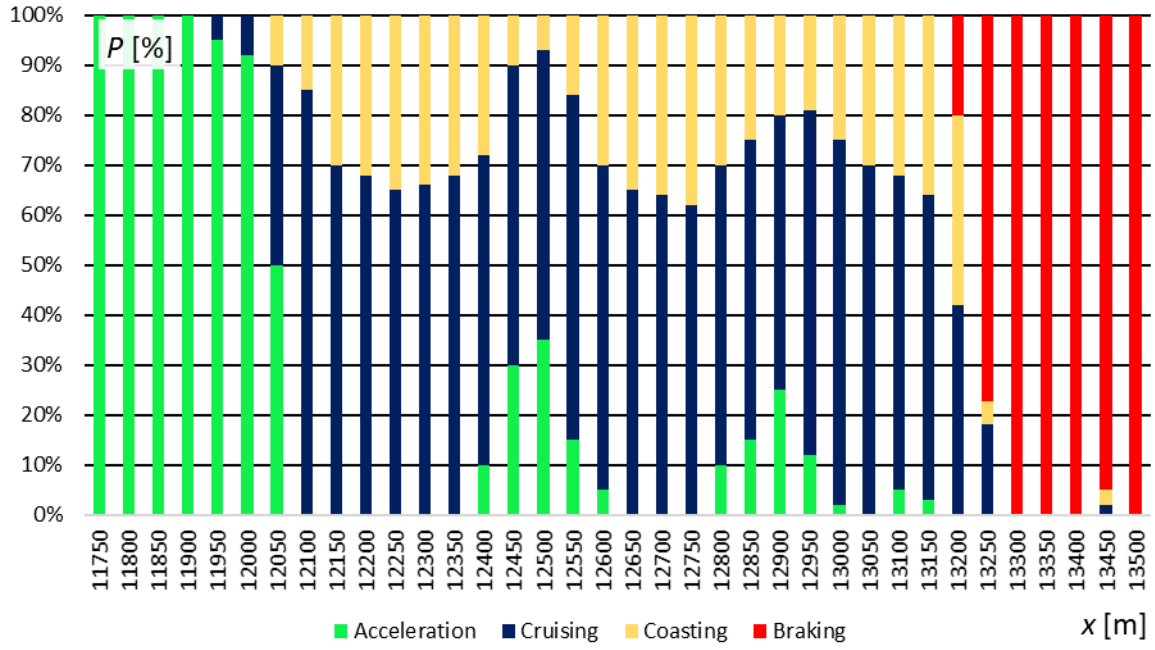

Fig. 5.31. Movement phases – route Sopot – Sopot Kamienny Potok, track 501 (direction Gdynia)

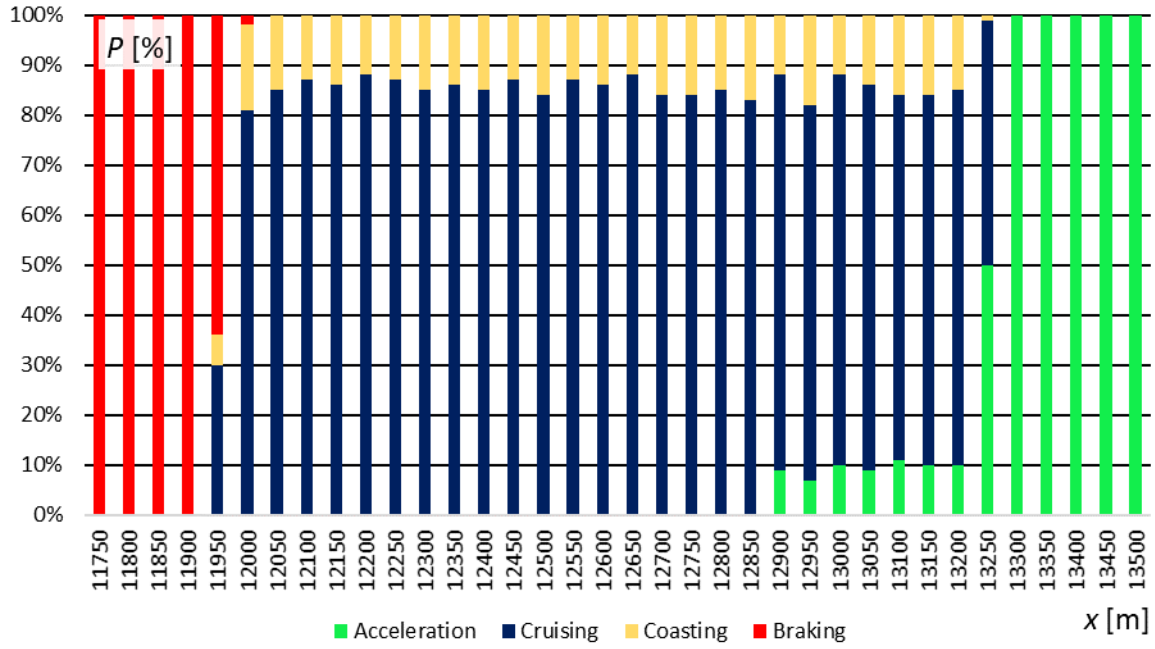

Fig. 5.32. Movement phases – route Sopot – Sopot Kamienny Potok, track 502 (direction Gdańsk)

Towards Gdynia, about 30% of the runs consisted of coasting and re–accelerations. In opposite direction, constant speed was dominating and some trains accelerated slowly. Next part ends at Gdynia Orłowo (Fig. 5.33, Fig. 5.34).

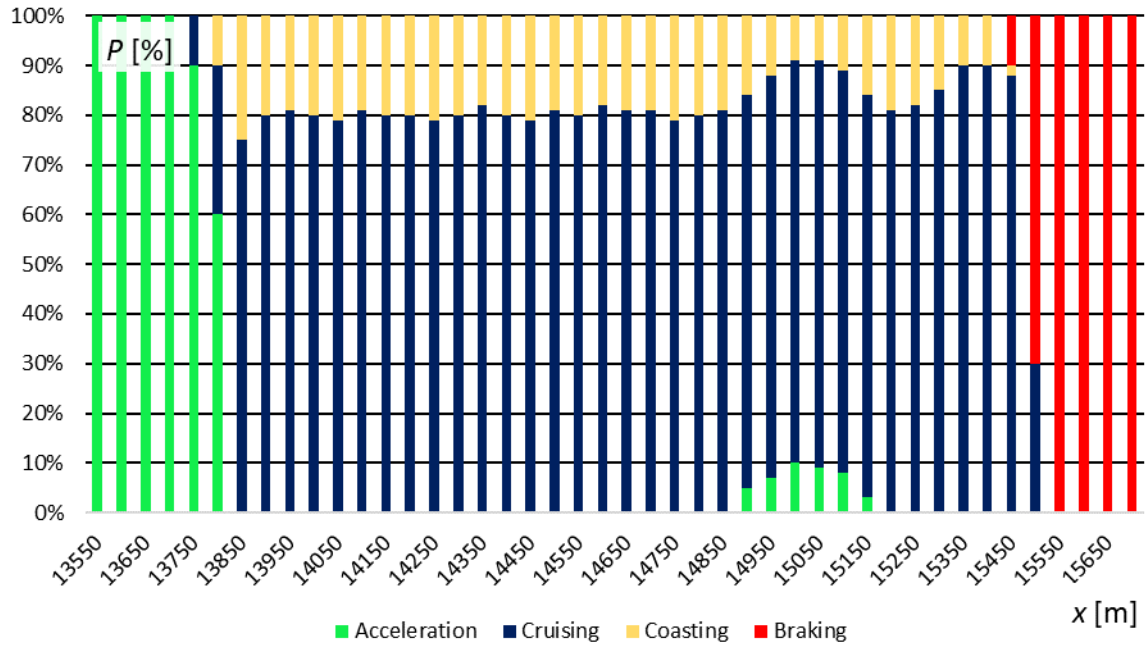

Fig. 5.33. Movement phases – Sopot Kamienny Potok – Gdynia Orłowo, track 501 (direction Gdynia)

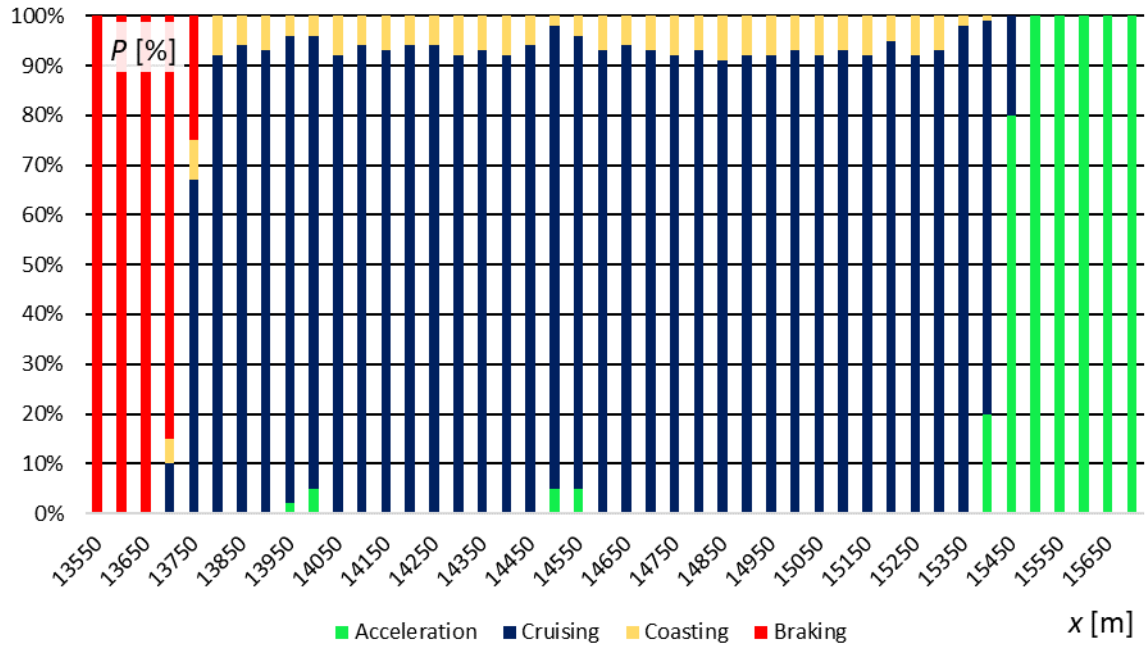

Fig. 5.34. Movement phases – Sopot Kamienny Potok – Gdynia Orłowo, track 502 (direction Gdańsk)

Cruising is again prevalent phase. Towards Gdańsk, acceleration is slightly slower and less runs contained coasting phase. Also, re–acceleration after coasting was recorded. Analyzed route ends at Gdynia Redłowo (Fig. 5.35, Fig. 5.36).

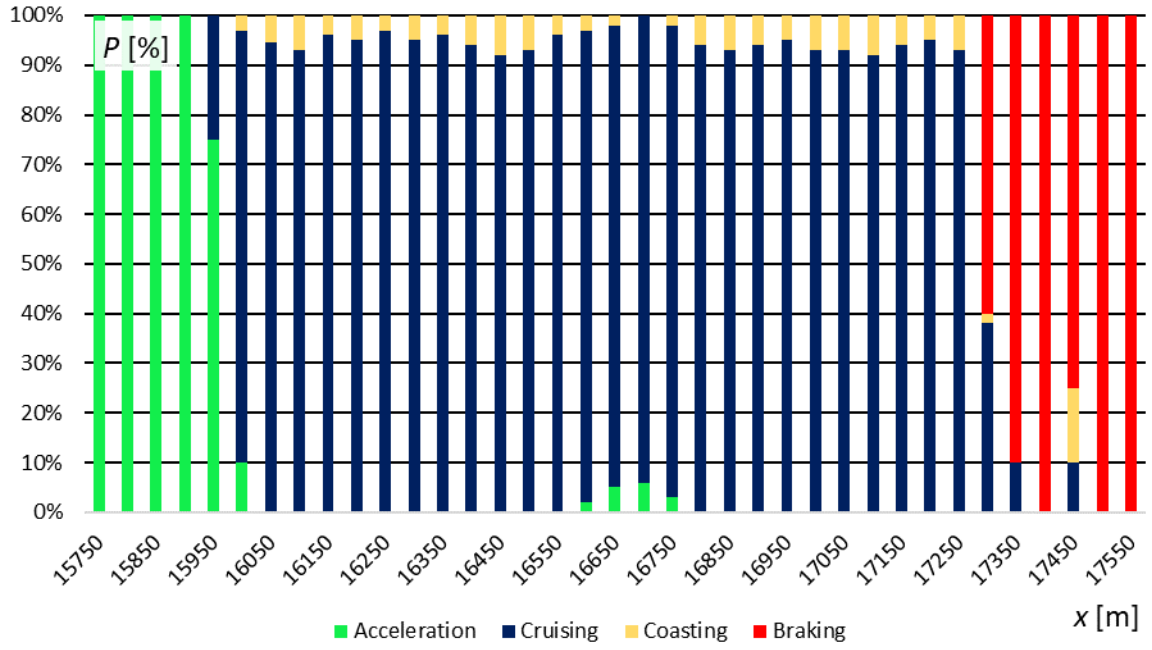

Fig. 5.35. Movement phases – Gdynia Orłowo – Gdynia Redłowo, track 501 (direction Gdynia)

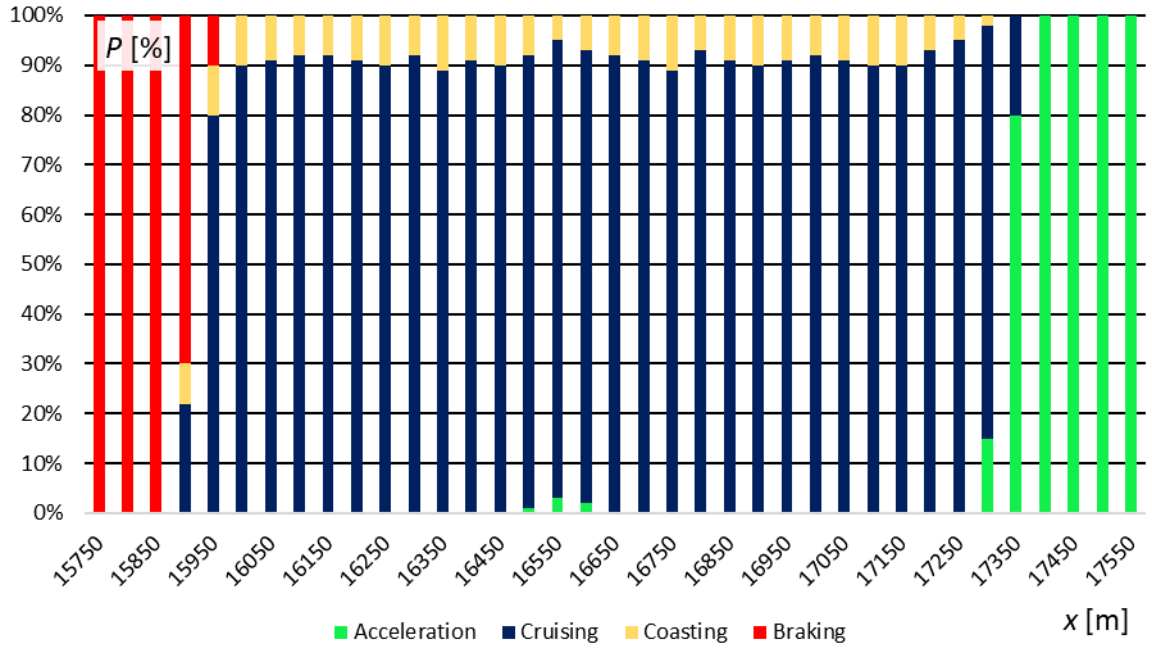

Fig. 5.36. Movement phases – Gdynia Orłowo – Gdynia Redłowo, track 502 (direction Gdańsk)

Again, significant majority of the recorded runs were driven with constant velocity. Despite section insulator installed at this fragment, there were no significant changes to velocity profiles that can be attributed to section change.

After analyzing velocity profiles, it can be concluded that vehicles equipped with induction motors are mostly driven with constant velocity, probably using cruise control, as velocity varies very slightly. Coasting phase can be observed when vehicle crosses section insulator, which is consistent with driver's reaction at trackside sign We9 and at certain route

fragments. Beyond that, runs with coasting phase were observed along the whole route, however they never constituted for more than 30% of recorded runs, often being at 20% or below. It is also worth noting that runs that feature coasting were driven that way consistently – therefore it is most likely that execution of velocity profile depends on the driver's habits, and any instructions were not in place at the time of recording. Braking to the station is mostly done with varying deceleration, sometimes with coasting phase in between. It is a result of manual control of the braking force and drivers using their personal experience for choosing the location where brakes are activated. There are points of uncertainty after acceleration and before braking because change of movement phase is a transient process interpretation of which is not necessary – because in simulation it is a result of controller regulation.

Both acceleration and braking require distance of 200 – 250 meters, despite recorded acceleration values being higher. This can be attributed to fact that the values described in 5.2.1 and 5.2.2 are assumed up to 40 km/h – which is close to base velocity for the analyzed vehicles. At higher speeds acceleration is considerably smaller; moreover, there is a possibility that the drivers reduced motive force during acceleration towards the target velocity. Similarly, deceleration was rarely linear during recorded runs, because the drivers regulated braking effort continuously – such variations would be problematic to simulate because of inconsistency of braking distance.

5.2.3. Cruising velocity

Significant number of the recorded runs were driven with constant velocity. However, not all trains were cruising with the same speed, therefore there is a need for a look into velocity values. The results were extracted from runs with more than four 50–m blocks covered with constant speed and grouped independently for each direction (Fig. 5.37, Fig. 5.38). Runs without cruising phase were skipped, as there is no constant velocity value to be obtained.

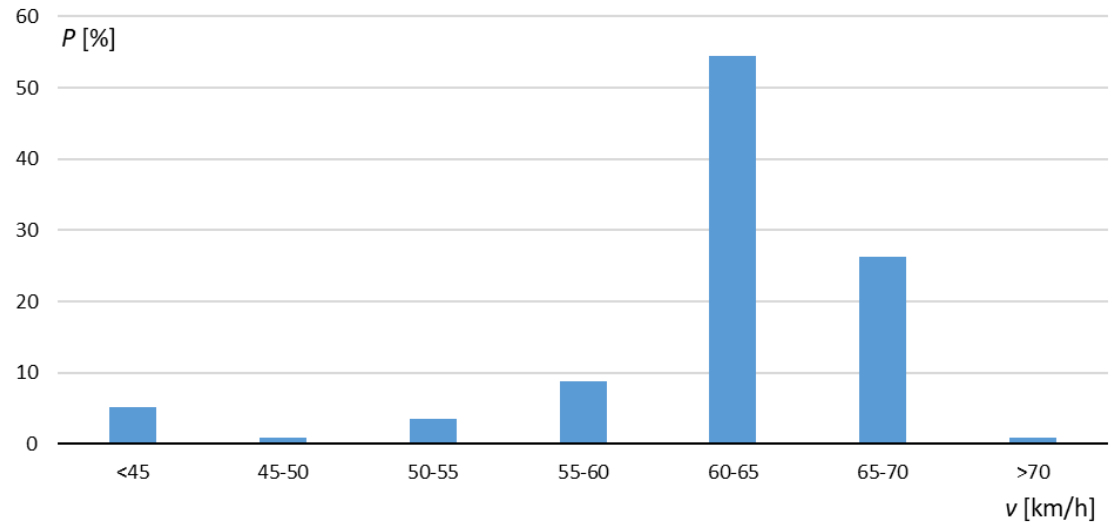

Fig. 5.37. Percentage of cruising velocities – track 501 (direction Gdynia)

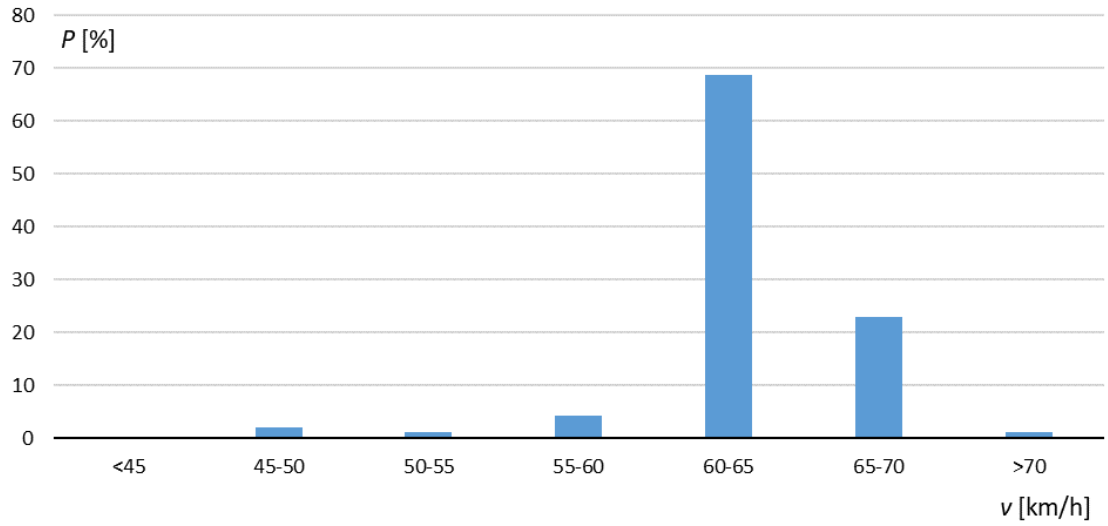

Fig. 5.38. Percentage of cruising velocities – track 502 (direction Gdańsk)

It can be concluded that in the most of the constant velocity runs trains had their speed set between 60 and 65 km/h, and speed limit of 70 km/h was achieved with significantly lower frequency. Runs with lower cruising speeds were rare, probably due to traffic situation and/or maintenance works. There was only one run with cruising velocity slightly exceeding 70 km/h, however this might also be a result of limited accuracy of GNSS recorder or satellite signal obstruction. It was also observed that vehicles were running slower thru the tunnel between Gdańsk Główny and Gdańsk Śródmieście (about 50 – 55 km/h). Runs under specific local speed limits were not considered in this comparison (e.g. pedestrian crossing at Gdańsk Zaspa station).

5.3. Reference velocity profiles

On the basis of the recorded runs analysis, reference runs for the simulation can be synthesized. Because trains run on dedicated track, traffic situation for regular operating conditions can be simplified into executable velocity profiles. In situations where analysis shown multiple possibilities, there are multiple reference velocity profiles, selected in relation to probability of their execution. The velocity profiles are a combination of target velocity and forced coasting. By default, vehicle try to accelerate towards the set speed and execute cruising phase. If value of "coasting" is set to true, the motive force upper limit is set at zero. In this case, "coasting" is a function of distance, specified in lookup table. Multiple velocity profiles are achieved by switching between the tables, depending on probability values.

Because the vast majority of recorded runs were executed with constant velocity, reference velocity profiles are also taking this into account. Therefore, typical run consists of acceleration with 0,6 m/s^2, cruising with 65 km/h and braking to stop with 0,6 m/s^2 (Fig. 5.39). Please note the arrow indicating direction of the run (in figure description).

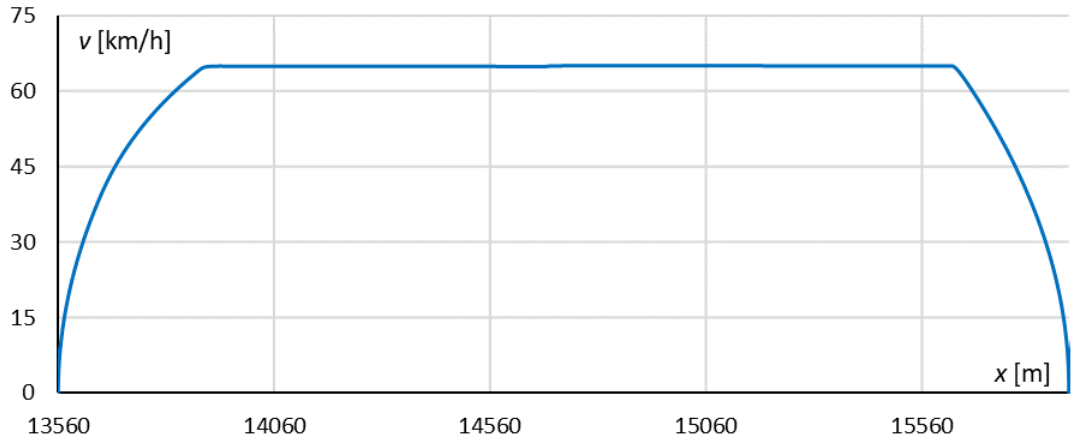

Fig. 5.39. Example of cruising–based velocity profile (Sopot Kamienny Potok – Gdynia Orłowo, track 501, direction →Gdynia)

There are also route fragments where vehicles run consistently with constant speed only thru part of the distance, either due to local speed limit or infrastructure characteristics (multiple switches). Such situation has been observed in tunnel between Gdańsk Śródmieście and Gdańsk Główny (both directions, Fig. 5.40, Fig. 5.41), between Gdańsk Główny and Gdańsk Stocznia (only track 501 bound for Gdynia, Fig. 5.42) and between Gdańsk Zaspa and Gdańsk Przymorze – Uniwersytet (only track 501 bound for Gdynia, Fig. 5.43). Other irregular velocity profiles were observed at the locations of section insulators. Trains were mostly coasting thru such route fragments (Fig. 5.44), however this was more visible with coincidence with acceleration phase, which is interrupted consistently (Fig. 5.45, Fig. 5.46). In other situations trains just cruised thru the insulator, and no visible velocity changes were observed.

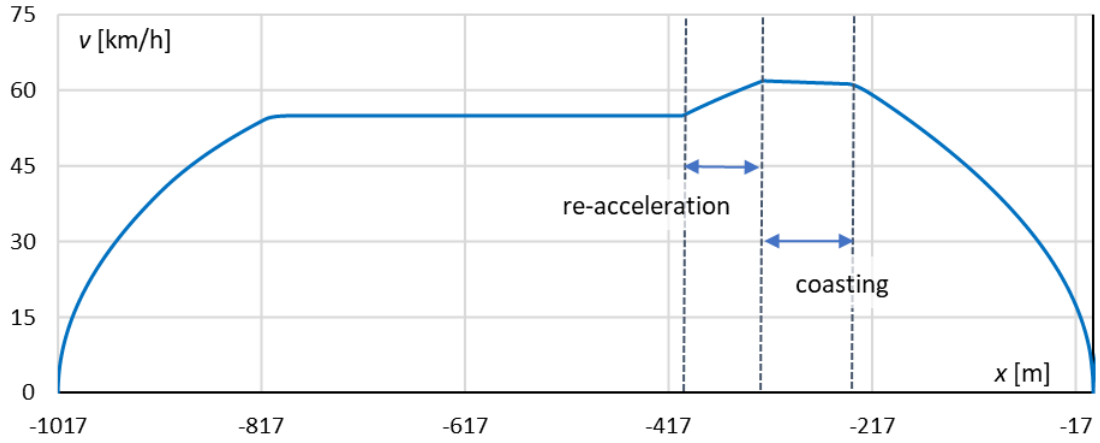

Fig. 5.40. Example of irregular velocity profile – re–acceleration and coasting (Gdańsk Śródmieście – Gdańsk Główny, track 501, direction →Gdynia)

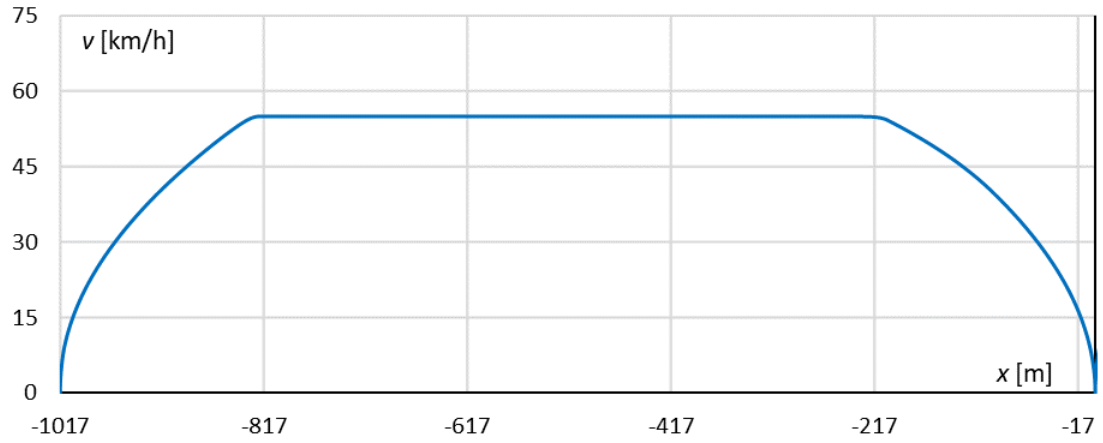

Fig. 5.41. Example of irregular velocity profile – lowered constant velocity (Gdańsk Śródmieście – Gdańsk Główny, track 502, direction Gdańsk←)

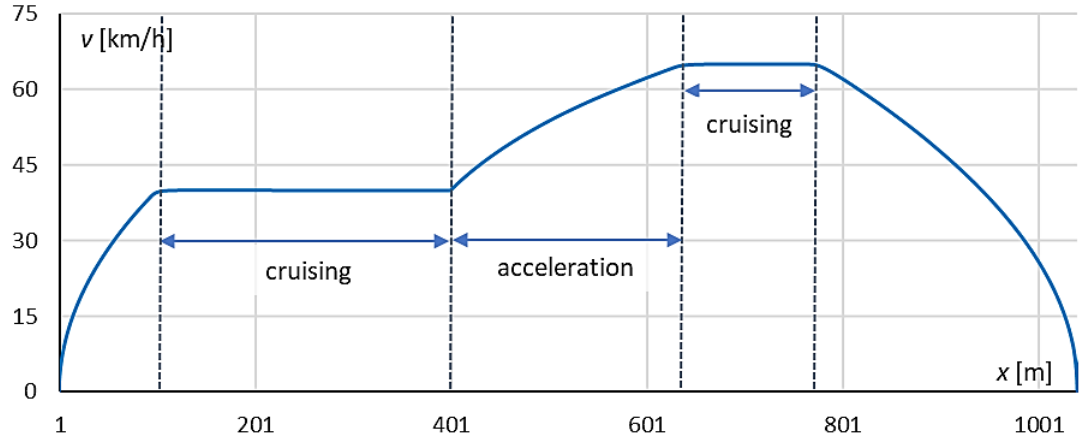

Fig. 5.42. Example of irregular velocity profile – slower run thru switches (Gdańsk Główny – Gdańsk Stocznia, track 501, direction →Gdynia)

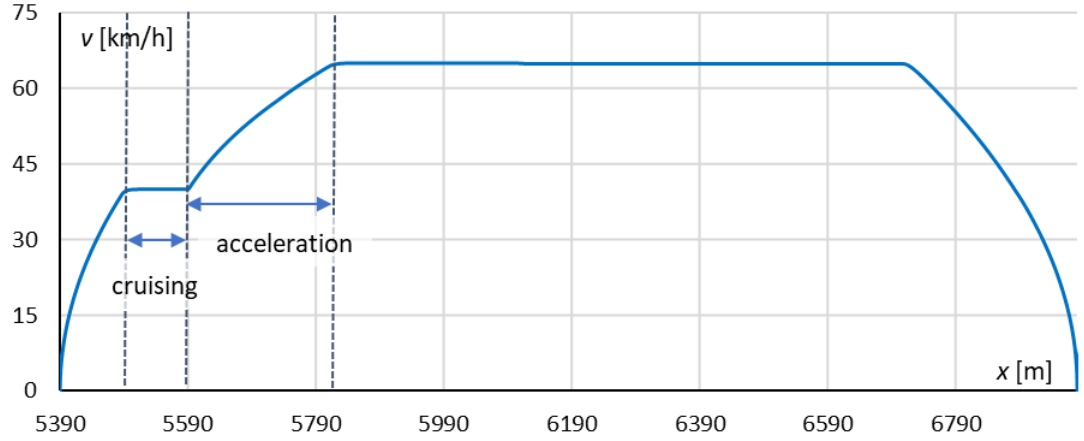

Fig. 5.43. Example of irregular velocity profile – local limit on pedestrian crossing (Gdańsk Zaspa – Gdańsk Przymorze, track 501, direction →Gdynia)

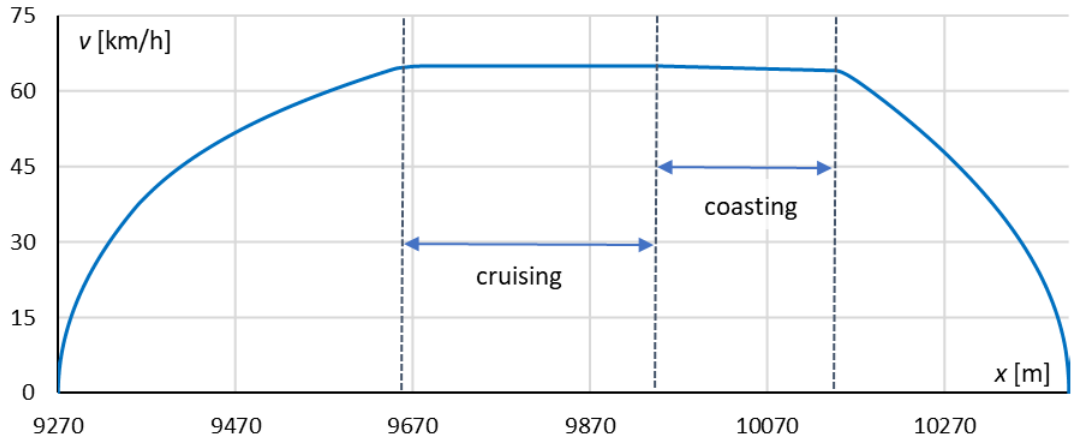

Fig. 5.44. Example of irregular velocity profile – coasting thru section insulator (Gdańsk Żabianka – Sopot Wyścigi, track 501, direction →Gdynia)

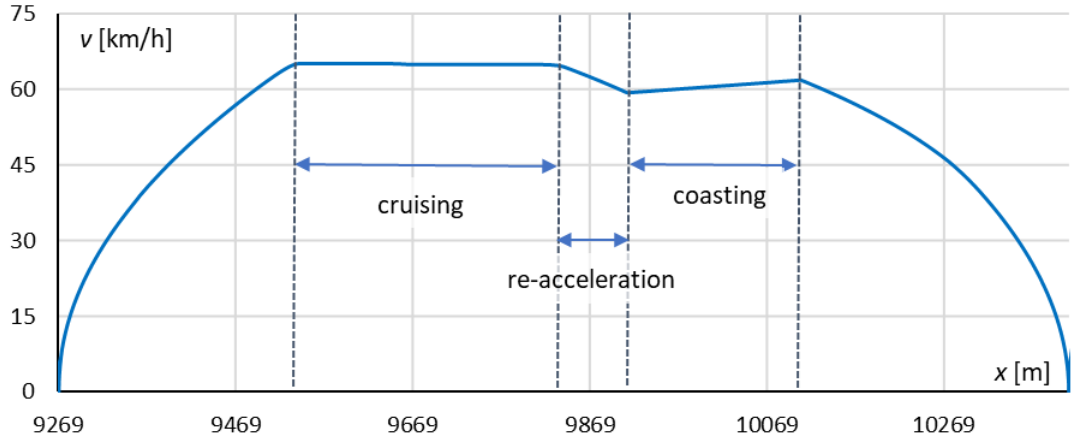

Fig. 5.45. Example of irregular velocity profile – coasting thru section insulator (Sopot Wyścigi – Gdańsk Żabianka, track 502, direction Gdańsk←)

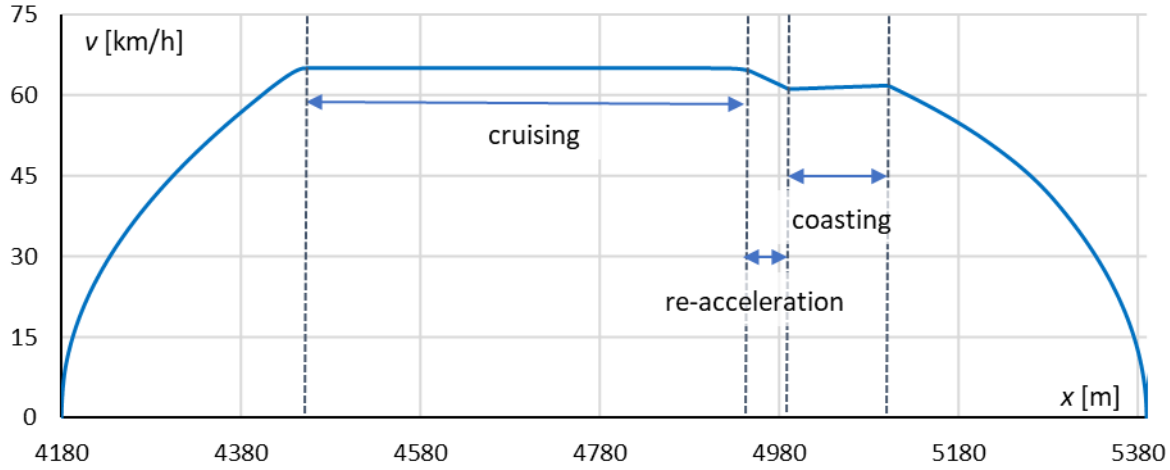

Fig. 5.46. Example of irregular velocity profile – coasting thru section insulator (Gdańsk Zaspa – Gdańsk Wrzeszcz, track 502, direction Gdańsk←)

Situations as shown above are assumed a part of the basic (most probable) velocity profiles set – as mentioned before, despite majority of the route is covered with constant velocity, there are parts where differences are occurring consistently. Author assumed that there are at most two possible profiles per station–to–station run: the basic one (constant velocity) and alternative one (coasting, with re–acceleration on longer route parts). Because of a limited impact on energy efficiency of the whole network of low–probability profiles, the threshold for implementing alternative profile was set at 20%. Consequently, some fragments will have only one profile possible, while others could be realized using one of the two. Probabilities of selection are determined based on the data computed by the Analyzer application and are shown in 5.2.2. The probability values are not dependent on time of the day, as there was no meaningful connection between velocity profile and time found within the recorded data. Similarly, the velocity profiles are the same for all the vehicles analyzed, despite differences in their parameters. This is done because in actual system timetable is calculated for the slowest vehicle in service (which in this case would be EN57AKM, with 0,8 m/s^2 acceleration), and the discrepancies between movement dynamics for different vehicles in recorded runs were not consistently repeated.

For the alternative runs, coasting and possible re–acceleration points were also set according to data presented in 5.2.2. Thanks to this, velocity profiles used in this analysis are realistic and based directly on large set of measurements done in real system. Overview of the assumed velocity profiles is shown in Tab. 7.

Tab. 7. Summary of velocity profiles with their probabilitites

No.	Run between stations	Direction Gdańsk/ Track 502		Direction Gdynia/ Track 501	
		Base	Alt.	Base	Alt.
1	Gdańsk Śródmieście – Gdańsk Główny*	100%	-	100%	-
2	Gdańsk Główny – Gdańsk Stocznia*	100%	-	100%	-
3	Gdańsk Stocznia – Gdańsk Politechnika*	100%	-	80%	20%
4	Gdańsk Politechnika – Gdańsk Wrzeszcz	85%	25%	85%	25%
5	Gdańsk Wrzeszcz - Gdańsk Zaspa	70%	30%	80%	20%
6	Gdańsk Zaspa – Gdańsk Przymorze	80%	20%	100%	-
7	Gdańsk Przymorze– Gdańsk Oliwa	80%	20%	100%	-
8	Gdańsk Oliwa - Gdańsk Żabianka – AWFiS	80%	20%	100%	-
9	Gdańsk Żabianka – AWFiS - Sopot Wyścigi	80%	20%	100%	-
10	Sopot Wyścigi – Sopot	100%	-	100%	-
11	Sopot – Sopot Kamienny Potok	80%	20%	80%	20%
12	Sopot Kamienny Potok – Gdynia Orłowo	100%	-	100%	-
13	Gdynia Orłowo – Gdynia Redłowo	100%	-	100%	-

*Smaller number of recorded runs

6. ENERGY EFFICIENCY ANALYSIS – OPERATION IN THE CURRENT STATE

This chapter describes obtained results of conducted simulation of SKM Trójmiasto route fragment, as described in chapter 5. In order to carry out comprehensive computation, developed model (as described in detail in chapter 3) was connected to depict analyzed transport system, and input parameters (as shown in chapter 5) were implemented. Timestep of this simulation was set at 1 s, which is adequate for such analysis [40,62,143,145]. The simulation includes the whole day (24 hours, from 2:00 till 2:00) of operation, including the odd night trains which run without the tact. Computed parameters include not only vehicle velocities, currents and pantograph voltages, but also drivetrain efficiency, passenger weight and drivetrain losses power. Similarly, parameters of power supply systems were also calculated – including substation voltages and currents and losses in catenary and feeder cables. For the whole system, energy consumption and energy regeneration efficiency was revealed.

As the analysis takes into account only fragment of the whole system, author suggests that simulating each vehicle that would cover the route in reality is not necessary – because it is possible to depict realistic schedule using lower number of vehicle models. Vehicles are "turning around" at Gdynia Redłowo, which is the last station on analyzed fragment; in real system trains continue towards Gdynia Główna and Wejherowo. This allows for considerable reduction of required computing resources, which results in shorter computation times – because the model of the vehicle is the most elaborate and thus, demanding part of the whole program. Synchronization necessary for tact retainment is done using permission function, specified beforehand. It is worth noting that the number of vehicles was selected to allow for schedule execution regardless from any prolonged runs. Possible stacking longer dwell times with slower velocity profiles will not impact the end result.

Timetable was assumed similar to real timetable from early 2021, as there were relatively little disturbances in schedule caused by maintenance works at the time. The implemented timetable is not identical in departure and arrival times, however it retains the tact and number of runs in each direction. As the station dwell time and, to an extent the velocity profiles are randomized, there are differences between the runs, as there would be in real transport system (this is an intentional feature).

The schedule depicts regular workday operation of the transport system (Fig. 6.1). It is worth noting that the network begins and ends its daily operation at Gdańsk Główny (former terminal), not Gdańsk Śródmieście.

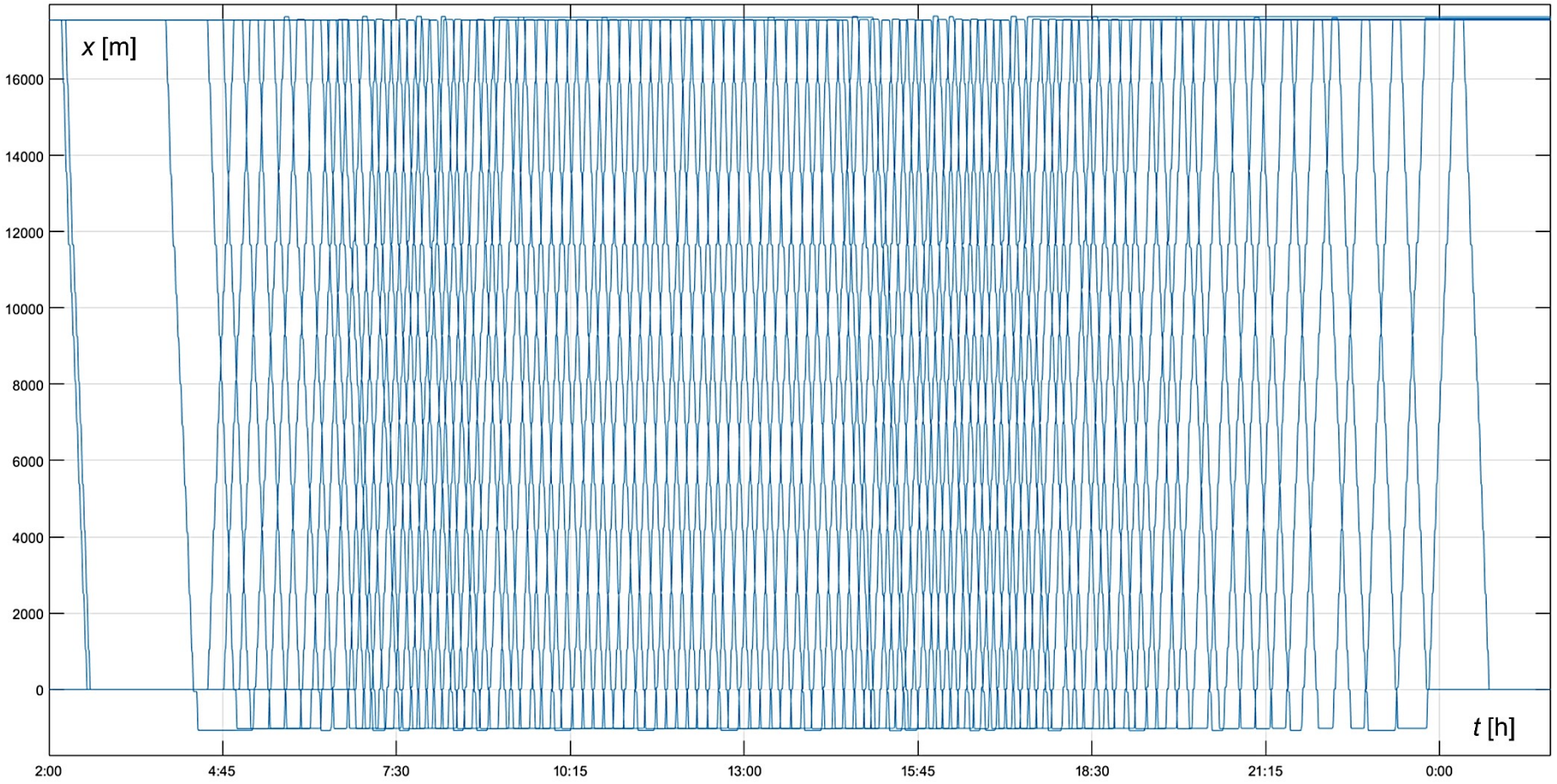

Fig. 6.1. Waveform of simulated vehicles' location – graphical timetable

6.1. Energy efficiency – vehicles

Vehicles are the main energy consumers in transport system – therefore, they should be the focus point of the analysis. Because the velocity profiles for the vehicles are selected with a degree of randomness, every run might be different, including variable station dwelling time and vehicle mass. The latter also impacts resulting velocity profiles directly, as the same motive force will take longer to accelerate heavier vehicle. Moreover, higher mass translates into higher movement resistance, which requires more energy for running with constant velocity and results in higher deceleration during coasting. The chart of relation between load mass and energy consumption allows for observation of a trendline, as shown on Fig. 6.2 for selected computed runs of EN57AKM train.

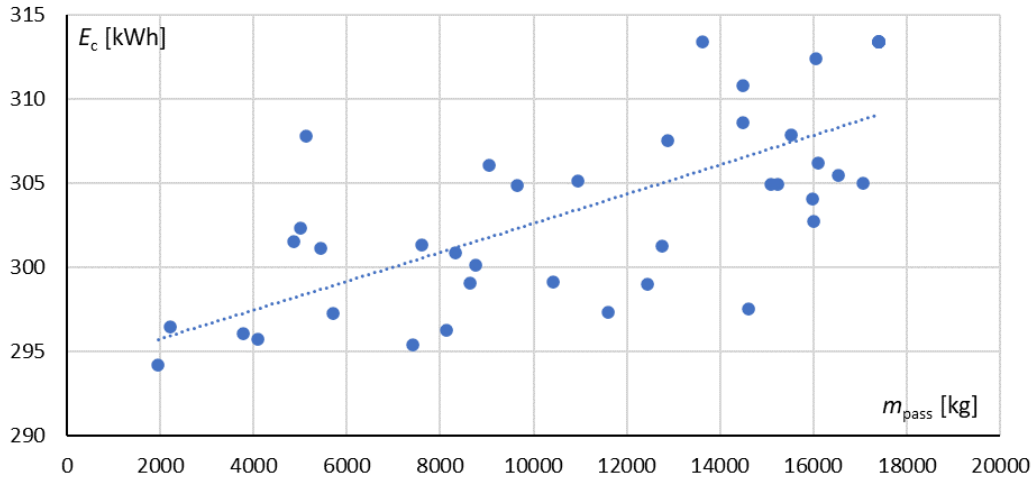

Fig. 6.2. Relation between average passenger mass and energy consumed during single run between Gdynia Orłowo and Gdańsk Śródmieście (track 502)

Energy regeneration is also not constant, being impacted by number of vehicles on route, correlation between movement phases of the vehicles and possibly, substation idle voltage. Because station dwelling time is randomized, the vehicles will not move in perfectly timed intervals, so recuperation will vary throughout the day. There are also slight differences in run times between each train run which also impacts energy consumption. This is an intentional feature, which allows for simulation of realistic conditions of network operation. Consequently, author decided to show waveforms only for selected run for one of the vehicles, while the general data from the simulation has been grouped into the charts and tables, which can be found in Appendix 2. It is not justified to present all the runs as there are over 100 services in each direction, and the simulation was executed multiple times to obtain large set of data. It should be noted that when vehicle exits analyzed area (between Gdynia Redłowo and Gdynia Orłowo station), the current value is zeroed, voltage value set at constant 3 kV (for solver stability) and all of the parameters connected with the energy figure are not counted. The air temperature was set to 7°C, resulting in HVAC duty cycle between 10 and 14%. Dry conditions were assumed ($\mu_0 = 0{,}3$), and remained as such throughout the whole analysis.

The exemplary set of waveforms (Fig. 6.2, 6.3, 6.4, 6.5, 6.6, 6.7, 6.8, 6.9) shows run of the EN57AKM vehicle towards Gdańsk Śródmieście, taking place between 12:46 and 13:15, outside the peak hours. Continuous rated power of this train is 2 MW, as it consists of two units coupled together. The run follows base, mostly constant velocity profile.

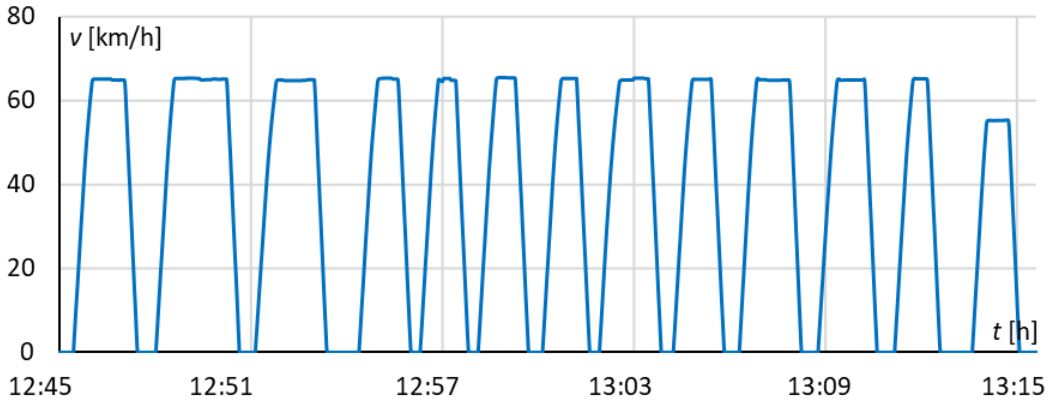

Fig. 6.3. Simulated velocity profile – EN57AKM, track 502

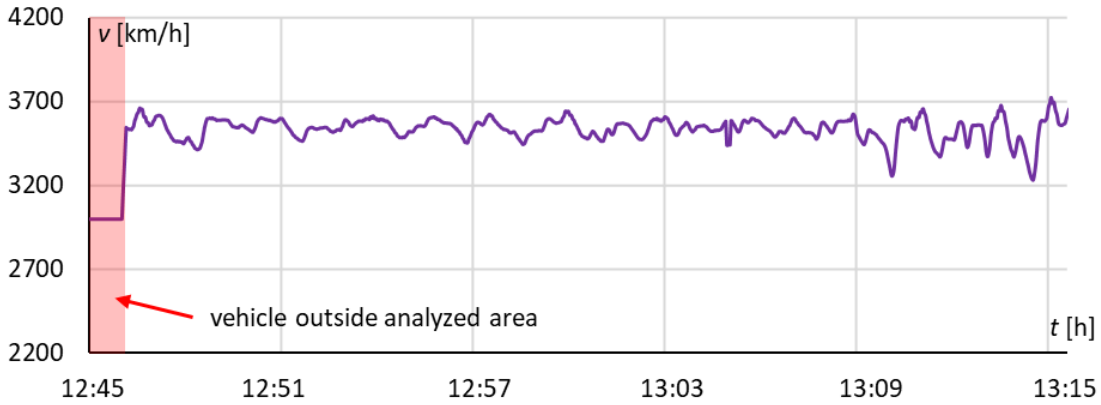

Fig. 6.4. Simulated pantograph voltage – EN57AKM, track 502

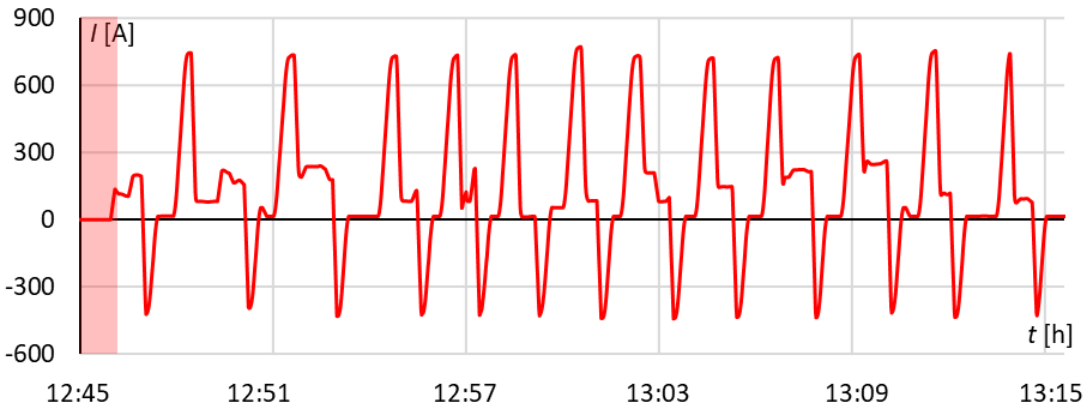

Fig. 6.5. Simulated vehicle current – EN57AKM, track 502

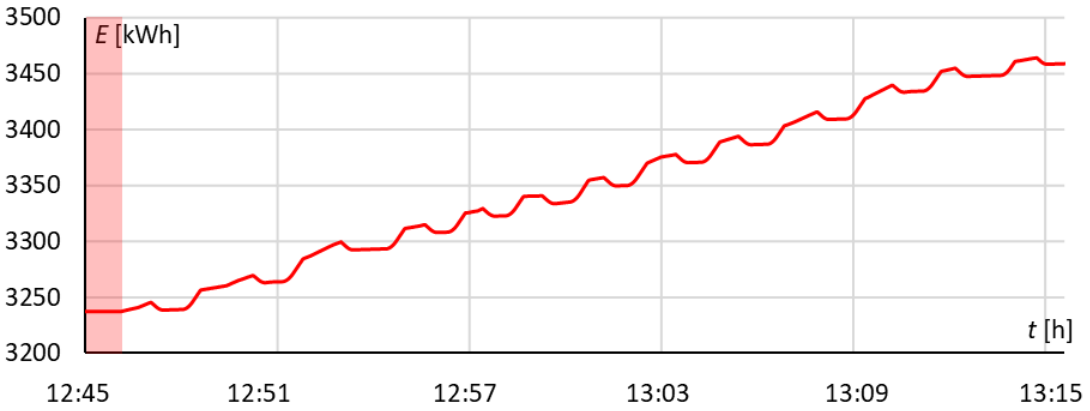

Fig. 6.6. Simulated energy balance – EN57AKM, track 502

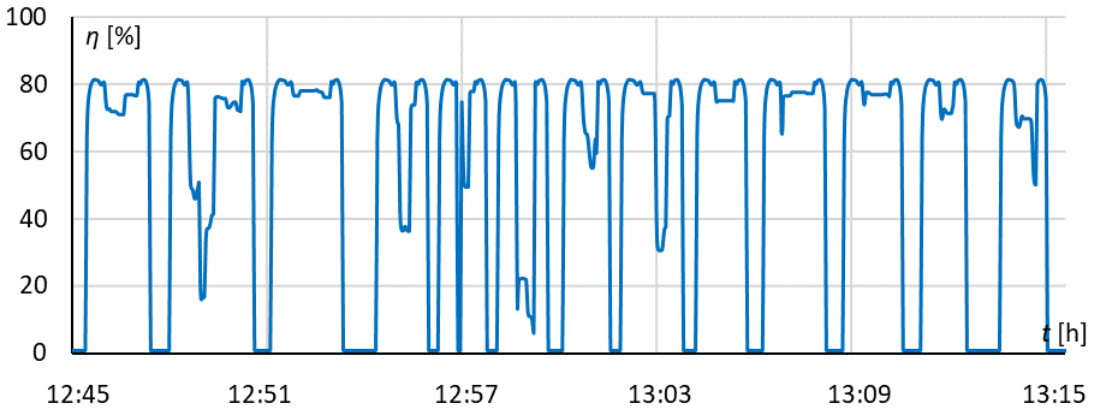

Fig. 6.7. Simulated traction drive efficiency – EN57AKM, track 502

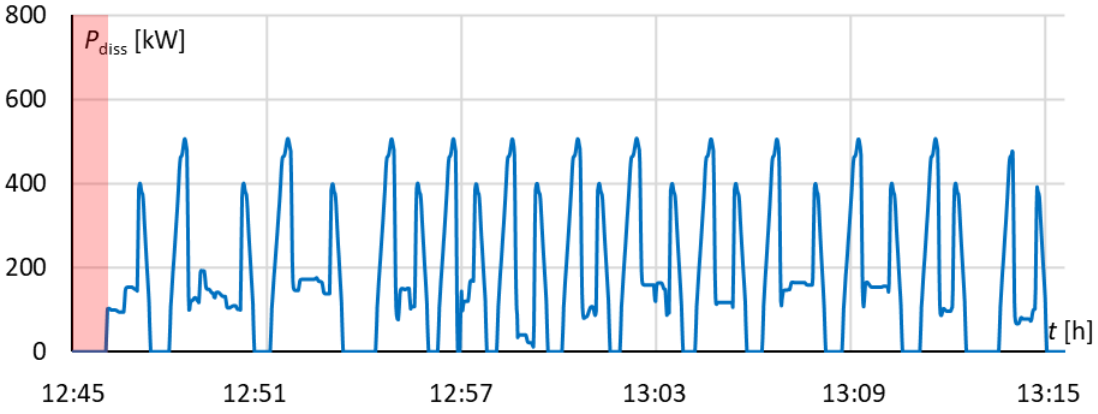

Fig. 6.8. Simulated traction drive losses power – EN57AKM, track 502

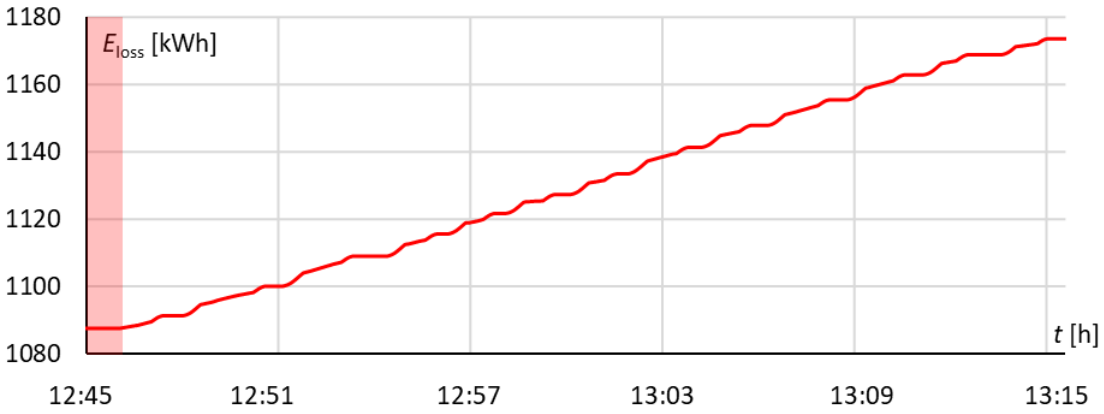

Fig. 6.9. Simulated traction drive losses energy – EN57AKM, track 502

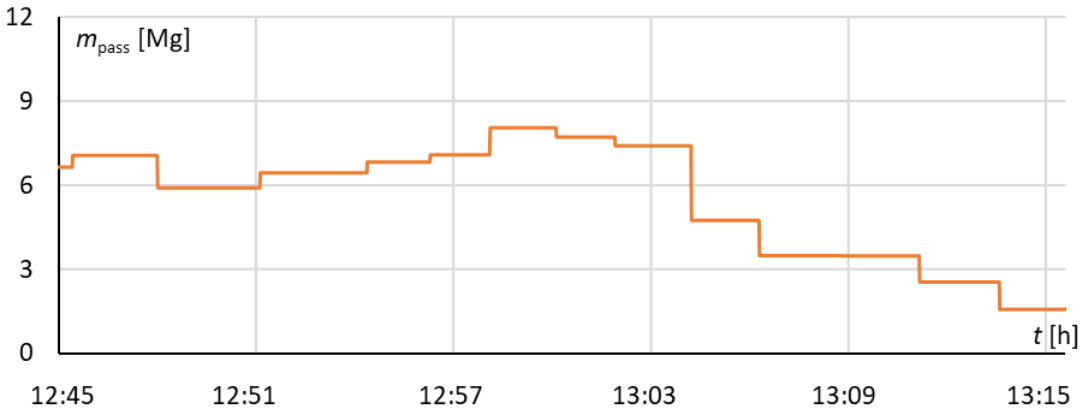

Fig. 6.10. Simulated passenger mass – EN57AKM, track 502

During the run, vehicle consumed 310,7 kWh and regenerated 79,4 kWh of energy, achieving 25,5% recuperation efficiency. This results in 13,2 kWh per km or 32,7 Wh per seat–km. Voltage on the vehicle pantograph remained at high level, mostly between 3400 and 3600 V, peaking at 3700 V and being the lowest at just above 3200 V. The highest voltage fluctuations were observed at the section powered only from one side, in proximity of Gdańsk Główny station. The losses in traction drive did not exceed 500 kW, being at around 100 – 150 kW during the cruising phase. During the run, total of 90 kWh of energy was dissipated in form of losses. Mass of the passengers decreased after passing Gdańsk Wrzeszcz, where typically many people leave the train for the shopping centers and business district located nearby. The difference in mass between stops can be minuscule, when similar amount of passengers boards and gets off a train (e.g. in Sopot).

Summary of energy consumption of EN57AKM class vehicles is shown in Fig. 6.11. The chart shows average, minimum and maximum value for each station–to–station route fragment, for trains running towards Gdańsk (track 502). Abbreviations used for stations names can be found in chapter 5 (Tab. 6).

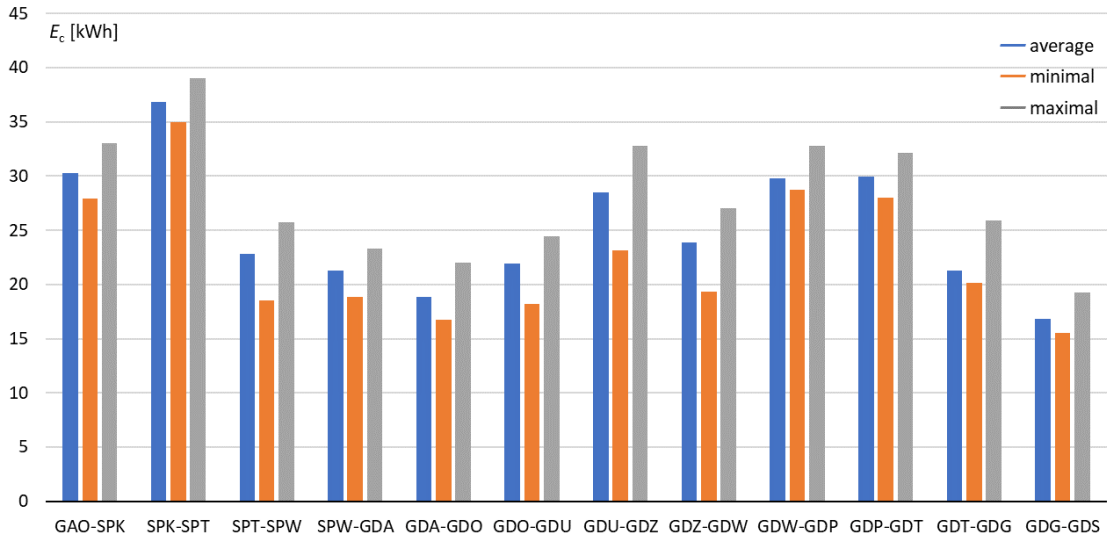

Fig. 6.11. Energy consumed for each route fragment – EN57AKM, train bound for Gdańsk (track 502)

It is worth noting that for most of the fragments, average value is closer to maximum than minimum. This is because the constant velocity based profiles have higher probability of execution than coasting based ones. The largest amount of energy is required for the longest parts of the route, and where the curvature and inclination is the highest.

Similar charts were compiled for regenerative braking, showing absolute energy regenerated (Fig. 6.12). Such data is useful to provide insight, where on the route energy recuperation is the highest.

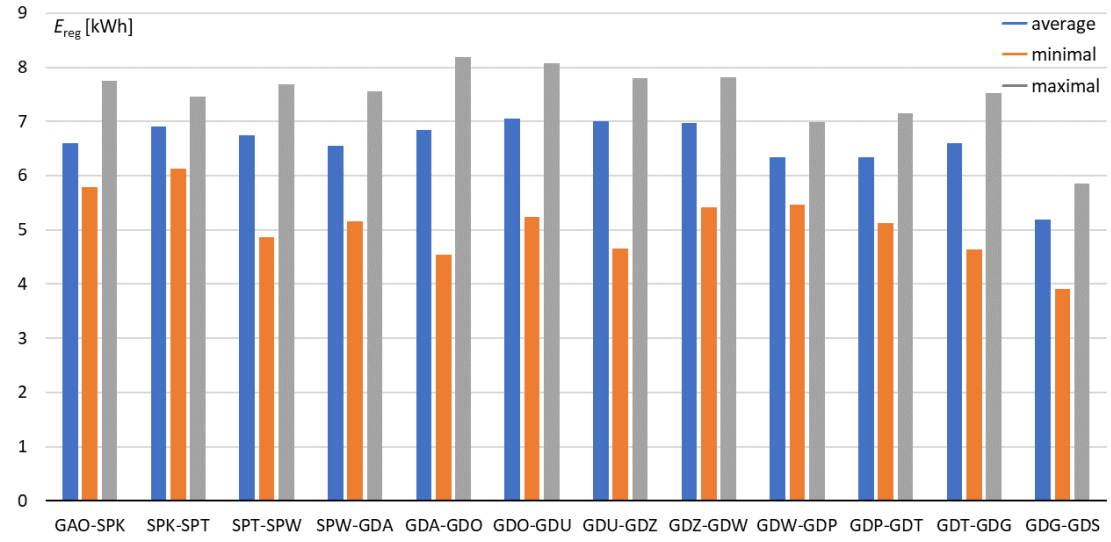

Fig. 6.12. Energy regenerated for each route fragment – EN57AKM, train bound for Gdańsk (track 502)

It can be concluded that despite the relatively long intervals between each service, energy recuperation is quite high. This is because power supply sections are short and catenary cross section is large. However, "regenerated energy" is not consumed by other vehicles in its entirety – some of the energy is dissipated in the catenary in form of losses.

Losses in vehicle drivetrain were also considered, and can be presented in similar way (Fig. 6.13). It should be noted that drivetrain losses occur not only during acceleration and cruising, but during regenerative braking as well – and in such case, their value is added to total losses figure. Mechanical losses during coasting phase are not considered as they do not impact consumed or recuperated energy.

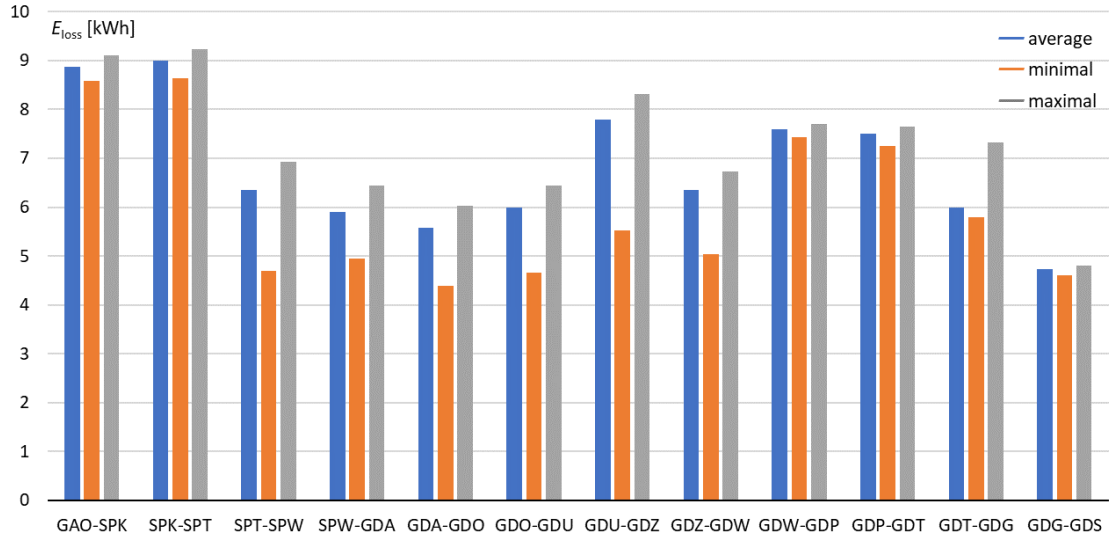

Fig. 6.13. Energy dissipated in vehicle drivetrain for each route fragment – EN57AKM, train bound for Gdańsk (track 502)

Route parts in which the difference between maximum and minimum losses is the highest are those where coasting runs are observed. In such cases, drivetrain losses could be reduced by more than 30% in relation to constant velocity runs. There are also differences in route fragments where vehicles typically run with constant velocity – those can be attributed to difference of required power caused by different mass of the passengers onboard.

Another interesting parameter is the relative energy consumption, given in kWh/km. Such data gives information on energy efficiency of the vehicle that can be compared against other vehicles. It can also show impact of driving technique and route inclination and curvature on energy consumption. Chart of relative energy usage for each route part is shown in Fig. 6.14.

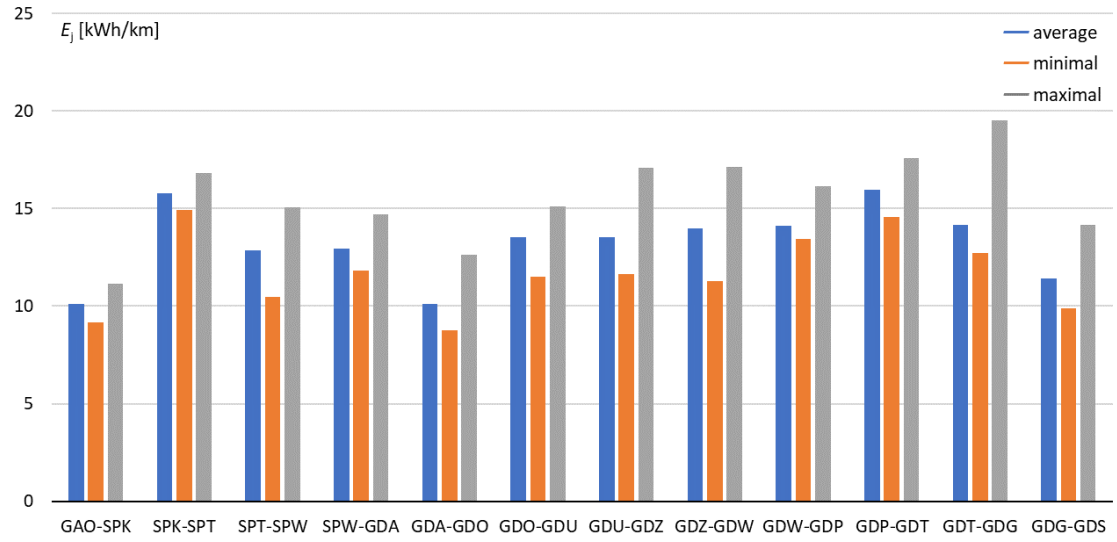

Fig. 6.14. Energy consumption per kilometer for each route fragment – EN57AKM, train bound for Gdańsk (track 502)

Average energy consumption falls between 10 and 16 kWh/km, which is a value expected for suburban electric train. It is worth noting that for longer fragments relative energy consumption can be lower than for shorter ones, as the energy–intensive acceleration phase constitutes for lower percentage of the run time and distance. Differences between minimal and maximal values are also emphasized, as those are influenced by the regenerative braking. Because the regenerative braking is influenced mostly by traffic situation (overlapping of movement phases), and energy regenerated is similar for each route part, the highest differences between minimum and maximum energy used is found in shortest fragments, notably between Gdańsk Stocznia and Gdańsk Główny stations.

The waveforms and charts shown earlier constitute only for one vehicle class moving in single direction. In order to show complete analysis data for the vehicles, author compiled the results for all the vehicles in form of a table (Tab. 8). Remaining waveforms and charts showing different vehicles, velocity profiles and direction of the run are included in Appendix 2. Presented equivalent emissions of CO2 were calculated using European Environment Agency (EEA) data for Polish energy mix [45].

Table 8. Comparison of energy efficiency of the vehicles

Vehicle	**Track 502** (direction Gdańsk)			**Track 501** (direction Gdynia)		
	Min.	Avg.	Max.	Min.	Avg.	Max.
EN57AKM						
Balance [kWh]	208,5	225,2	242,0	208,9	229,0	244,8
Drivetrain losses [kWh]	78,7	81,7	84,8	76,2	83,3	86,5
Losses/total energy [%]	21,0	21,4	21,9	21,0	21,4	21,8
Regeneration [%]	22,8	25,8	27,2	23,0	25,8	27,8
Relative consumption [kWh/km]	12,6	13,3	14,3	12,4	13,6	14,5
Emissions [g CO2/km]	8812	9290	9983	8618	9448	10099
EN71SKM						
Balance [kWh]	201,1	206,3	211,4	203,4	210,1	216,0
Drivetrain losses [kWh]	61,3	63,7	65,9	63,5	65,5	66,9
Losses/total energy [%]	17,4	17,8	19,0	17,5	17,9	18,4
Regeneration [%]	24,3	26,9	28,1	26,0	27,2	27,9
Relative consumption [kWh/km]	11,9	12,2	12,5	12,0	12,4	12,8
Emissions [g CO2/km]	8297	8511	8722	8391	8668	8912
31WE						
Balance [kWh]	213,4	239,4	258,4	221,2	241,0	251,0
Drivetrain losses [kWh]	82,6	89,9	94,6	89,2	92,7	95,3
Losses/total energy [%]	20,7	21,1	21,5	21,0	21,2	21,7
Regeneration [%]	25,5	28,1	31,7	27,5	29,0	30,9
Relative consumption [kWh/km]	12,6	14,2	15,1	13,1	14,2	14,8
Emissions [g CO2/km]	8805	9880	10516	9127	9925	10352

It should be noted that despite the lowest energy consumption, EN71SKM class vehicle is used for significantly less services and has the smallest passenger capacity of the considered multiple units. Therefore, comparison of relative energy consumption is desirable, showing results per passenger–kilometer. Because the model operates using only load mass of the vehicle, passenger numbers were approximated by division of the load mass by average

passenger mass of 70 kg, as given by standard UIC 566 [148]. Complete comparison is presented in Fig. 6.15.

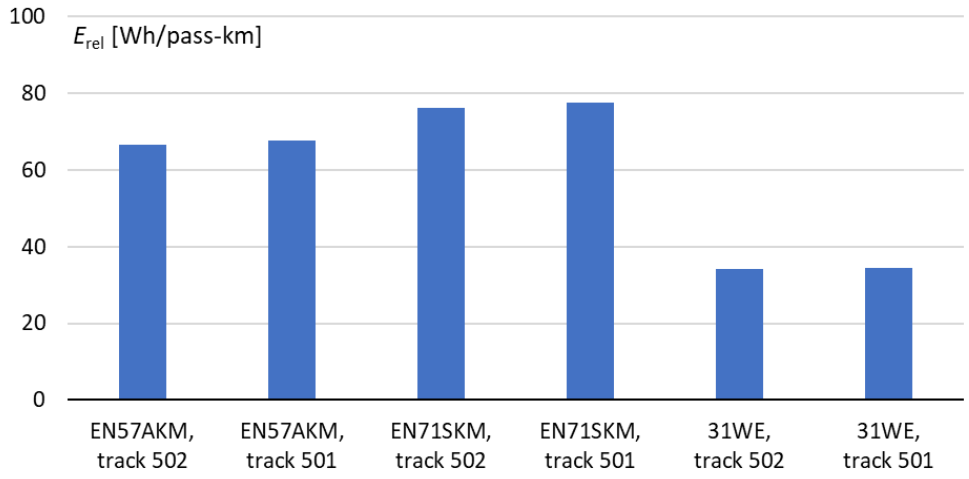

Fig. 6.15. Relative average energy use by analyzed vehicles – both directions

The figure shows that the most efficient is the new 31WE class train – despite the highest power, the vehicle has the highest passenger capacity and the lowest movement resistance. Modernized vehicles of EN57AKM and EN71SKM class are less efficient, and the difference can be as high as 40%. It should be pointed out that shown figure uses daily average numbers, including trains running outside peak hours with very little occupancy rate. During peak hours the values can decrease up to 45%, showing maximum potential for energy efficient passenger transportation. Trains running towards Gdynia (track 501) require more energy per passenger–km, which is expected as the route goes uphill. The difference is, however relatively small – because of night trains bound for Gdańsk, which have very small occupancy rate, thus enlarging the figure for trains going thru track 502.

Comparing the figures with the most popular mode of transport, automobile, shows the advantage of the rail vehicles. Considering electric car, Peugeot e–208 with average car occupancy for Europe of 1,45 person/vehicle [101] and energy consumption of 164 Wh/km of the automobile [7], the relative energy consumption equals 113,1 Wh/pass–km. This is almost double the figure for modernized railroad vehicles, and three times higher than the new ones. For combustion engine powered car, the difference would be likely much higher.

6.2. Catenary

The catenary along the route is uniform, made with 4 wires: one catenary line, 95 mm^2, two contact lines, 100 mm^2 each and a booster cable, 120 mm^2 cross section. The tracks are built using welded S49 steel rails, connected in parallel to reduce the voltage drops. Such a large catenary cross–section, along with relatively short section length (effectively no more than 6 km) results in relatively small voltage drops and reduces losses. It is also a factor in regenerative braking efficiency improvement – as there are typically 3 to 4 trains

moving in each direction, chance for one of the vehicles consuming regenerative braking energy of other is increased.

The largest losses were observed in section between substation Gdańsk Wrzeszcz and end of the line beyond the Gdańsk Śródmieście station. The section is powered only from one side, but the catenary installed over both tracks is connected at the end. It should be also noted that within this section, terminal station is located – therefore, energy is being used for heating of the vehicles waiting for their scheduled service. The section has also the most stop–to–stop route parts, so acceleration and braking occurs there most often. For the section, power and energy of the losses were calculated (Fig. 6.16, 6.17):

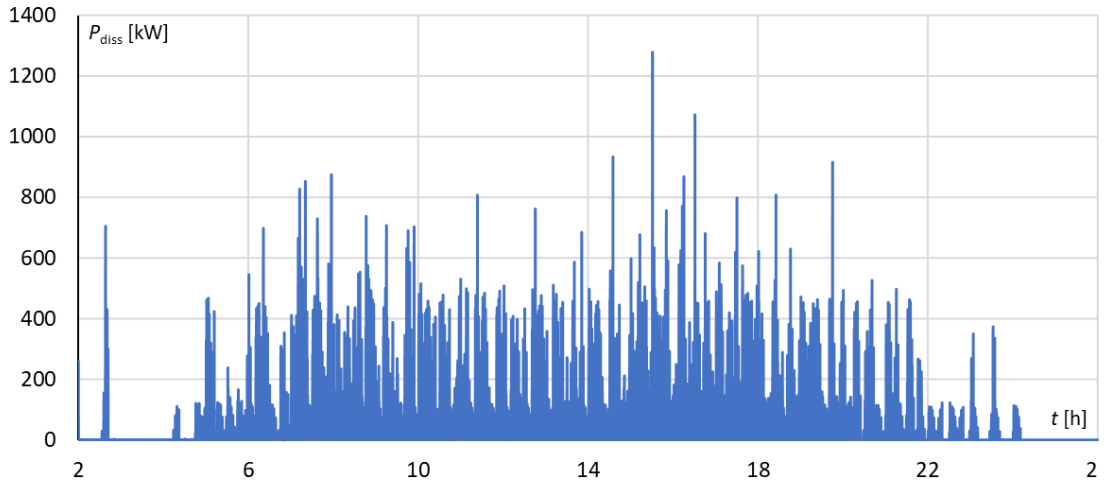

Fig. 6.16. Power of losses on section between Gdańsk Śródmieście and substation Gdańsk Wrzeszcz

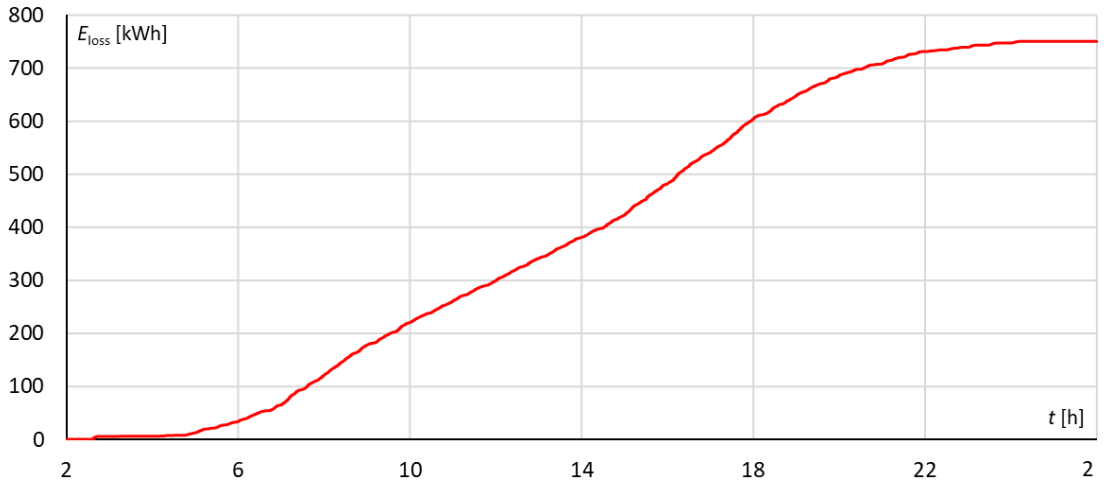

Fig. 6.17. Energy of losses on section between Gdańsk Śródmieście and substation Gdańsk Wrzeszcz

The highest losses coincide with the afternoon peak hours, when multiple vehicles operate with nearly full occupancy. The peak exceeding 1200 kW of power loss is a combination of multiple vehicles accelerating and braking at the same time. There are also peaks of

losses power outside the rush hours, as the regenerative braking energy is dissipated in the catenary. Total losses within this section amount to about 750 kWh.

The second analyzed power supply section is located between substations Gdańsk Wrzeszcz and Sopot, and fed from both sides. It is the shortest section on this route. Waveforms of losses for power (Fig. 6.18) and energy (Fig. 6.19) are shown below.

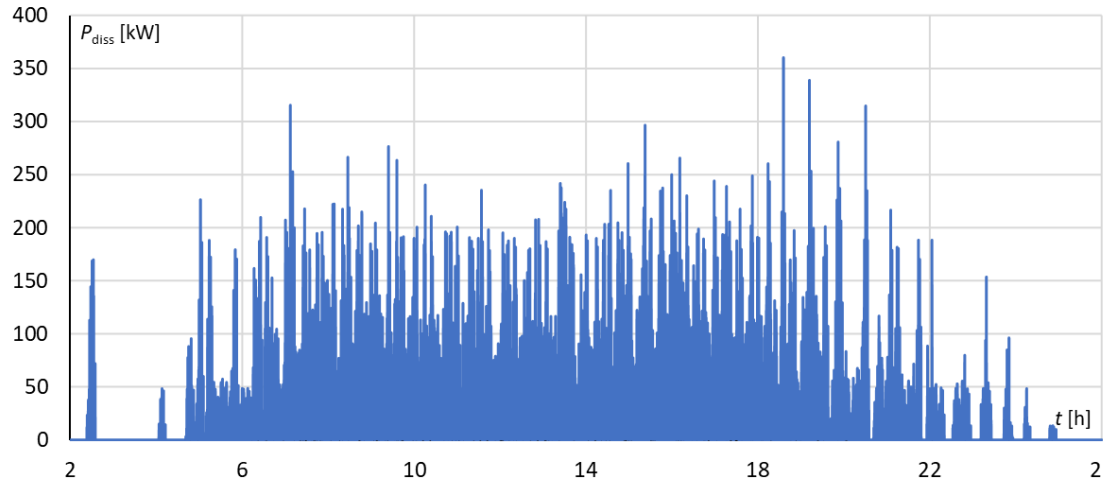

Fig. 6.18. Power of losses on section between substation Gdańsk Wrzeszcz and substation Sopot

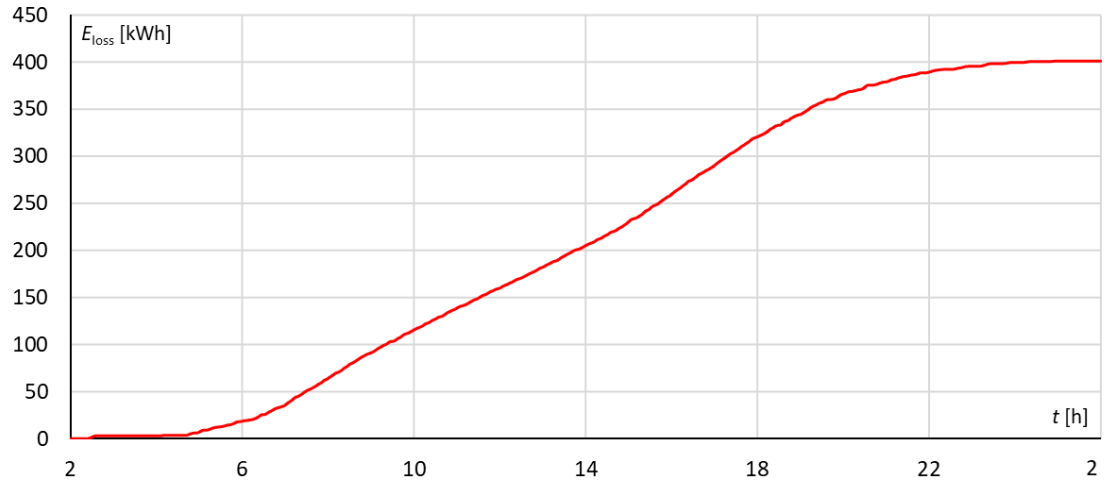

Fig. 6.19. Energy of losses on section between substation Gdańsk Wrzeszcz and substation Sopot

Losses within this section are substantially smaller than the first one. This is because of less accelerating–braking cycles occurring within. There are also no vehicles dwelling for prolonged time, as this section does not contain terminal station. Losses power peaks are significantly smaller in value, and occur in similar moments in time. Dissipated energy is also lower, nearing 60% of former section.

The third and last considered sections powers route from substation Sopot to substation Gdynia Redłowo. This route fragment is the longest, and is also fed from both sides. However, there is the lowest number of stops located within this section, so the acceleration

and braking does not occur as often. Waveforms of dissipated power and energy are shown in Fig. 6.20 and Fig. 6.21.

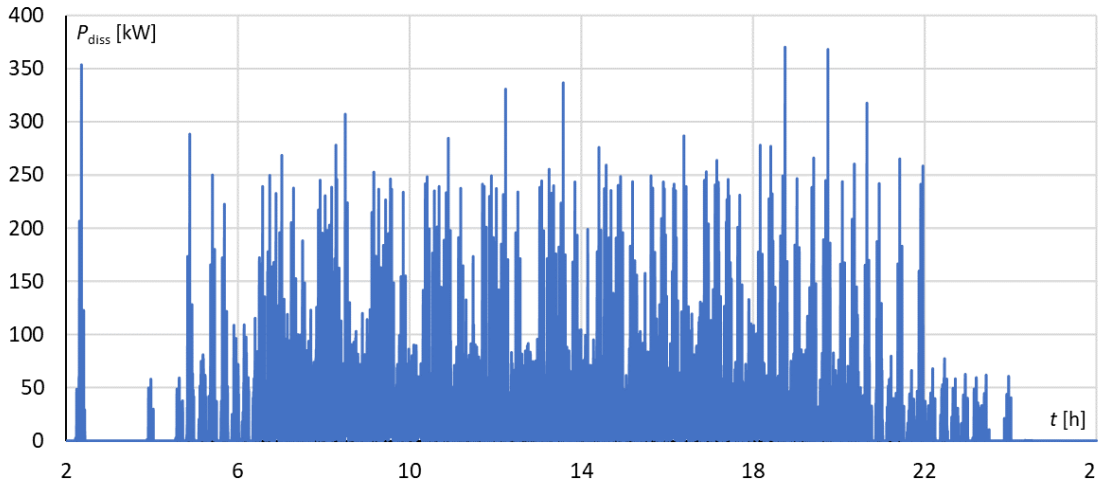

Fig. 6.20. Power of losses on section between substation Sopot and substation Gdynia Redłowo

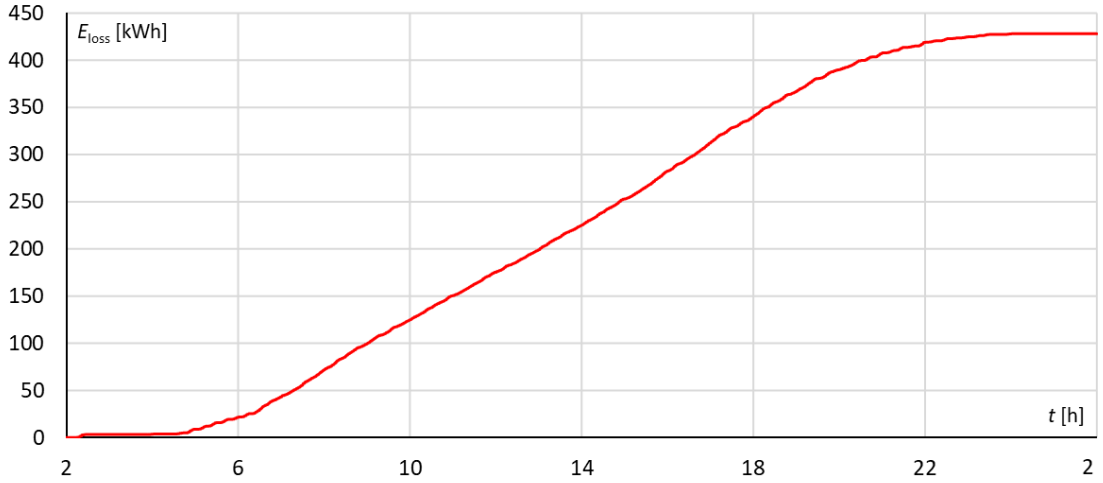

Fig. 6.21. Energy of losses on section between substation Sopot and substation Gdynia Redłowo

The losses within this section are slightly higher than between Wrzeszcz and Sopot. This is because this part of the route is longer and covered with higher average speed, so distance between the vehicles is larger. This translates to higher losses as the current needs to flow longer distance to and from vehicle. This also increases losses associated with regenerative braking.

Total energy dissipated in catenary amounts to approximately 1,6 MWh (Fig. 6.22), which is about 3% of energy balance of the vehicles, or 8% of total losses. While this is not the largest part of energy consumption in the system, it still translates to about 1108 kg of CO2 in equivalent emissions, considering Polish energy mix. Difference between peak and outside of peak hours is small – this is probably a result of long intervals between the services.

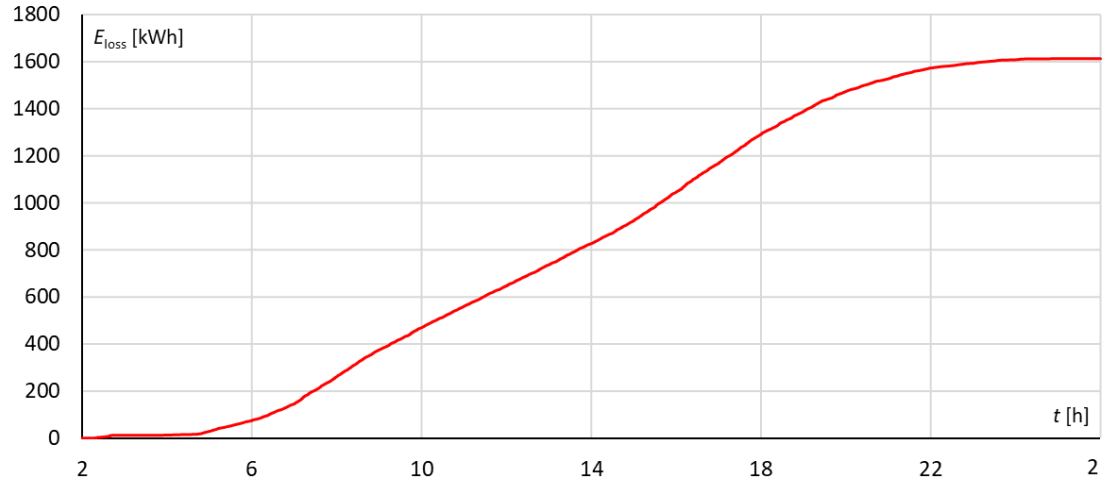

Fig. 6.22. Energy of catenary losses on the whole analyzed route

In order to obtain clearer view of catenary losses, 15 minute average power was computed (Fig. 6.23). Losses outside the peak hours are only slightly smaller than during the morning or evening rush. This is because on the two power supply sections between substations Gdynia Redłowo and Gdańsk Wrzeszcz, there is mostly one vehicle going thru each section in one direction (because of tact being 7 minutes at maximum). Consequently, current from regenerative braking must flow thru the whole section length substations to other sections.

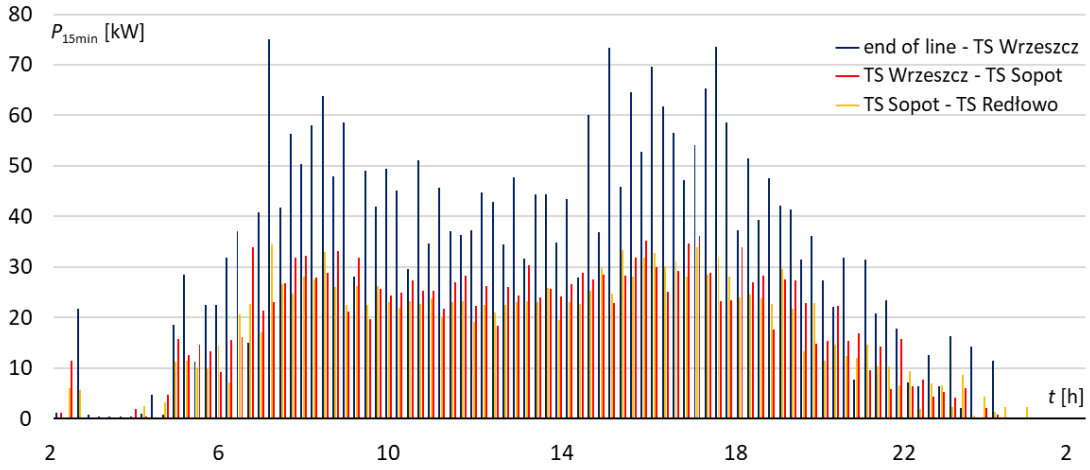

Fig. 6.23. 15 minute average power of catenary losses on the whole analyzed route

The section between TS Gdańsk Wrzeszcz and Gdańsk Śródmieście station has the highest losses – because of the largest amount of vehicles, the most stops of all the sections and powering only from one side.

6.3. Substations and feeders

There are three traction substations on the analyzed route, fitted with PD16 transformer–rectifier units. While those are fitted with three–four units each, at least one of those is decoupled from the substation output bars, acting as a reserve. For the sake of this analysis,

author assumed two units online in substations Wrzeszcz and Sopot, and one in substation Redłowo. For each substation values of output voltage, current and power were computed. Losses occurring in feeder cables were also considered. Idle voltage value of 3600 V was assumed for all three substations.

Substation Gdańsk Wrzeszcz is connected to two power supply sections, with one being fed from one side. Waveforms of voltage, current and power are shown on Fig. 6.24, 6.25 and 6.26.

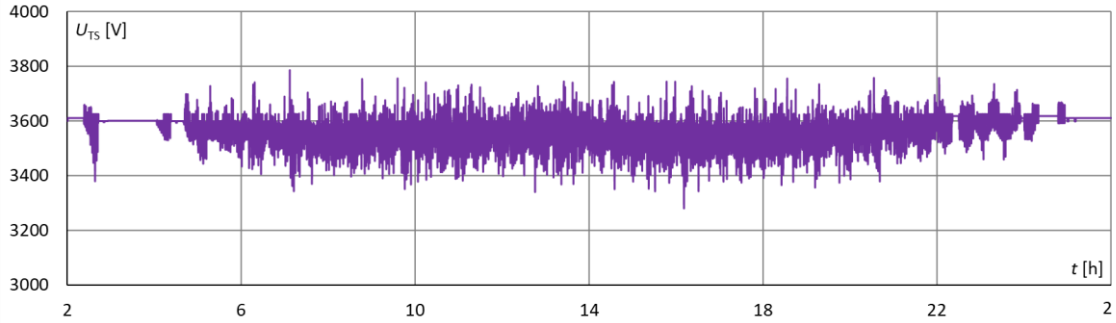

Fig. 6.24. Output voltage – substation Gdańsk Wrzeszcz

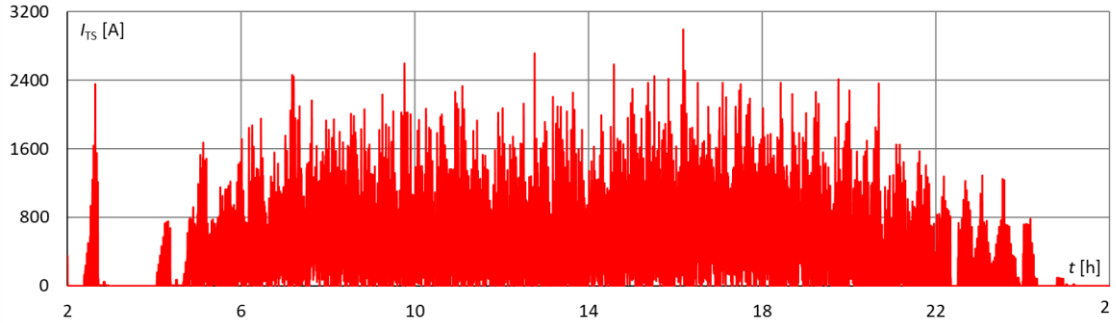

Fig. 6.25. Output current – substation Gdańsk Wrzeszcz

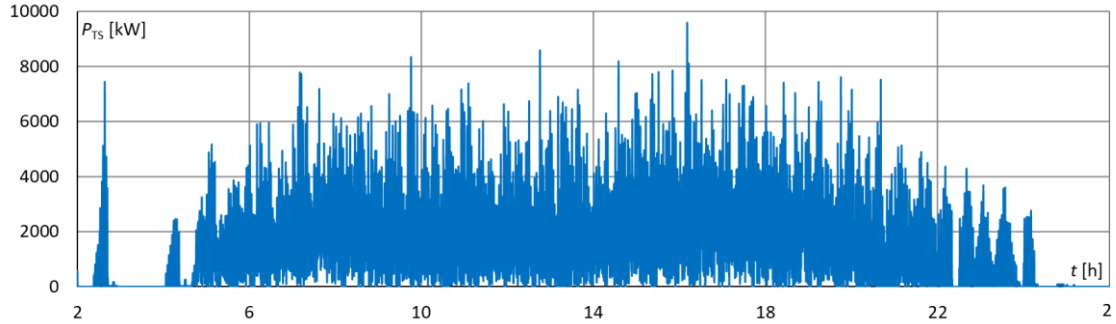

Fig. 6.26. Output power – substation Gdańsk Wrzeszcz

Power spike at the beginning (around 2:30) is caused by night trains going towards Gdańsk in short interval. This causes voltage drop to below 3400 V; such voltage drops occur regularly as the value lies within nominal parameters of substation. The lowest value of output voltage is around 3300 V, and occurs only once during early afternoon peak hours. Regenerative braking causes voltage to rise to about 3800 V, but only for a short periods of time (seconds) as the rheostatic braking chopper is active at this voltage levels.

The substation has four feeders connected. Because the cables have large cross section and relatively short length, the losses are relatively small in comparison to other transport system elements (Fig. 6.27, Fig. 6.28).

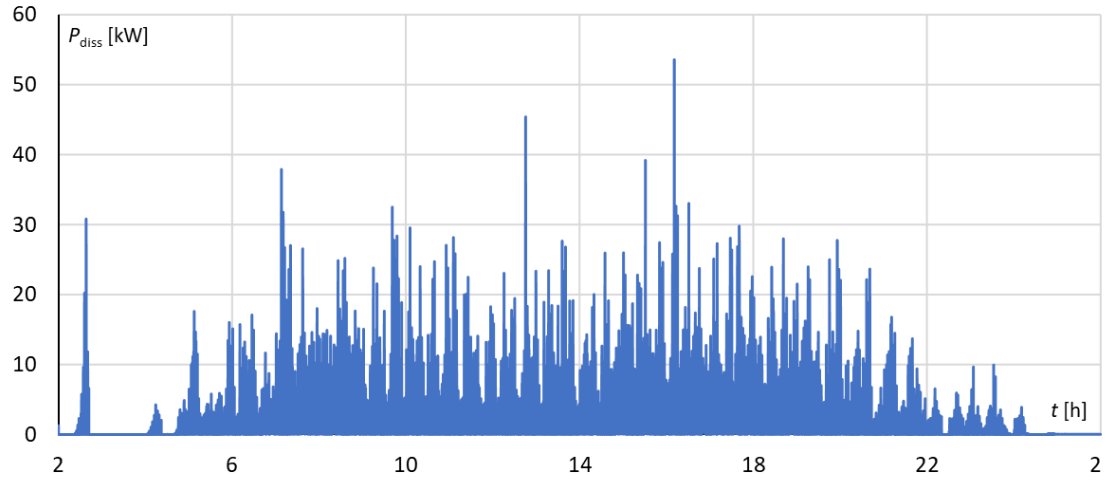

Fig. 6.27. Feeder losses power – substation Gdańsk Wrzeszcz

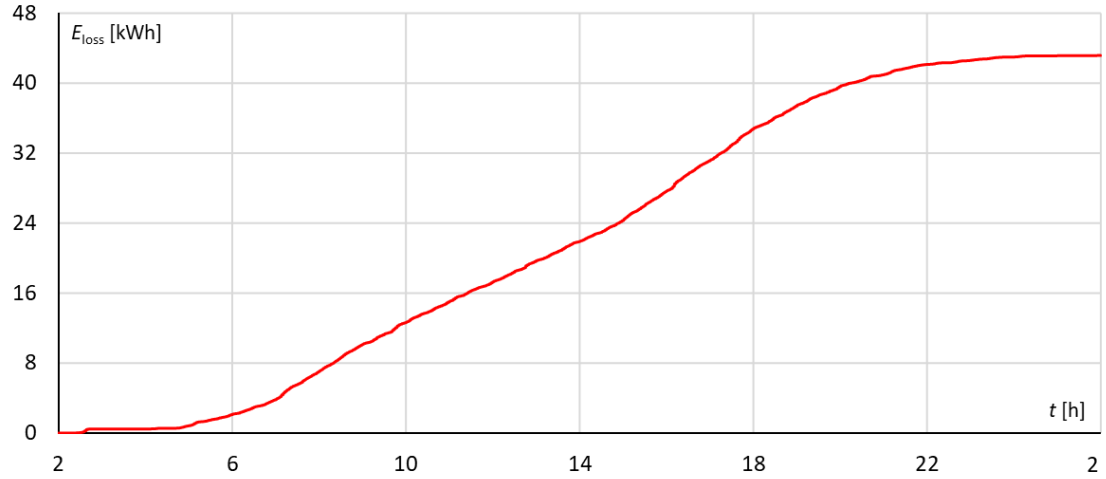

Fig. 6.28. Feeder losses energy – substation Gdańsk Wrzeszcz

Maximum value of losses in feeders slightly exceed 50 kW, and this also happens only for a short periods of time – when multiple vehicles accelerate or brake at the same time. Total dissipated energy is at 43 kWh, which is an order of magnitude less than losses computed in catenary.

The next substation is located near Sopot Wyścigi station, south from the platform. It is also connected to two power supply sections, both powered from two sides. The section between Gdańsk Wrzeszcz and Sopot Wyścigi is the shortest, has less stations within and does not contain terminal. The section towards Gdynia Redłowo contains only four stops located in the longest distances from each other on the analyzed route. Computed waveforms of voltage, current and power are shown on Fig. 6.29, 6.30 and 6.31.

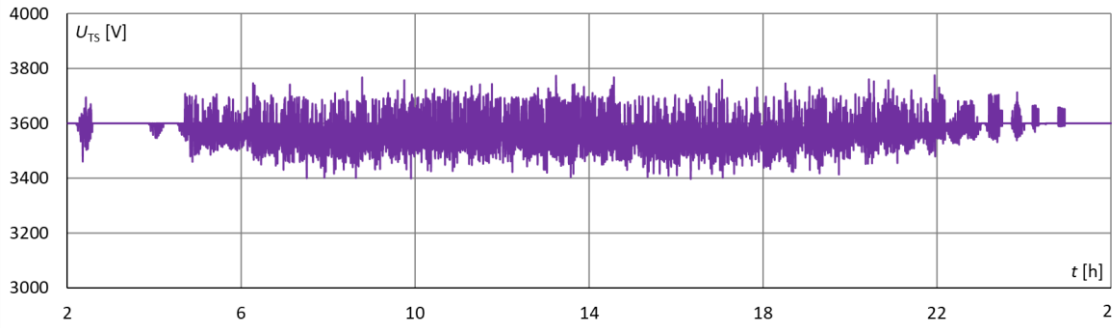

Fig. 6.29. Output voltage – substation Sopot

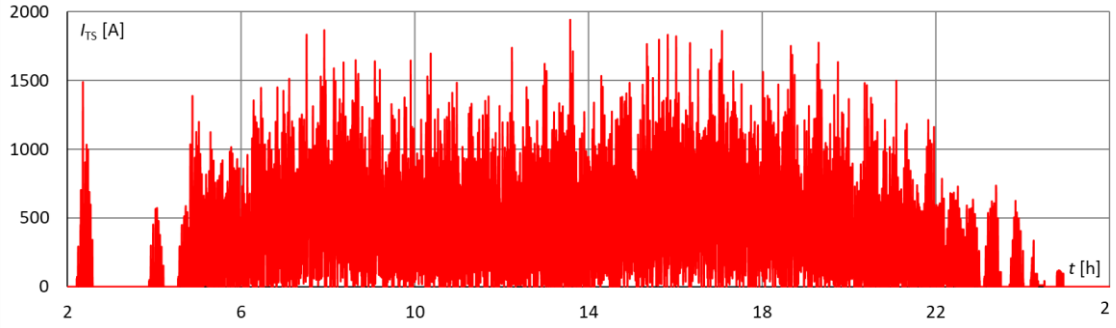

Fig. 6.30. Output current – substation Sopot

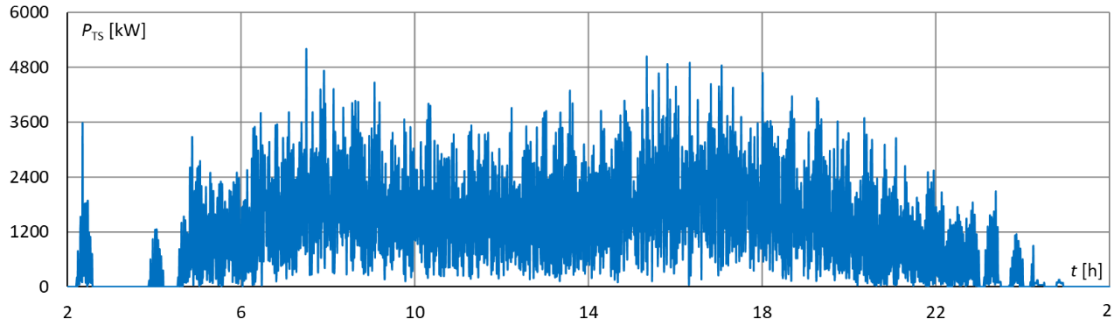

Fig. 6.31. Output power – substation Sopot

Voltage fluctuates during the day within bounds similar to TS Wrzeszcz, but the peaks are less notable, as the substation operates under more consistent load. The peak hours are less visible, with maximum currents of about 2000 A. Output power is smaller, as the section is shorter and there are typically less vehicles going thru at the same time.

Lower substation load is also reflected in feeder losses. There are also four feeder cables, but the maximal power of dissipation is about 22 kW, less than half of TS Wrzeszcz maximum feeders losses. The energy wasted amounts to about 30 kWh (Fig. 6.32, Fig. 6.33), which is close to energy consumption of the vehicle for single station to station run.

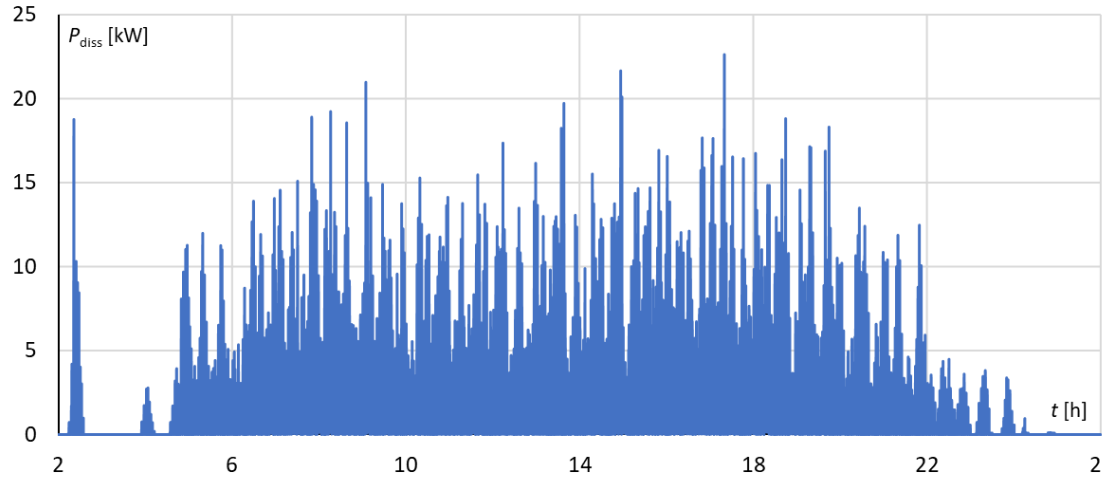

Fig. 6.32. Feeder losses power – substation Sopot

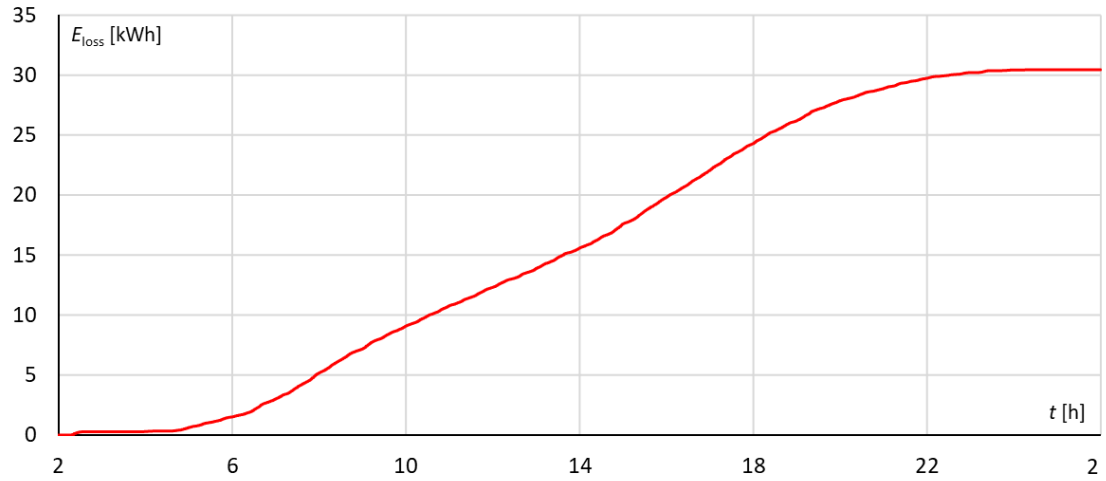

Fig. 6.33. Feeder losses energy – substation Sopot

The last analyzed substation is located in Gdynia Redłowo, between stations Gdynia Orłowo and Gdynia Redłowo. The substation is connected to catenary installed on SKM line, but further north power supply is interconnected with intercity line and port connection. Therefore, in order to analyze suburban line separately, author assumed that one transformer–rectifier unit is connected to analyzed route. The rest of the units inside substation are powering the next section independently, thus are not under consideration. As a result, this substation is powering only one power supply section – but the section itself is fed by two substations – from TS Redłowo and TS Sopot.

Similarly to substations described earlier, output voltage, current and power were computed (Fig. 6.34, 6.35, 6.36).

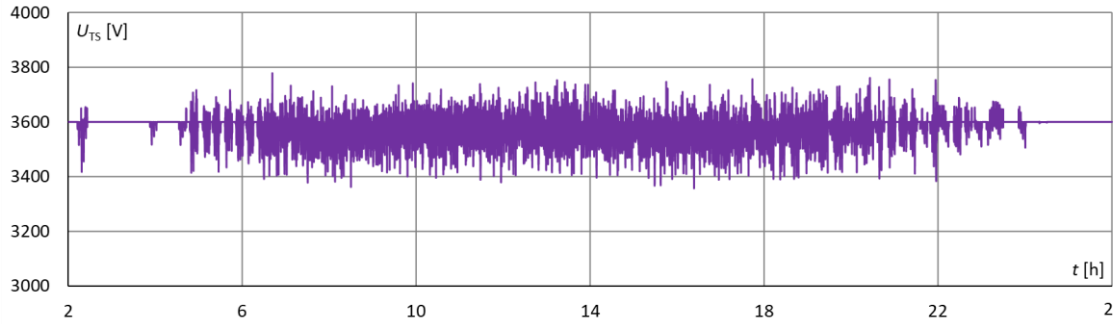

Fig. 6.34. Output voltage – substation Gdynia Redłowo

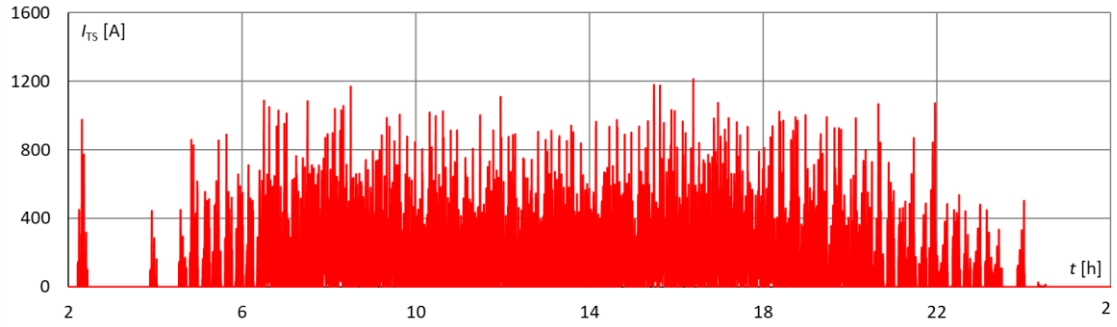

Fig. 6.35. Output current – substation Gdynia Redłowo

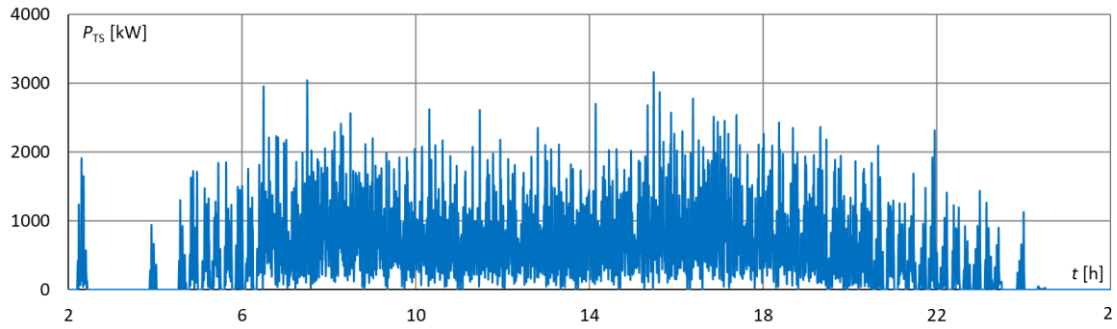

Fig. 6.36. Output power – substation Gdynia Redłowo

Output voltage rises to about 3800 V during regenerative braking and falls to slightly below 3400 V under the highest load. The highest current does not exceed 1400 A – this is because there are rarely more than one vehicle going in each direction at the same time. Despite the section between Sopot Wyścigi and Gdynia Redłowo is the longest within the analyzed route, there are relatively few stops and those are separated by the longest distances. Because of this, the vehicles cover this part of the route quicker than the other two, which also translates to lower power load (rarely above 2 MW, as the probability of multiple vehicles accelerating at the same time is very low). Less frequent accelerations are a factor too.

Feeder losses also reflect the fact of only one transformer–rectifier unit powering the route (Fig. 6.37, 6.38), and the feeders are half in number.

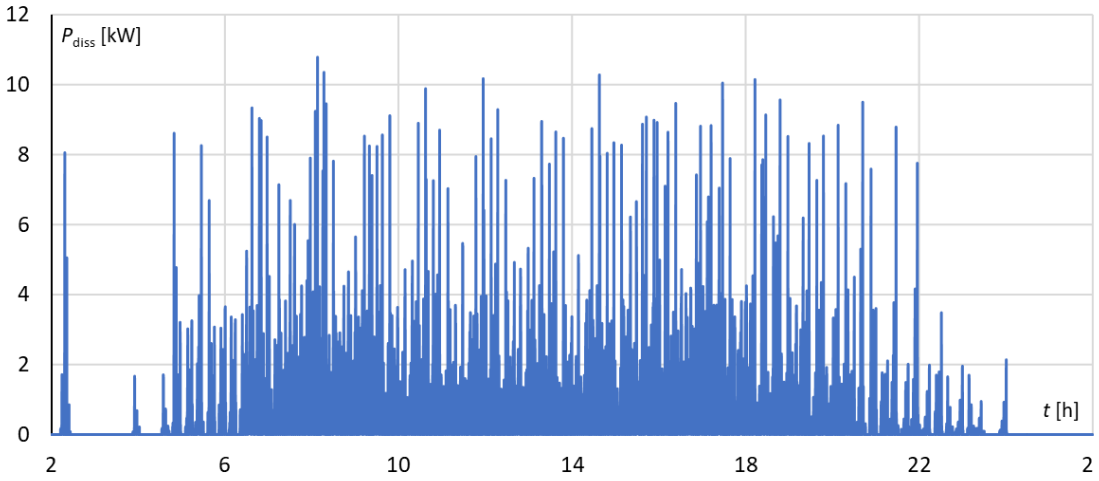

Fig. 6.37. Feeder losses power – substation Gdynia Redłowo

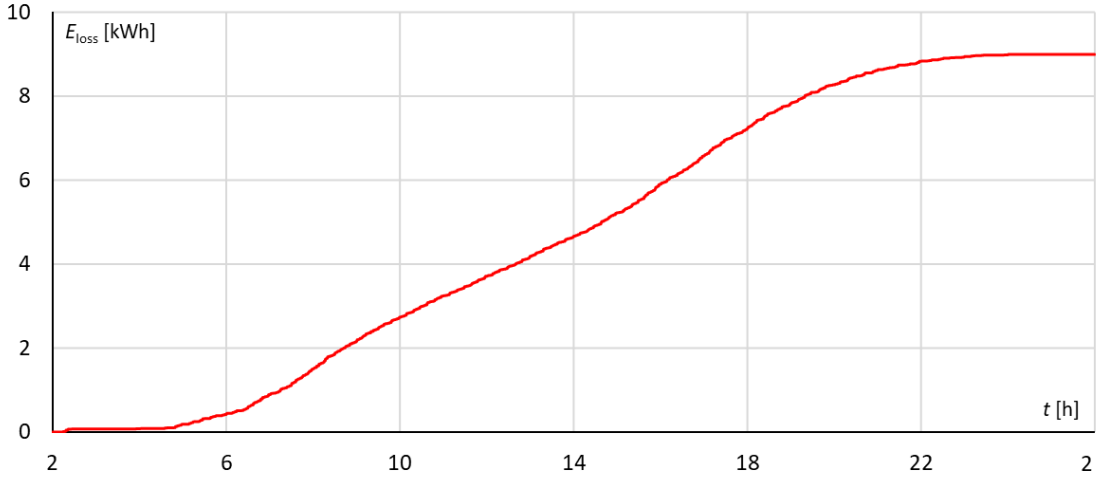

Fig. 6.38. Feeder losses energy – substation Gdynia Redłowo

Maximum power of dissipation is about 10 kW, which is an expected value as there are only two feeder pairs connected. In terms of energy, only 9 kWh were wasted – the least of the analyzed substations. This is a result of lower substation load, which stems from powering only one section that has the least stops and shortest travel time.

6.4. System total

Comprehensive analysis should focus not only on parts of the transport system, but on cumulative results for the whole network as well. For comparable results, author compiled cumulative energy consumption chart, showing total energy figures in relation to time of the day (Fig. 6.39). Please note that "vehicles movement" include energy recuperation, so it shows the total balance.

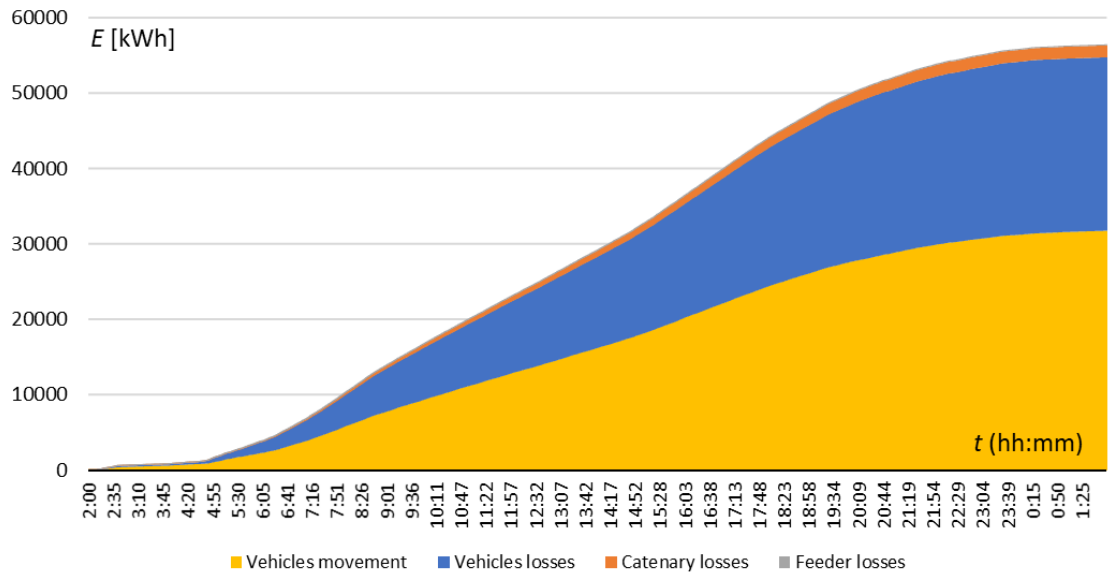

Fig. 6.39. Cumulative energy consumed by the transportation system

The most energy in transportation system is used by the vehicles, for both movement and losses. The losses are significant in value, amounting to almost 40% of vehicle energy requirement – this is because energy is dissipated not only during the acceleration and cruising phases, but also during the regenerative braking. Losses in catenary are about 3% of total energy balance, because of short power supply sections and large cross–section. Losses in feeder cables are significantly smaller, below 1% of total consumed energy – because of very large cross–section and relatively short length of the cables. However, neither catenary nor feeders should be neglected, as their parameters impact value of vehicle pantograph voltage, which, in turn, directly influences energy recuperation and possible movement dynamics. Moreover, the distribution of energy consumption depends on infrastructure and rolling stock in use, so it can be different for different routes and modes of transport.

Energy dissipation by the traction substations (power transformer, rectifier, LC filter etc.) was not considered within the scope of this analysis. However, author tested early version of the presented model using exemplary transportation network [61], with results showing losses in substations on level similar to the catenary.

The vehicles' energy consumption is a key factor in analysis of efficiency of transport systems. However, it is directly influenced by the regenerative braking, which, in certain conditions, may result in significant energy savings. In this case, short length of power supply sections and large catenary cross section were the main causes of good recuperation efficiency (Fig. 6.40). This is despite the relatively long time intervals between the services, often leading to single vehicle movement thru section in each direction.

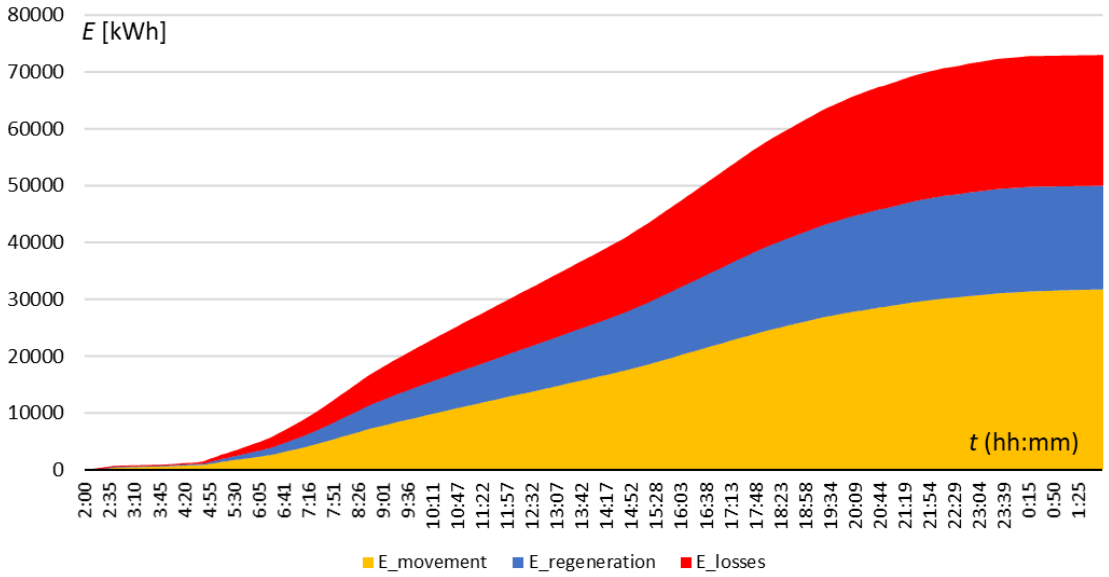

Fig. 6.40. Energy balance of all the vehicles

Figure shows that without regenerative braking, the vehicles would consume total of over 72 MWh of energy during the day of operation. However, energy recuperation lowers this to about 54 MWh, so 25,5% of the required energy is provided by vehicles themselves thru regenerative braking. In numbers, this translates to about 18,3 MWh of energy saved, and equivalent emissions reduction of 12,7 Mg of CO2. This proves the significance of energy recuperation and main advantage of electric vehicles over diesel–powered ones.

However, energy recuperation is highly dependent on traffic organization – if there is no intersection of acceleration and braking phase between the vehicles, the energy could not be regenerated. In case of suburban transport systems this is mitigated to an extent by regular tact, leading to vehicles accelerating and decelerating often. Because of connecting the whole system together by substations and utilization catenary with large cross section, improvement of energy regeneration is achievable.

Nonetheless, looking into possible variability of energy recuperation efficiency can be interesting, especially when developed model allows for execution of multiple velocity profiles, with varying probability. Therefore, author carried out the simulation multiple times with the same input parameters, changing only the seed values for the random number generators in vehicles to look into possible impact of changed dwelling time and velocity profiles on energy recuperation. The seed values were also obtained using RNG. The result of this analysis is shown in Fig. 6.41.

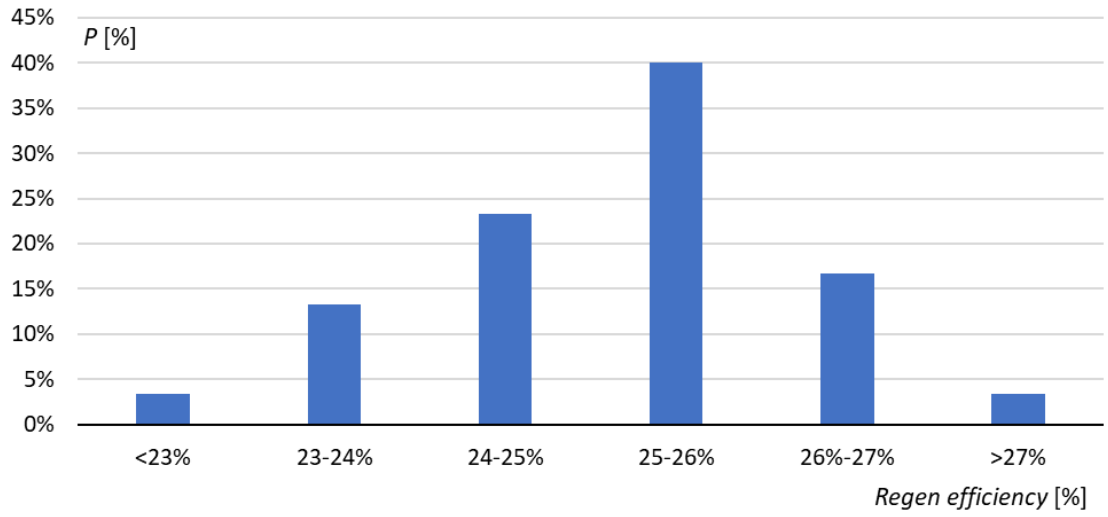

Fig. 6.41. Percentage of runs (out of 30) with specified regeneration efficiency

Analysis shows that 25,5% of regeneration efficiency was the most probable outcome of the simulation. Higher efficiency is less probable, and was caused by combination of less consumption (more "alternative", coasting–based runs) and slightly better synchronization between acceleration and braking. Less efficient runs were more numerous, and contained more constant–velocity movement. Overall, the differences between maximum and minimum recuperation efficiency are small, mostly due to limited variability within the system. However, it is still valuable to be able to see how the energy recuperation can change during the normal operation.

7. PROPOSED OPTIMIZATION METHOD

Optimization of velocity profile and timetable for electrified transport systems is growing in importance as the energy prices increase. The subject matter is studied since 1960s, and during those years multiple methods for energy consumption reduction were developed. Currently there are algorithms that allow for simultaneous optimization of both velocity profile and timetable, some of which are designed to work and adjust the parameters to actual traffic situation.

However, those advanced methods rely on precise execution of computed velocity profile and following the timetable rigorously. This implies reliance of the system on advanced signaling systems which send information to the driver, or even fully autonomous operation, which is understandable, as the most papers are written with autonomous subway systems in mind. Transportation networks that were presented as examples with such automated and optimized control within the literature review were:

- Valencia Metro, Spain [151],
- Naples Metro, Italy [21],
- Taipei Metro, Republic of China (Taiwan) [147],
- Beijing Metro, People's Republic of China [159],
- Subway systems in United States (BART/San Francisco, MARTA/Atlanta, New York, Washigton, Los Angeles) [140,146],
- S–Bahn Hamburg, Germany (only one line) [46].

In reality, suburban railway systems are rarely fitted with such equipment – therefore control of train movement is generally done manually. Even systems using various forms of optimization (like JR Central and JR East in Japan, or Munich S–Bahn in Germany) rely on human operation, using cab signaling as an information for the driver. Moreover, it is harder to control departures and arrivals precisely, as rolling stock used by urban rail operators is often not designed for quick passenger exchange, especially when passengers with limited mobility are considered [15,27,97] – in Poland, vehicles used in suburban operation have only two pairs of doors per carriage, while in Japan, the usual number is four.

Because of this, author proposed optimization method designed for simple implementation that does not require expensive advanced signaling, while allowing for considerable energy savings. It is worth noting that in recorded runs, consistent use of cruise control was observed. Because of this, presumed potential for savings is high.

7.1. Methods of optimization in electrified transport systems

Significance of lowering the energy consumption in electrified transport systems motivated the research into possible improvements in this matter. Because of this, multiple methods of optimization were proposed, varying in complexity, requirements and objectives [6,18,31,95,166]. Existing optimization methods can be classified in relation to their realization method or objective (Fig. 7.1). Methods selected by the author for this work are highlighted.

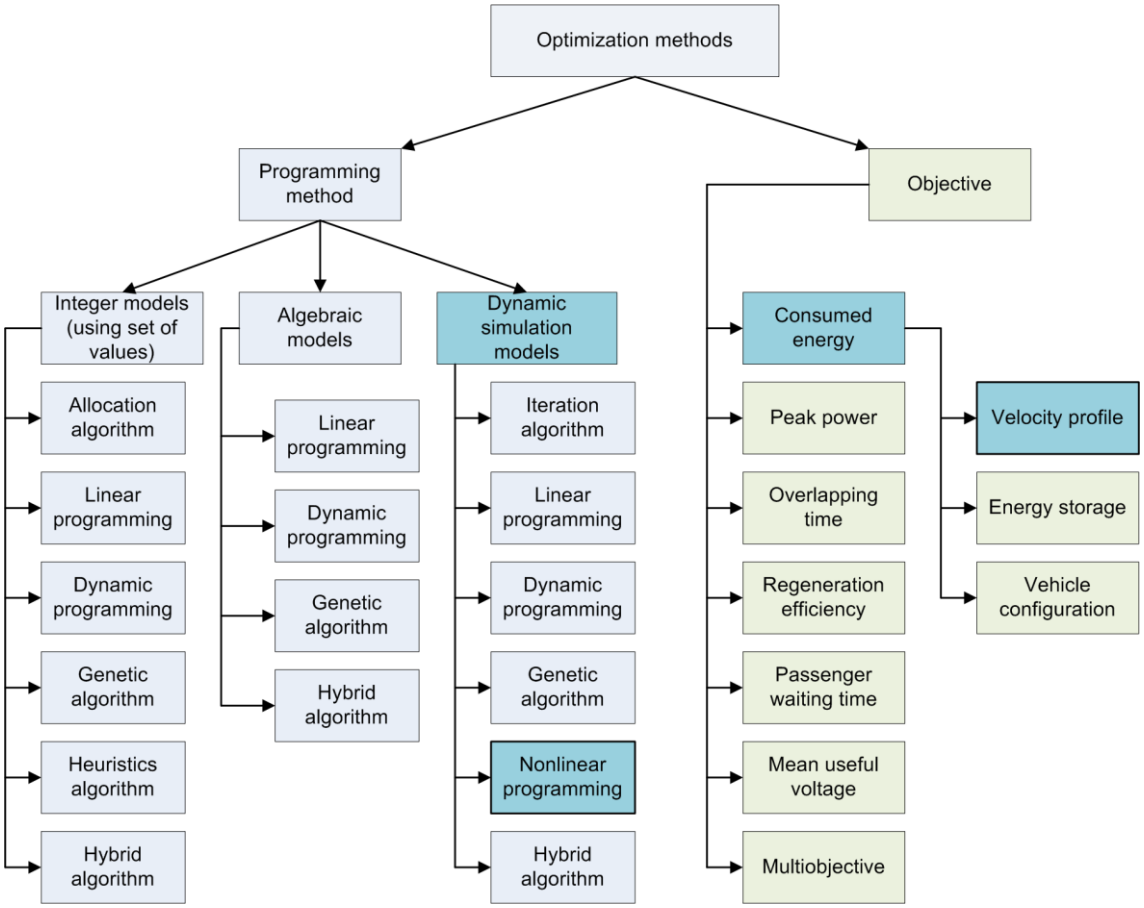

Fig. 7.1. Classification of existing optimization methods used for electrified transport networks [28,44,56,68,78,86,90,125,147,151,161]

Conducting optimization requires use of model that can be different depending on selected algorithm. While some of the algorithms can be used for most of the models, it is advisable to use those which are efficient in analyzed case, e.g. nonlinear programming algorithms are considered slow for multicriterial optimization problems with multiple design variables [28,100,161].

There are also multiple possible objectives of optimization – while this dissertation is aiming for reduction in energy consumption, there are other criterions that can be taken into account, depending on requirements of analyzed transport system. The most advanced are multiobjective optimization methods, which attempt to optimize multiple variables simultaneously. While their potential is the highest, their practical implementation usually requires the highest investment in both infrastructure and rolling stock.

Within the methods meant for reduction of energy consumption, author was interested the most in velocity profile optimization. There are many solutions to such problem, but significant part of them require precise velocity control. Therefore, for suburban railway application methods that optimize velocity profile by determining location of movement phase change might be useful. Those algorithms choose between acceleration, cruising, coasting and braking, as shown in Fig. 7.2 for the run between two stops. While velocity profiles obtained this way are not necessarily resulting in the highest theoretically

achievable savings, they are possible to deploy without large investment in equipment, as they can be realized by the human driver.

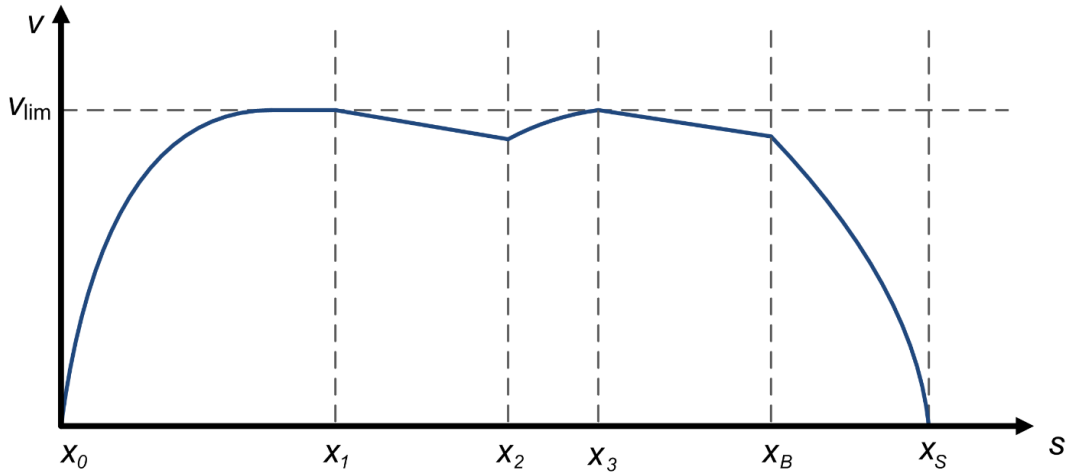

Fig. 7.2. Principle of phase change point setting: x_0 – starting location, x_1 – cruising to coasting, x_2 – coasting to acceleration, x_3 – acceleration to coasting, x_b – coasting to braking, x_s – target station location

It is necessary to consider the methods carefully, and select the best suited one for the analyzed transport system. Because even the simplest optimization will result in energy savings, using the most advanced methods might not be necessary as they will provide only small further improvement. Moreover, high cost of required additional infrastructure (about $260000 per track–km) might outweigh savings from reduced energy consumption [112].

7.2. Proposed optimization approach

Author decided to use the relatively simple algorithm, which is cheap and easy to implement (trackside signs are sufficient). In comparison to precise trajectory computation, it does not require cab signaling and modification of vehicle that allow for autonomous operation – it can be realized fully by the human driver.

Therefore, optimization through setting cruising and coasting points, as well as their number has been chosen. Starting point and target station location are loaded from external file. Braking point is not calculated thru optimization algorithm – in order to reduce number of design variables, vehicle is braking using deceleration curve with constant deceleration value. Exemplary vehicle used for the optimization was the EN57AKM, as this is the least powerful vehicle. Acceleration was executed with maximum available motive force, and braking with constant deceleration of 0,9 m/s^2. For the EN57AKM vehicle (with the lowest nominal power), hourly power was assumed – it is justified to do so, as the vehicle does not operate continuously, so overheating of the motors is not an issue.

Optimization was carried out using the developed Simulink vehicle model and programming tools from Matlab Optimization Toolbox. For this task model of a single vehicle, identical to vehicle models used in the main transport system model, was used. It should be noted that the vehicle model used throughout this work was fully parametrized,

similar to elements from block libraries. Such model will work correctly as long as sufficient parameters are provided (Fig. 7.3).

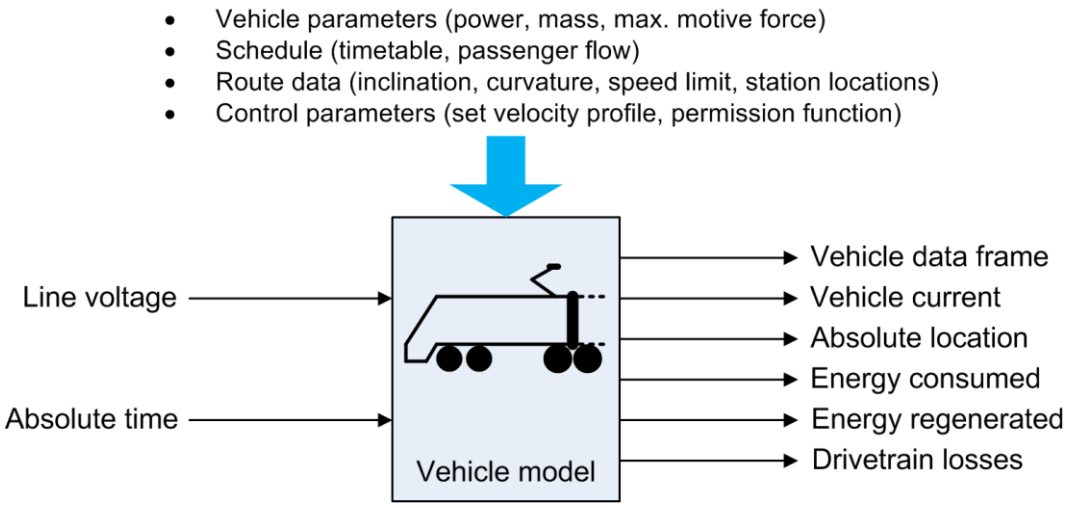

Fig. 7.3. Simplified diagram of vehicle model block with its inputs and outputs (data possible to access within not shown)

Assumed simplifications are as follows:

- Input voltage was assumed constant. Such simplification is allowed, as the pantograph voltage value does not impact energy consumption unless it is within the power limiter bounds,
- The regenerative braking controller was switched off – as the timetable adjusting is not considered, the optimization should provide energy savings without being overly reliant on regenerative braking,
- There is no initial cruising point defined – because the model is designed so the cruising phase is a default movement phase; vehicle will try to accelerate and retain the set velocity,
- Similarly, braking distance or location of braking point is not a subject of optimization, as the model still uses the braking curve for stopping on stations.

Therefore, the algorithm was set to minimize consumed energy. Optimization calculations were performed separately for each part of the route (station to station) in both directions.

In order to perform calculations, objective function was assumed as combination of energy, computed through simulation of developed model and nonlinear cost function, which ensured satisfaction of the timetable:

$$F = E(\text{model}(v_{cr}, \mathbf{X}_{co}, \mathbf{X}_{cr}) + C(t)) \tag{7.1}$$

where: F – objective function, E – consumed energy, v_{cr} – set cruising velocity, $\mathbf{X}_{co} = \{x_{co1}, x_{co2}, x_{co3}\}$, $\mathbf{X}_{cr} = \{x_{cr1}, x_{cr2}, x_{cr3}\}$ – localization of coasting/cruising points, $C(t)$ – cost function, dependent on time.

The design variables are as follows:

- values of set cruising velocity: 50 km/h $\geq v_{cr} \geq$ 70 km/h;

- values of coasting/cruising points location x_{co}, x_{cr}: they should fit between 50 m and 1500 m from each other (there can be up to 3 cruising or coasting points defined, depending on the distance between stations and route inclination/curvature).

The constraints are defined as follows:

- Maximum allowed velocity, equal to speed limit of 70 km/h;
- Maximum run time between stops, equal to time specified in timetable for each route part (optimization cannot cause delays).

There is also cost function C(t) implemented, with value being dependent on run time. Its value equals zero, when vehicle is within bounds of the schedule, and begins rising steeply after run time enters time reserve. This is done in order to prevent computing impractical velocity profiles, which prolong travel time.

Optimized velocity profile does not influence the braking phase – it is still executed in accordance with set braking curve. This way, train will reliably stop on station regardless of computed velocity profile. Such assumption allows for decrease of number of design variables, improving calculation performance.

In Matlab, the objective function is defined using script, which is linked to optimization task thru custom requirement option (Fig. 7.4). It can be decided, if output function value should be minimized, maximized or to certain value.

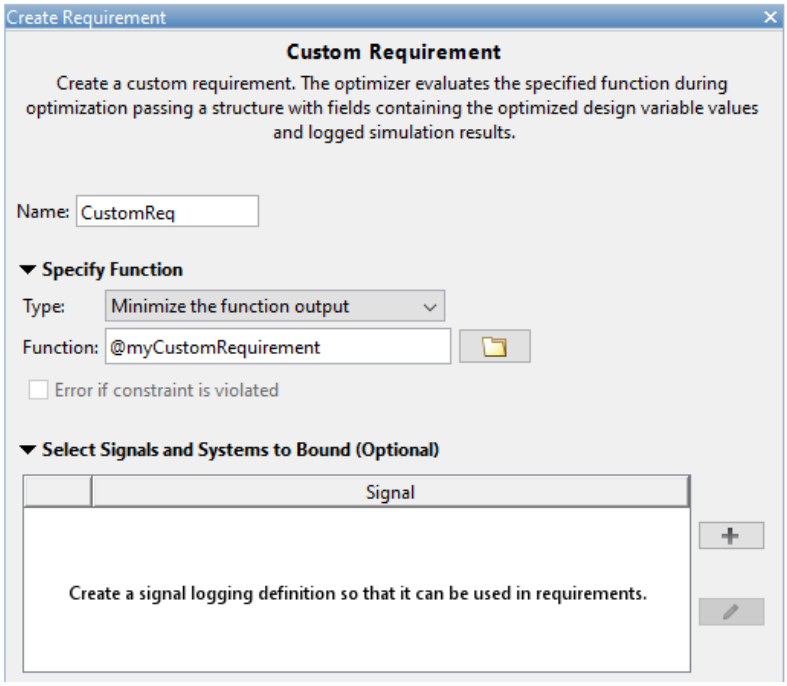

Fig. 7.4. Specification of custom requirement – Matlab Optimization Toolbox

The script–based objective function can be complex, being factually a sub–program within the analysis. This also includes interaction with the model itself, as there is a possibility of

binding signals from the model. Those signals can be then referenced in the objective function, being minimized directly or acting as arguments of the function.

For this problem, author specified the objective function using signal outputs of energy balance and run time. The value of run time was used as an argument for the cost function, which was added to energy value. This way, the objective function value was minimized using the vehicle model, not just system of algebraic equations. This results in consistency between all the developed models.

The design variables are defined by their name and maximum and/or minimum values. Naming of the variables need to be consistent throughout the whole simulation, including the main Matlab Workspace and the model diagram. It should be noted that numerical input of the design variables parameters is required, so relations between them must be specified differently.

Consequently, author modified Control Function used by the model – measurement–based selection of probable velocity profiles, specified in lookup tables as coasting points and speed limits location was removed. Instead, function accepting the location of cruising and coasting points as well as set velocity value was implemented. The function specifies sequence of the points, converting them from relative values used by the optimizer to absolute values, required by the model.

Optimization process is conducted by running the model multiple times, with design variables changed every time, according to selected algorithm [89]. Sequential quadratic programming (SQP) algorithm (implemented in Matlab Optimization Toolbox) proven to be the most reliable for this task – it can efficiently optimize any non–linear problem, regardless from degree of non–linearity. It can still provide meaningful results even if the non–linearity is found within the constraints. However, large number of design variables or constraints can slow down the computation. For this problem, SQP algorithm was a very good match, allowing for better precision and quicker computation than iterative methods [60,100].

7.3. Optimized velocity profiles

Including the above–mentioned constraints, series of simulations were performed for each route part. For the short and relatively flat fragments of the route, the vehicle accelerated to 60–65 km/h (depending on length and curvature), coasted and braked to station stop. Interestingly, optimized velocity profiles for longer and steeper fragments still included only one coasting and cruising point – kinetic energy amassed during the acceleration was enough to allow the train to cover distance between stops without need for re–acceleration.

The optimal speed vs. distance profile is shown in Fig. 7.5. for track 502 (direction Gdańsk) and in Fig. 7.6 for track 501 (direction Gdynia). Please note the movement direction, as the figures present velocity in relation to absolute route distance (consistent with infrastructure data [157]).

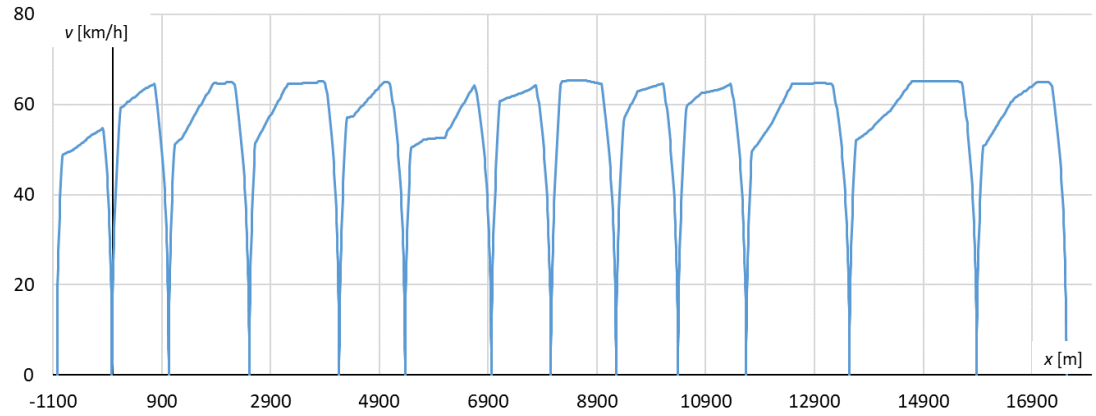

Fig. 7.5. Optimized velocity profile in relation to absolute location – track 502, direction Gdańsk (movement: right to left)

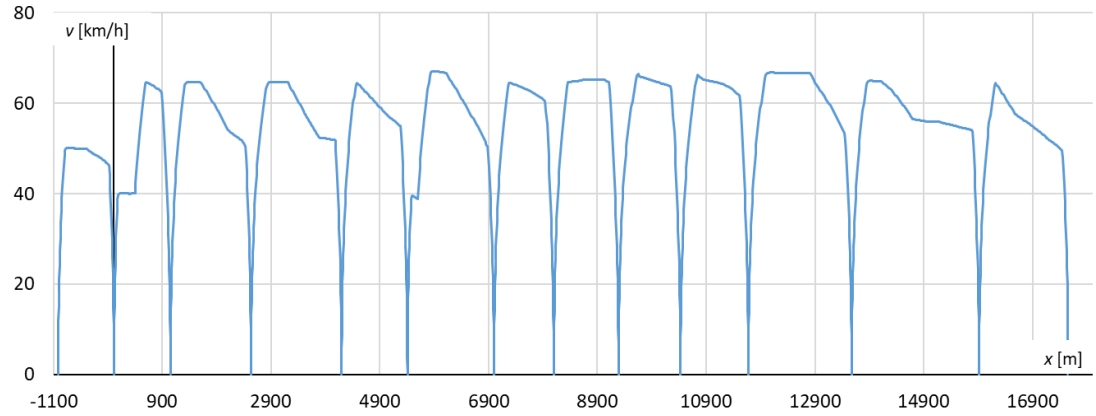

Fig. 7.6. Optimized velocity profile in relation to absolute location – track 501, direction Gdynia (movement: left to right)

The cruising, coasting and braking points location along with set velocity limits are the same for all the rolling stock considered. Because of this, there is a possibility of easy implementation of this method, using the trackside signs (Fig. 7.7).

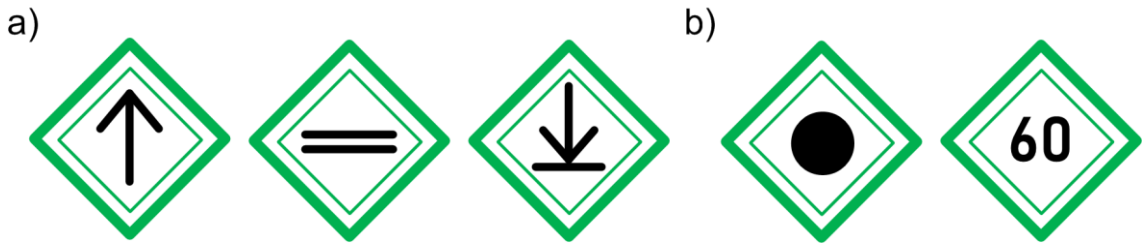

Fig. 7.7. Proposed trackside signs for optimized velocity profile: a) phase change signs for accelerating/cruising, coasting, and decelerating; b) additional signs to be placed with phase change signs: for station and set velocity

The phase change signs could be placed at computed location, being an information for the driver about the velocity profile. Additional signs are intended to be installed along the phase change signs to specify information about the velocity: sign "60" placed with sign "accelerate/cruise" would mean that the set speed for cruising is 60 km/h, and should be achieved with pre–calculated acceleration (in case of this system: 0,8 m/s^2). Additional sign "station" should be used with phase change sign "decelerate" informing the driver about necessity of applying brakes to stop on station. Example of signs placement along with their computed location is shown in Fig. 7.8 for route fragment between Gdańsk Główny and Gdańsk Stocznia stations. Table with complete velocity profiles data for the whole analyzed route can be found in Appendix 3.

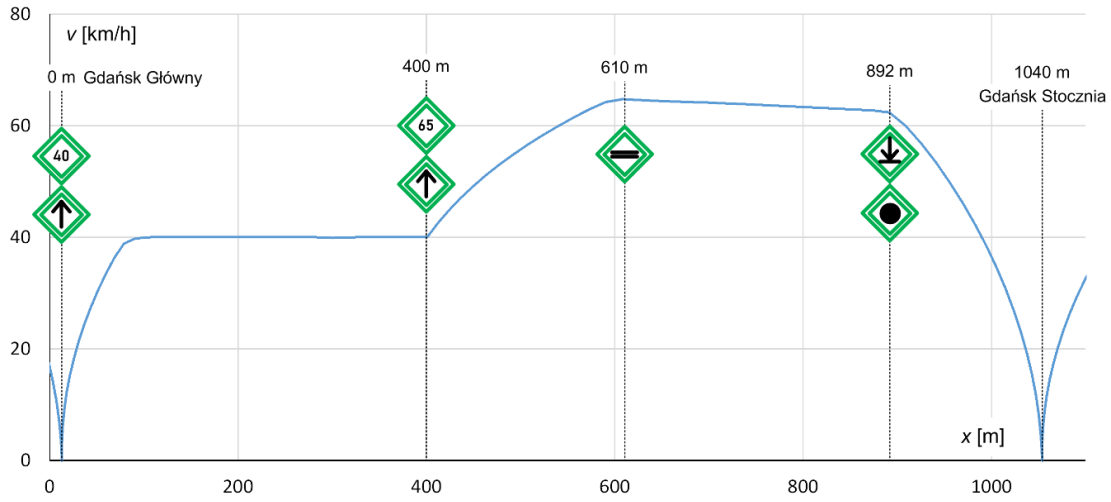

Fig. 7.8. Example of optimized velocity profile and its proposed realization

The optimized run covers the same distance in nearly the same time (28 min actual vs 29 min optimized), satisfying the timetable. There is a possibility of further improvement, however it would require lowering the velocity on certain parts of the route. Consequently, travel time would be prolonged by a few minutes, making the passenger service less attractive. Some offset to this can be achieved by reducing station dwelling time, but this would require making the passenger exchange more efficient. However, rolling stock in service of SKM Trójmiasto have only two pairs of doors per carriage, so acceleration of boarding process is very unlikely as it would require purchasing uniform fleet of radically different vehicles.

7.4. Analysis of energy efficiency improvement

Proposed improvement of energy efficiency was implemented in transport system model described in detail in earlier chapters. The optimized velocity profile data was implemented in velocity profile generator for all the vehicles with 100% probability along the whole route. It is worth noting that the optimized velocity profile is considered a set velocity. Because there are differences between the vehicles (mass, power, motive force, movement

resistance etc.), there are also slight differences between the set and actual velocity. There can also be minuscule differences between peak hours and outside of peak, as the mass of the vehicle varies. This is, however accounted for to an extent, as the optimization was carried out considering the full load of the vehicle. The HVAC controls were modified, so the heating system will try to overlap with the regenerative braking, improving regeneration efficiency, similarly to what was proposed by Pascal et al. [106]. The schedule for the whole system remained the same, similar to power supply system settings. Random parameters were also consistent with un–optimized simulation results shown in chapter 6, as RNG function used returns repeatable values for any given seed. Because of this, presented results for unoptimized and optimized runs can be compared directly.

7.4.1. Optimization results – current power supply structure

In order to provide insight in vehicle operation, the selected waveforms were plotted. For exemplary vehicle (EN57AKM), values of velocity (Fig. 7.9), line voltage (Fig. 7.10), current (Fig. 7.11), energy balance (Fig. 7.12), traction drive efficiency (Fig. 7.13), traction drive losses (Fig. 7.14) and vehicle mass in relation to time (Fig. 7.15) are presented. Author selected the same exact service towards Gdańsk Śródmieście station as shown in chapter 6 to ensure comparability of the presented results.

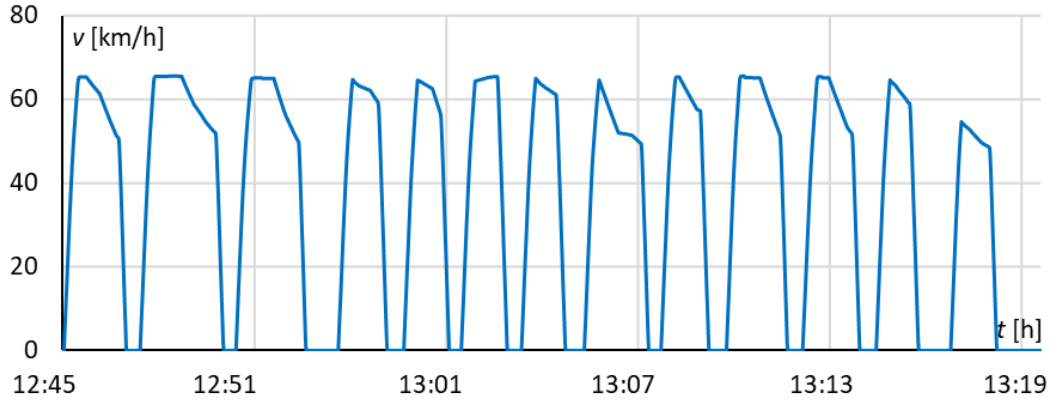

Fig. 7.9. Optimized velocity profile – EN57AKM, track 502

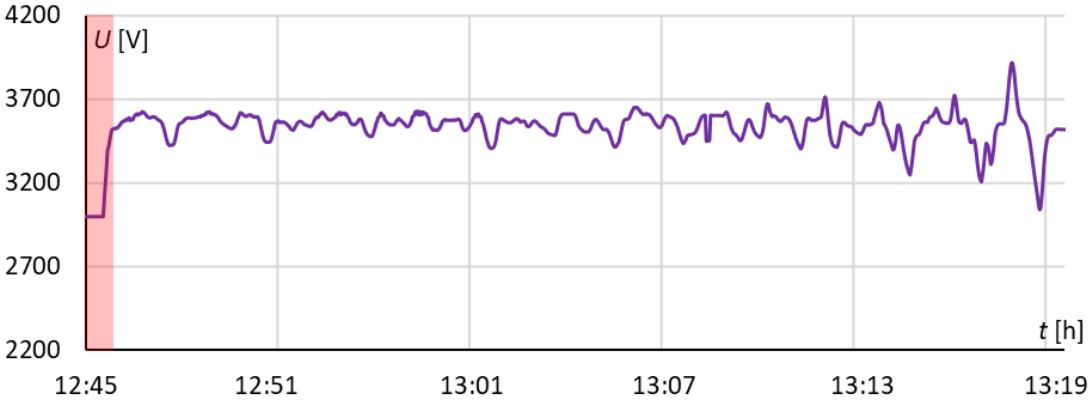

Fig. 7.10. Pantograph voltage, optimized velocity profile – EN57AKM, track 502

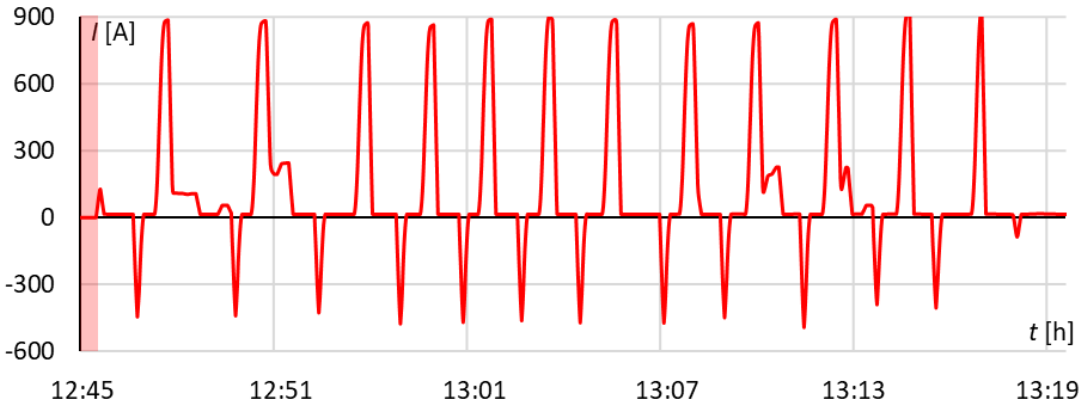

Fig. 7.11. Pantograph current optimized velocity profile – EN57AKM, track 502

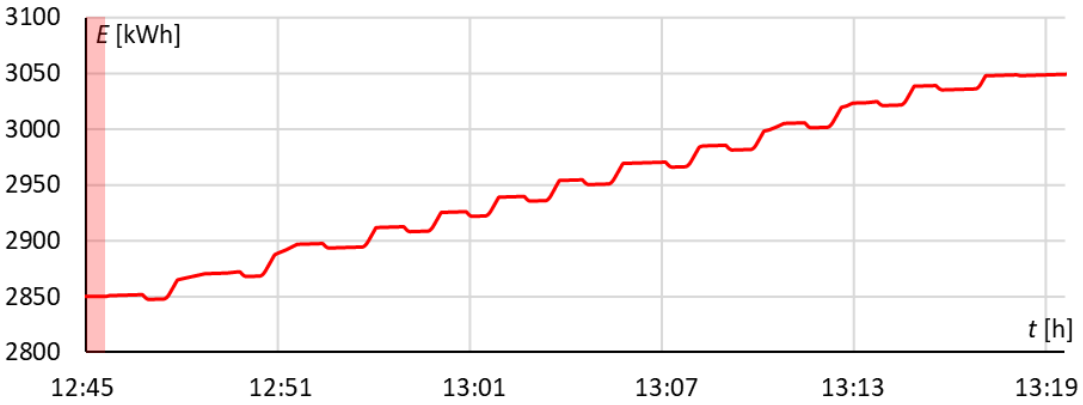

Fig. 7.12. Energy balance, optimized velocity profile – EN57AKM, track 502

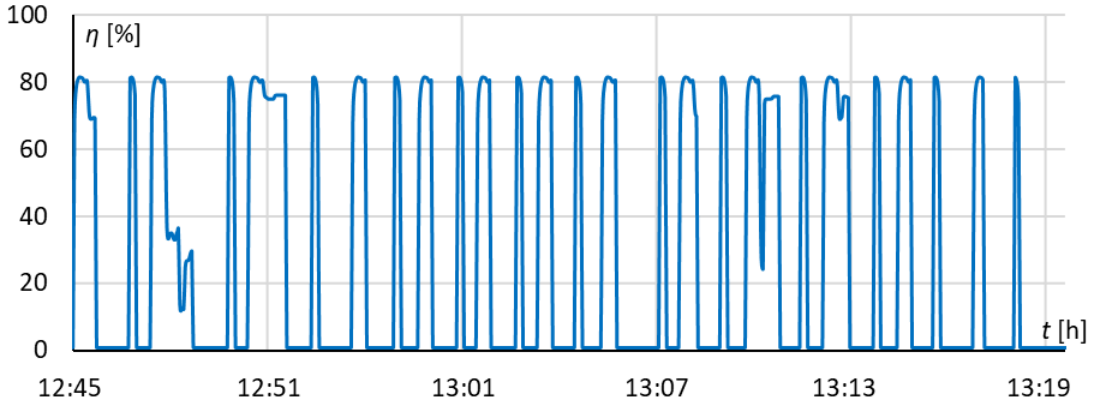

Fig. 7.13. Drive efficiency, optimized velocity profile – EN57AKM, track 502

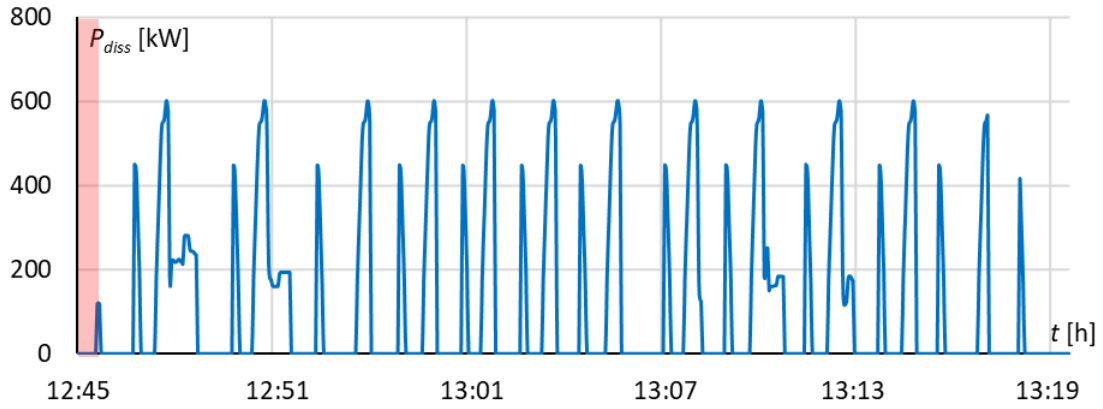

Fig. 7.14. Losses power, optimized velocity profile – EN57AKM, track 502

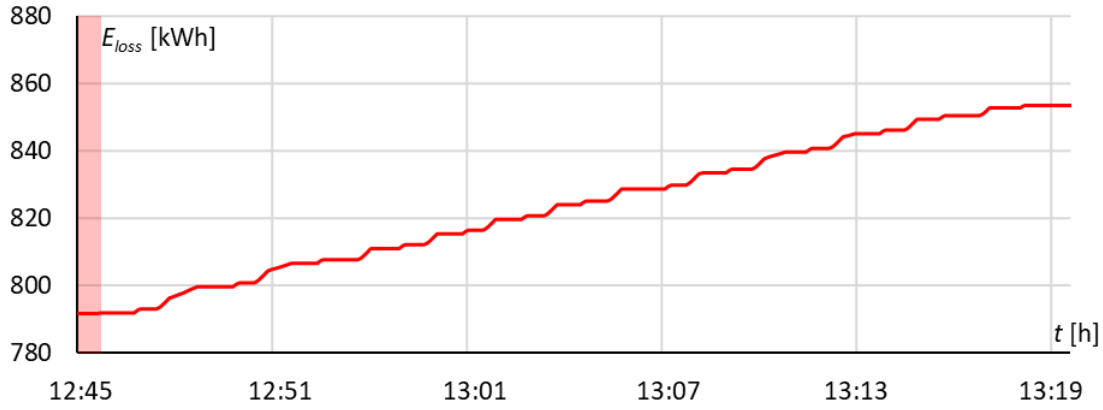

Fig. 7.15. Energy dissipation, optimized velocity profile – EN57AKM, track 502

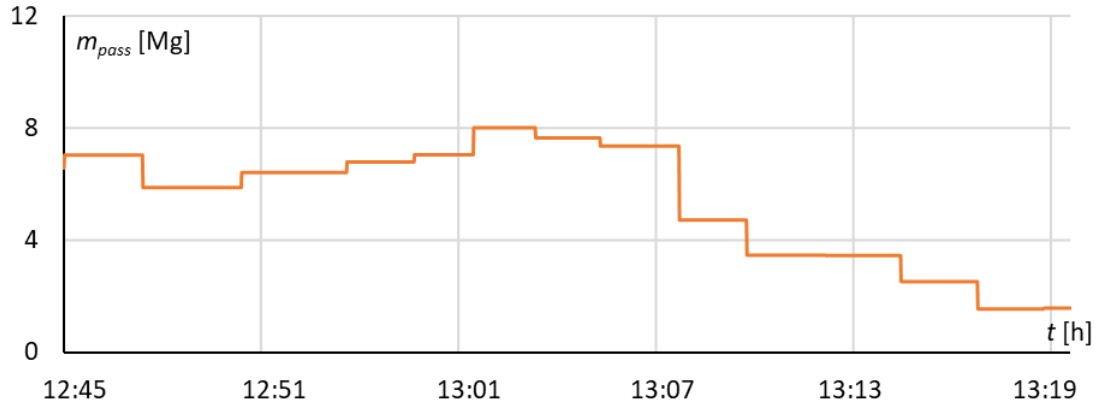

Fig. 7.16. Passenger mass, optimized velocity profile – EN57AKM, track 502

The results indicate that vehicle consumed 249,6 kWh, which is an improvement of 24% in relation to constant velocity run. The regenerated energy equals to 51,0 kWh, resulting in 20,4% regenerative braking efficiency – less than the constant velocity run. This is caused by less vehicles ready to consume the energy surplus at given moment and mostly, lower kinetic energy at the beginning of the braking phase as the vehicles dissipated part of this energy for overcoming movement resistances during the coasting phase. However, the relative energy consumption is at 11,3 kWh/km, almost 17% less than for the exemplary

constant velocity run. Losses amounted to 66,8 kWh, which is 29% less than exemplary run (presented in chapter 6). This results show the potential of the presented optimization method.

Moreover, cruising over short distance proven less energy–intensive than coasting and re–accelerating, especially on uphill parts. This also leads to reduction of substation load; drivetrain and catenary losses are reduced too. It is also worth noting that parts of the route which were longer and/or going uphill have higher target velocity set. This is a consequence of two factors: necessity for amassing more kinetic energy by the vehicle for the coasting phase and need for the run time to fit within the specified timetable bounds. Such occurrence is, however taking place mainly for trains running on track 501, from Gdańsk towards Gdynia – where the route goes uphill for the longest part.

Exemplary waveforms of run in the opposite direction are attached in the Appendix 4. Summary of the average vehicles operation parameters under optimized regime is shown below, in Tab. 9.

Tab. 9. Summary of vehicle energy efficiency – before and after optimization

Vehicle	**Track 502** (direction Gdańsk)			**Track 501** (direction Gdynia)		
	Optimized	Current	Diff. %	Optimized	Current	Diff. %
EN57AKM						
Balance [kWh]	194,7	225,2	**-15%**	225,2	229,0	**-2%**
Drivetrain losses [kWh]	64,2	81,7	**-27%**	66,5	83,3	**-25%**
Regeneration [%]	22,5	25,8	-3%	18,9	25,8	-7%
Relative consumption [kWh/km]	11,6	13,3	**-15%**	13,3	13,6	**-2%**
EN71SKM						
Balance [kWh]	162,8	206,3	**-27%**	174,5	210,1	**-20%**
Drivetrain losses [kWh]	48,3	63,7	**-32%**	50,1	65,5	**-31%**
Regeneration [%]	21,9	26,9	-5%	20,0	27,2	-7%
Relative consumption [kWh/km]	9,9	12,2	**-23%**	10,6	12,4	**-17%**
31WE						
Balance [kWh]	208,7	239,4	**-15%**	232,5	241,0	**-4%**
Drivetrain losses [kWh]	64,5	89,9	**-39%**	66,8	92,7	**-39%**
Regeneration [%]	21,3	28,1	-6,8%	18,6	29,0	-10,4%
Relative consumption [kWh/km]	11,92	14,2	**-19%**	13,28	14,2	**-7%**

Higher savings occur for trains going towards Gdańsk, as the most of the route goes downhill. Because of this, less energy is dissipated for overcoming the route gradient; therefore, it is easier to coast over a longer distance. In opposite direction, savings still exist – but are lower. Energy recuperation decreased, which is a consequence of higher movement dynamics – acceleration and braking phases take less time, so there is lower probability of phase overlapping between the vehicles. However, drivetrain losses decreased significantly for all vehicles, improving the overall efficiency.

The highest differences are for the EN71SKM vehicle, mainly because it is the only EMU operating as a single unit (4 carriages), while other trains consist of two coupled units (EN57AKM – 6 carriages, 31WE – 8 carriages). Consequently, the vehicle has the lowest mass and movement resistance, but also the smallest passenger capacity. Moreover, it is used for the least number of runs, so "lucky overlapping" between acceleration and braking with other vehicles will have bigger impact on the analysis outcome.

After optimization, voltage variations increased, especially within power supply section between the TS Gdańsk Wrzeszcz and end of the line in Gdańsk Śródmieście, where maximum value peaks at over 3900 V and minimum falls below 3000 V. This, in turn, limits the recuperation efficiency as the regenerative braking energy is dissipated in braking rheostat under such conditions – as visible at about 13:14 in the vehicle current waveform. The fluctuations on output bars of the substation are also larger than for unoptimized operation (Fig. 7.17). Complete results can be found in Appendix 5.

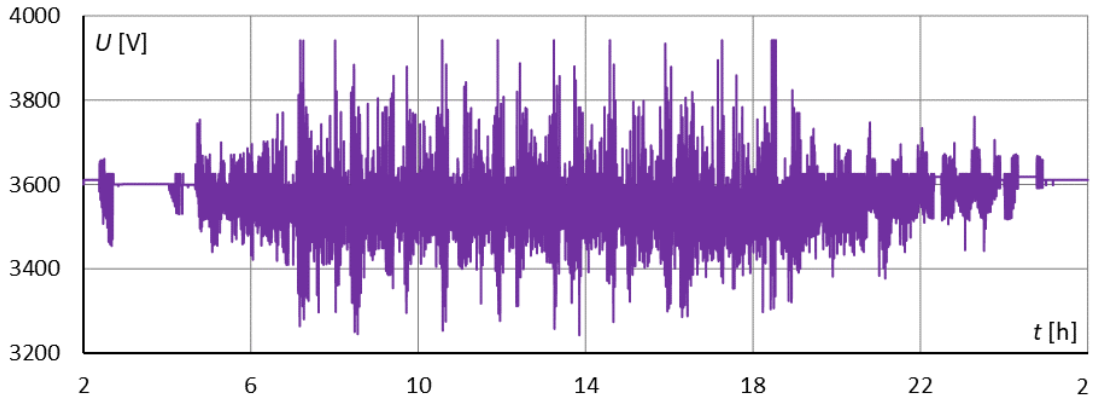

Fig. 7.17. Output voltage – TS Gdańsk Wrzeszcz

This is a direct result of acceleration and deceleration being more dynamic – there is higher current flowing within shorter time. Consequently, energy recuperation is lower as voltage over 3900 V prevents the regenerative braking entirely. Acceleration and braking phases are also shorter in duration, making the overlapping less likely. Higher value of deceleration also means higher involvement of friction brakes, which also reduces energy recuperation.

The losses within power supply system rose very slightly, as the currents are higher in value and vehicles are less likely to consume energy surplus. The difference is however insignificant, amounting to 14 kWh (1661 vs 1675 kWh losses). Interestingly, losses in catenary after optimization decreased by 10 kWh (Fig. 7.18), but losses in feeders rose by 24 kWh or 29% (Fig. 7.19). Those figures can be considered acceptable, because

optimization allowed for significant reduction of losses in the vehicles. Therefore, much less energy is wasted overall.

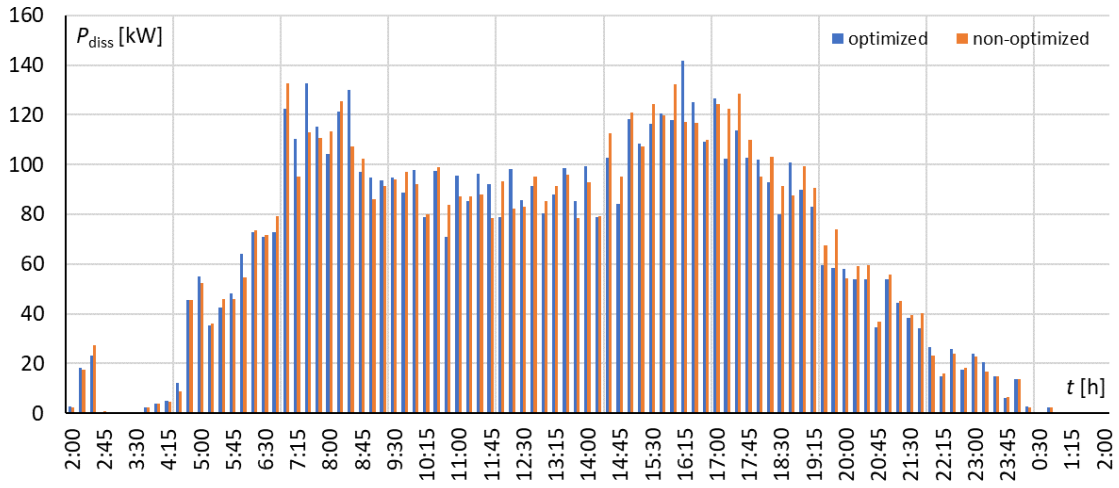

Fig. 7.18. Difference between catenary losses after optimization and losses before optimization – 15 min average power

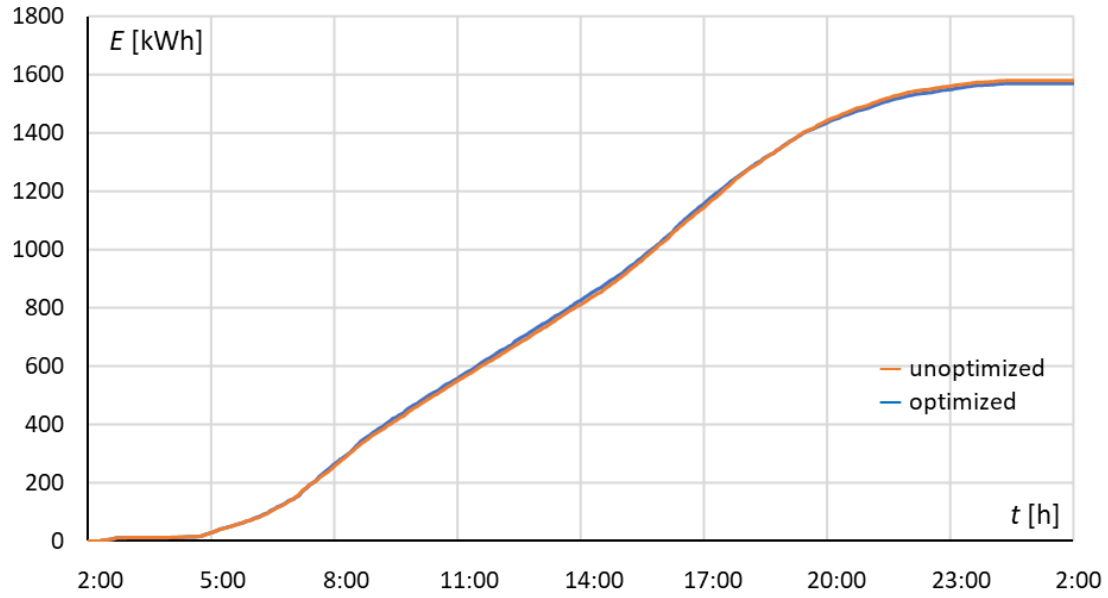

Fig. 7.19. Difference between catenary losses after optimization and losses before optimization – energy

Despite overall reduction of catenary losses, average 15 minute losses power can still be higher after optimization, with visible peaks during morning and afternoon rush hours. The difference is 20 kW at its highest, which amount to 20% – and this is a result of reduced regenerative braking efficiency, but also higher currents resulting from higher movement dynamics of the vehicles.

Feeder losses are presented in Fig. 7.20 (15 minute average power) and 7.21 (total dissipated energy).

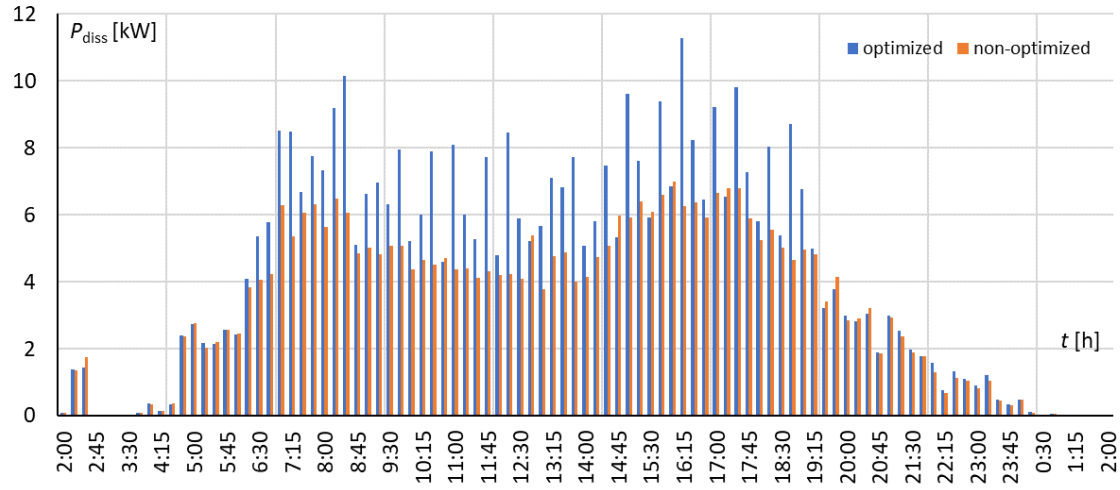

Fig. 7.20. Difference between feeder losses after optimization and losses before optimization – 15 min average power

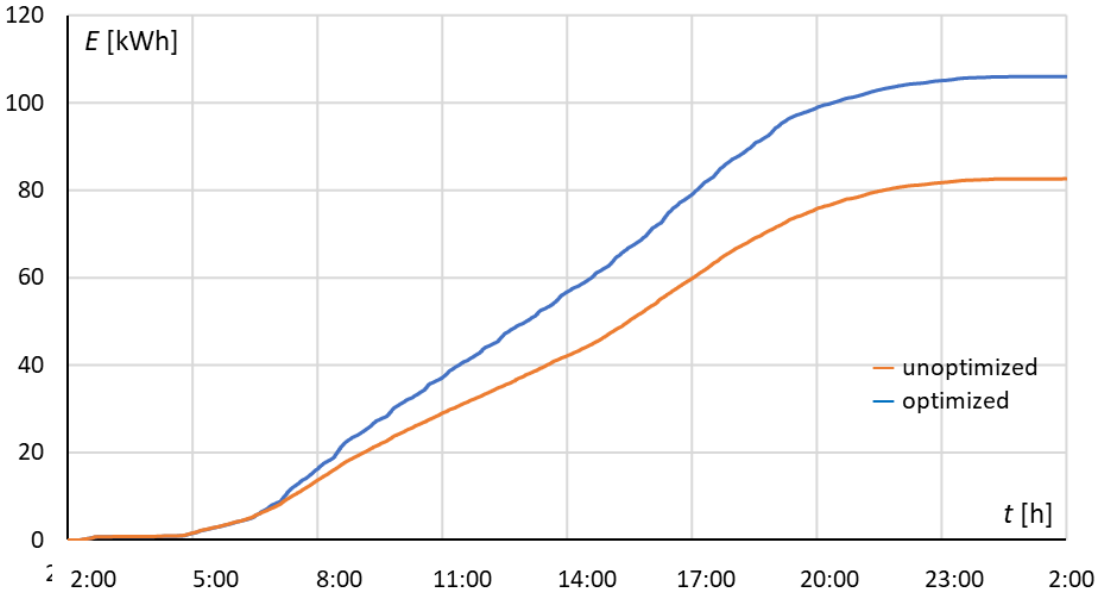

Fig. 7.21. Difference between total feeder losses after optimization and losses before optimization – energy

Feeder losses increased in value – because of reduced local energy recuperation, the surplus is more likely to be pushed thru the substations (and consequently, the feeders) to other power supply sections. At the same time, current values are higher as the vehicles accelerate and decelerate faster and thus, are more likely to require full power.

Total energy dissipated by the vehicles in form of losses were significantly decreased: from 22990 kWh down to 17912 kWh, or by 28% (Fig. 7.22). Savings of 5 MWh translate to roughly 20 train runs or emissions reduction by 3500 kg of CO2 equivalent – and this is a daily figure. For the whole year (counting only workdays, 251 days in total) energy dissipated by the vehicles in form of losses would be lowered by 1,25 GWh, improving system efficiency.

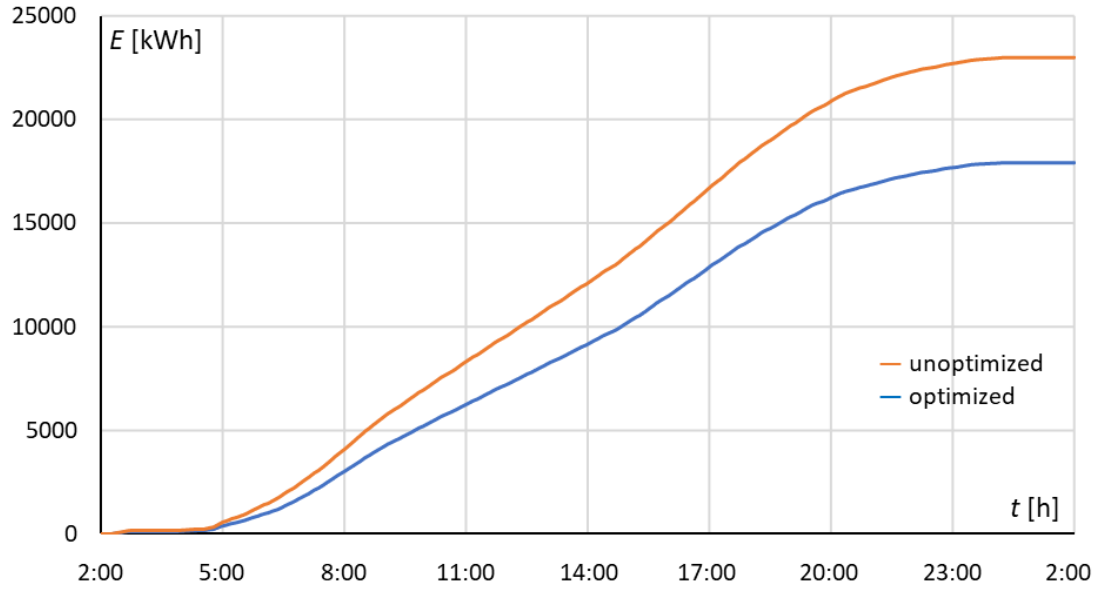

Fig. 7.22. Difference between total drivetrain losses after optimization and losses before optimization (sum for all vehicles)

The losses are reduced along the whole day, as no energy is dissipated by the drivetrain when the vehicle is coasting (power necessary for control, cooling etc. of the inverter is considered as an auxiliary device, and its energy use is not included in losses).

For the whole system, energy consumption was lowered by 8%, from 56,4 MWh to 52,2 MWh. This translates to 4,2 MWh of energy saved daily, and equivalent CO2 emissions lowered by 2,9 Mg. In scale of one year, the savings will equal to about 1,1 GWh, and emissions by over 3000 Mg. The advantages of using optimized velocity profile are significant, even if the method used is quite simple. Further improvement would require synchronized timetable or implementation of energy storage.

7.4.2. Energy storage implementation

Energy storages used for improvement of energy recovery are growing in popularity – they are successfully used by trolleybus, tram and subway operators. Therefore, author conducted simplified analysis of impact that possible energy storage would have on energy efficiency of the whole system.

There are multiple approaches to energy storage implementation – they can be installed inside the vehicle, inside the traction substation and in some location between the substations, coupled to catenary directly. Appropriate storage can improve energy recuperation and reduce voltage fluctuations. There is also a possibility of coupling the storage to the smart grid system, when energy can be exchanged with renewable sources or electric vehicles chargers [37].

In this analysis, the highest volatility of voltage was detected in the power supply section between TS Gdańsk Wrzeszcz and end of the line (Gdańsk Śródmieście station). Regenerative braking efficiency was also reduced there. Because of this, author decided to locate the storage inside the TS Gdańsk Wrzeszcz – not only will it help to reduce voltage

fluctuations within mentioned section, but will also absorb braking currents from section between TS Gdańsk Wrzeszcz and TS Sopot.

The storage itself is modelled in simplified version, as this is not the focus point of the analysis. It is represented by controller, implemented as custom function and integrator calculating energy stored inside. The controller feeds power to the integrator, and its value is dependent on charge/discharge current and substation output voltage. The thresholds for activation of the storage can be customized, however they should be set in such a way that will prevent the storage from charging with energy coming from the transformer–rectifier unit (Fig. 7.23).

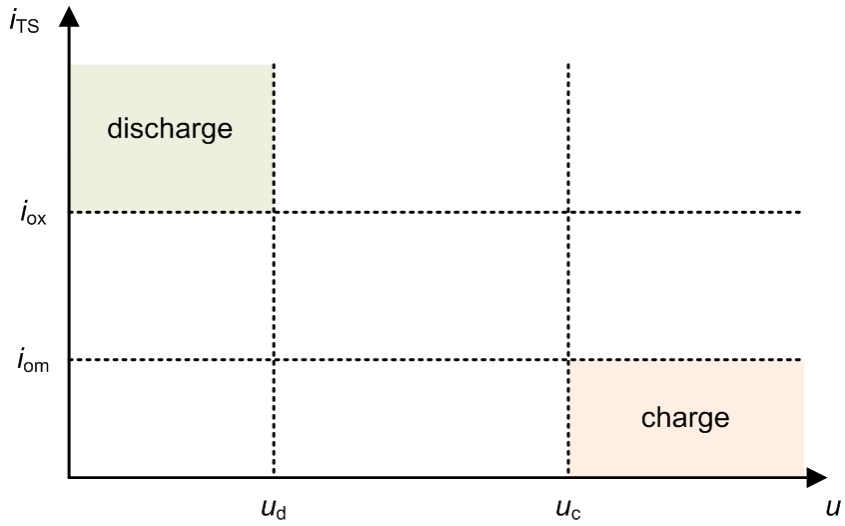

Fig. 7.23. Principle of energy storage control – in relation to substation current and voltage

The discharge happens, when output voltage decreases and substation load current increases – this way, the storage stabilizes output voltage providing additional energy. Moreover, the controller function prevents the storage from charging when the state of charge (SoC) is at 100% and from discharging when it is at 50% or lower. The discharge current is controlled so it will not be higher than the maximum specified value.

Additionally, there is set of basic parameters defined – including maximum discharge current, storage capacity and maximum depth of discharge. The type of the device is not specified – there are just required parameters. Summary of the assumed parameters is shown in Tab. 10.

Tab. 10. Energy Storage Parameters

Parameter	**Unit**	**Value**
Capacity	kWh	50
Max. depth of discharge (DoD)	%	30
Max. discharge current	A	2000
Max. charging current	A	1000
Charge thresholds i_{om},u_c	A/V	10/3600
Discharge thresholds i_{ox},u_d	A/V	1000/3550

Storage with presented parameters was coupled into the substation model, being between the voltage output of the transformer–rectifier units and the feeders connection. Initial charge for the analysis was assumed at 40% SoC. Notable are high values of required charging and discharging current, so such storage could be realized only as supercapacitor–based or hybrid (supercapacitor coupled with electrochemical battery).

The simulation was conducted using the same setup parameters (timetable, velocity profiles, HVAC duty cycle etc.) from optimized system operation. Waveforms of SoC and stored energy were obtained (Fig. 7.24, Fig. 7.25).

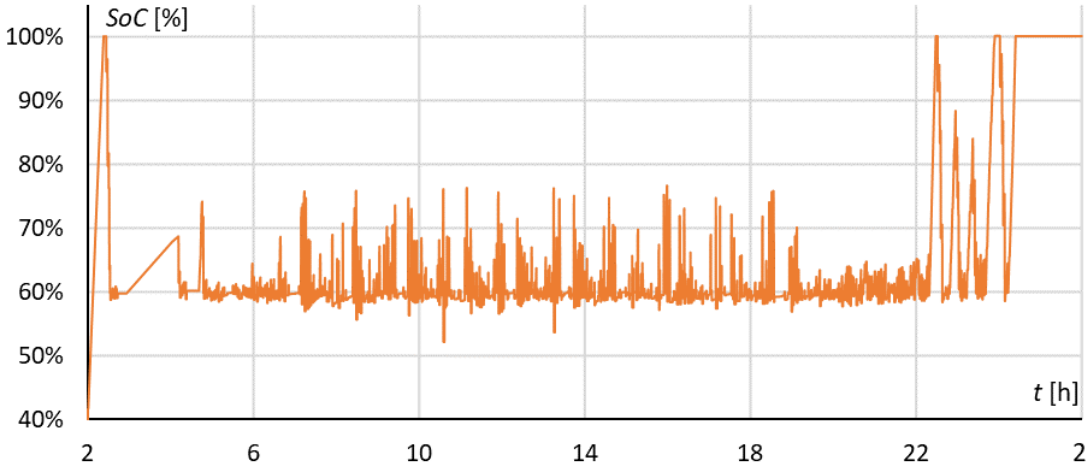

Fig. 7.24. State of charge (SoC) – energy storage

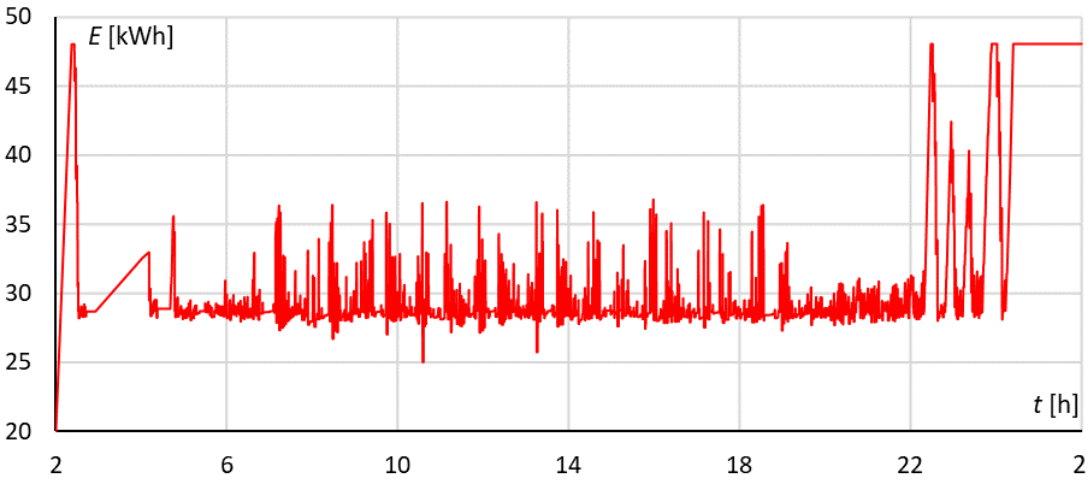

Fig. 7.25. Stored energy

It is worth noting that the full capacity of the storage is rarely used – in most cases SoC oscillates between 50 and 75%. Only during the night train runs it is charged up to 100%, as there are less vehicles able to consume the energy surplus. Therefore, there is a room for optimization of storage parameters, including capacity – because of high cost of such device.

Implementation of storage decreased voltage volatility significantly – now vehicles are able to regenerate energy, charging the storage. It is visible on the Fig. 7.26 and 7.27, showing waveforms of current and voltage for the same vehicle, timeframe and input parameters that was presented earlier. Flattened voltage peaks mean that vehicle is able to recuperate energy, as for the most part the waveform falls below the rheostatic braking engage threshold of 3700 V.

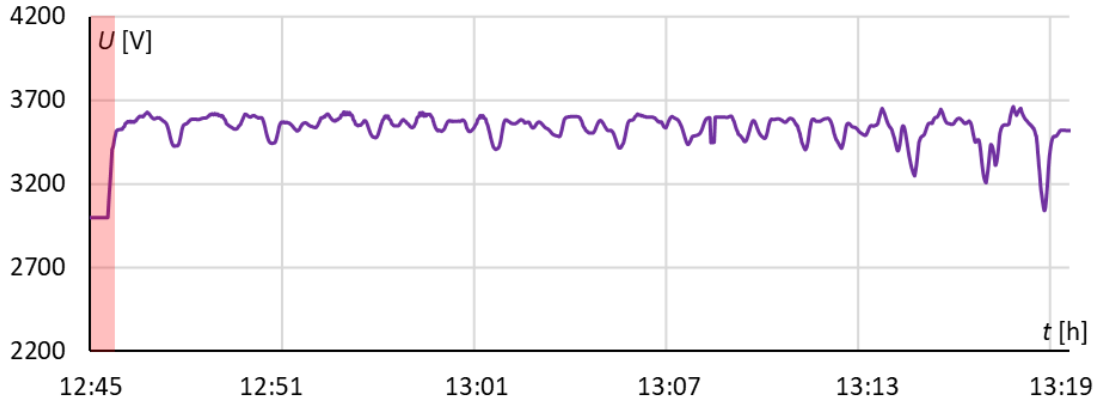

Fig. 7.26. Pantograph voltage, EN57AKM – storage online

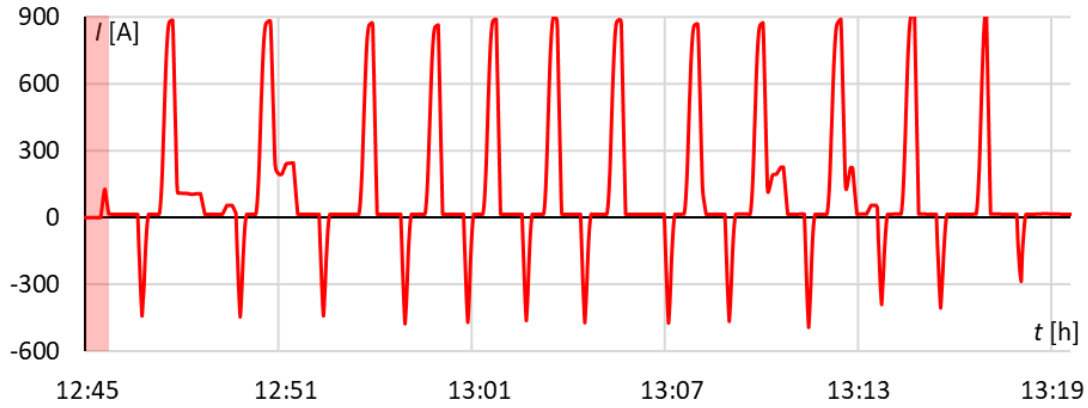

Fig. 7.27. Vehicle current – EN57AKM, storage online

It can be observed that installation of the storage allowed vehicle on approach to Gdańsk Główny – Gdańsk Śródmieście stations to regenerate energy. This time voltage was below 3700 V during braking, and did not exceed that value.

Improvement of regenerative braking efficiency is noticeable despite the storage being installed only in one substation. Without the storage, recuperation efficiency was at 18,1%, and at 19,5% with the storage. While the difference is not very large, it still can add up thru the year – and considering dynamics of energy prices, it may allow for not only energetic, but also monetary gains.

Total system energy consumption fell to 50,8 MWh, by 3% in relation to optimized run without storage and by 11% in relation to unoptimized run. The storage can, therefore, save at least 1,4 MWh daily, reducing emissions by 970 kg of CO2. There is also room for further improvements, if the storage was coupled into smart grid system, which could

consume surplus of energy at night (e.g. for EV charger) or provide additional energy for accelerating vehicles during the day, thru wind or solar generator.

7.5. Optimization – conclusions

Within the scope of this dissertation, author proposed algorithm for optimization of energy efficiency of the electric multiple units in service of suburban railway operator. The analysis shows that with minimal investment, energy consumption can be reduced. Shown method is easily implementable in real systems, as it requires only trackside signs to be placed – which is possible to do within single technical break at night. Author also proposed the signs appearance, which would distinguish them from other signals thus avoiding confusion.

There was also stationary energy storage considered – simplified analysis shown potential for further improvement of energy efficiency, as the storage reduced the consumption while improving voltage stability. In future work, author is planning implementation of more advanced storage models, for both vehicles and infrastructure.

Summary of obtained results are grouped in Tab. 11. It is worth noting that non–optimized run consumed significantly more energy that was mostly dissipated in form of losses. Because of this, better regeneration efficiency is not as helpful as it could seem.

Table 11. Summary of energy efficiency analysis

Run/Parameter	Non–optimized	Optimized	Optimized with storage
Energy consumed [MWh]	70,8	61,6	60,8
Energy regenerated [kWh]	18054	11150	11856
Drivetrain losses [kWh]	22990	17912	17910
Average recuperation efficiency [%]	25,5	18,1	19,5
Catenary losses [kWh]	1579	1569	1577
Feeder losses [kWh]	82	106	104
Total energy balance [MWh]	56,4	52,2	50,8
Difference vs. non–optimized run [%]	-	**-8%**	**-11%**
CO2 emissions [Mg]	39085	36175	35204
Energy saved (per year)* [MWh]	-	1,05 GWh	1,41 GWh
Monetary savings/year** [PLN]	-	298296,00 (2019) 311850,00 (2021) 526050,00 (2022)	397728,00 (2019) 418770,00 (2021) 706410,00 (2022)
*only workdays, 251 days in total (weekends and holidays not included) **based on electrical energy price for 2019, Bt21L tariff [22] and data for 2021/22 [88]			

Proposed method allows for reducing not only global energy efficiency, but losses as well. The most energy is dissipated by the vehicle drivetrain – therefore, implementation of velocity profile that can reduce such losses is advantageous. Energy savings translate into significant reduction of CO2 emissions, as the most of the Polish power plants are coal–fired. Rapidly rising costs of electrical energy show how much money can be saved, and this number is significant, as the net profit of the SKM Trójmiasto is within 1 million PLN range. Therefore, optimization of velocity profile is advisable.

Energy efficiency can be improved further by installing the energy storage. Despite the improvement over optimized velocity profile without additional infrastructure is not very large, it allows for enhancing power quality (reduction of voltage fluctuations) and can be connected with smart grid system. It also consistently increases regenerative braking efficiency (Fig. 7.28). However, price of such device might be a major drawback, especially considering necessary capacity and charge/discharge currents required.

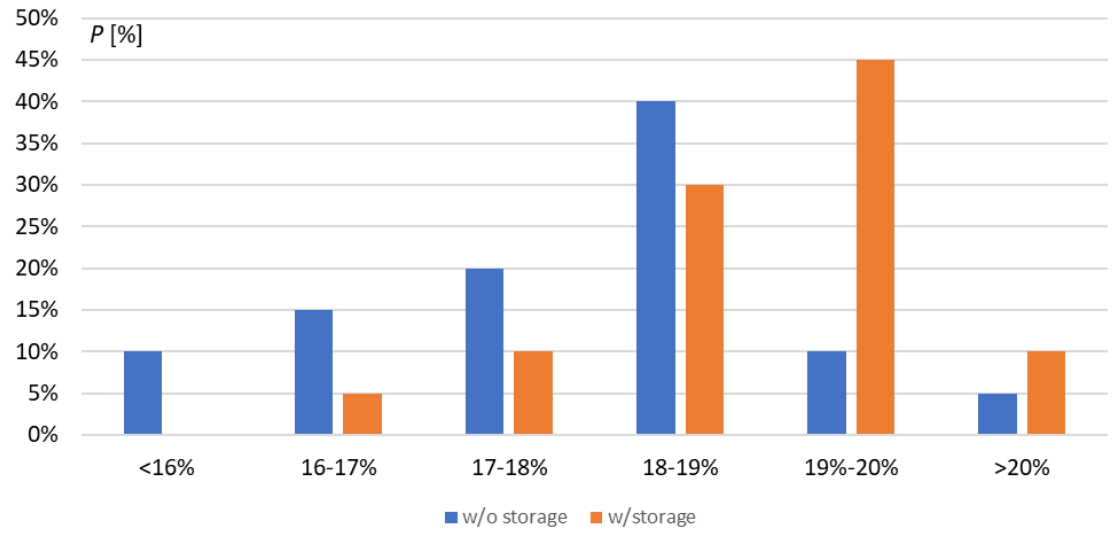

Fig. 7.28. Comparison of energy recuperation efficiency – probability of achieving certain value for optimized system without and with storage (data from 20 simulations for each option)

Author resigned from using precise optimization of velocity profile that would require advanced signaling equipment or ATO. This is because analyzed route is not fitted with any cab signaling system and there is no information if plans for installation of such equipment exist. Similarly, optimizing the timetable would prolong the travel time significantly requiring precise following of the timetable (time interval between the vehicles is shortest at 7 minutes, optimized subway systems operate with 4–5 minute tact).

Another possibility is to regulate substation idle voltage using tap–switch, where lowering the voltage value might increase energy recuperation, as the controller is voltage–dependent. Author conducted such analysis for trolleybus system in Pilsen, concluding that improvement is achievable in this way. Example of obtained results for the substation MR5, as described in chapter 4, is shown in Fig. 7.29.

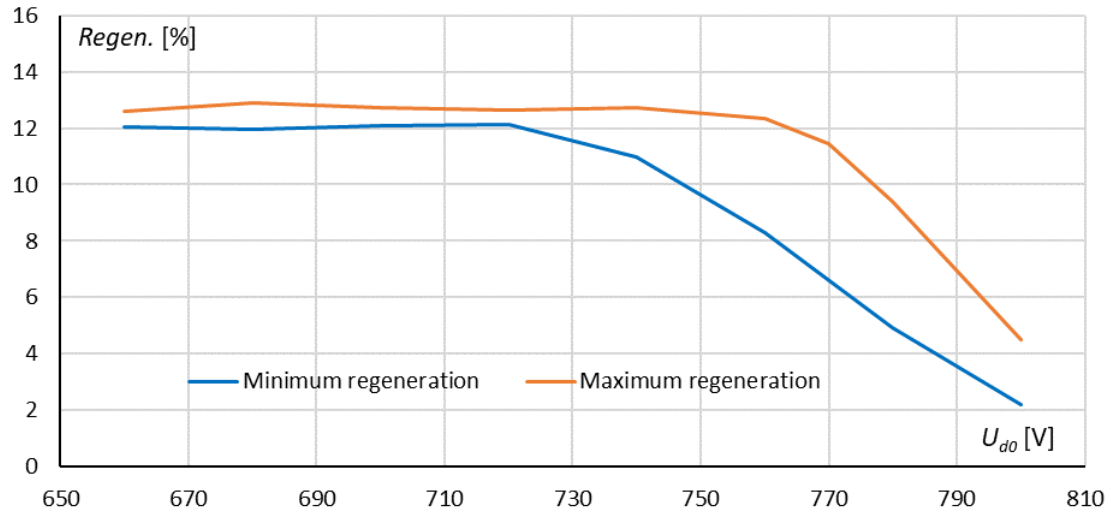

Fig. 7.29. Regenerative braking efficiency (min. and max.) in relation to substation idle voltage (Pilsen trolleybuses)

Lowering the voltage can increase regenerative braking efficiency, but only to a certain degree – if there is no vehicle or storage receiving the energy, it cannot be recuperated. Moreover, lower value of the substation voltage results in higher currents within the system, and this leads to losses increase.

In this dissertation, author resigned from implementing such measure, as the voltage was falling down to about 3200 V. Pushing down the value would result in voltage dips that could result in engaging power limitation in vehicles and disrupt the velocity profiles.

8. CONCLUSIONS AND FURTHER WORK

Increase in fuel and electrical energy prices and ecological consciousness motivates research into improvement of energy efficiency in all branches of the economy. Because the transportation consumes up to 30% of total energy produced, seeking savings there is the natural outcome. This translates to not only electrification of means of transport (like electric cars, bicycles or buses) but also to reduction of energy consumption in existing systems. Moreover, within agglomerations with large number of inhabitants and high population density, enlargement of existing electrified transport networks is a plausible solution for a rising need for mobility. However, all of those investments require careful planning, as the cost of both vehicles and infrastructure is high, and its reliable operation thru decades is needed. Consequently, need for simulation software dedicated for analyzing electrified transport systems arise – such software should provide precise data about operation of the transport network, but also allow for testing multiple variants of modernization.

As the importance of energy efficiency improvement in electrified transportation is widely recognized, many programs dedicated to this task exist. However, there is still room for further development, especially in the versatility matter. Large number of the existing programs also realize rigid schedules and velocity profiles, so the possibility of statistical analysis of the results is limited.

Seeing the room for possible improvements, author developed novel models that use architecture inspired by industrial communication networks. Implementation of data bus structure improves their scalability and versatility, as the subsystems are standardized, "library–like" elements that require providing parameters to work. Consequently, implementing larger network would require adding vehicles and supply sections, and providing them with parameters.

This was achieved, because there is dynamic link between the vehicles and the power supply, as the data circulates within the frames, addressed by unique identifiers. Complex power supply structure, like branch lines and roundabouts can be therefore easily implemented – linking vehicle to corresponding power supply section is done based on its location. Structure of the equivalent electrical circuit does not change throughout the simulation, and only values are loaded using the so called "Selectors" – there is no need for CPU–intensive algorithm for connecting elements of equivalent circuit every timestep. Everything necessary for conducting the analysis is included in the model, so it is only single program to execute. As the model is Matlab/Simulink based, its compatibility is very high, because every computer equipped with this environment can run the model, regardless of operating system.

In order to present capabilities of the developed program, examples from two different electrified transport systems were shown: trolleybus network from Pilsen, Czech Republic and suburban railway system of SKM Trójmiasto. Both cases allowed to highlight versatility of the proposed structure, as they included variable tact, multiple possible

velocity profiles and complex power supply structure. Computation performance was also proven to be very high – using PC computer (Intel Core i7@2.30 GHz), calculation of the whole day of transport system operation took in both cases below 1 minute, or around 2000 timesteps per second. This performance can be improved further, thru better multitasking optimization or GPU acceleration

The model was validated against recorded vehicle run at selected route fragment on suburban railway system of SKM Trójmiasto. Moreover, the power supply system model was verified using large set of data recorded in trolleybus system, indicating relatively high precision of the developed application, with error in energy balance below 5% and in computed catenary voltage – below 2%. Such accuracy was achieved thru use of large set of measurement data, enabling statistics–based parameter setting. This degree of variability, which included velocity profiles, station dwell time and vehicle mass leads to large set of results obtained, which allow to see a bigger picture than only single answer. This opens a possibility for statistical analysis of the simulation results.

Then, in–depth analysis of the transport system of SKM Trójmiasto was carried out. Velocity profiles were determined basing on large set of recorded data, and power supply layout was assumed using published technical parameters of the infrastructure and tender documentation. Series of simulations were carried out, uncovering energy consumption, regeneration efficiency and energy usage of each vehicle. As the obtained results constitute a large set of data, they can be used as plausible information about energy efficiency in analyzed systems.

Consequently, obtained data was used as a basis for energy efficiency optimization. Author proposed unique approach, which contrary to existing ones is simple, quick and cheap to implement – as the trackside signs are sufficient. Then, simulation of the whole system with optimized velocity profiles was executed, showing improvement of total energy balance of around 8 %. Potential savings stemming from use of substation–mounted energy storages were indicated, lowering energy consumption of analyzed railway system by 11%.

Author underlines the original achievements of this dissertation:

- Introduction of industrial data network structure into electrified transport system model, which improves versatility and computation performance;
- Adaptive structure of the model: elements of the vehicle or power supply are easily replaceable for different analyses; simulating every part independently is possible also outside the main program;
- Simulation of interconnected systems: each vehicle can be of different type, follow different route and schedule; power supply can have different parameters for each section; Interconnected systems (e.g. tram and trolleybus) or smart grids can be analyzed;
- Statistic–based determination of input parameters for the analysis;
- Original algorithm for automatic analysis of large set of recorded vehicle run data, that returns the summary of all velocity profiles;

- Implementation of original semi–randomized velocity profile selection, with variable probabilities based on runs recorded in real system;
- Unique control algorithm: vehicle movement is controlled by the set of logical functions, with the Permission function being the highest in hierarchy;
- Implementation of passenger flow data, which impacts mass of the vehicle, and consequently, its movement dynamics and energy consumption;
- Variability of station dwelling time: this includes not only prolonged stops at main stations, but also random variability occurring in real systems;
- Consideration of weather conditions: air temperature has an impact on heating and air conditioning, and dry, wet or icy conditions have a consequences in wheel adhesion. This can vary with time and/or distance;
- Differentiation between route and power supply section: parameters of the route (inclination, curvature) are independent from power supply – the vehicle can change track during the run or travel outside the electrified route if equipped with energy storage;
- Scalability: it is possible to simulate a whole day of the network operation or focus only on short timeframe, with reduced timestep – as the initial parameters are loaded from external file.

Publications author was involved in during the PhD course include, but are not limited to:

- Journal article in Energies (MDPI) [62],
- Journal article in Vehicle System Dynamics (Taylor & Francis) [154],
- Journal article submitted to Sensors (MDPI),
- Journal article in Electrotechnical Review [64],
- WoS–listed conference papers, IEEE [58,60] and CETRA [61].

Author was also involved in peer review process for MDPI journals, with two articles in JCR–listed ones (Sustainability, Applied Sciences).

Author also took part (as contractor) in international research projects, including:

- Development of an innovative method for determining the precise trajectory of a railway vehicle. Program Operacyjny Inteligentny Rozwój 2014–2020, The National Centre for Research and Development. Projekt w ramach Wspólnego Przedsięwzięcia BRIK (POIR.04.01.01–00–0017/17),
- EfficienCE – Energy Efficiency for Public Transport Infrastructure in Central Europe. Interreg CENTRAL EUROPE Programme (CE1537),
- POWER 3.5 Zintegrowany Program Rozwoju Politechniki Gdańskiej. European Social Fund programme (POWR.03.05.00–00–Z044/17).

Author considers this work to be a basis for further development, as the developed model had already seen its first application. Being used for determination of possibilities of energy efficiency improvement in trolleybus system in Pilsen, the model proven to be powerful tool for analysis of electrified transport systems. In future, there are plans for:

- Implementation of energy storages and their control algorithms, including onboard applications and vehicles moving thru partially electrified routes,

- Improvement of losses and voltage drops calculation within rail tracks,
- Implementation of smart–grid interconnections,
- Modeling of AC power supply systems,
- Broadening the weather part of the model, implementing influence of air temperature and currents within on catenary resistance and losses,
- Implementation of reliability–focused features, including calculation of stray currents and EMC compatibility.

The long–term goal is to combine all the developed models into single program with broad functionality. Such software can be usable within the industry providing improvements over existing commercial programs.

References

[1] A survey on wheel/rail friction. Federal Railroad Administration, Washington 2017.
[2] Abad G., Power Electronics and Electric Drives for Traction Applications. Wiley, Chichester 2017.
[3] Abouzeid A.F., Guerrero J.M., Endemano A, Muniategui I., Ortega D., Larrazabal I., Briz F: Control strategies for induction motors in railway traction applications. Energies 13/2020
[4] Abrahamsson, L.: Optimal Railroad Power Supply System Operation and Design, KTH Stockholm, 2012.
[5] Abramov E.Y., Shchurov N.I., Rozhkova M.V. Energy efficiency matching of electric traction Network with Double and Single-Way Circuits. 18th INTERNATIONAL CONFERENCE ON MICRO/NANOTECHNOLOGIES AND ELECTRON DEVICES EDM 2017
[6] Açikbaş, S.; Söylemez, M. T. Parameters Affecting Braking Energy Recuperation Rate in DC Rail Transit. In ASME/IEEE 2007 Joint Rail Conference and Internal Combustion Engine Division Spring Technical Conference; ASMEDC: Pueblo, Colorado, USA, 2007; pp 263–268.
[7] All new Peugeot 208. Equipment and technical specifications. Peugeot Motor Company, 2020.
[8] Alnuman, H., Gladwin, D., Foster, M.: Electrical modelling of a DC railway system with multiple trains, Energies, 11, 2018.
[9] Amrani A., Hamida A., Liu T., Langlois O.: Train speed profiles optimization using a genetic algorithm based on a random forest model to estimate energy consumption. Transport Research Arena (TRA) 2018, Apr 2018, Vienna, Austria.
[10] Apostolidou N, Papanikolaou N.: Energy saving estimation of Athens trolleybuses considering regenerative braking and improved control scheme. Resources 7(43)/2018
[11] Bartłomiejczyk M. Super capacitor energy bank MEDCOM UCER-01 in Gdynia trolleybus system. IECON 2016 - 42nd Annual Conference of the IEEE Industrial Electronics Society, Florence, Italy.
[12] Bartłomiejczyk M., Mirchevski S., Jarzębowicz L., Karwowski K., How to choose drive's rated power in electrified urban transport? EPE'17 ECCE Europe, Warszawa 2017.
[13] Baumeister D. (red.) Modelling and simulation of a public transport system with battery-trolleybuses for an efficient e-mobility integration. 1st E-Mobility Power System Integration Symposium, Berlin 23 October 2017
[14] Bellure A., Aspalli M.S. Dynamic d-q Model of Induction Motor Using Simulink. International Journal of Engineering Trends and Technology (IJETT) – Volume 24 Number 5- June 2015
[15] Biliński J., Buta S., Gmurczyk S., Kaska J. Asynchroniczny napęd z hamowaniem odzyskowym dla elektrycznych zespołów trakcyjnych serii EN57 I EN71. TTS 10/2009.
[16] Birr K., Jamroz K., Dziedzic T., Kustra W. Wybrane wyniki badań potrzeb transportowych mieszkańców województwa Pomorskiego. Zeszyty Naukowo-Techniczne SITK RP, oddział w Krakowie Nr 1(103)/2014
[17] Bosyi, D.; Kosariev, Y. Modeling of the controlled traction power supply system in the space-time coordinates. Transp. Probl. 2017, 12 (3), 5–19.
[18] Botte M., D'Acierno L., Mottola F., Pagano M. Optimization of Railway Operating in terms of Distribution System Voltage Drop. 2020 IEEE Vehicle Power and Propulsion Conference (VPPC)
[19] Brona P., Calvet B., Szarata A., Klemba S. Kolej Metropolitalna w Trójmieście. Badanie podróży. Praca konsultingowa, Instytut Kolejnictwa, Warszawa 2010
[20] Buja G., Casadei D., Serra G. Direct torque control of induction motor drives. Proceedings of the IEEE International Symposium on Industrial Electronics ISIE '97.

[21] Caramia P., Mottola F., Natale P., Pagano M. Energy saving approach for optimizing speed profiles in metro application. 2016 International Conference on Electrical Systems for Aircraft, Railway, Ship Propulsion and Road Vehicles & International Transportation Electrification Conference (ESARS-ITEC)
[22] Cennik dla energii elektrycznej – PKP Energetyka S.A. Warszawa, 2019.
[23] Chakravarthy B.K, Sree Lakshmi G.: Power Savings with all SiC Inverter in Electric Traction applications. E3S Web of Conferences 87, 01014 (2019)
[24] Czucha J., Karwowski K., Mizan M., Pazdro P.: Efektywność odzysku energii hamowania elektrodynamicznego w komunikacji miejskiej. Przegląd Elektrotechniczny 2004, R. 80, nr 10, s. 1016–1019. ISSN 0033-2097.
[25] Czucha J., Pazdro P.: Badania ruchowe tyrystorowego układu rozruchu impulsowego zespołu trakcyjnego EN 57. Konferencja naukowa „Energoelektronika w taborze trakcyjnym" zorganizowana przez Komitet Elektrotechniki PAN, Instytut Elektrotechniki oraz Politechnikę Warszawską. Warszawa, 10-11 listopada 1987 r.
[26] Dębiński M., Kiercz K., Kowalski S., Kądziołka T. Przegląd rozwiązań konstrukcyjnych wybranych elektrycznych zespołów trakcyjnych. Pojazdy Szynowe 1/2011
[27] Dokumentacja systemu utrzymania EZT 31WE Nr NS/31WE/3117/16. Newag SA, grudzień 2016
[28] Douglas, H., Roberts, C., Hillmansen, S., Schmid, F.: An assessment of available measures to reduce traction energy use in railway networks. Energy Conversion and Management, 106, pp. 1149-1165, 2015.
[29] Drążek Z., Maciołek T., Szeląg A., Steczek M. Energy efficiency of a railway line supplied by 3 kv supply system – a case study of the application of an inverter in a traction substation. TECHNICAL TRANSACTIONS 10/2018 ELECTRICAL ENGINEERING
[30] Du G., Wang C., Liu J., Li G., Zhang D.: Effect of Over Zone Feeding on Rail Potential and Stray Current in DC Mass Transit System. Mathematical Problems in Engineering vol. 2016.
[31] Durzyński Z., Podstawy metody wyznaczania parametrów energooszczędnej jazdy pojazdów trakcyjnych na obszarach aglomeracyjnych, Pojazdy Szynowe, rok 2011, nr 3, str. 1 – 5
[32] Dynamis. IVE GmbH - Ingenieurgesellschaft für Verkehrs-und Eisenbahnwesen mbH. https://www.ivembh.de/softwareprodukte/simulation/dynamis.html Access: 2021-06-25.
[33] Dynamis® - Driving Dynamic Calculations of any Train Configuration. IVE - Consulting Company for Traffic and Railway Engineering Ltd. (data dostępu 9.07.2018 r.) http://www.ivembh.de
[34] EfficienCE. Interreg Central Europe. https://www.interreg-central.eu/Content.Node/EfficienCE.html, access: 2021-03-12.
[35] EN 50163: Railway applications – Supply voltages of traction systems, European Committee for Electrotechnical Standardization (CENELEC), 2004
[36] Enache S., Campeanu A., Vlad I., Zlatian R., Enache M.A. Dynamic Analysis of New Induction Motor for Electrical Traction. 2020 International Symposium on Power Electronics, Electrical Drives, Automation and Motion
[37] Energy Storage: A Key Enabler for the Decarbonisation of the Transport Sector. EASE Position Paper on Energy Storage and Mobility, Brussels 2019
[38] F. Du, J. H. He, L. Yu, M. X. Li, Z. Q. Bo, A. Klimek: Modeling and Simulation of Metro DC Traction System with Different Motor Driven Trains. 2010 Asia-Pacific Power and Energy Engineering Conference, Chengdu, China.
[39] Filipović Z., Elektrische Bahnen. Springer-Verlag, Berlin 2015.
[40] Frilli, A., Meli E., Nocciolini, D., Pugi, L., Rindi, A.: Energetic optimization of regenerative braking for high speed railway systems. Energy Conversion and Management, 129, pp. 200-215, 2016.
[41] Furuta R., Kawasaki J., Kondo K. Hybrid Traction Technologies with Energy Storage Devices for Nonelectrified Railway Lines. IEEJ Transactions on Electrical and Electronic Engineering IEEJ Trans 2010, 5: 291-297.

[42] Gerben M. Scheepmaker, Rob M.P. Goverde, Leo G. Kroon: Review of energy-efficient train control and timetabling. European Journal of Operational Research 257 (2017) 355–376.
[43] Ghani P., Arasteh M., Reza Taeybi H. Analysis of Electromechanical Model of Traction System with Single Inverter Dual Induction Motor. 7th Power Electronics, Drive Systems & Technologies Conference (PEDSTC 2016) 16-18 Feb. 2016, Iran University of Science and Technology, Tehran, Iran
[44] González-Gil, A., Palacin, R., Batty, P., Powell, J. P.: A systems approach to reduce urban rail energy consumption. Energy Conversion and Management, 80 (2014), 509–524.
[45] Greenhouse gas emission intensity of electricity generation. European Environment Agency data visualization, published 8 December 2020. https://www.eea.europa.eu/data-and-maps/daviz/co2-emission-intensity--6
[46] Hamburg. DB i Siemens prezentują pierwszy kolejowy pojazd autonomiczny. https://www.transport-publiczny.pl/wiadomosci/hamburg-db-i-siemens-prezentuja-pierwszy-kolejowy-pojazd-autonomiczny-70798.html, access: 2021-10-12.
[47] Hao L., Zedong Z., Qin D., Zheng X. A novel urban rail transit system based on DC distribution and energy internet architecture. 2017 IEEE Conference on Energy Internet and Energy System Integration (EI2), Beijing, China.
[48] Hata H. What drives electric multiple units? Japan Railway & Transport Review 17/1998.
[49] Hayashiya H., Makino T., Akiyama T., Kobayashi S., Ogiwara M., Nakajima M., Matsumoto A. Evaluation of energy saving effect of traction power supply voltage in urban electric railway system. EPE'18 ECCE Europe
[50] Hayashiya H., Suzuki T., Kawahara K., Yamanoi T. Comparative study of investment and efficiency to reduce energy consumption in traction power supply. 16th International Power Electronics and Motion Control Conference and Exposition, Antalya, Turkey 21-24 Sept 2014.
[51] Hirano T., Kikuchi S., Suzuki T., Hayashiya H. Evaluation of energy loss in d.c. traction power supply system. 2015 17th European Conference on Power Electronics and Applications (EPE'15 ECCE-Europe 2015). Geneva, Switzerland 2015.
[52] Hõimoja H., Vinnikov D., Lehtla M., Rosin A., Zakis J. Survey of Loss Minimization Methods in Tram Systems. International Symposium on Power Electronics, Electrical Drives, Automation and Motion SPEEDAM 2010.
[53] IEEE Guide for the Calculation of Braking Distances for Rail Transit Vehicles. IEEE Vehicular Technology Society (VTS), New York, USA 2009
[54] Inarida S., Kaneko T. A novel power control method achieving high reliability of auxiliary power supply system for trains. 2005 European Conference on Power Electronics and Applications. Dresden, Germany.
[55] Instrukcja o prowadzeniu ruchu pociągów Ir-1. PKP Polskie Linie Kolejowe S.A. Warszawa, 2017 r.
[56] Ishikawa K., Application of optimization theory for bounded state variable problems to the operation of trains, Bull. Jpn. Soc. Mech. Eng., vol. 11, no. 47, pp. 857–865, Oct. 1968.
[57] Iwnicki S., Handbook of Railway Vehicle Dynamics. Taylor & Francis, 2006.
[58] Jakubowski A., Jarzębowicz L. Constant vs. Variable efficiency of electric drive in train run simulations. 2019 26th International Workshop on Electric Drives: Improvement in Efficiency of Electric Drives (IWED), Moskwa.
[59] Jakubowski A., Jarzębowicz L., Karwowski K., Wilk A. Analiza energochłonności pojazdu szybkiej kolei miejskiej z uwzględnieniem zmiennej sprawności napędu trakcyjnego. Zeszyty Naukowe WEiA PG nr 60, Gdańsk 2018.
[60] Jakubowski A., Jarzębowicz L., Practical eco-driving strategy for suburban electric multiple unit. 2021 28th International Workshop on Electric Drives: Improving Reliability of Electric Drives (IWED), Moskwa 2021.

[61] Jakubowski A., Karwowski K., Wilk A., Analysis of energy efficiency of suburban transport network. 6th International Conference on Road and Rail Infrastructure (CETRA 2020), Zagreb 2021.
[62] Jakubowski, A., Jarzębowicz, L., Bartłomiejczyk, M., Skibicki, J., Judek, S., Wilk, A., & Płonka, M. (2021). Modeling of Electrified Transportation Systems Featuring Multiple Vehicles and Complex Power Supply Layout. ENERGIES, 14, 8196
[63] Jakubowski, A., Jarzębowicz, L., Karwowski, K., & Wilk, A. (2018). Efektywność energetyczna pojazdu szynowego w różnych warunkach obciążenia. Technika Transportu Szynowego, 44-48.
[64] Jakubowski, A., Karkosińska-Brzozowska, N., Karwowski, K., & Wilk, A. (2020). Storage electric multiple units on partially electrified suburban railway lines. Przegląd Elektrotechniczny, 158-161.
[65] Jarzębowicz L., Judek S., Karwowski K., Lipiński L., Miszewski M., Kompleksowa analiza symulacyjna układu napędowego zespołu trakcyjnego. Czasopismo Techniczne Vol. R. 108., nr z.13 (2011).
[66] Jefimowski W. Analiza wybranych aspektów efektywności energetycznej układu zasilania 3 kV DC zelektryfikowanej linii kolejowej. Praca Doktorska. Wydział Elektryczny PW, Warszawa 2018
[67] Jefimowski W., Szeląg A. Assessment of AC traction substation influence on energy quality in a supplying grid. TECHNICAL TRANSACTIONS 12/2018 ELECTRICAL ENGINEERING.
[68] Johnson J., Benefits of all-electric braking. Final report. RSSB Research Programme Engineering, Rail Safety and Standards Board, London 2012.
[69] Judek S., Skibicki J. Wyznaczanie parametrów elektrycznych trakcyjnego układu zasilania dla złożonych warunków ruchu przy wykorzystaniu programu PSpice. PRZEGLĄD ELEKTROTECHNICZNY (Electrical Review), ISSN 0033-2097, R. 85 NR 12/2009
[70] Kalman R. E., Falb P. L., Arbib M. A.: Topics in Mathematical System Theory. New York, Mc Graw Hill
[71] Kamel T., Tian Z., Zangiabadi M., Wade N., Pickert V., Tricoli P. Optimized Localization for the inverting substation to maximize the braking efficiency of the DC railways. 2021 IEEE 15th International Conference on Compatibility, Power Electronics and Power Engineering (CPE-POWERENG).
[72] Karwowski K. (red.), Energetyka transportu zelektryfikowanego. Poradnik inżyniera. Wyd. Politechniki Gdańskiej. Gdańsk, 2018.
[73] Karwowski K. Architektura, analiza i praktyka mikrokomputerowych systemów sterowania elektrycznych pojazdów trakcyjnych. Praca habilitacyjna. Politechnika Gdańska, Gdańsk 1996.
[74] Kinki Sharyo – Products. https://www.kinkisharyo.co.jp/english/ourproducts/?cat=1, access: 2021-03-16.
[75] Koleje pasażerskie w województwach. Dynamika zmian w latach 2010 – 2020. Urząd Transportu Kolejowego, Warszawa 2021.
[76] Kondo M., Ebizuka R., Yasunaga A. Rotor Design for High Efficiency Induction Motors for Railway Vehicle Traction. 2009 International Conference on Electrical Machines and Systems, Tokyo Japan.
[77] Kornaszewski M., Sierociński M. Proces przygotowania rozkładu jazdy pociągów. Autobusy 1809, 12/2016.
[78] Koseki, T.: Technologies for Saving Energy in Railway Operation: General Discussion on Energy Issues Concerning Railway Technology. IEEJ Transactions on Electrical and Electronic Engineering, 5, pp. 285-290, 2018.
[79] Kovacik M., Pospisil S. Design of electric multiple unit for Tatra electric Railway. 2020 Elektro, Taormina, Italy.
[80] Krzysztoszek K., Luft M., Lukasik Z.: Digital control model for electric traction vehicles. Procedia Computer Science 149 (2019) 274-277.

[81] Krzysztoszek K.: MATHEMATICAL MODEL OF TRACTION VEHICLE MOVEMENT. Journal of Automation, Electronics and Electrical Engineering vol. I iss. I 2019.
[82] Lawrence Shampine, Mark Reichelt. The MATLAB ODE Suite. SIAM Journal on Scientific Computing, Society for Industrial and Applied Mathematics, 1997
[83] Li, C.; Wang, H.; Bi, H. The Calculation Method of Energy Consumption of Air-Conditioning System in Subway Vehicle Based on Representative Operating Points. IOP Conf. Ser. Earth Environ. Sci. 2020, 455, 012177
[84] Lipiński L., Praktyczne metody regulacji trakcyjnych silników indukcyjnych optymalne pod względem energetycznym. Zeszyty Problemowe – Maszyny Elektryczne Nr 78/2007.
[85] Liu C., Meerman E. Increased recuperation efficiency by increment of the recuperation voltage to 1950V in a 1500V DC catenary system. 2007 European Conference on Power Electronics and Applications, Aalborg, Denmark 2007.
[86] Liu P., Yang L., Gao Z., Huang Y., Li S., Gao Y., Energy-Efficient Train Timetable Optimization in the Subway System with Energy Storage Devices, IEEE Transactions on Intelligent Transportation Systems.
[87] Luo J., Ying K., Bai J. Savitzky–Golay smoothing and differentiation filter for even number data. Signal Processing 85 (2005) 1429–1434.
[88] Madrjas J. Pomorskie: Drożejący prąd wymusi podwyżkę cen biletów kolejowych? https://www.rynek-kolejowy.pl/wiadomosci/pomorskie-rosnace-ceny-energii-wymusza-podwyzke-cen-biletow-105043.html, access: 2021-10-24.
[89] Matlab programming fundamentals. MathWorks Inc., https://www.mathworks.com/help/pdf_doc/matlab/matlab_prog.pdf, Access: 2021-04-11
[90] Matsuoka K., Kondo M., Energy Saving Technologies for Railway Traction Motors. IEEJ TRANSACTIONS ON ELECTRICAL AND ELECTRONIC ENGINEERING 2010, 5: 278-284.
[91] Matysiak, M., Michna, M., Ronkowski, M., & Wilk, A. (2014). DYNAMICZNA APLIKACJA INTERNETOWA SYMULACJI OBWODOWEJ MASZYNY INDUKCYJNEJ. UJĘCIE OBIEKTOWE. Maszyny Elektryczne : Zeszyty Problemowe, 104, 213-218
[92] Michalski L. (red.), STRATEGIA TRANSPORTU I MOBILNOŚCI OBSZARU METROPOLITALNEGO GDAŃSK-GDYNIA-SOPOT DO ROKU 2030. Diagnoza sytemu transportowego Obszaru Metropolitalnego. Gdańsk, 2015
[93] Miyatake M., Ko H.: Optimization of Train Speed Profile for Minimum Energy Consumption. IEEJ TRANSACTIONS ON ELECTRICAL AND ELECTRONIC ENGINEERING IEEJ Trans 2010; 5: 263–269
[94] Morimoto M. Iron Loss of Non-Rare Earth Traction Motor for Electric Vehicle. 2010 IEEE Vehicle Power and Propulsion Conference, Lille France.
[95] Muginshtein, L. A.; Yabko, I. A. Power Optimal Traction Calculation for Operation of Trains of Increased Mass and Length, In 2009 9th International Heavy Haul Conference ,Shanghai, China, 2009
[96] Mwambeleko J.J., Somsai K., Kulworawanichpong T. The potential of battery electric multiple units to replace diesel commuter trains and reduce fuel cost. 2016 IEEE/SICE International Symposium on System Integration, Sapporo Japan.
[97] Nalewajko J., Szkliniarz S., Hałaśkiewicz J. Vademecum maszynisty elektrycznych pojazdów trakcyjnych. Część III - opisy obwodów elektrycznych i pneumatycznych pojazdów trakcyjnych serii EN57, ET21, EU07, ET41, ET22. Śląska DOKP, Katowice 1982.
[98] Nevezak V., Shatokhin A. Interaction's Simulation Modeling of Electric Rolling Stock and Electric Traction System. 2019 International Ural Conference on Electrical Power Engineering (UralCon)
[99] Nikolaidis P., Poulikkas A. A comparative review of electrical energy storage systems for better sustainability. Journal of Power Technologies 97 (3) (2017) 220–245

[100] Nocedal, J. and Wright, S. Numerical Optimization, 2nd. ed., Ch. 18. Springer, 2006
[101] Occupancy rates in passenger transport. EEA European Environment Agency Indicator Assesment. https://www.eea.europa.eu/data-and-maps/indicators/occupancy-rates-of-passenger-vehicles/occupancy-rates-of-passenger-vehicles, access: 2021-07-12.
[102] Ogawa T., Manabe S., Yoshikawa G., Imamura Y., Kageyama M.: Method of calculating running resistance by the use of the train data collection devices. QR of RTRI, vol. 58, No. 1, Feb. 2017
[103] Olofsson, Ulf & Zhu, Yi & Abbasi, Saeed & Lewis, Roger & Lewis, Stephen. (2013). Tribology of the wheel−rail contact – aspects of wear, particle emission and adhesion. Vehicle System Dynamics. 51. 1091-1120.
[104] OpenPowerNet Simulation Software for traction power supply systems. Institut fuer Bahntechnik GmbH. https://www.openpowernet.de/ Access: 2021-05-15.
[105] P. -S. Murvay and B. Groza, "Efficient Physical Layer Key Agreement for FlexRay Networks," in IEEE Transactions on Vehicular Technology, vol. 69, no. 9, pp. 9767-9780, Sept. 2020
[106] Pascal J., Hoummas A., Letrouvé T., Lhomme W. Energetic Benefits of Trains by Overrunning the Heating System during the Regenerative Braking. 2017 IEEE Vehicle Power and Propulsion Conference (VPPC), Belfort, France.
[107] Patel, A. ; Chandwani, H.; Patel, V.; Patel, K. Prediction of IGBT power losses and junction temperature in 160kW VVVF inverter drive Journal of Electrical Engineering 2014, 12 (2) 1–7
[108] Pazdro P., Karwowski K., Czucha J., Mizan M., Kamonciak A., Skibicki J. Optymalizacja efektów hamowania odzyskowego w komunikacji miejskiej przez sterowanie adaptacyjne. Raport projektu badawczego KBN nr 10A07422, Gdańsk 2003
[109] Pellegrino G., Armando E., Mahmoudi A., Soong W. L. Efficiency Maps of Electrical Machines. IEEE Energy Conversion Congress and Exposition (ECCE), Montreal 2015.
[110] Perpinya X. (Ed.), Lozano J.A., Felez J., de Dios Sanz J., Mera J.M. Railway Traction. Reliability and Safety in Railways. InTech 2012, ISBN:978-953-51-0451-3. Available from: http://www.intechopen.com/books/reliability-and-safety-in-railway/railway-traction
[111] PKP Energetyka uruchomiła największy trakcyjny magazyn energii w Europie, który zasili polską kolej. Aktualności PKP Energetyka. http://www.pkpenergetyka.pl/Aktualnosci/2021/PKP-Energetyka-uruchomila-najwiekszy-trakcyjny-magazyn-energii-w, access: 2021-07-11.
[112] Positive train control: is the US on track? https://www.railway-technology.com/analysis/featurepositive-train-control-is-the-us-on-track-5825798/, access: 2018-03-25.
[113] Quantification of benefit of train mass reduction. Research Programme –Engineering, research project T712. Rail Safety and Standards Board, London 2010.
[114] Radtke A., Muller L., Schumacher A. DYNAMIS: a model for the calculation of running times for an efficient time-table construction. Transactions on the Built Environment vol 34, © 1998 WIT Press
[115] Radu P.V., Szeląg A., Steczek M. On-Board Energy Storage Devices with Supercapacitors for Metro Trains—Case Study Analysis of Application Effectiveness. Energies 2019, 12, 1291
[116] Rawicki S., Energooszczędne przejazdy tramwajów ze sterowanymi wektorowo silnikami indukcyjnymi w dynamicznym ruchu miejskim. Wyd. Politechniki Poznańskiej, Poznań 2013.
[117] Rimpas D., Kaminaris S. D., Aldarraji I., Piromalis D., Vokas G., Papageorgas P. G., Tsaramirsis G., Energy management and storage systems on electric vehicles: A comprehensive review, Materials Today: Proceedings, Volume 61, Part 3, 2022, Pages 813-819, ISSN 2214-7853
[118] Rodriguez A.F.: Design of robust and energy efficient ATO speed profiles of metropolitan lines considering train load variations and delays

[119] Rojek A., Kaniewski M., Czarnecki R. Interoperacyjność układu zasilania trakcji elektrycznej – nowe normy EN 50367 i EN 50388. TTS Technika Transportu Szynowego 1-2/2006 pp. 52-56.
[120] Rojek A., Zasilanie trakcji elektrycznej w systemie prądu stałego 3 kV. Kolejowa Oficyna Wydawnicza, Warszawa 2012
[121] Rufer A., Energy Storage Systems and Components. Taylor & Francis Group, 2018.
[122] Ryu J-H., Lee J-H., Lee J-S.: Switching Frequency Determination of SiC-Inverter for High Efficiency Propulsion System of Railway Vehicle. Energies 13/2020
[123] Sakamoto Y., Kashiwagi T., Sasakawa T., Fujii N. Linear Eddy Current Brake for Railway Vehicles Using Dynamic Braking. Proceedings of the 2008 International Conference on Electrical Machines
[124] Sapoń G., Starowicz W. Wyniki badań potoków pasażerów korzystających z przejazdów w pociągach regionalnych na terenie województwa Łódzkiego. TTS Technika Transportu Szynowego 11/2003, pp. 33-38
[125] Shashaj A., Bohlin M., Ghaviha N.: Joint optimization of multiple train speed profiles, 10th International Conference on Compatibility, Power Electronics and Power Engineering (CPE-POWERENG), Bydgoszcz, 29.06 – 01.07 2016.
[126] Sikora A., Kulesz B. Effectiveness of different designs of 12- and 24-pulse rectifier transformers. Proceedings of the 2008 International Conference on Electrical Machines
[127] Šimanek J., Novák J., Dolecek R., Cerny O., Control algorithms for permanent magnet synchronous traction motor. IEEE International Conference "Computer as a tool", Warszawa 2007.
[128] Song Y., Song W. A Novel Dual Speed-Curve Optimization Based Approach for Energy-Saving Operation of High-Speed Trains. IEEE Transactions on Intelligent Transportation Systems, vol. 17 no. 6, June 2016.
[129] Spiridonov E.A., Yarolavtsev M.V. Research of energy recuperation efficiency in Electric Transport Systems. 18th INTERNATIONAL CONFERENCE ON MICRO/NANOTECHNOLOGIES AND ELECTRON DEVICES EDM 2017.
[130] Spiroiu M-A., About the influence of wheel-rail adhesion on the maximum speed of trains. MATEC Web of Conferences 178, 06004 (2018)
[131] Stana G., Brazis V. Analyses of Trolleybus Recuperation Energy Utilisation Losses Considering Different Efficiency Ratios of Traction Inverter and DC/DC Converter IEEE 2019
[132] Stana G., Brazis V. Trolleybus Motion Simulation by Dealing with Overhead DC Network Energy Transmission Losses. 2017 18th International Scientific Conference on Electric Power Engineering (EPE), Kouty nad Desnou, Czech Republic.
[133] Steimel A., Electric traction – motive power and energy supply. Oldenbourg Industrieverlag, München 2008.
[134] Sugimoto T. A study to estimate of effective coefficient of regenerative energy in electric railway. Transactions on the Built Environment vol 34, Computers in Railways 1998.
[135] Susz S., Pawęska M. Model oceny potencjału pasażerskiego dla województwa Dolnośląskiego. Przegląd Komunikacyjny 4/2014
[136] Szeląg A. ELECTRICAL POWER INFRASTRUCTURE FOR MODERN ROLLING STOCK WITH REGARD TO THE RAILWAY IN POLAND. Archives of Transport, Volume 42, Issue 2, 2017
[137] Szeląg A., Wpływ napięcia w sieci trakcyjnej 3 kV DC na parametry energetyczno-trakcyjne zasilanych pojazdów. Instytut Naukowo-Wydawniczy „SPATIUM", Radom 2013. ISBN 978-83-62805-01-3
[138] Szeląg, A.: Electric traction – basics. Oficyna Wydawnicza Politechniki Warszawskiej, 2019.
[139] The new N700S Shinkansen: More comfortable and earthquake-proof. https://www.jrailpass.com/blog/shinkasen-n700s, access: 2021-07-22.
[140] The Train Operations Model (data dostępu 9.07.2018 r.) http://www.railsystemscenter.com/tom.htm

[141] Tian Z., Hillmansen S., Roberts C., Weston P.: Modeling and simulation of DC rail traction systems for energy saving. 2014 17th International IEEE Conference on Intelligent Transportation Systems.
[142] Tian Z., Zhao N., Hillmansen S., Su S., Wen C.: Traction power substation load analysis with various train operating styles and substations fault modes. Energies 13/2020.
[143] Tian, Z., Hillmansen, S., Roberts, C., Weston, P., Zhao, N., Chen, L., Chen, M.: Energy evaluation of the power network of a DC railway system with regenerating trains. IET Electrical Systems in Transportation, 10, pp. 1-9, 2015.
[144] Tian, Z., Zhang, G., Zhao, N., Hillmansen, S., Tricoli, P., Roberts, C.: Energy Evaluation for DC Railway Systems with Inverting Substations. 2018 IEEE International Conference on Electrical Systems for Aircraft, Railway, Ship Propulsion and Road Vehicles and International Transportation Electrification Conference, ESARS-ITEC 2018.
[145] Train Energy and Dynamics Simulator (TEDS). U.S. Department of Transportation, Federal Railroad Administration. https://railroads.dot.gov/rolling-stock/current-projects/train-energy-and-dynamics-simulator-teds, access 2021-05-30.
[146] TranSys Research Ltd.; RailTEC at the University of Illinois at Urbana-Champaign; CPCS Transcom; Lawson Economics Research Inc.; National Cooperative Railroad Research Program; Transportation Research Board; National Academies of Sciences, Engineering, and Medicine. Comparison of Passenger Rail Energy Consumption with Competing Modes; Transportation Research Board: Washington, D.C., 2015; p 22083.
[147] Tseng K. H., Shiao Y. F., THE ANALYSIS OF REGENERATIVE BREAKING POWER FOR TAIPEI RAPID TRANSIT SYSTEMS ELECTRICAL MULTIPLE UNITS.
[148] UIC 566: Loading of coach bodies and their components. International Union of Railways, 1994.
[149] Vagnguide – Motorvagn X31K/ET. https://www.jarnvag.net/vagnguide/x31k, access: 2018-09-04.
[150] Valentini P.P., Pennestri E. A Review of Formulas for the Mechanical Efficiency Analysis of Two Degrees-of-Freedom Epicyclic Gear Trains. Journal of Mechanical Design 9/2003
[151] Villalba Sanchis I., Salvador Zuriaga P.: An energy-efficient metro speed profiles for energy savings: application to the Valencia metro. Transportation Research Procedia 18 (2016) 226 – 233.
[152] Wang W., Wang Q., Yu Y., Zeng X., Zou N. Study on the Operation Region of Induction Traction Motor for Electric Vehicle. 2009 International Conference on Measuring Technology and Mechatronics Automation
[153] Wei, K.; Zhang, C.; Gong, X.; Kang, T. The IGBT Losses Analysis and Calculation of Inverter for Two-Seat Electric Aircraft Application. Energy Procedia 2017, 105, 2623–2628
[154] Wilk, A., Gelman, L., Judek, S., Karwowski, K., Mizan, M., Maciołek, T., Lewandowski, M., Jakubowski, A., & Klimowska, K. (2021). Novel method of estimation of inertial and dissipative parameters of a railway pantograph model. VEHICLE SYSTEM DYNAMICS, 1-23.
[155] Wilk, A.; Koc, W.; Specht, C.; Judek, S.; Karwowski, K.; Chrostowski, P.; Czaplewski, K.; Dabrowski, P.S.; Grulkowski, S.; Licow, R.; Skibicki, J.; Specht, M.; Szmaglinski, J. Digital Filtering of Railway Track Coordinates in Mobile Multi–Receiver GNSS Measurements. Sensors2020, 20, 5018.
[156] Wongprasert S., Sapaklom T., Konghirun M. Efficiency Improvement of Traction Drive System with Induction Motor using Dynamic DC bus Voltage Adjustment Over a Wide Speed Range Operation. The 23rd International Conference on Electrical Machines and Systems (ICEMS)
[157] Wykaz odległości taryfowych SKM Trójmiasto (WOT-SKM). Gdynia 2020.

[158] X. He, E. Li and H. Zhang, "ASR Control of Distributed Drive Vehicles based on CAN Bus and FlexRay Bus," 2021 IEEE 5th Advanced Information Technology, Electronic and Automation Control Conference (IAEAC), 2021, pp. 749-755
[159] Y. Zhou, Y. Bai, J. Li, B. Mao, and T. Li, “Integrated Optimization on Train Control and Timetable to Minimize Net Energy Consumption of Metro Lines,” Journal of Advanced Transportation, 2018
[160] Yang H., Yan J., Zhang K. Braking Process Modeling and Simulation of CRH2 Electric Multiple Unit. 2012 Third International Conference on Digital Manufacturing & Automation, Guilin, China.
[161] Yang X., Li X., Ning B., Tang T.: A Survey on Energy-Efficient Train Operation for Urban Rail Transit, IEEE Transactions on Intelligent Transportation Systems, Volume: 17, Issue: 1, Jan. 2016.
[162] Z. Xiao, Q. Wang, P. Sun, B. You, X. Feng, “Modeling and energy optimal control for high speed trains”. IEEE Transactions on transportation electrification, vol. 6, no. 2, pp. 797–807, June 2020
[163] Zarifian A., Kolpahchyan P., Pshihopov V., Medvedev M., Grebennikov N., Zak V.: EVALUATION OF ELECTRIC TRACTION'S ENERGY EFFICIENCY BY COMPUTER SIMULATION. 19th IMACS World Congress, San Lorenzo del Escorial (Spain) 26-30.08.2013
[164] Zhang C., Li H., Luo W., Liu H. Fast Method for Calculating Power Flow of Metro Traction Power Supply. The 16th IET International Conference on AC and DC Power Transmission (ACDC 2020)
[165] Zhang G., Tian Z., Tricoli P., Hillmansen S., Wang Y., Liu Z. Inverter Operating Characteristics Optimization for DC Traction Power Supply Systems. IEEE TRANSACTIONS ON VEHICULAR TECHNOLOGY, VOL. 68, NO. 4, APRIL 2019.
[166] Zhang Q., Zhang T. Speed-optimal setting of electric multiple units based on energy-efficient operation. 2015 IEEE Advanced Information Technology, Electronic and Automation Control Conference (IAEAC), Chongqing, China.
[167] Żurkowski A. Modelowanie przewozów międzyaglomeracyjnych. Problemy Kolejnictwa - zeszyt 148 pp. 5-48.

Appendix 1 – Code and subsystems examples

1a – Permission function setting

```
%permission table - vehicle #1, EN57AKM (571)
%starting from Gdansk Srodmiescie

rjat = 2*3600+75*60;

sd1 = randi([1 2000],1,1);

rjay = [0 0 1 1 0 0 1 1 0 0 1 1 0 0 1 1 0 0 1 1 0 0 1 1 0 0 1 1 0 0 1 1 0 0 1 1 0 0];

rjax = [0                          %0
        4*3600+30*60-1             %0
        4*3600+30*60               %1
        4*3600+30*60+75*60*5-1     %1
        4*3600+30*60+75*60*5          %0
        4*3600+30*60+75*60*5+5*60-1   %0
        4*3600+30*60+75*60*5+5*60        %1
        4*3600+30*60+75*60*5+5*60+75*60-1   %1 #1
        4*3600+30*60+75*60*5+5*60+75*60     %0
        4*3600+30*60+75*60*5+5*60*2+75*60-1 %0
        4*3600+30*60+75*60*5+5*60*2+75*60      %1 #2
        4*3600+30*60+75*60*5+5*60*2+75*60*2-1  %1
        4*3600+30*60+75*60*5+5*60*2+75*60*2    %0
        4*3600+30*60+75*60*5+5*60*3+75*60*2-1  %0
        4*3600+30*60+75*60*5+5*60*3+75*60*2    %1 #3
        4*3600+30*60+75*60*5+5*60*3+75*60*3-1  %1
        4*3600+30*60+75*60*5+5*60*3+75*60*3    %0 14.45
        4*3600+30*60+75*60*5+5*60*4+75*60*3-1  %0
        4*3600+30*60+75*60*5+5*60*4+75*60*3    %1 #4
        4*3600+30*60+75*60*5+5*60*4+75*60*4-1  %1
        4*3600+30*60+75*60*5+5*60*4+75*60*4         %0 16.05
        4*3600+30*60+75*60*5+5*60*4+75*60*4+2*60-1  %0
        4*3600+30*60+75*60*5+5*60*4+75*60*4+2*60    %1 16.07
        4*3600+30*60+75*60*5+5*60*4+75*60*4+2*60+75*60*2-1  %1
        4*3600+30*60+75*60*5+5*60*4+75*60*4+2*60+75*60*2    %0
        4*3600+30*60+75*60*5+5*60*4+75*60*4+2*60+75*60*2+3*60-1 %0
        4*3600+30*60+75*60*5+5*60*4+75*60*4+2*60+75*60*2+3*60   %1 18.40
        4*3600+30*60+75*60*5+5*60*4+75*60*4+2*60+75*60*2+3*60+75*60-1   %1
        4*3600+30*60+75*60*5+5*60*4+75*60*4+2*60+75*60*2+3*60+75*60     %0
        4*3600+30*60+75*60*5+5*60*5+75*60*4+2*60+75*60*2+3*60+75*60-1   %0
        4*3600+30*60+75*60*5+5*60*5+75*60*4+2*60+75*60*2+3*60+75*60     %1 20.00
        4*3600+30*60+75*60*5+5*60*5+75*60*4+2*60+75*60*2+3*60+75*60*4-1   %1
        4*3600+30*60+75*60*5+5*60*5+75*60*4+2*60+75*60*2+3*60+75*60*4     %0
        4*3600+30*60+75*60*5+5*60*8+75*60*4+2*60+75*60*2+3*60+75*60*4-1   %0
        4*3600+30*60+75*60*5+5*60*8+75*60*4+2*60+75*60*2+3*60+75*60*4     %1
        4*3600+30*60+75*60*5+5*60*8+75*60*4+2*60+75*60*2+3*60+75*60*5-1   %1
        4*3600+30*60+75*60*5+5*60*8+75*60*4+2*60+75*60*2+3*60+75*60*5     %0
        4*3600+30*60+75*60*5+5*60*8+75*60*4+2*60+75*60*2+3*60+75*60*10    %0
        ]


%4 obieg, potem +5
%4 obieg +5min
```

1b – HVAC duty cycle setting

```
%HVAC duty cycle setting

temp = 7;       %temperature (degree C)

TV = [-10 -8 -6 -4 -2 0 2 4 6 8 10 12 14 16 18];    %temperatures (arguments)
TU = [100 97 80 68 59 50 40 30 20 12 6 2 0 0 0];    %duty cycle (up)
TD = [80 75 60 45 35 25 16 10 5 0 0 0 0 0 0];       %duty cycle (down)

UB = interp1(TV,TU,temp)*100;       %interpolate upper curve
LB = interp1(TV,TD,temp)*100;       %interpolate lower curve

ADC = randi([LB UB],1,1)/100;       %random HVAC duty cycle - within curves
```

1c – Reverser

```
function rev = fcn(cnt,do)

pom = mod(cnt,2);    %2 possible directions

if do == 1           %reverser dependent on starting direction 'do'
if pom == 0          %and number of circulations
    rev = 1;
else rev = -1;
end
else
    if pom == 0
    rev = -1;
else rev = 1;
    end
end

%y = u;
```

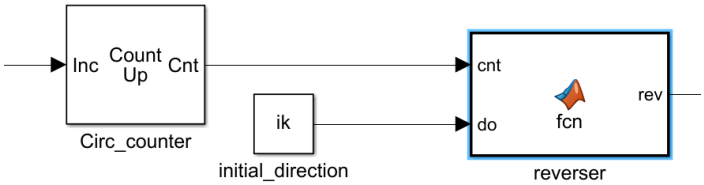

1d – Supply section selection

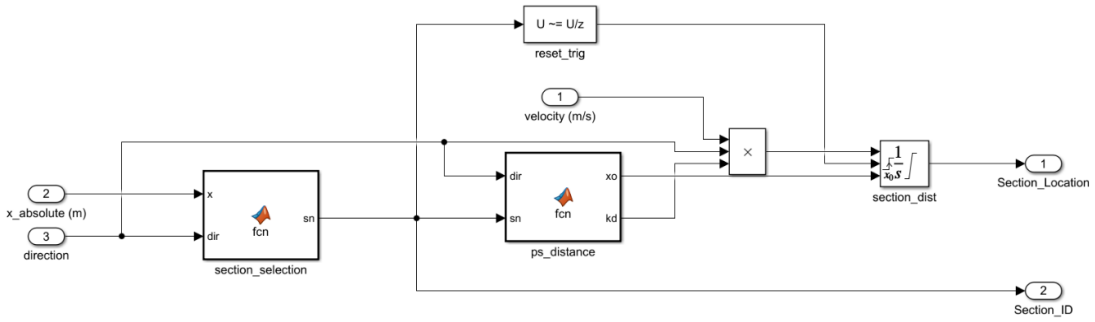

```
function sn = fcn(x,dir)

%power supply section selection
%section 11: PT Wrzeszcz (one sided, closed)
%section 21/22: PT Wrzeszcz - PT Sopot (two sided, track 501 & 502)
%section 31/32: PT Sopot - PT Redlowo (two sided, track 501 & 502)
%section 999: out of bounds of analysis (ignored)

switch(dir)
    case 1
if x<4744
    sn = 11;
elseif x>=4744 && x<10352
    sn = 21;
elseif x>=10352 && x<17131
    sn = 31;
else sn = 999;
end
    case -1
if x<4744
    sn = 11;
elseif x>=4744 && x<10352
    sn = 22;
elseif x>=10352 && x<17131
    sn = 32;
else sn = 999;
end
    otherwise sn = 999;
end
%y = u;
```

```
function [xo,kd] = fcn(dir,sn)

%power suppply section beginning relative distance
%0 for track 501 (positive velocity integration, distance increase)
%section length for track 502 (negative integration)
%section 11 converted into two sided - integration always positive
%k is correction of reverser for section distance integration

if dir == 1
    kd = 1;
    if sn == 11
    xo = 6144;
    else
        xo = 0;
    end
else
    switch sn
        case 11
            xo = 0;
            kd = -1;
        case 22
            xo = 5608;
            kd = 1;
        case 32
            xo = 6779;
            kd = 1;
        otherwise xo = 0;
            kd = 1;
    end
end
```

1e – mass and stop time variability

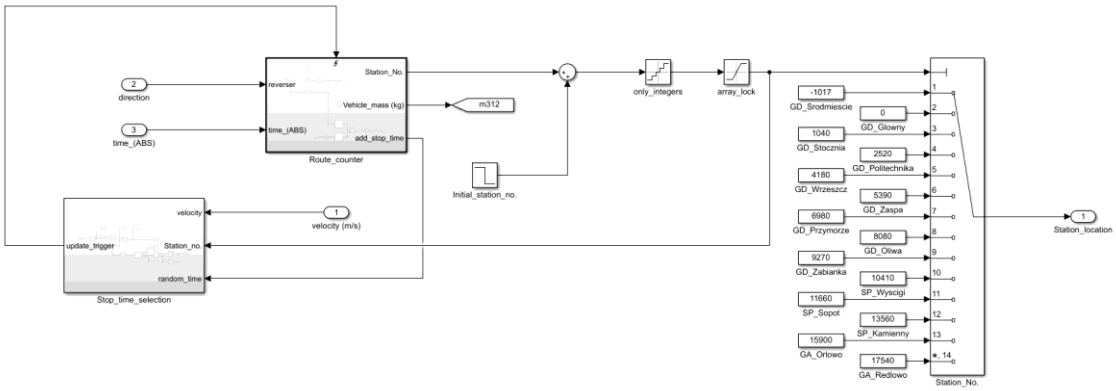

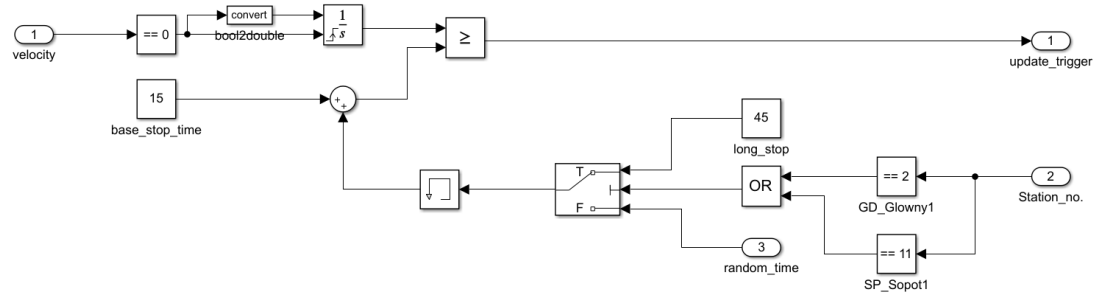

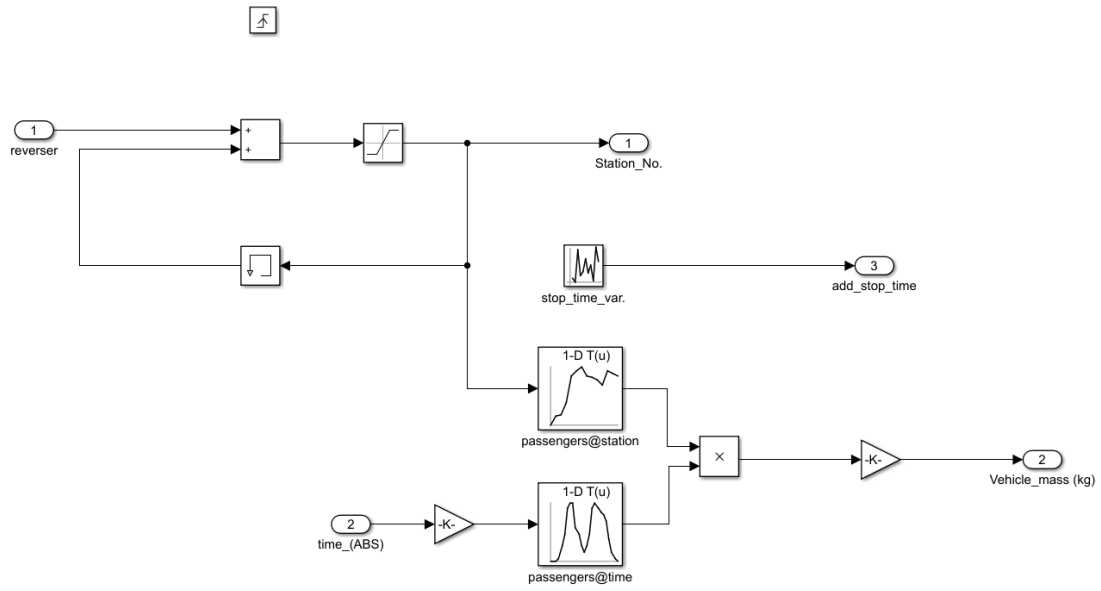

Appendix 2 – Simulation results for other vehicles

2a – EN57AKM, track 501 (direction Gdynia)

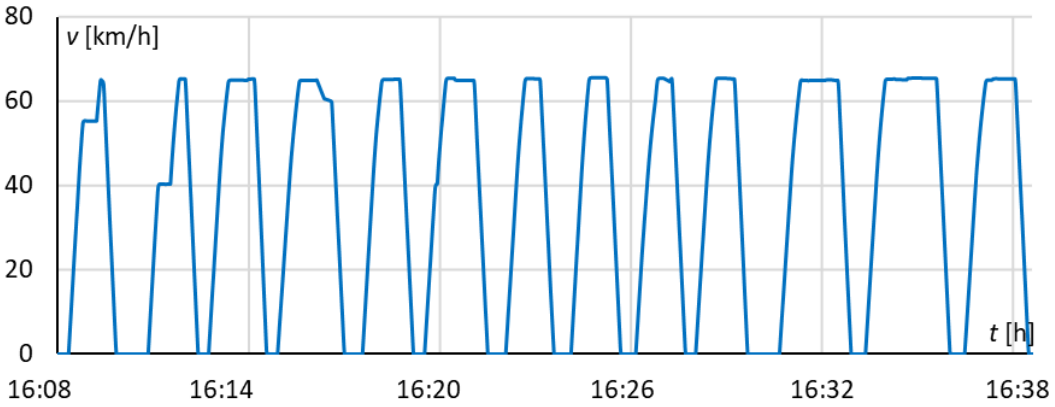

EN57AKM – velocity waveform, track 501

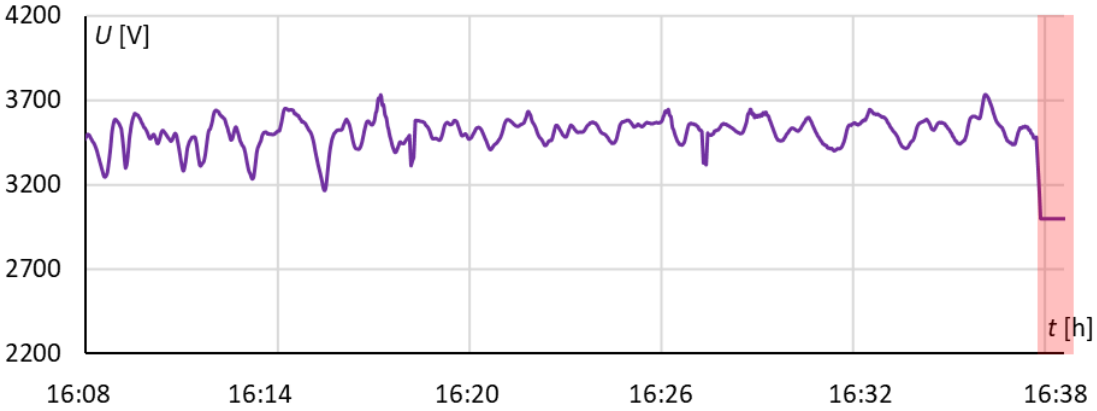

EN57AKM – pantograph voltage waveform, track 501

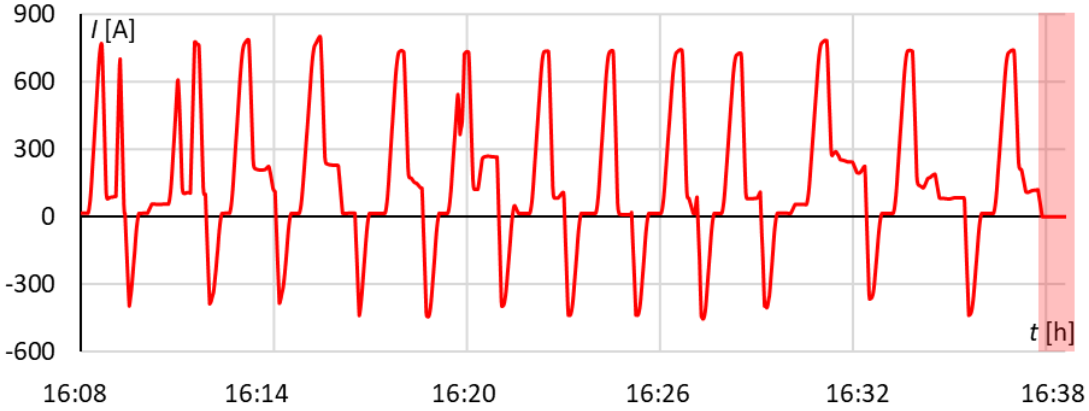

EN57AKM – vehicle current waveform, track 501

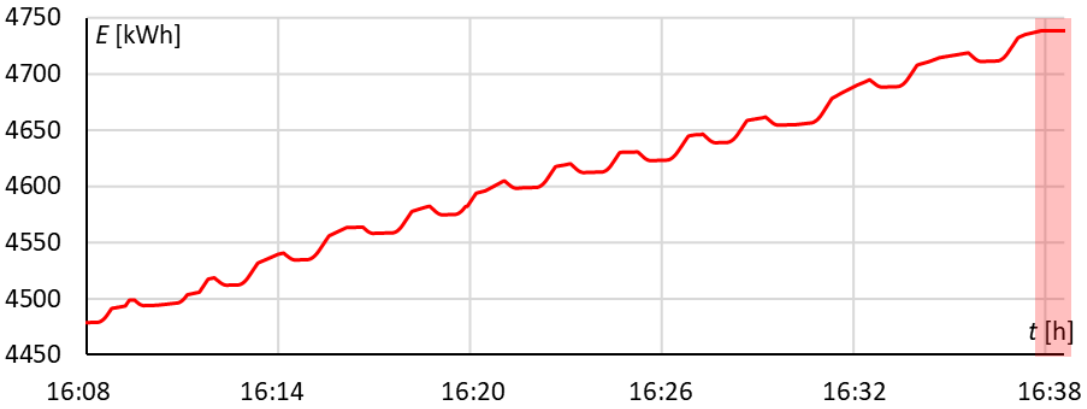

EN57AKM – vehicle energy balance waveform, track 501

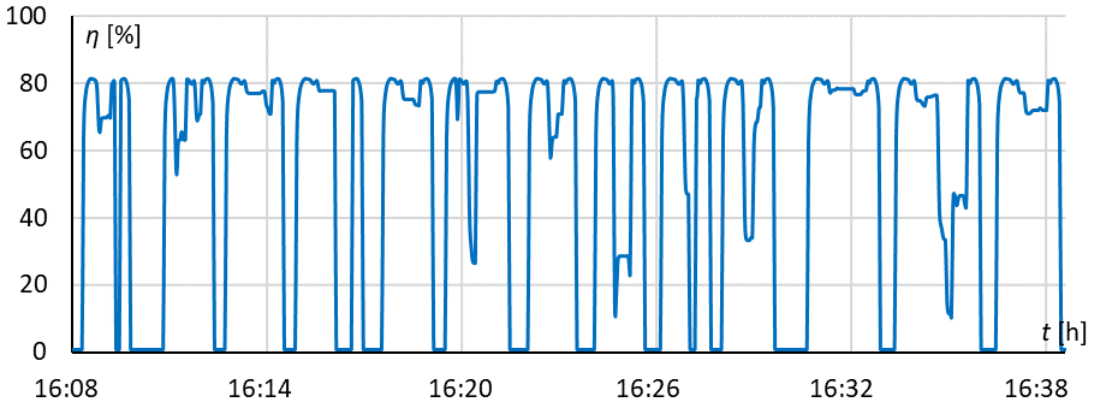

EN57AKM – drivetrain efficiency waveform, track 501

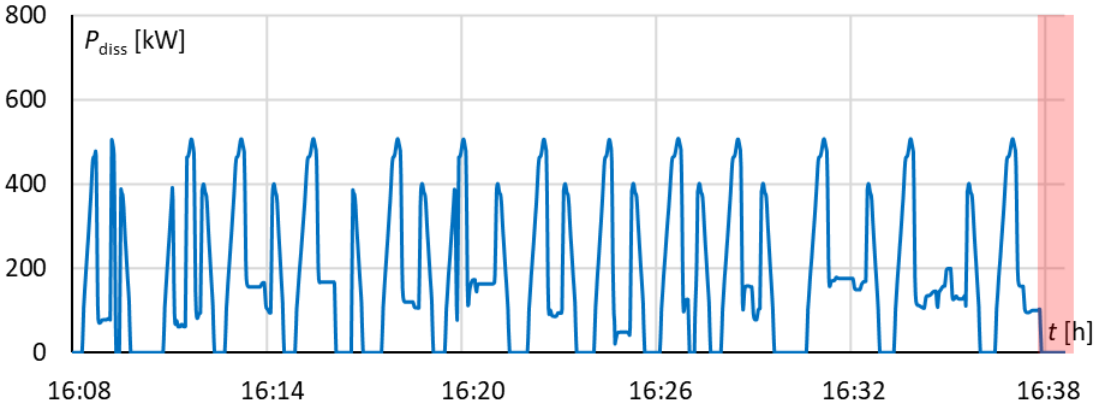

EN57AKM – drivetrain losses waveform, track 501

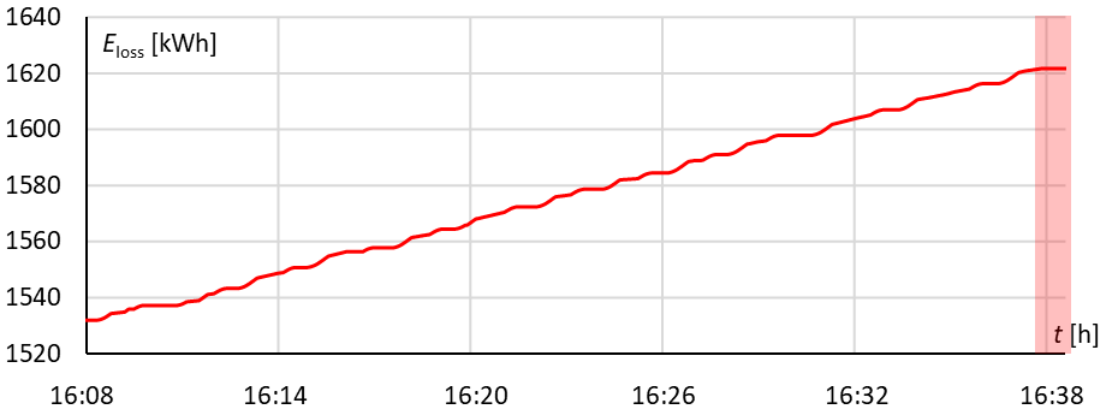

EN57AKM – dissipated energy waveform, track 501

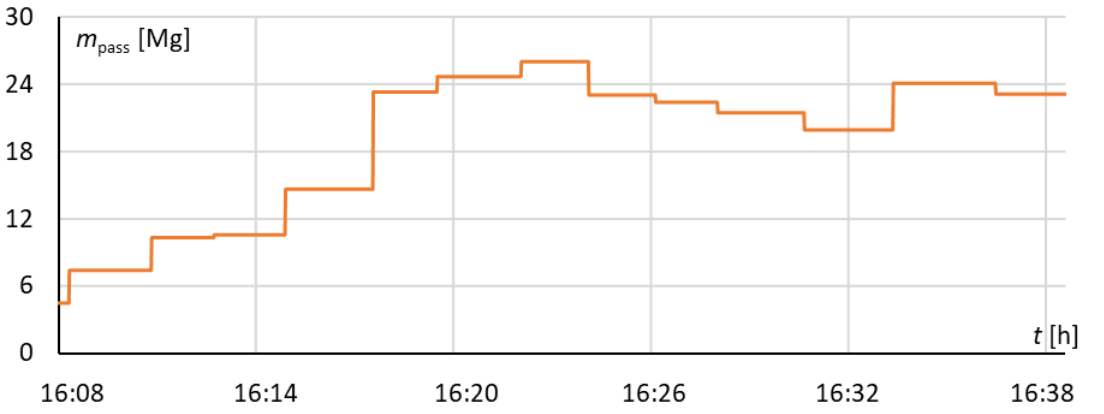

EN57AKM – passenger mass waveform, track 501

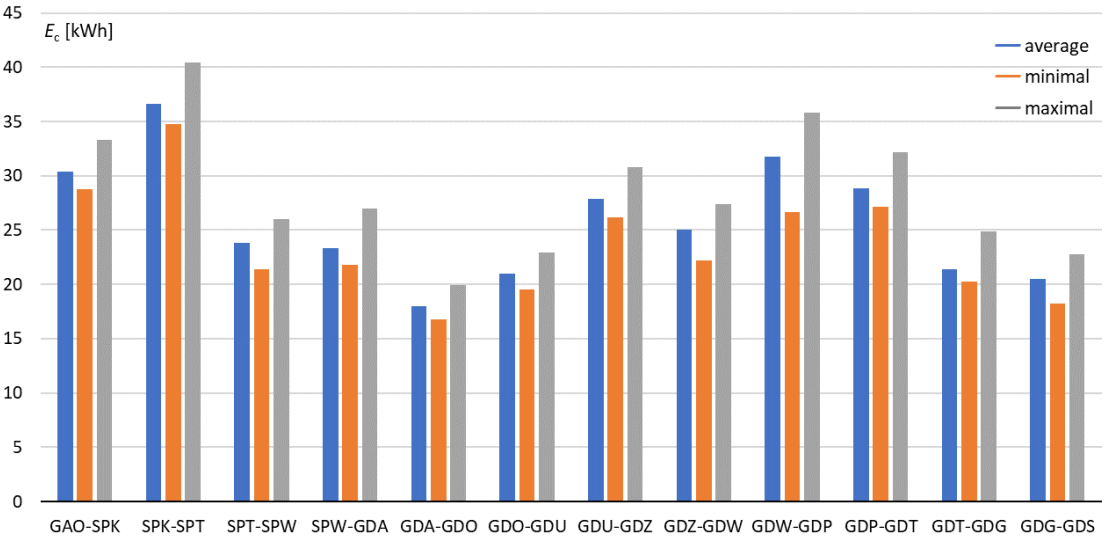

EN57AKM – consumed energy for each route part, track 501

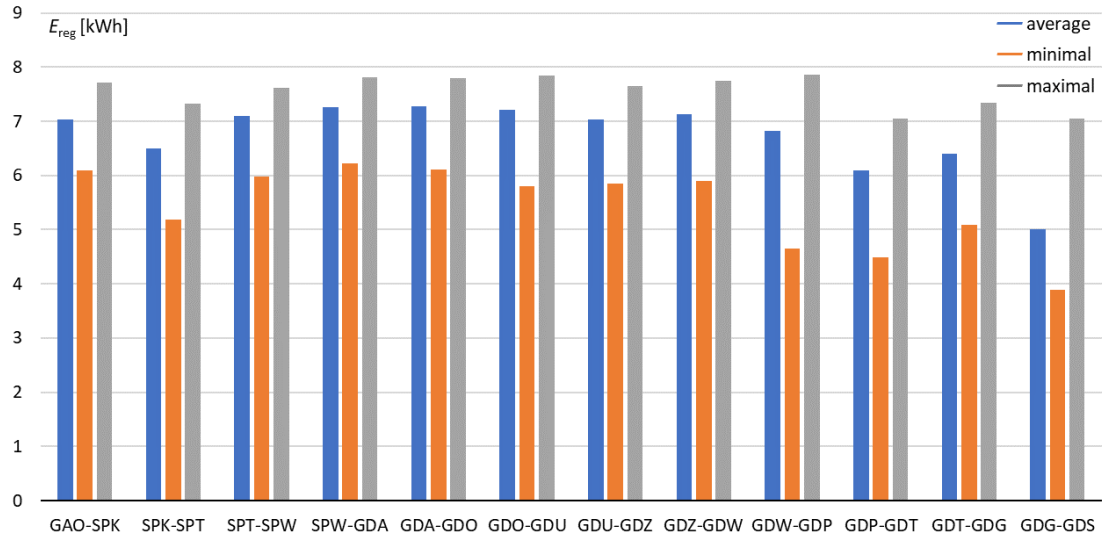

EN57AKM – regenerated energy for each route part, track 501

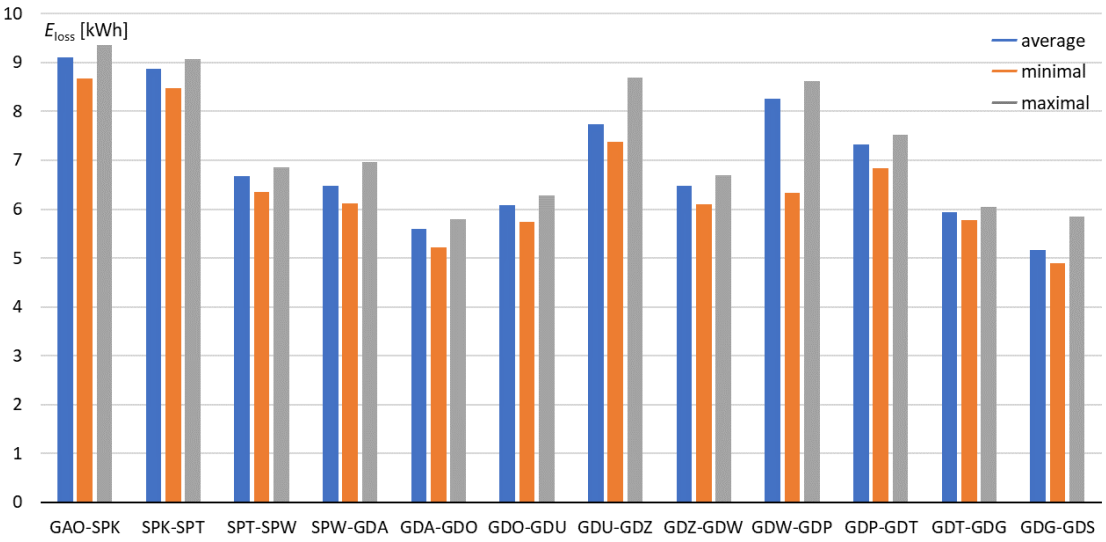

EN57AKM – dissipated energy for each route part, track 501

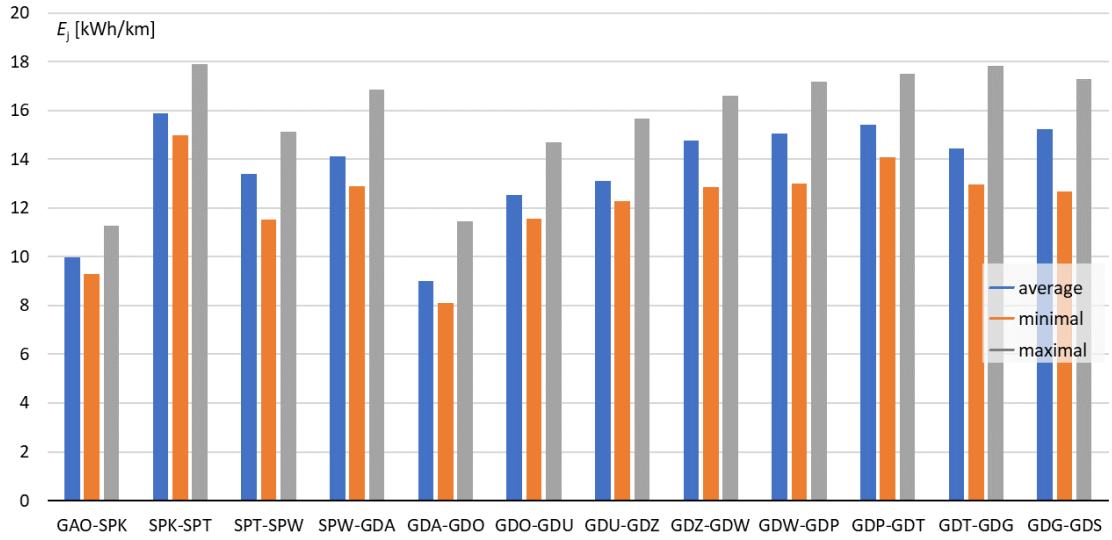

EN57AKM – energy consumption per 1 km, track 501

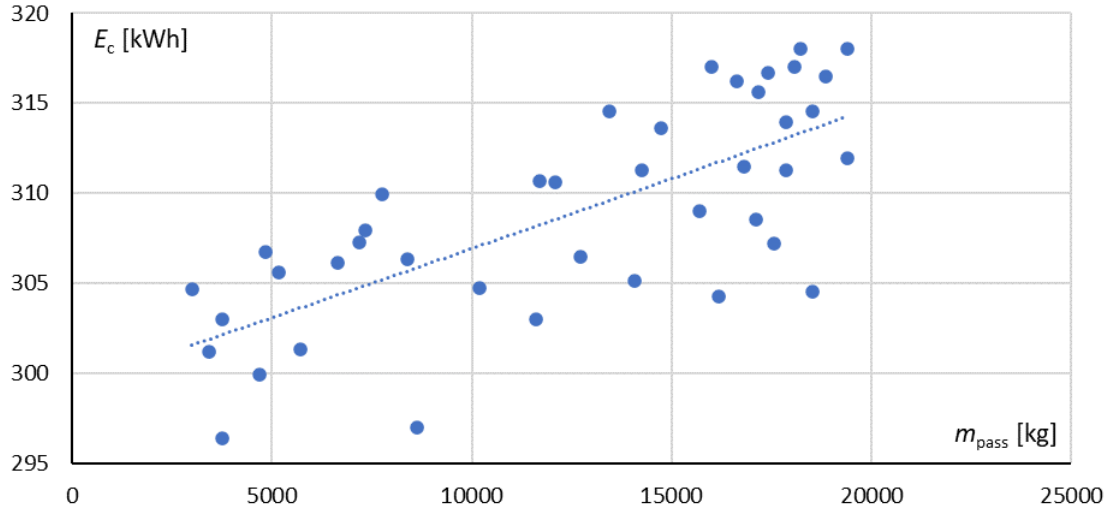

EN57AKM – consumed energy vs load mass, track 501

2b – EN71SKM, track 502 (direction Gdańsk)

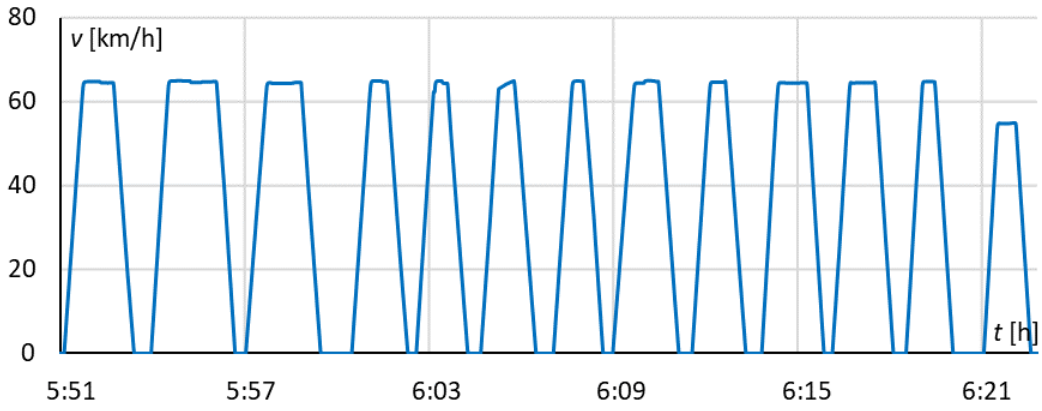

EN71SKM – velocity waveform, track 502

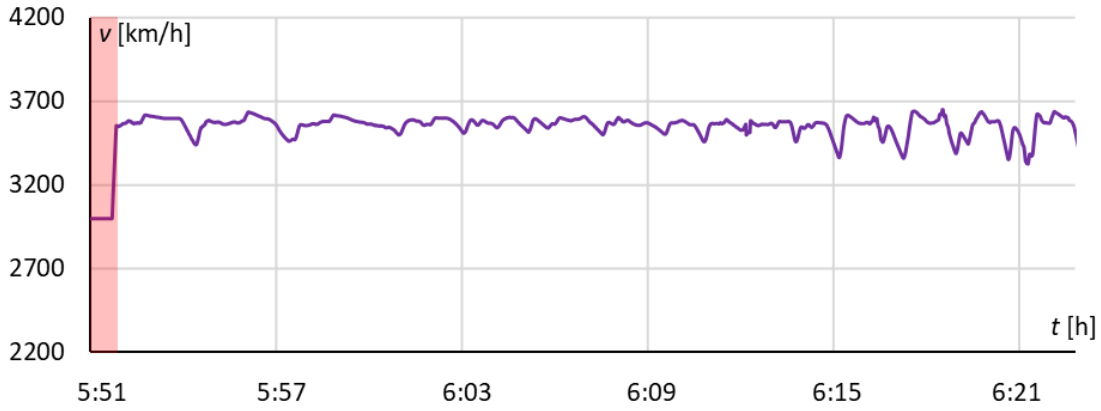

EN71SKM – pantograph voltage waveform, track 502

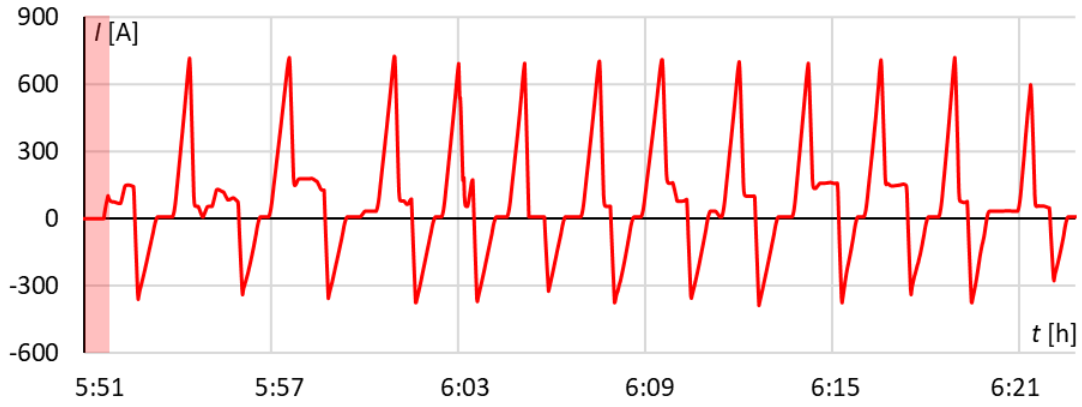

EN71SKM – vehicle current waveform, track 502

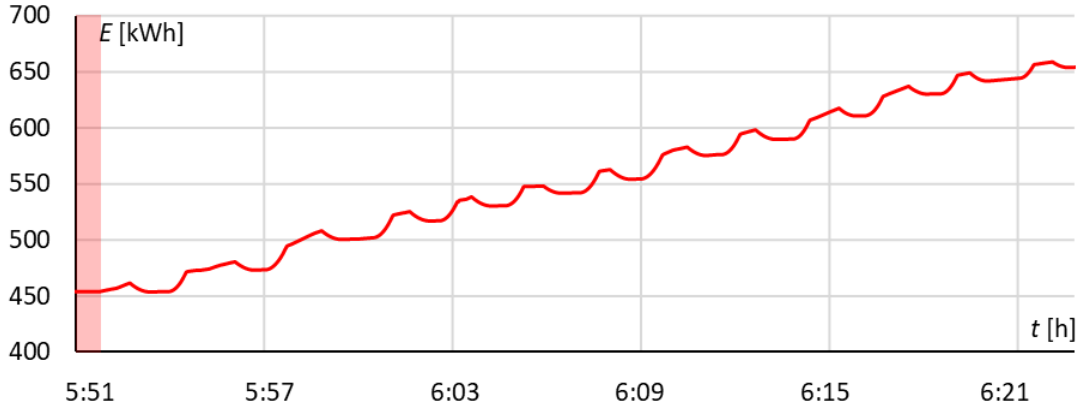

EN71SKM – vehicle energy balance waveform, track 502

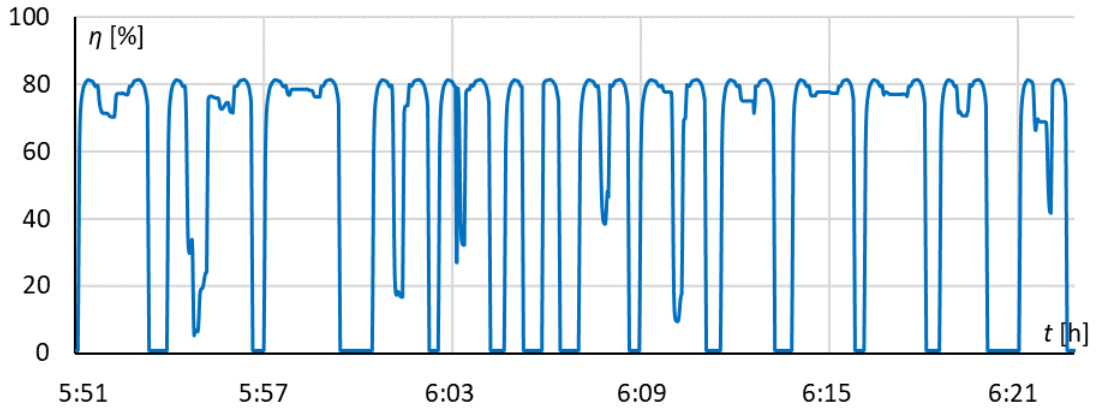

EN71SKM – drivetrain efficiency waveform, track 502

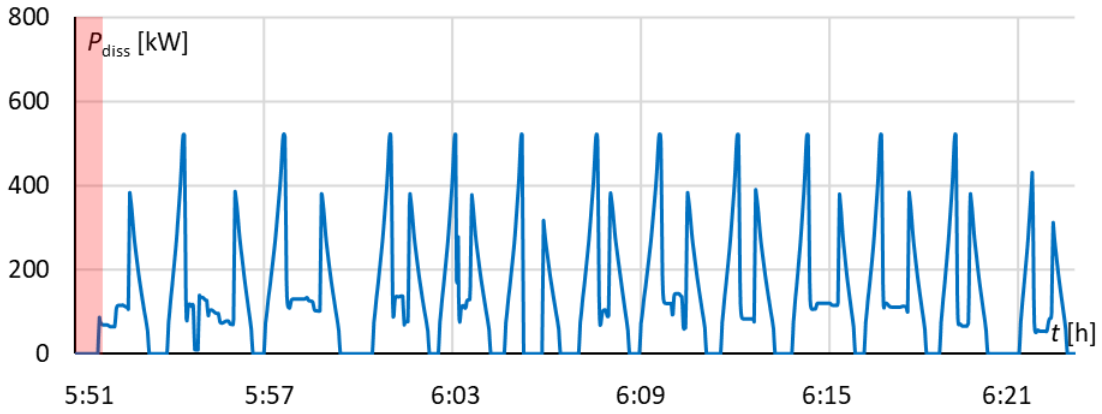

EN71SKM – drivetrain losses waveform, track 502

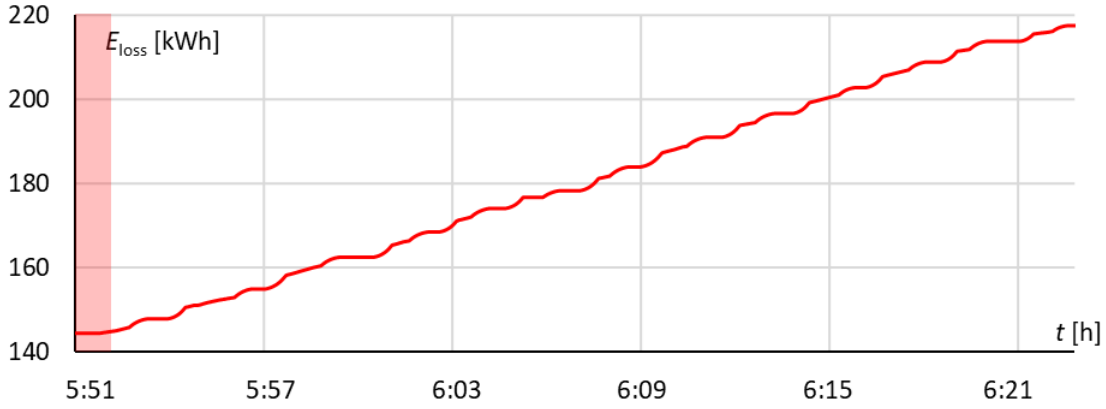

EN71SKM – dissipated energy waveform, track 502

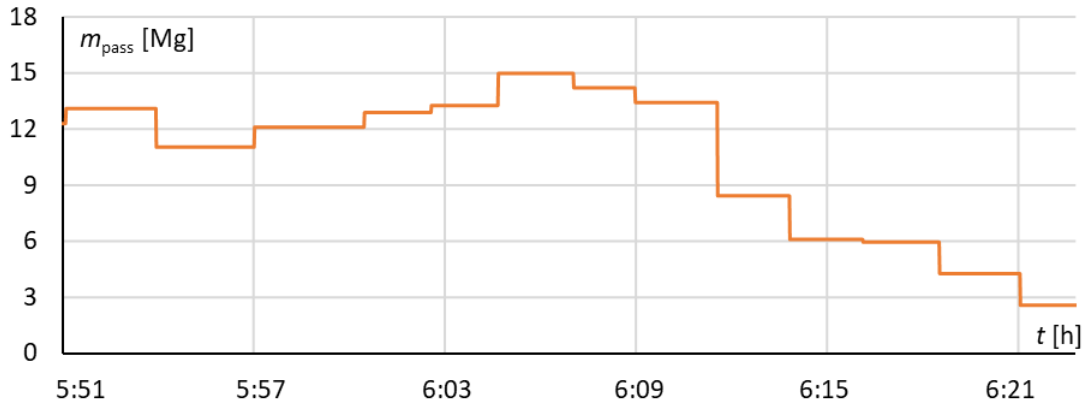

EN71SKM – passenger mass waveform, track 502

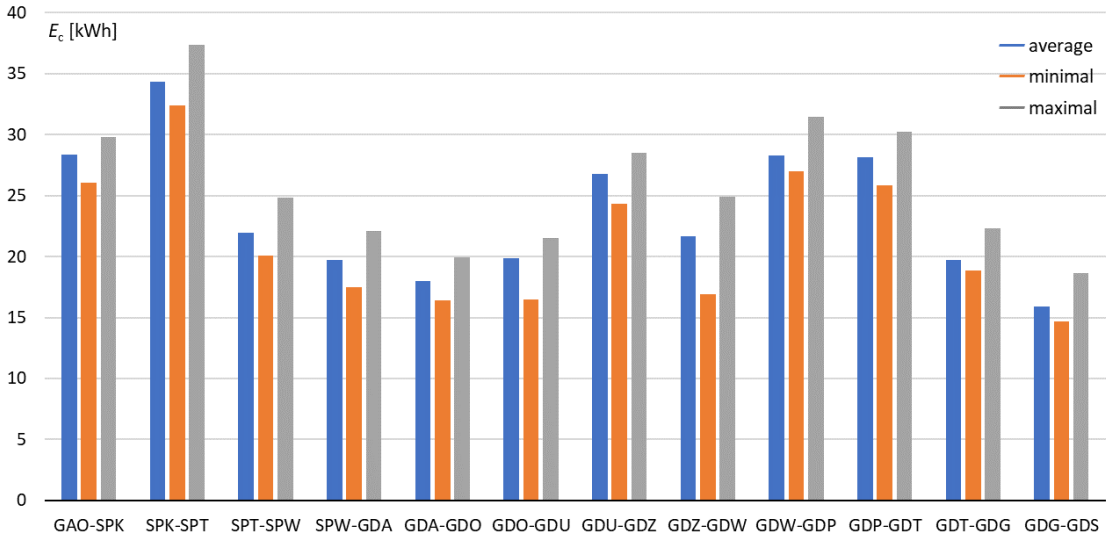

EN71SKM – consumed energy for each route part, track 502

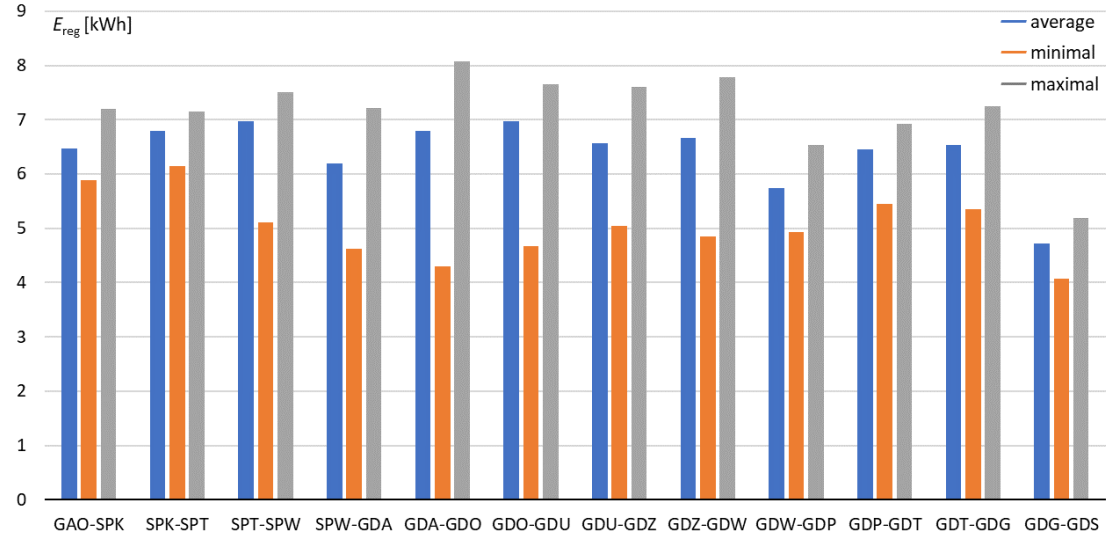

EN71SKM – regenerated energy for each route part, track 502

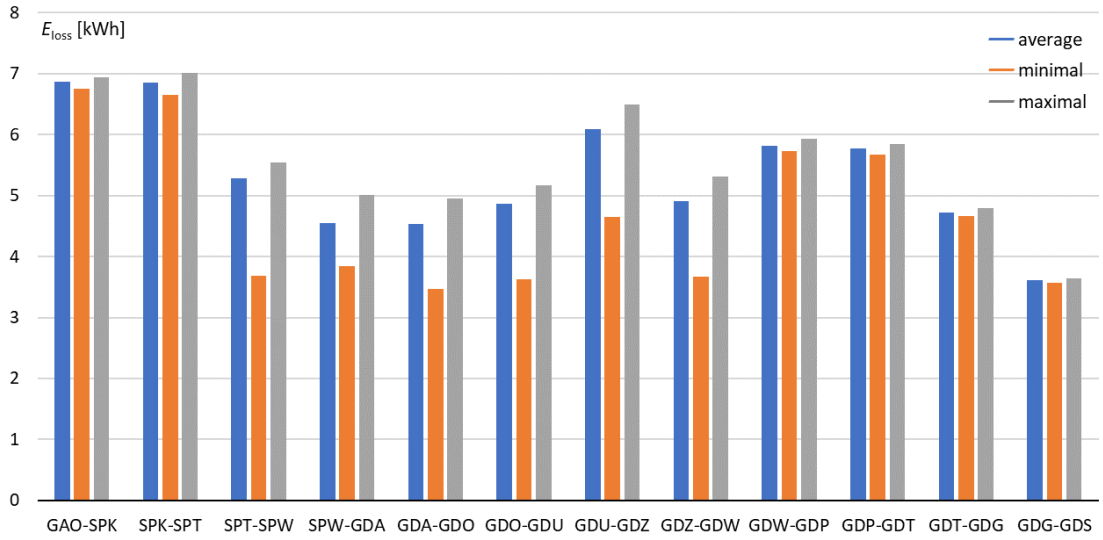

EN71SKM – dissipated energy for each route part, track 502

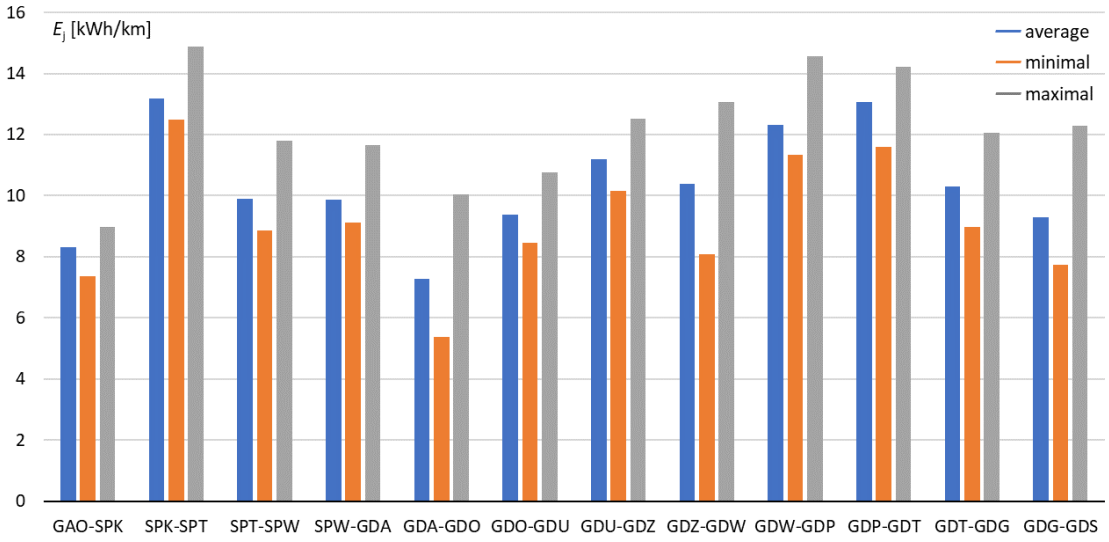

EN71SKM – energy consumption per 1 km, track 502

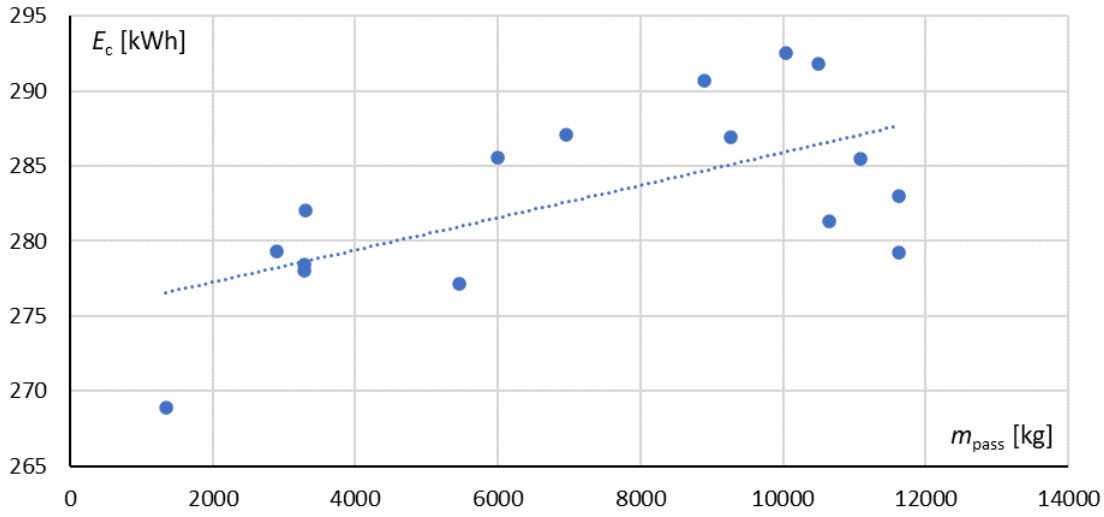

EN71SKM – consumed energy vs load mass, track 502

2c – EN71SKM, track 501 (direction Gdynia)

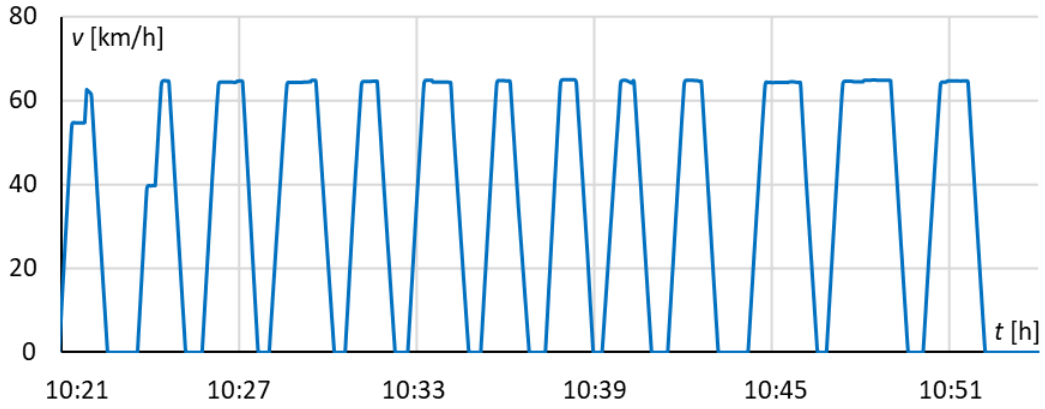

EN71SKM – velocity waveform, track 501

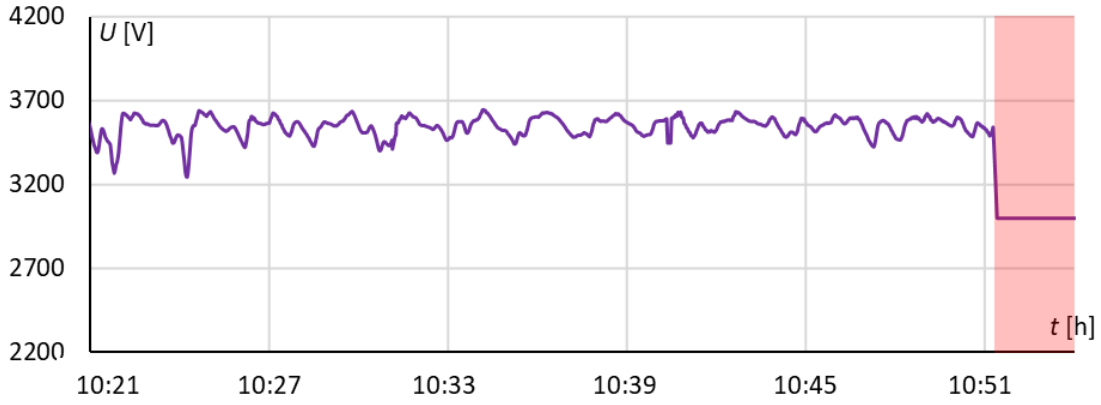

EN71SKM – pantograph voltage waveform, track 501

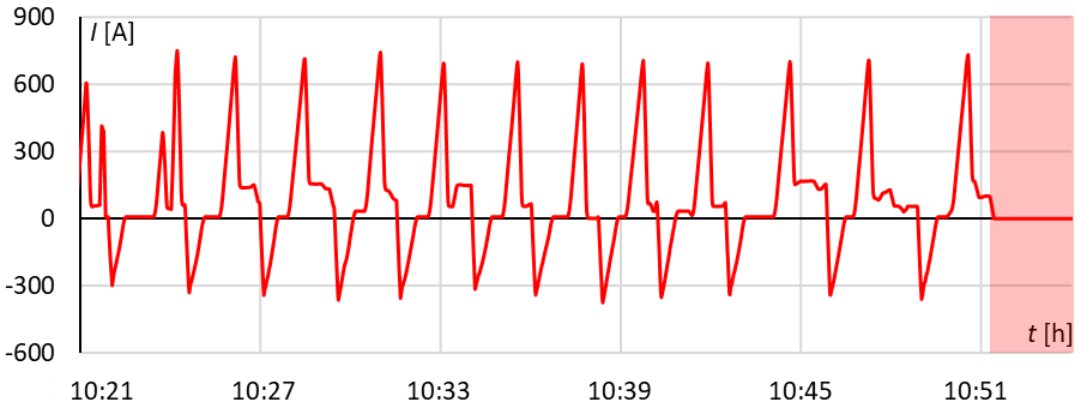

EN71SKM – vehicle current waveform, track 501

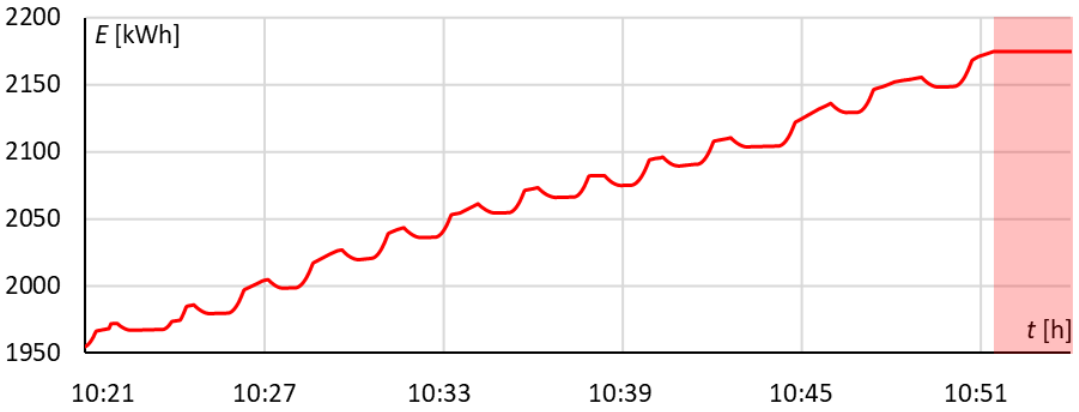

EN71SKM – vehicle energy balance waveform, track 501

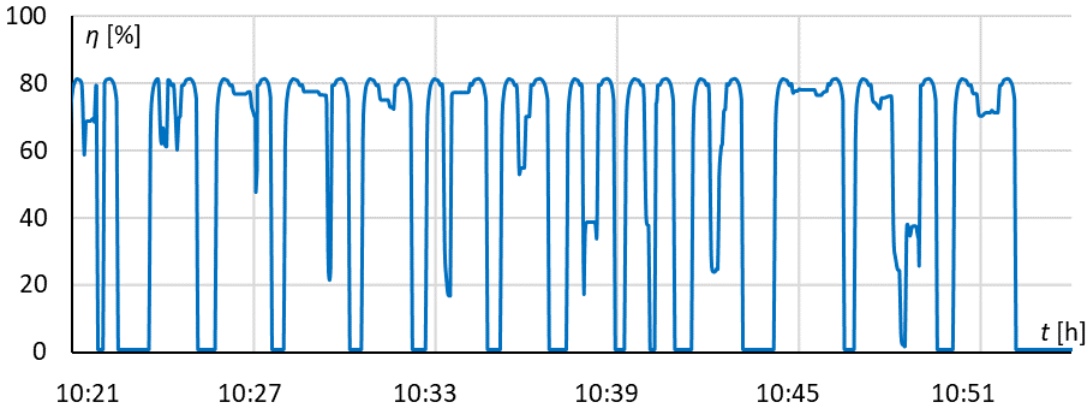

EN71SKM – drivetrain efficiency waveform, track 501

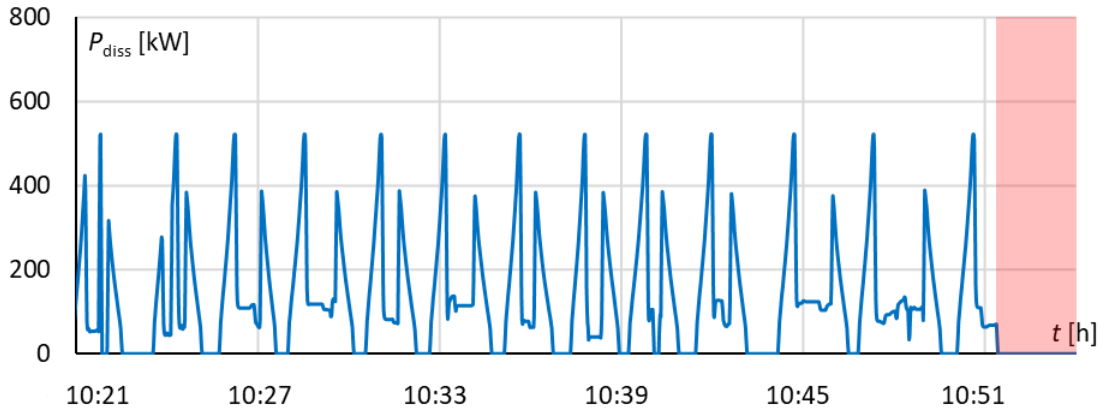

EN71SKM – drivetrain losses waveform, track 501

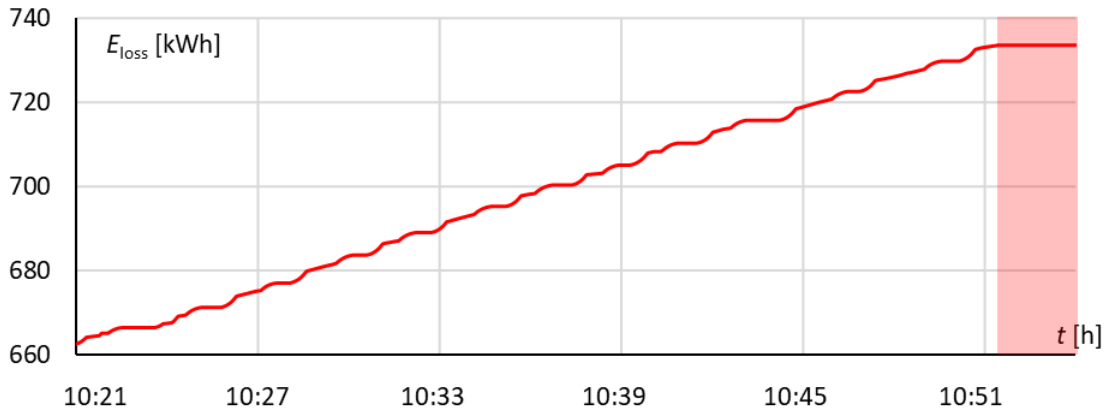

EN71SKM – dissipated energy waveform, track 501

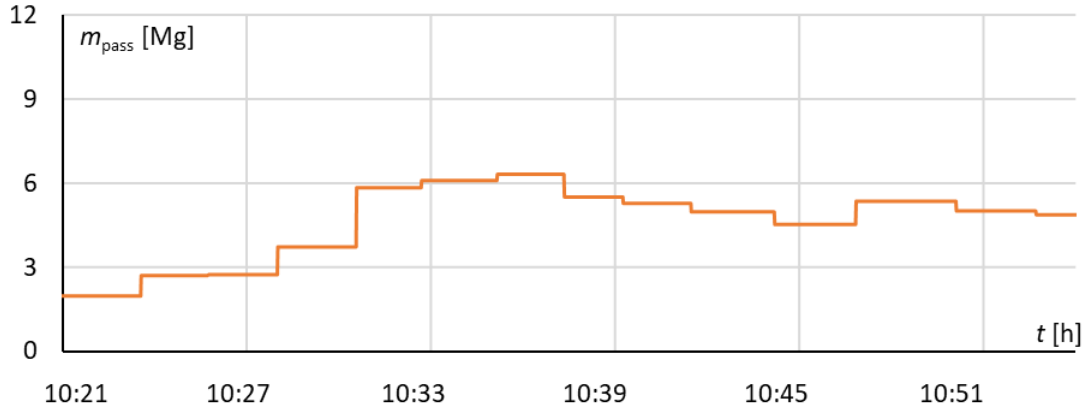

EN71SKM – passenger mass waveform, track 501

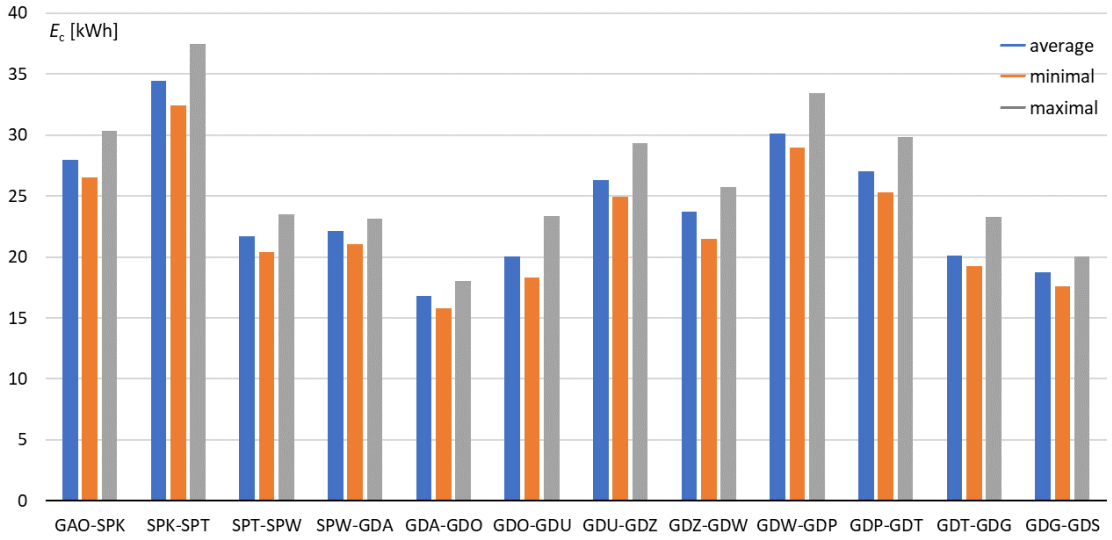

EN71SKM – consumed energy for each route part, track 501

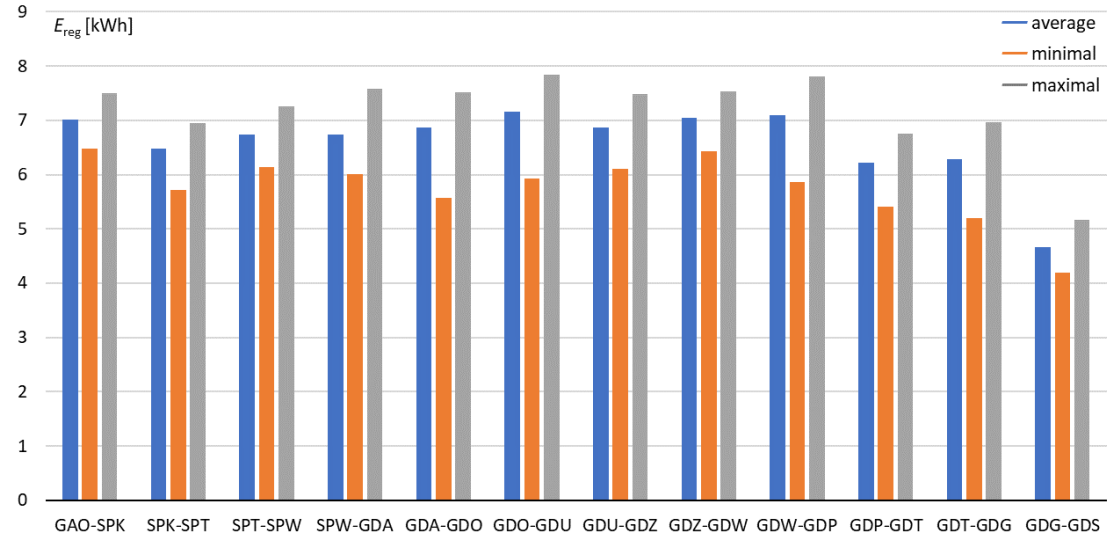

EN71SKM – regenerated energy for each route part, track 501

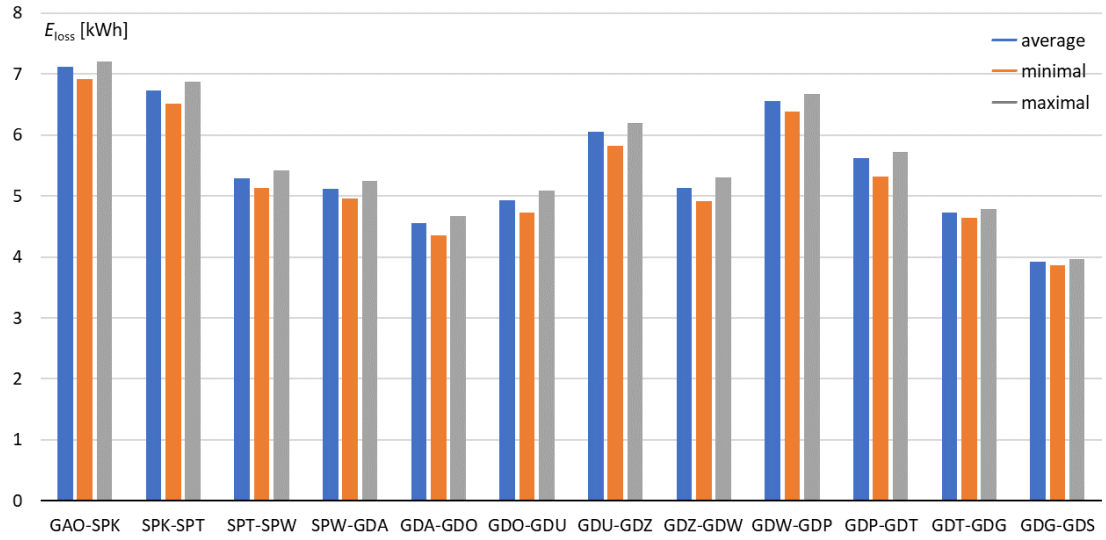

EN71SKM – dissipated energy for each route part, track 501

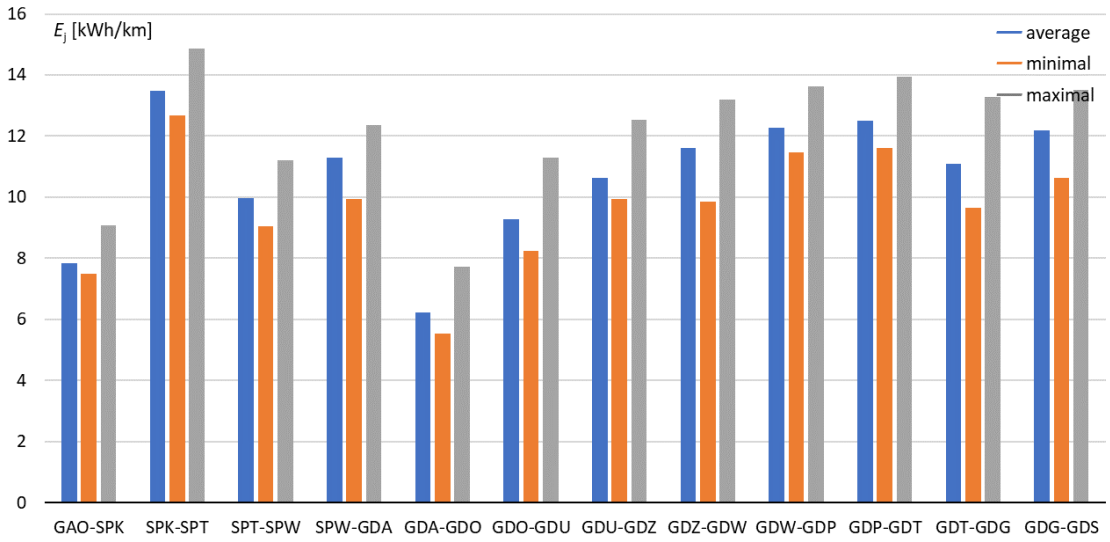

EN71SKM – energy consumption per 1 km, track 501

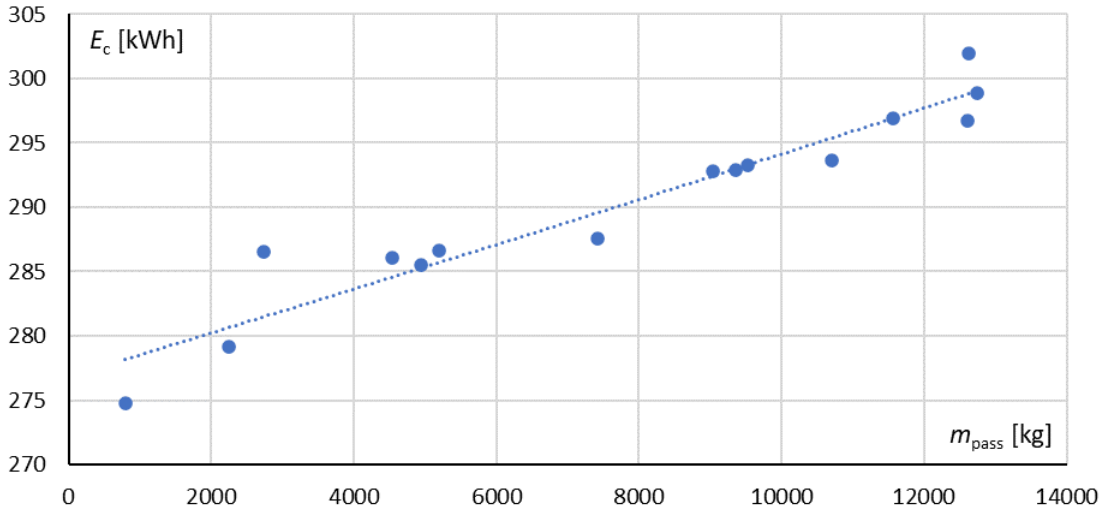

EN71SKM – consumed energy vs load mass, track 501

2d – 31WE, track 502 (direction Gdańsk)

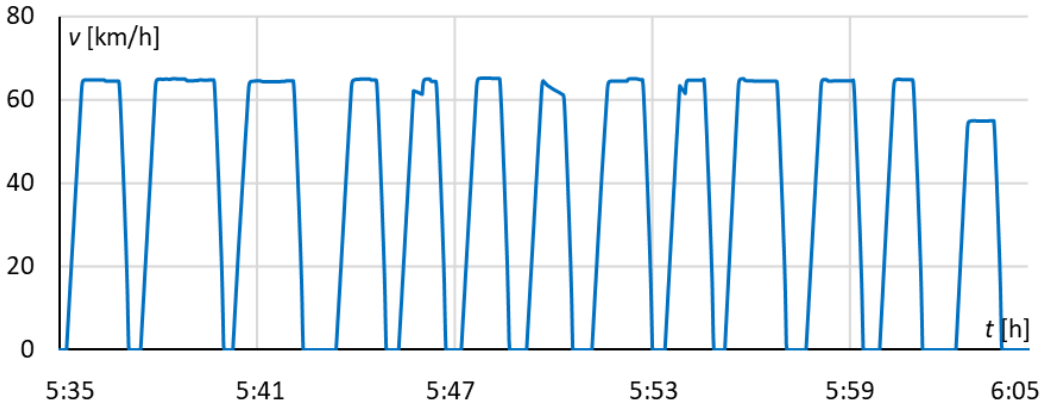

31WE – velocity waveform, track 502

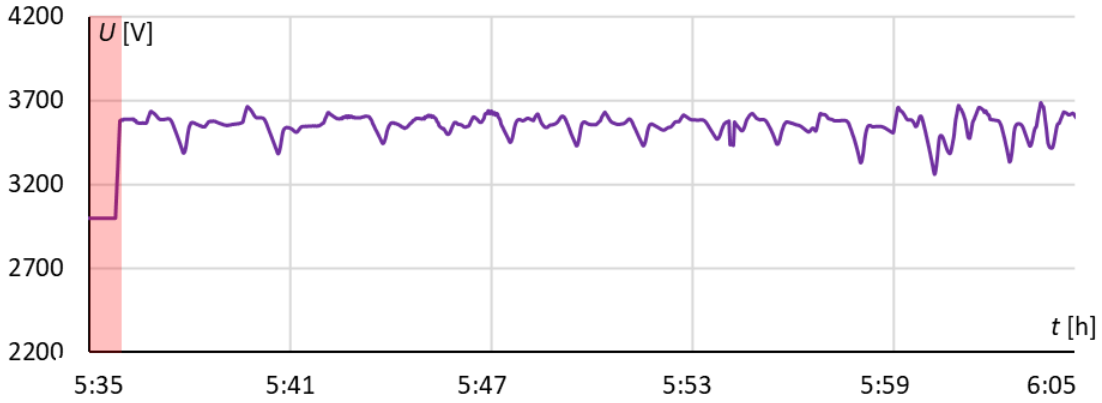

31WE – pantograph voltage waveform, track 502

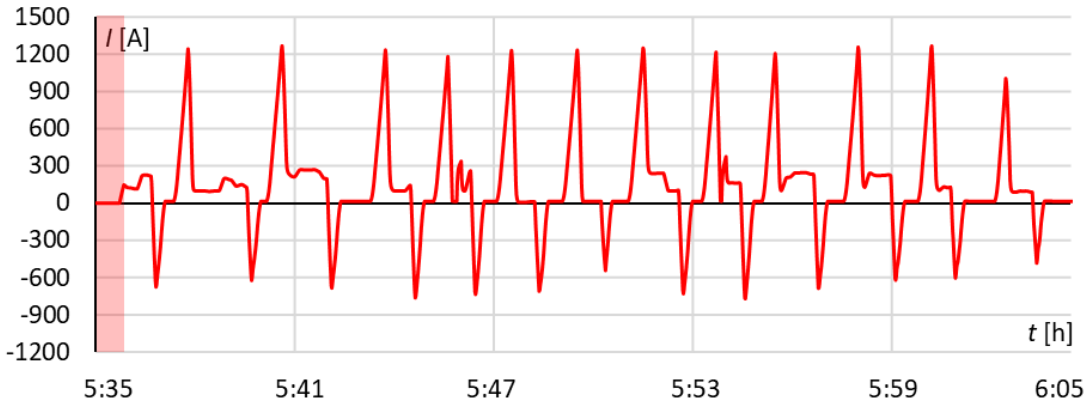

31WE – vehicle current waveform, track 502

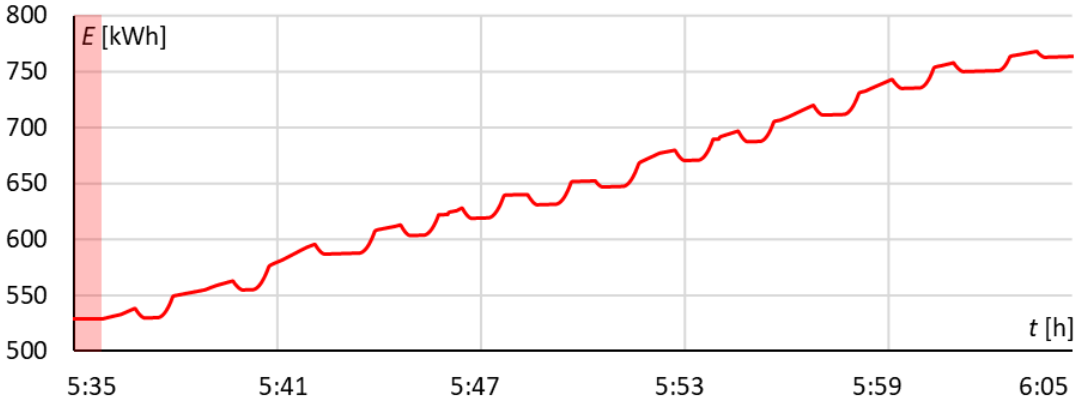

31WE – vehicle energy balance waveform, track 502

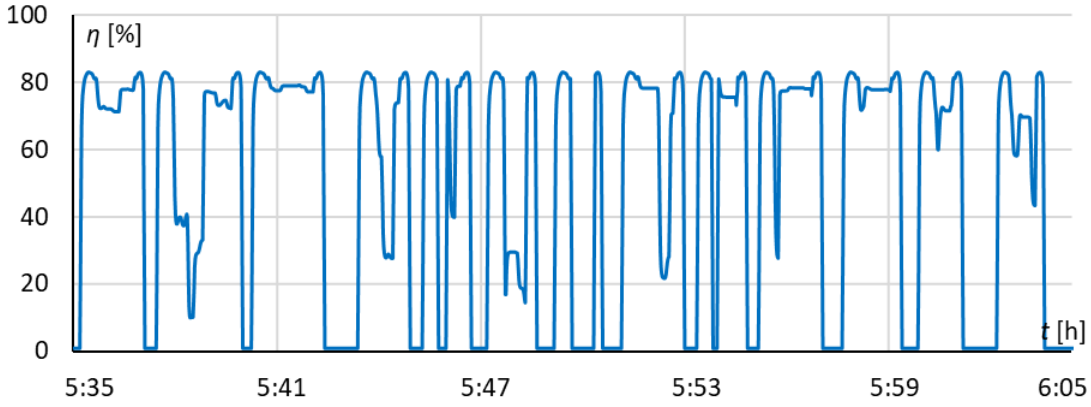

31WE – drivetrain efficiency waveform, track 502

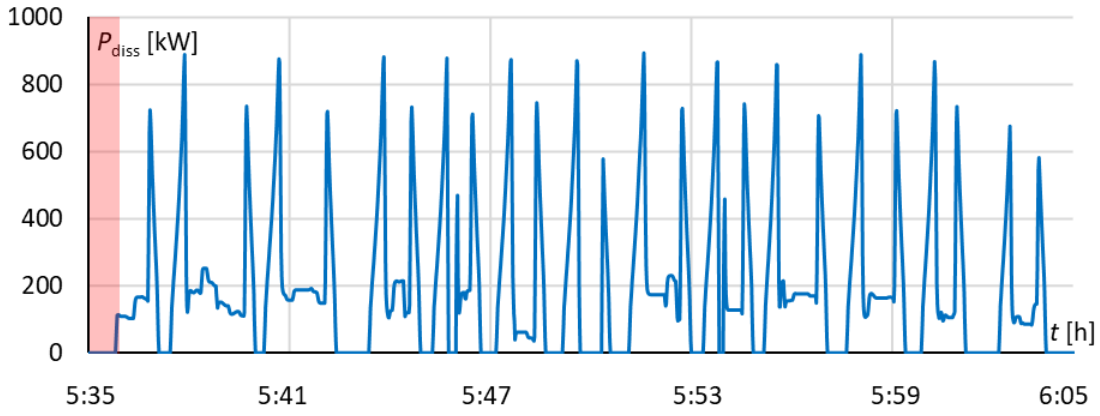

31WE – drivetrain losses waveform, track 502

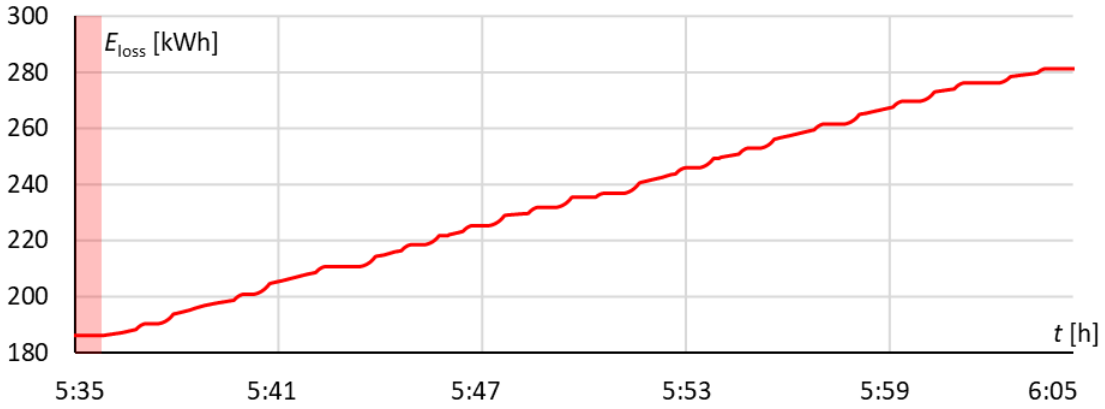

31WE – dissipated energy waveform, track 502

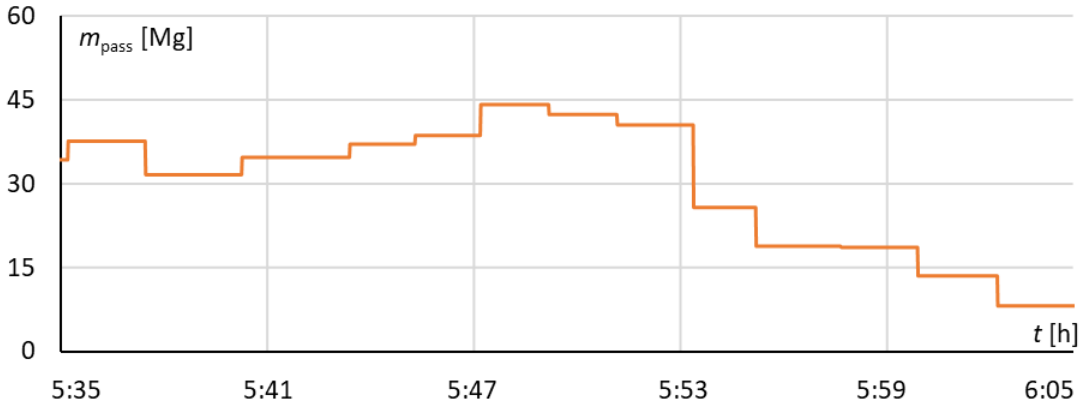

31WE – passenger mass waveform, track 502

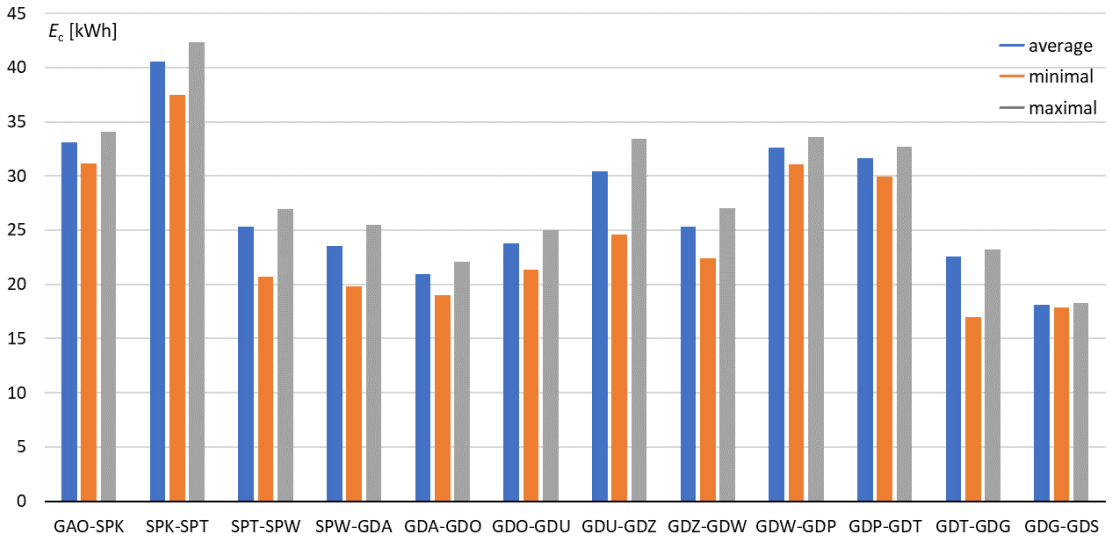

31WE – consumed energy for each route part, track 502

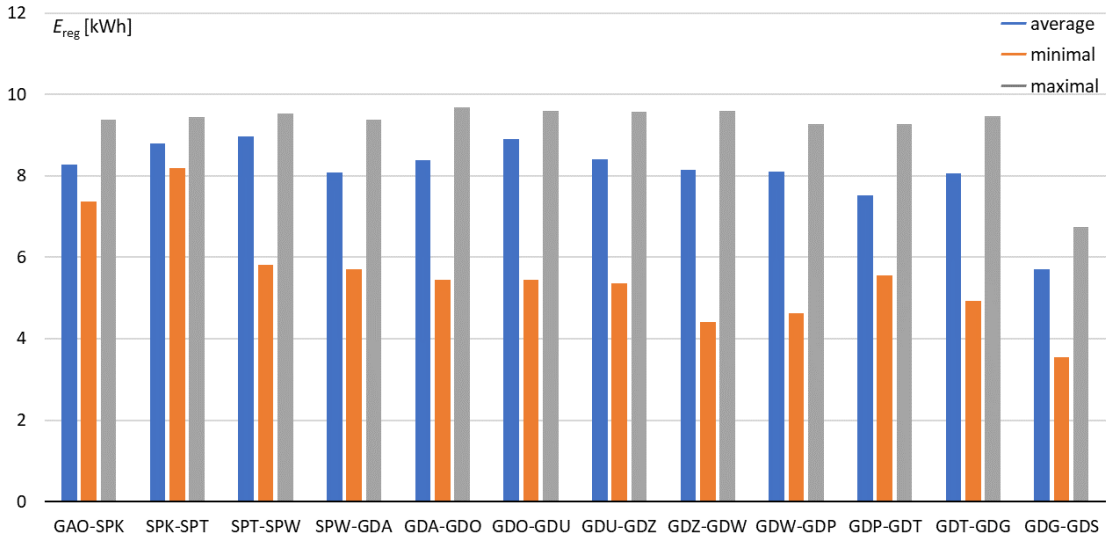

31WE – regenerated energy for each route part, track 502

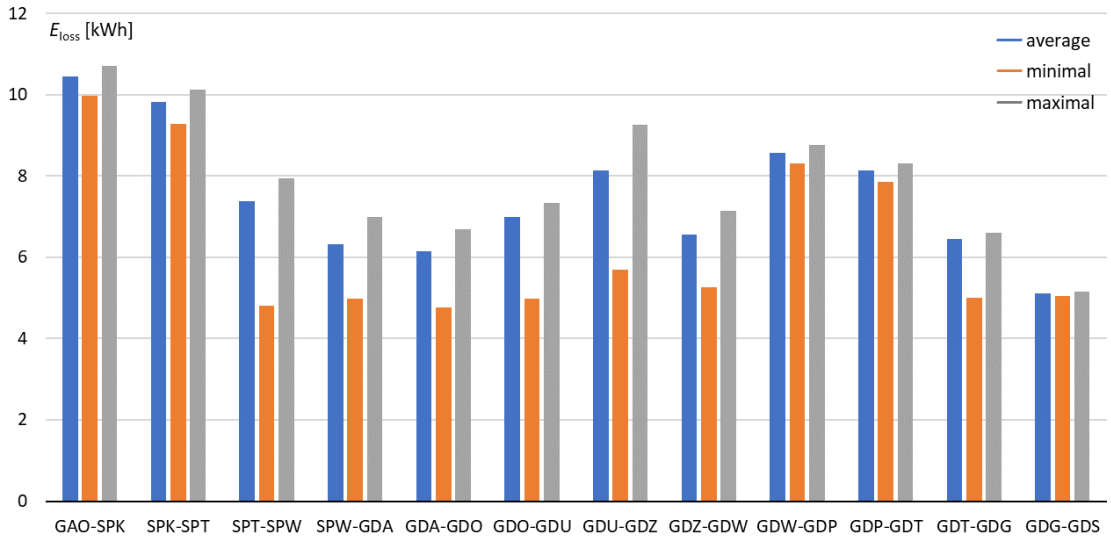

31WE – dissipated energy for each route part, track 502

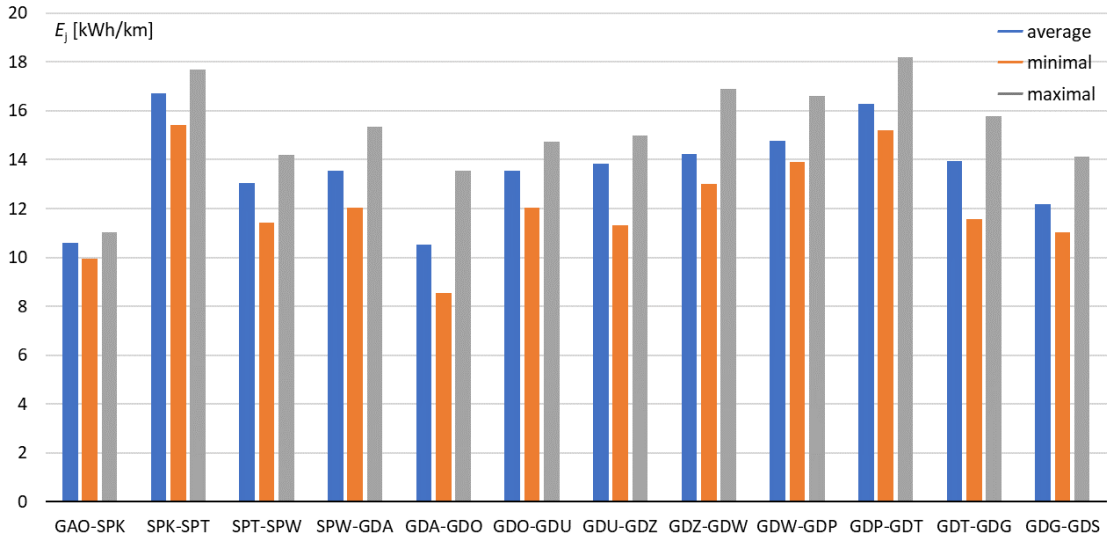

31WE – energy consumption per 1 km, track 502

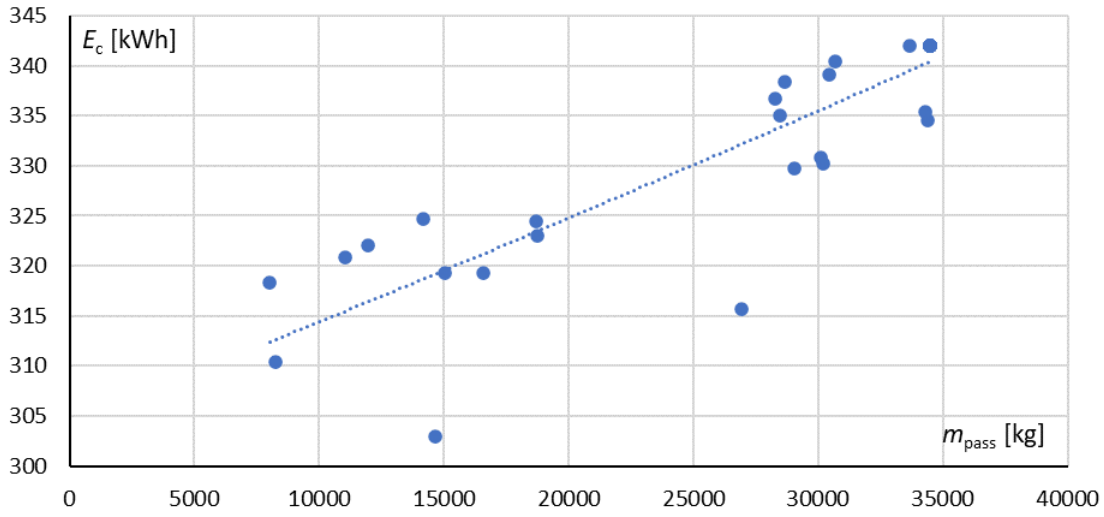

31WE – consumed energy vs load mass, track 502

2e – 31WE, track 501 (direction Gdynia)

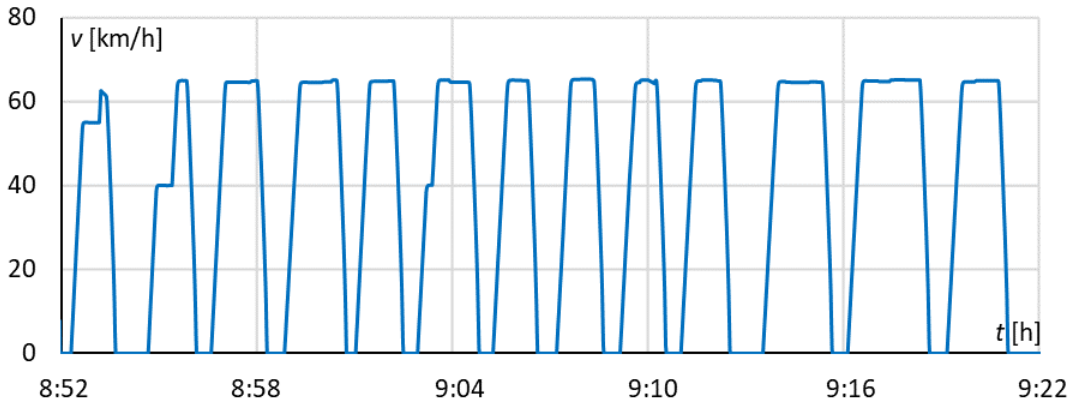

31WE – velocity waveform, track 501

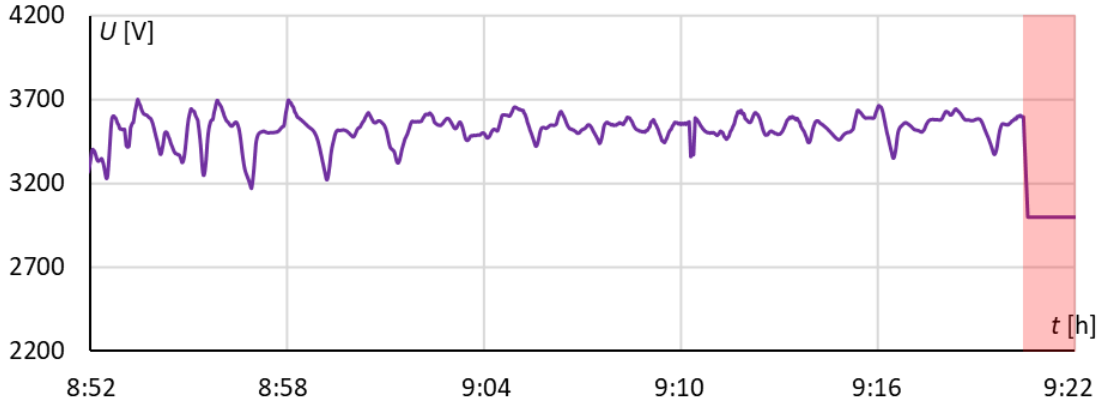

31WE – pantograph voltage waveform, track 501

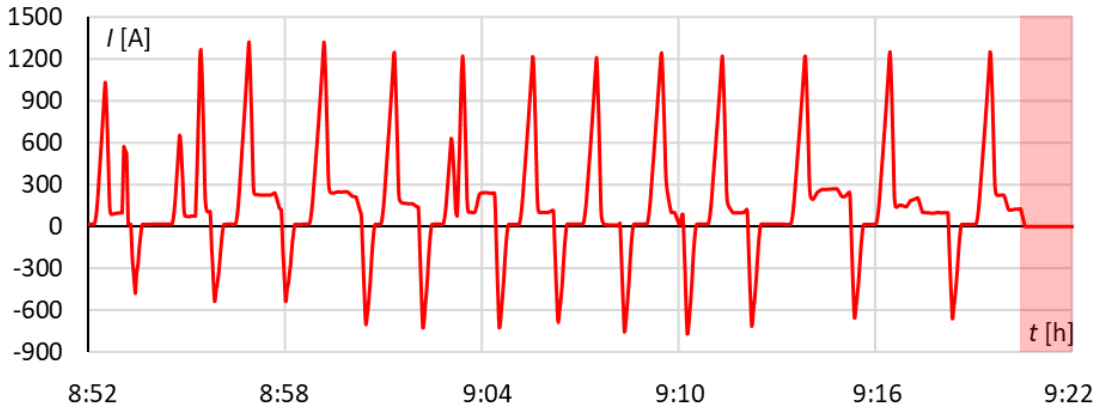

31WE – vehicle current waveform, track 501

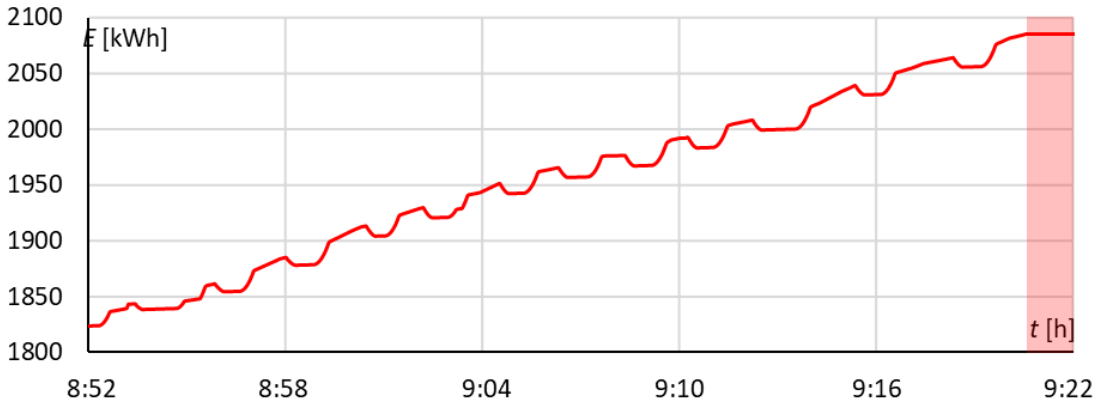

31WE – vehicle energy balance waveform, track 501

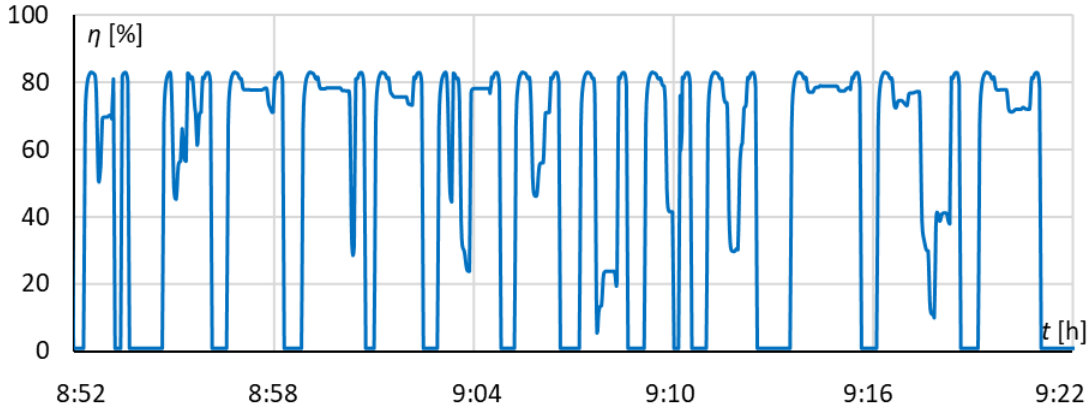

31WE – drivetrain efficiency waveform, track 501

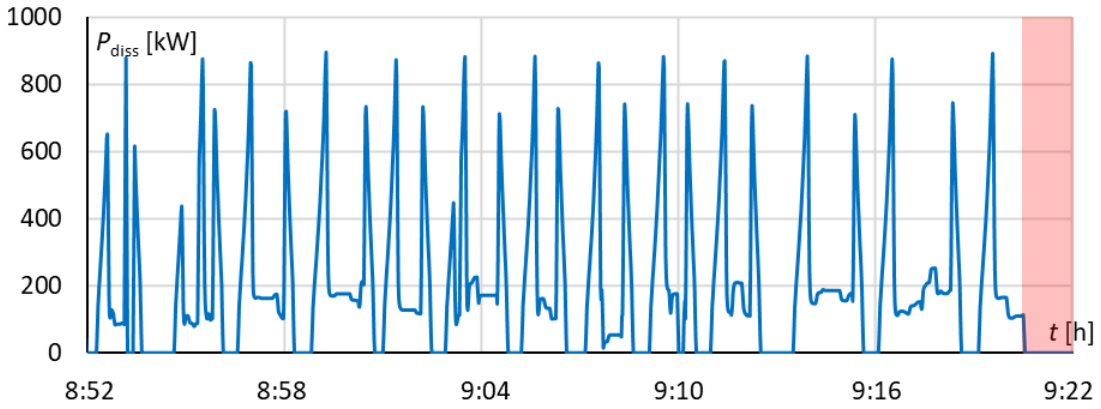

31WE – drivetrain losses waveform, track 501

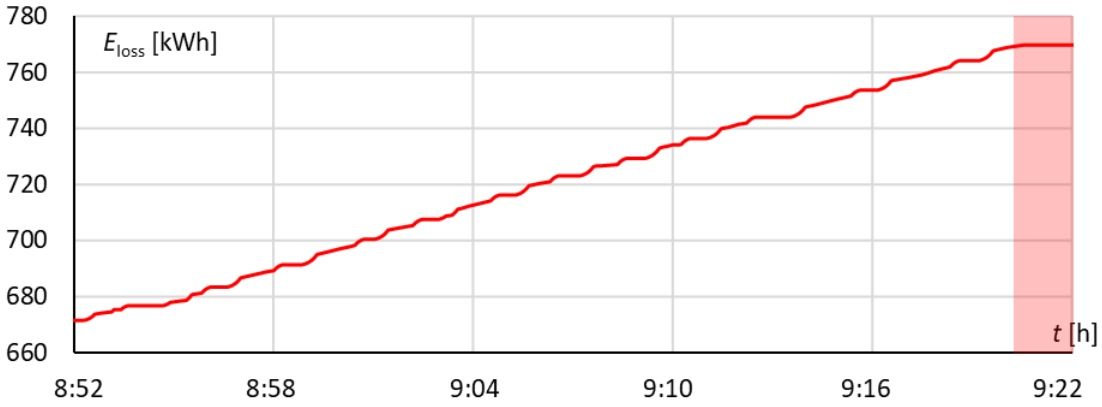

31WE – dissipated energy waveform, track 501

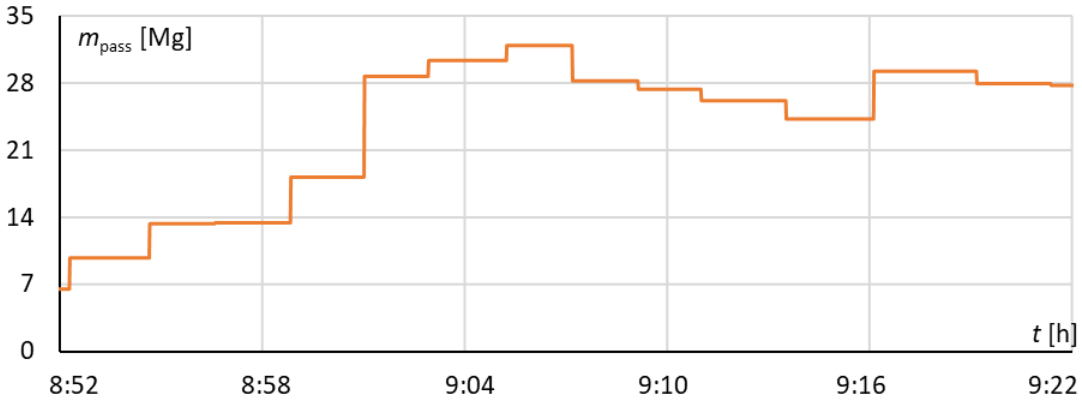

31WE – passenger mass waveform, track 501

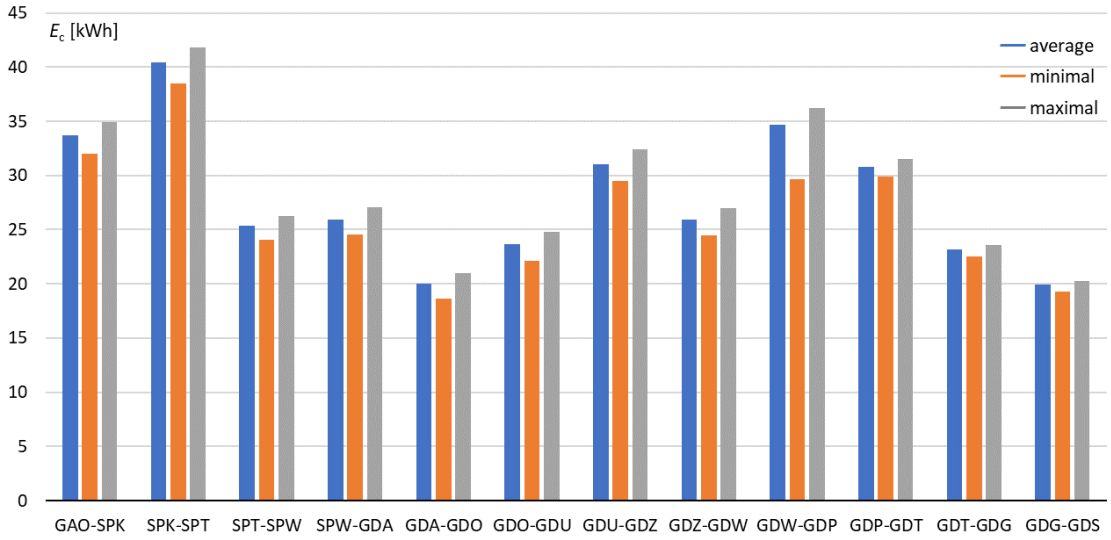

31WE – consumed energy for each route part, track 501

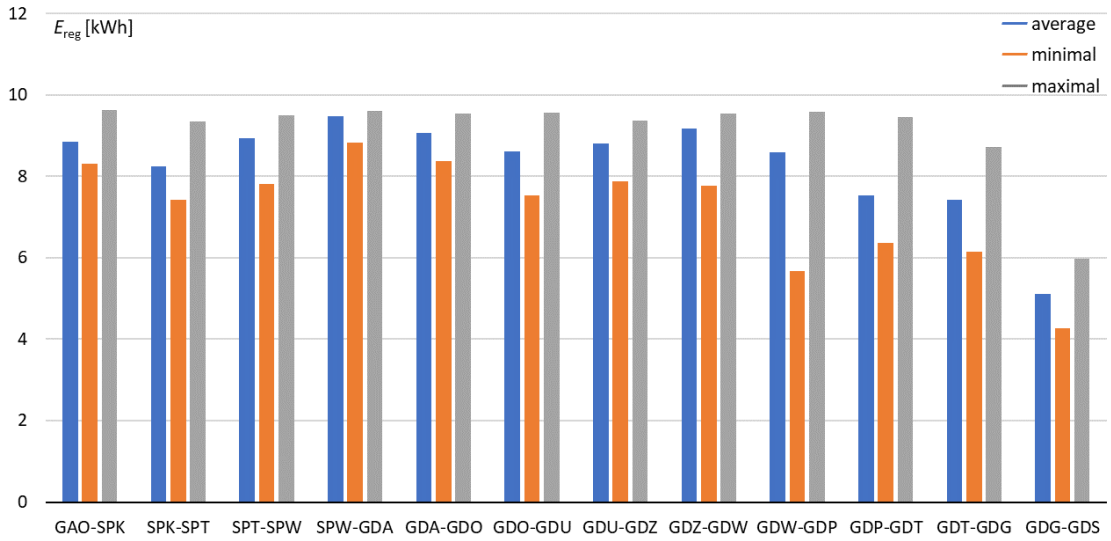

31WE – regenerated energy for each route part, track 502

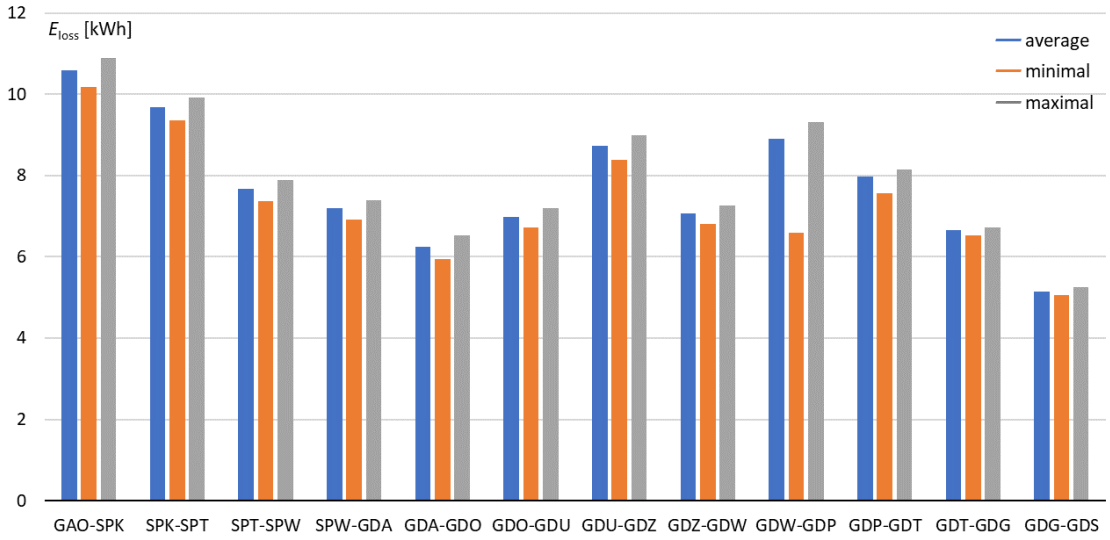

31WE – dissipated energy for each route part, track 502

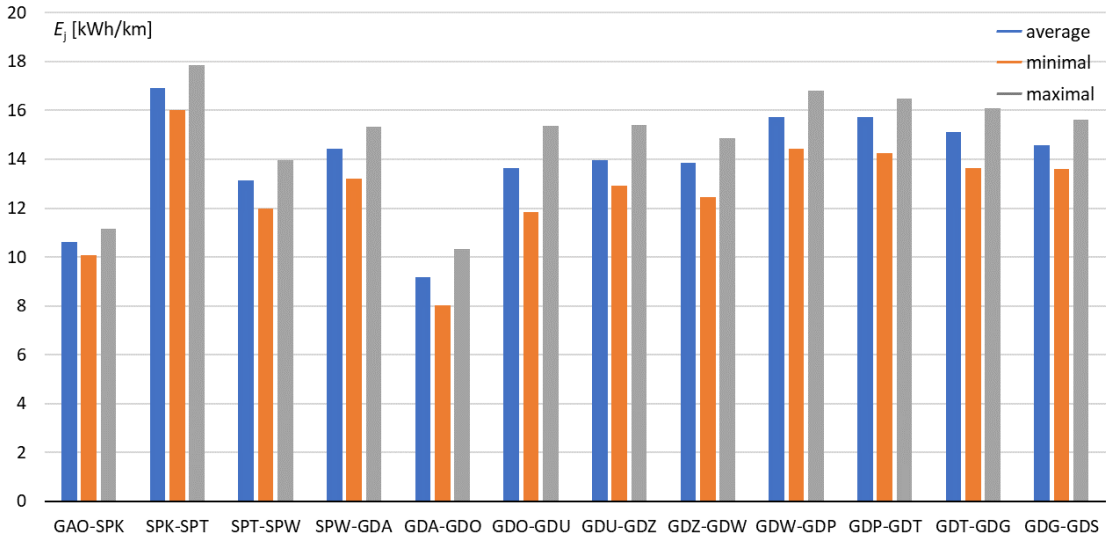

31WE – energy consumption per 1 km, track 502

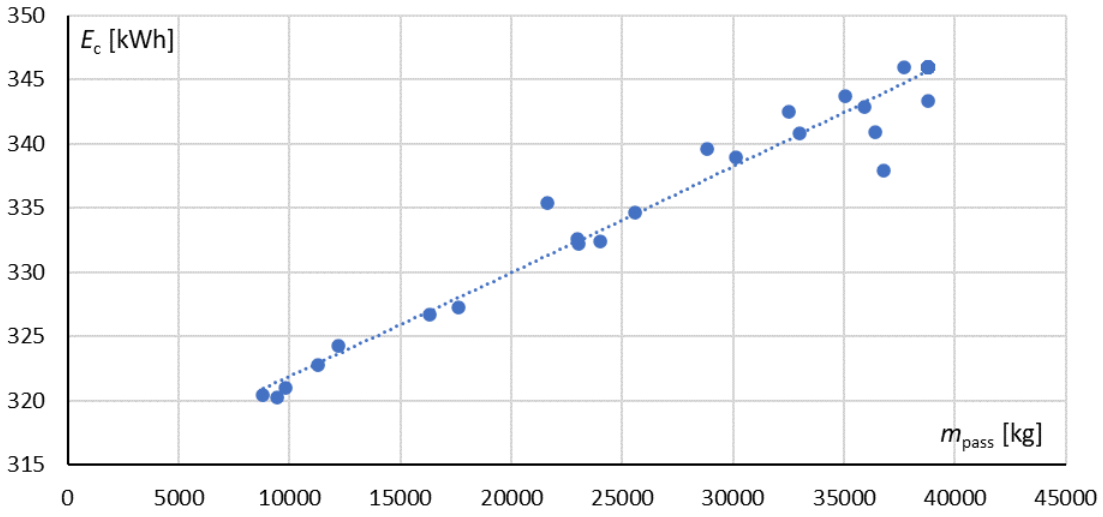

31WE – consumed energy vs load mass, track 501

Appendix 3 – Optimized velocity profiles data

Table. Data for implementing optimized velocity profiles

Track 501 (direction Gdynia)		**Route distance [km] Station**	**Track 502 (direction Gdańsk)**	
Action	Set velocity		Set velocity	Action
Accelerate	55	-1,017 Gdańsk Śródmieście	0	Stop
		-0,876	0	Brake
Cruise	55	-0,822		
Coast		-0,498		
		-0,186		Coast
Brake	0	-0,125		
Accelerate	40	0,000 Gdańsk Główny	55	Accelerate
Cruise	40	0,083		
		0,154	0	Brake
Accelerate	65	0,400		
Coast		0,610		
		0,759		Coast
Brake	0	0,892		
Accelerate	66	1,040 Gdańsk Stocznia	65	Accelerate
		1,139	0	Brake
Cruise	66	1,434		
Coast		1,585		
		1,857		Coast
		2,199	65	Cruise
Brake	0	2,373		
Accelerate	65	2,520 Gdańsk Politechnika	65	Accelerate
		2,638	0	Brake
Cruise	65	2,932		
		3,256		Coast
Coast		3,391		
		3,904	65	Cruise
Brake	0	4,018		
Accelerate	64	4,180 Gdańsk Wrzeszcz	65	Accelerate
		4,311	0	Brake

Coast		4,459		
		4,930		Coast
		5,092	65	Cruise
Brake	0	5,269		
Accelerate	40	5,390	65	Accelerate
		Gdańsk Zaspa		
Cruise	40	5,477		
		5,489	0	Brake
Accelerate	64	5,592		
Coast		5,792		
		6,649		Coast
Brake	0	6,890		
Accelerate	64	6,980	64	Accelerate
		Gdańsk Przymorze		
		7,155	0	Brake
Coast		7,292		
		7,744		Coast
Brake	0	7,925		
Accelerate	64	8,080	64	Accelerate
		Gdańsk Oliwa		
		8,290	0	Brake
Coast		8,349		
		8,977		Coast
Brake	0	9,098		
Accelerate	64	9,270	65	Accelerate
		Gdańsk Żabianka		
		9,421	0	Brake
Coast		9,597		
		10,117		Coast
Brake	0	10,258		
Accelerate	64	10,410	65	Accelerate
		Sopot Wyścigi		
		10,556	0	Brake
Coast		10,716		
		11,338		Coast
Brake	0	11,514		
Accelerate	67	11,660	65	Accelerate
		Sopot		
		11,751	0	Brake
Cruise	67	12,027		
		12,505		Coast
Coast		12,785		
		13,223	65	Cruise
Brake	0	13,438		
Accelerate	67	13,560	65	Accelerate

		Sopot Kamienny Potok		
		13,661	0	Brake
Cruise	67	13,912		
Coast		14,092		
		14,667		Coast
		15,571	66	Cruise
Brake	0	15,770		
Accelerate	64	15,900	66	Accelerate
		Gdynia Orłowo		
		16,012	0	Brake
Coast		16,215		
		16,992		Coast
		17,244	65	Cruise
Brake	0	17,420		
Stop		17,540	65	Accelerate
		Gdynia Redłowo		
All velocities are given in km/h All distances are given in absolute route km				

Appendix 4 – Results of optimization – track 501 waveforms

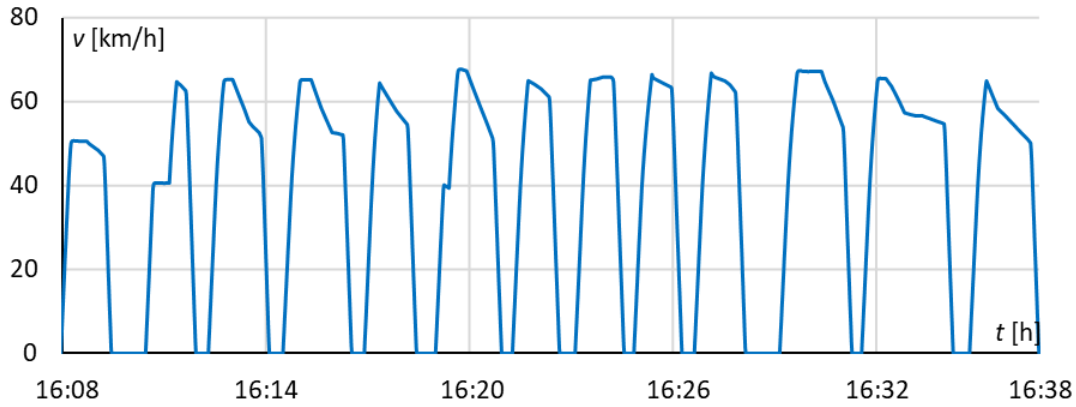

EN57AKM – velocity waveform, track 501 (optimized run)

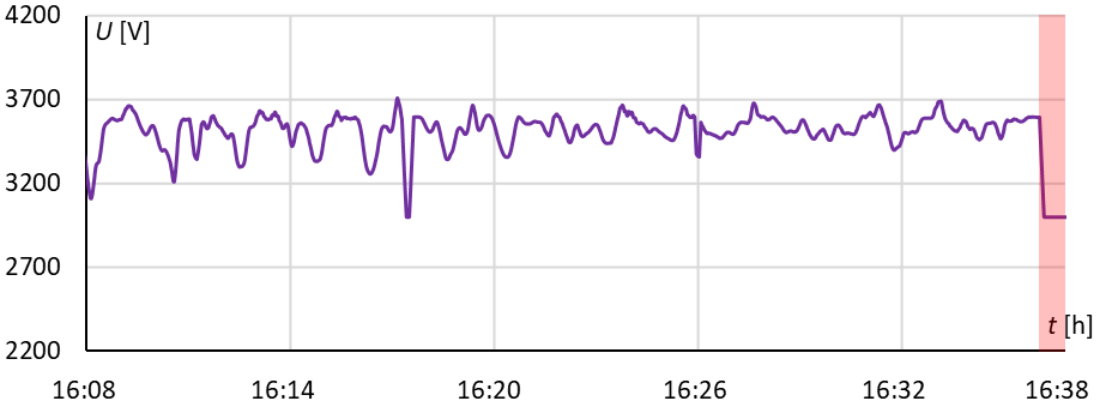

EN57AKM – pantograph voltage waveform, track 501 (optimized run)

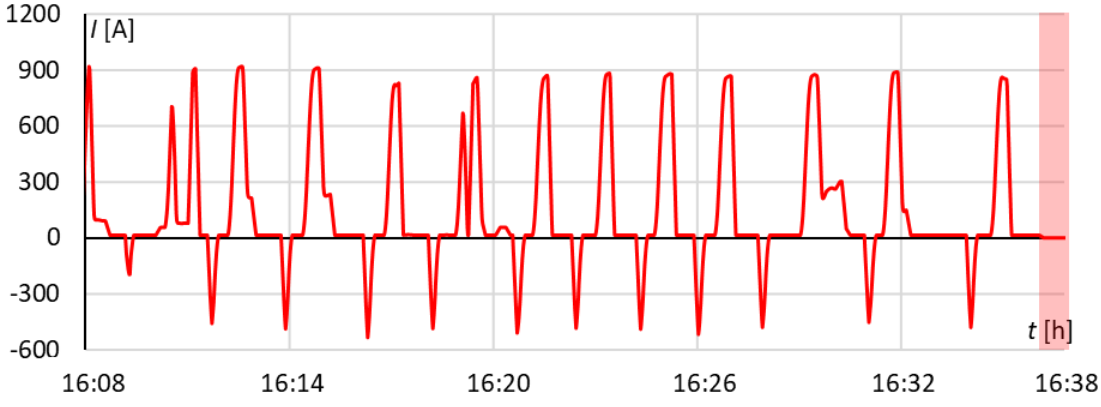

EN57AKM – vehicle current waveform, track 501 (optimized run)

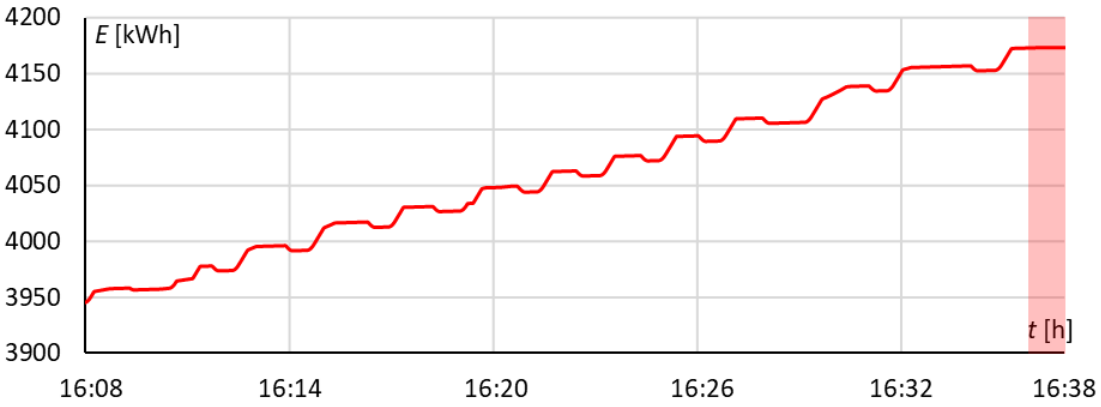

EN57AKM – vehicle energy balance waveform, track 501 (optimized run)

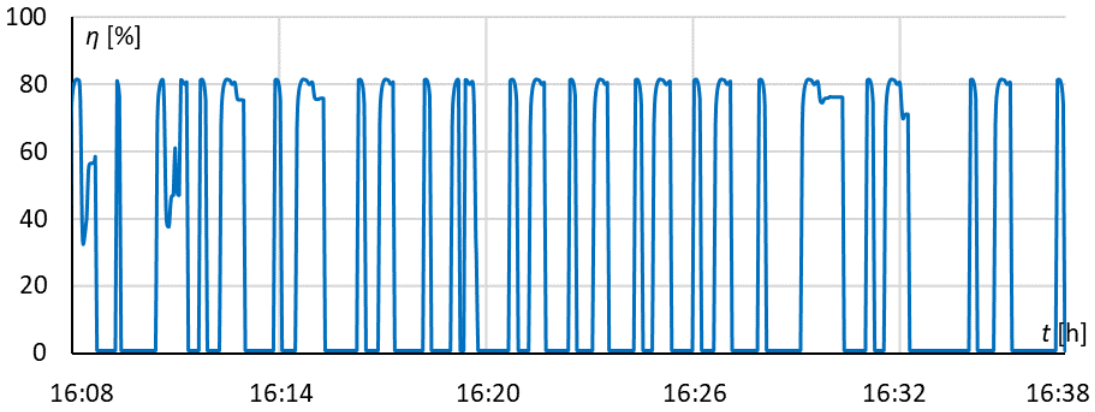

EN57AKM – drivetrain efficiency waveform, track 501 (optimized run)

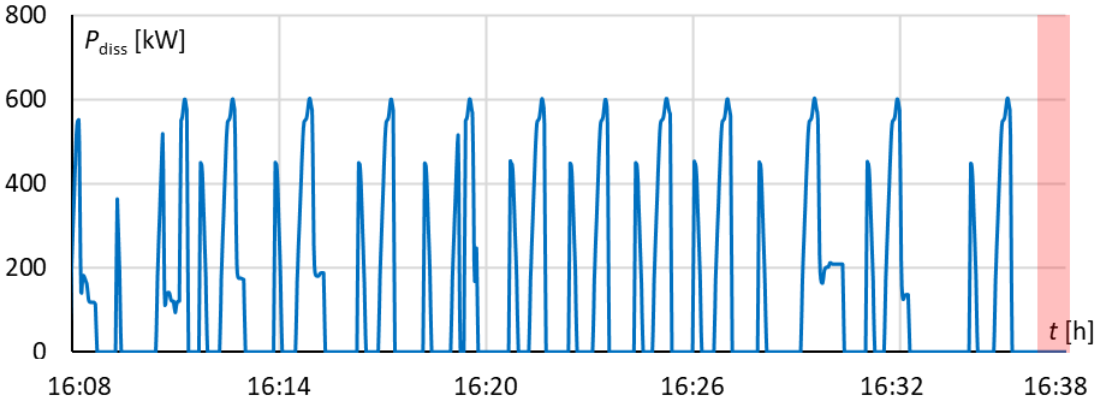

EN57AKM – drivetrain losses waveform, track 501 (optimized run)

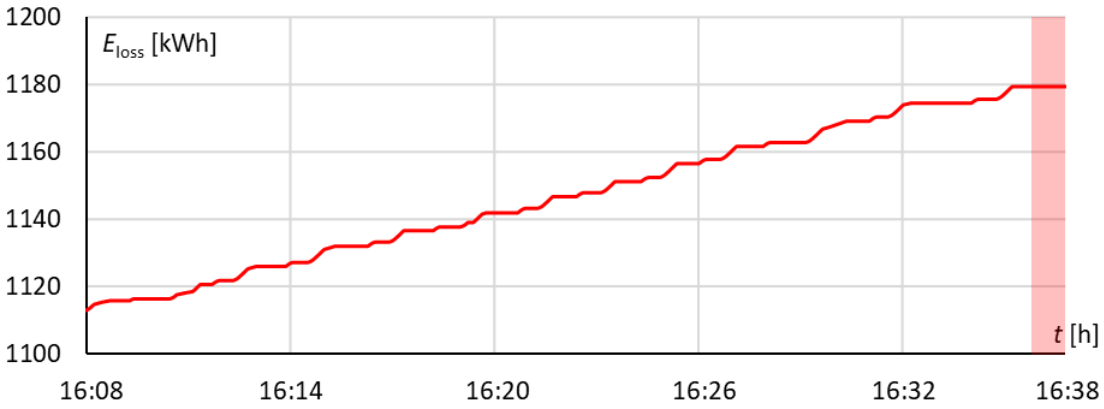

EN57AKM – dissipated energy waveform, track 501 (optimized run)

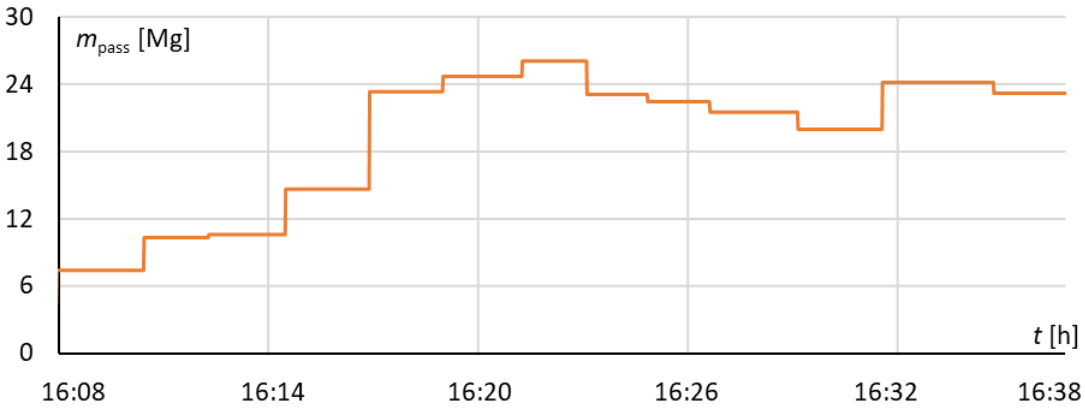

EN57AKM – passenger mass waveform, track 501 (optimized run)

Appendix 5 – Results of optimization – power supply

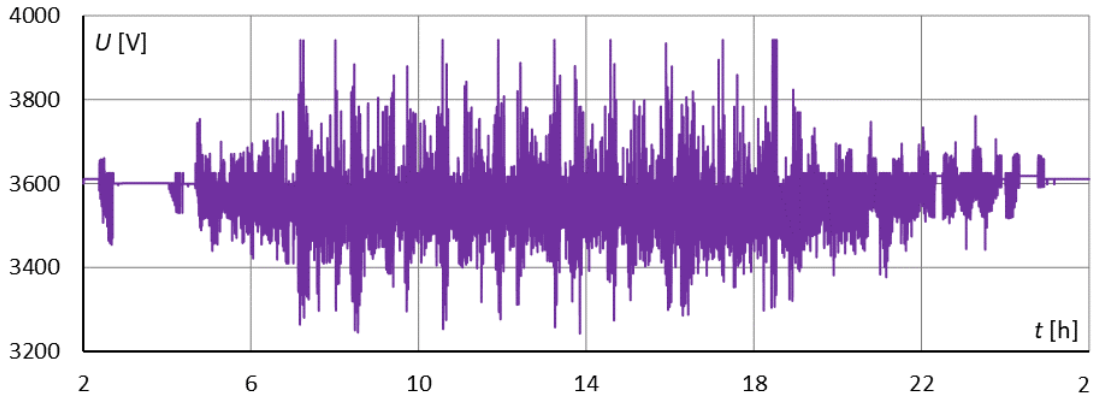

Output voltage – substation Gdańsk Wrzeszcz (optimized run)

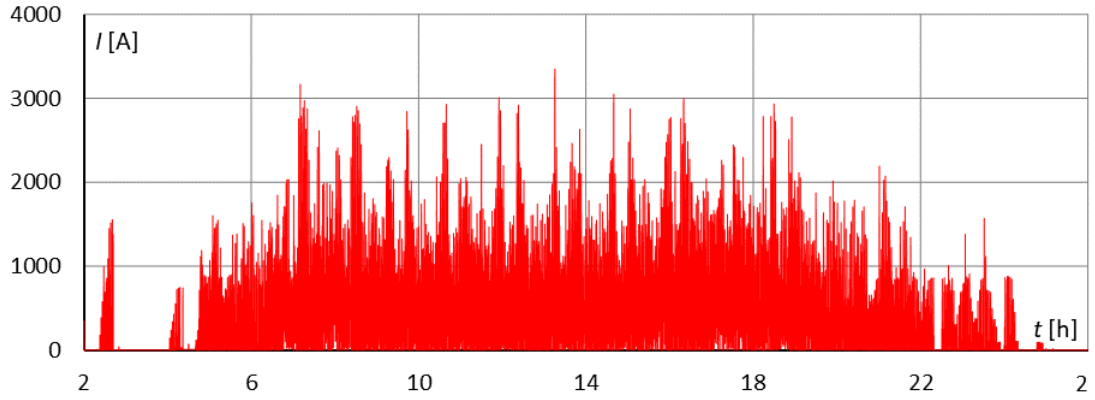

Output current – substation Gdańsk Wrzeszcz (optimized run)

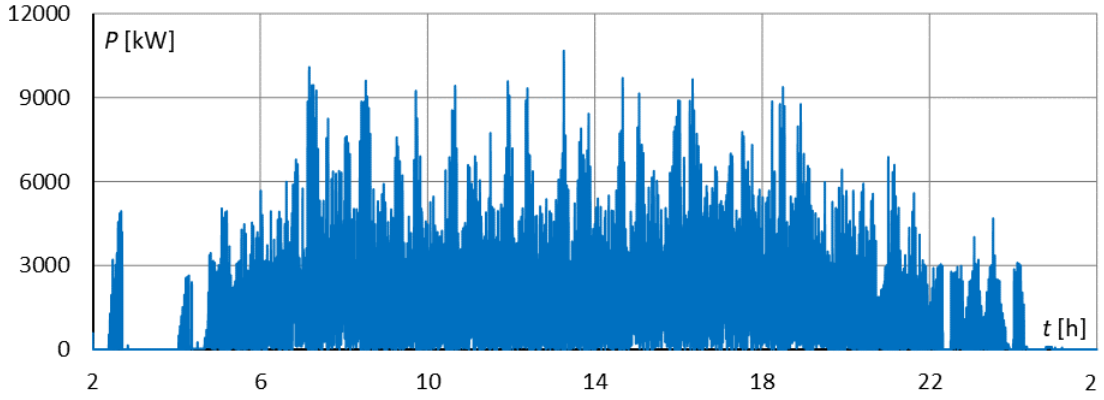

Output power – substation Gdańsk Wrzeszcz (optimized run)

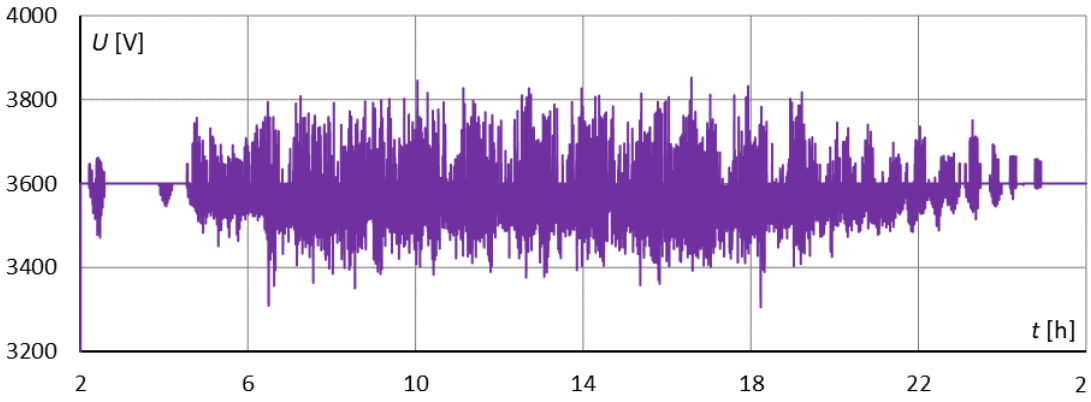

Output voltage – substation Sopot (optimized run)

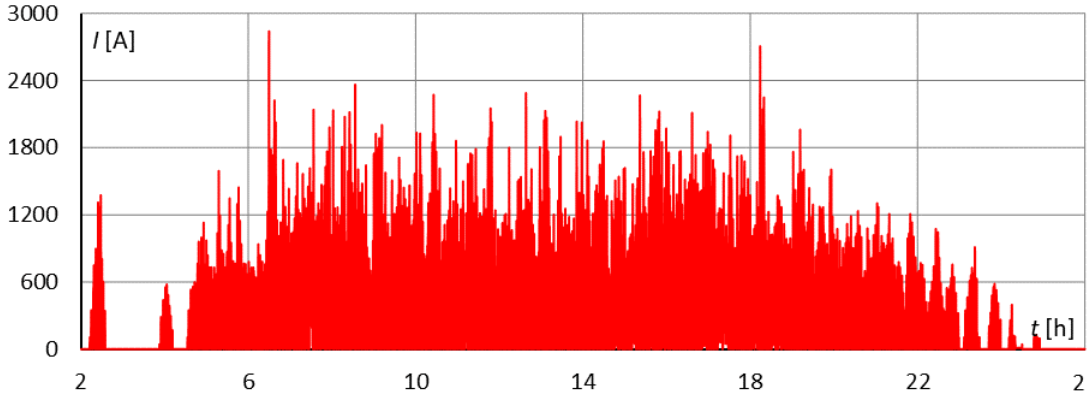

Output current – substation Sopot (optimized run)

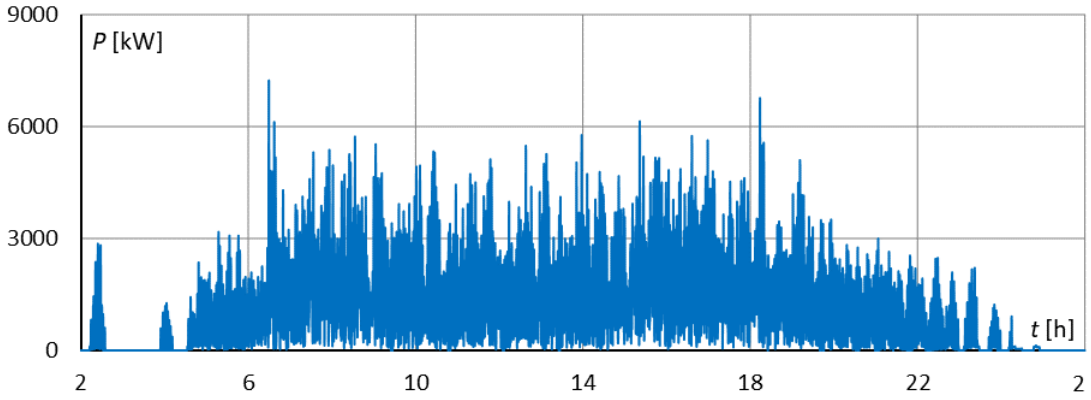

Output power – substation Sopot (optimized run)

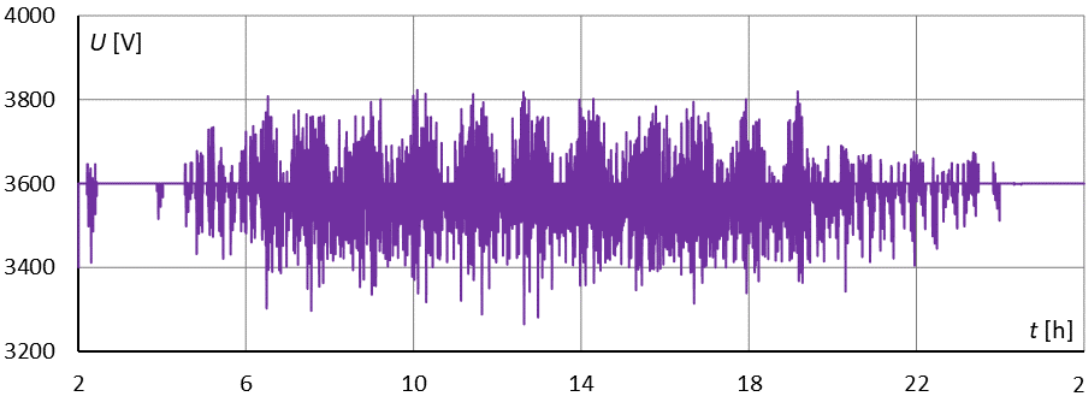

Output voltage – substation Gdynia Redłowo (optimized run)

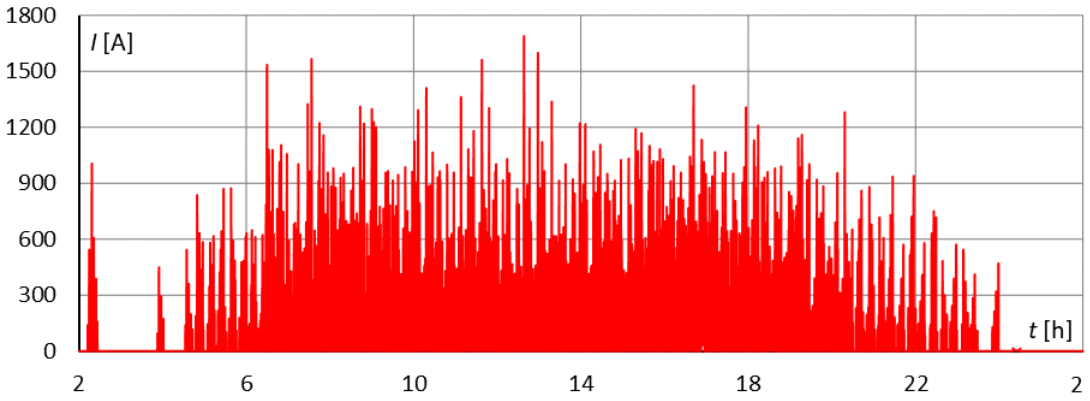

Output current – substation Gdynia Redłowo (optimized run)

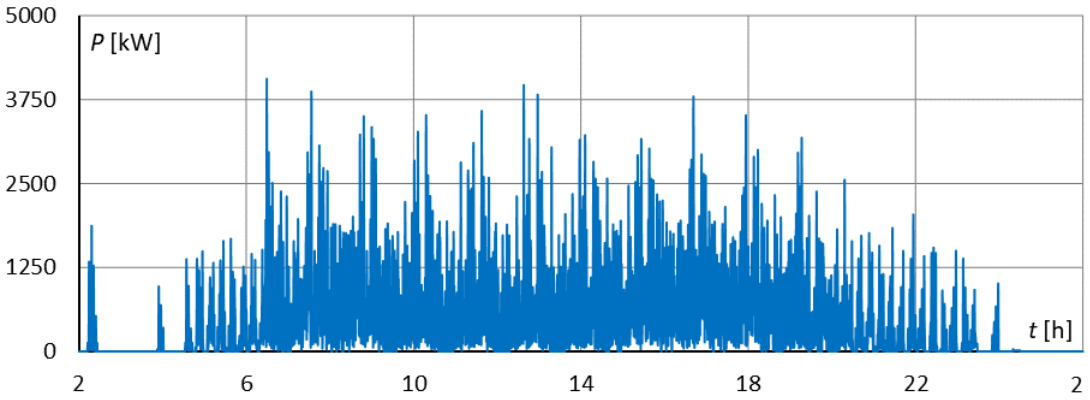

Output power – substation Gdynia Redłowo (optimized run)